

**PROPERTIES AND HYDRATION OF CEMENTITIOUS SYSTEMS CONTAINING
LOW, MODERATE AND HIGH AMOUNTS OF
NATURAL ZEOLITES**

**A THESIS SUBMITTED TO
THE GRADUATE SCHOOL OF NATURAL AND APPLIED SCIENCES
OF
THE MIDDLE EAST TECHNICAL UNIVERSITY**

BY

BURAK UZAL

**IN PARTIAL FULFILLMENT OF THE REQUIREMENTS
FOR
THE DEGREE OF DOCTOR OF PHILOSOPHY
IN
CIVIL ENGINEERING**

SEPTEMBER 2007

Approval of the thesis:

**PROPERTIES AND HYDRATION OF CEMENTITIOUS SYSTEMS
CONTAINING LOW, MODERATE AND HIGH AMOUNTS OF
NATURAL ZEOLITES**

submitted by **BURAK UZAL** in partial fulfillment of the requirements for the degree of **Doctor of Philosophy in Civil Engineering Department, Middle East Technical University** by,

Prof. Dr. Canan Özgen
Dean, Graduate School of **Natural and Applied Sciences**

Prof. Dr. Güney Özcebe
Head of Department, **Civil Engineering**

Assoc.Prof. Dr. Lutfullah Turanlı
Supervisor, **Civil Engineering Dept., METU**

Prof. Dr. Hayrettin Yücel
Co-Supervisor, **Chemical Engineering Dept., METU**

Examining Committee Members:

Prof. Dr. Ömer Z. Cebeci
Metalurgical and Materials Engineering Dept.,
Marmara University

Assoc. Prof. Dr. Lutfullah Turanlı
Civil Engineering Dept., METU

Prof. Dr. M. Cemal Göncüoğlu
Geological Engineering Dept., METU

Prof. Dr. Ali Çulfaz
Chemical Engineering Dept., METU

Prof. Dr. Mustafa Tokyay
Civil Engineering Dept., METU

Date: September 25, 2007

I hereby declare that all information in this document has been obtained and presented in accordance with academic rules and ethical conduct. I also declare that, as required by these rules and conduct, I have fully cited and referenced all material and results that are not original to this work.

Burak Uzal

Signature:

ABSTRACT

PROPERTIES AND HYDRATION OF CEMENTITIOUS SYSTEMS CONTAINING LOW, MODERATE AND HIGH AMOUNTS OF NATURAL ZEOLITES

Uzal, Burak

Ph.D., Department of Civil Engineering

Supervisor: Assoc. Prof. Dr. Lutfullah Turanlı

Co-Supervisor: Prof. Dr. Hayrettin Yücel

September 2007, 171 pages

The extent of the benefits provided by use of SCMs in cementitious systems increases as their percentage amounts in total binder increases. However, the proportion of SCMs in cementitious systems is limited, especially for natural pozzolans, by some factors such as increase in water requirement and decrease in rate of strength development. Therefore investigations are needed to increase the amount of natural pozzolans in blended cements or in concrete as much as possible without decreasing their performance. This aim requires studies on cementitious systems with more reactive natural pozzolans than widely-used ones.

The objective of the study was to investigate the pozzolanic activity of natural zeolites (clinoptilolite) from two localities in Turkey, and properties of cementitious systems containing low (15%), moderate (35%) and high (55%) amount of them.

The study covers characterization of the natural zeolites used, evaluation of their pozzolanic activity in comparison with some popular mineral admixtures, and properties of pastes, mortars, and concrete mixtures containing low, moderate, and high amounts of natural zeolites.

Reactivity of the natural zeolites with Ca(OH)_2 was found to be higher than those of the fly ash and the non-zeolitic pozzolan, but lower than that of the silica fume.

Natural zeolite blended cements were characterized with the following highlighted properties; faster setting than portland cement, low amounts of Ca(OH)_2 and capillary pores larger than 50 nm in hardened pastes, relatively dense microstructure of hardened paste than portland cement, more compatibility with melamine-based superplasticizer than being with naphthalene-based one, and excellent compressive strength performance.

Concrete mixtures containing natural zeolites as partial replacement for portland cement were characterized with the following properties; 7-day compressive strength of ~25 MPa and 28-day strength of 45-50 MPa with only 180 kg/m³ portland cement and 220 kg/m³ zeolite dosages (55% replacement), comparable modulus of elasticity with plain portland cement concrete, “low” and “very low” chloride-ion penetrability for low and large levels of replacement, respectively.

Keywords: Blended Cement, Concrete, Natural Pozzolan, Pozzolanic Activity, Zeolite

ÖZ

DÜŞÜK, ORTA VE YÜKSEK MİKTARLARDA DOĞAL ZEOLİT İÇEREN BAĞLAYICI SİSTEMLERİN ÖZELLİKLERİ VE HİDRATASYONU

Uzal, Burak

Doktora, İnşaat Mühendisliği Bölümü

Tez Yöneticisi: Assoc. Prof. Dr. Lutfullah Turanlı

Yardımcı Tez Yöneticisi: Prof. Dr. Hayrettin Yücel

Eylül 2007, 171 sayfa

İlave bağlayıcı malzemelerin katkılı çimentolardaki veya betondaki miktarları arttıkça, bu malzemelerin kullanımıyla sağlanan yararların büyüklüğü de artmaktadır. Ancak ilave bağlayıcı malzemelerin bağlayıcı sistemlerdeki miktarı, özellikle doğal puzolanlar için, su ihtiyacındaki artış ve dayanım kazanma hızındaki azalma gibi faktörler tarafından kısıtlanmaktadır. Bundan dolayı katkılı çimentolarda veya betonda kullanılan doğal puzolan miktarını, performans kaybı olmaksızın mümkün olduğu kadar artırmak amacıyla araştırmalar gerekmektedir. Bu amaç yaygın olarak kullanılan doğal puzolanlardan daha reaktif doğal malzemeleri içeren bağlayıcı sistemler üzerinde çalışılmasını gerektirmektedir.

Bu çalışmanın amacı, Türkiye'deki iki farklı rezervden temin edilmiş doğal zeolitlerin (klinoptilolit) puzolanik aktivitelerini ve bu zeolitlerden düşük (%15 ikame), orta (%35 ikame) ve yüksek (%55 ikame) düzeyde içeren bağlayıcı

sistemlerin özelliklerinin araştırılmasıdır. Çalışma, doğal zeolitlerin karakterizasyonunu, puzolanik aktivitelerinin diğer yaygın kullanılan mineral katkıları ile karşılaştırmalı olarak değerlendirilmesini, ve düşük, orta ve yüksek düzeyde zeolit içeren çimento hamuru, harç ve beton karışımlarının özelliklerini kapsamaktadır.

Doğal zeolitlerin Ca(OH)_2 ile olan reaktivitelerinin, uçucu küllün ve zeolitik olmayan puzolanın reaktivitelerinden daha yüksek, silis dumanının reaktivitesinden ise bir miktar düşük olduğu tespit edilmiştir.

Doğal zeolit içeren katkılı çimentolar şu önemli özellikleri ile karakterize edilmişlerdir; portland çimentosundan daha hızlı priz, sertleşmiş hamurlarda düşük Ca(OH)_2 miktarı ve düşük miktarda 50 nm'den büyük gözenekler, portland çimentosu hamuruyla karşılaştırıldığında göreceli olarak yoğun mikro yapı, naftalin bazlı akışkanlaştırıcıya kıyasla melamin-bazlı akışkanlaştırıcı ile daha iyi uyumluluk, ve çok iyi basınç dayanımı performansı.

Portland çimentosunun belirli miktarlarda doğal zeolite ile ikamesi yoluyla hazırlanan beton karışımları şu özellikleri ile karakterize edilmişlerdir; sadece 180 kg/m^3 portland çimentosu ve 220 kg/m^3 zeolit dozajı ile (%55 ikame) 7. günde ~25MPa, 28.günde 45-50 MPa basınç dayanımı, normal portland çimentosu betonu ile karşılaştırılabilir ölçüde elastik modül değeri, düşük ve yüksek ikame oranları için sırasıyla “düşük” ve “çok düşük” klor iyon geçirgenliği.

Anahtar Kelimeler: Beton, Doğal Puzolan, Katkılı Çimento, Puzolanik Aktivite, Zeolit.

To My Parents

ACKNOWLEDGEMENT

I wish to express my sincere gratitude to my supervisor Assoc. Prof. Dr. Lutfullah Turanlı and co-supervisor Prof. Dr. Hayrettin Yücel for their perfect assistance guidance, recommendations and support throughout this research and preparation of this thesis.

I would also like to thank Prof. Dr. M. Cemal Göncüođlu, Prof. Dr. Mustafa Tokyay, and Prof. Dr. Ali ulfaz for their suggestions and comments.

I would like to thank Res. Assist. Fatih Bektas, Res. Assist Raci Bayer, and Dr. Mustafa Sahmaran for their contributions.

The technical assistance of Mr. Cuma Yıldırım, Mr. Ali Sümbüle, Mr. Ali Yıldırım, Mr. Harun Koralay are gratefully acknowledged.

Finally, I would like to express my deepest gratitude to my wife, Mrs. Nimet Uzal, and to my family for their endless patience, encouragements, and all kind of supports during this study.

This study was supported by The Scientific and Technological Research Council of Turkey (TUBITAK) Project No:104M393.

The measurements of particle size distribution by laser diffraction, thermal analysis, and mercury intrusion porosimetry were conducted by METU Central Laboratory.

TABLE OF CONTENTS

ABSTRACT.....	iv
ÖZ.....	vi
DEDICATION.....	viii
ACKNOWLEDGEMENTS.....	ix
TABLE OF CONTENTS.....	x
LIST OF TABLES.....	xiv
LIST OF FIGURES.....	xvi
LIST OF ABBREVIATIONS.....	xxii
LIST OF CEMENT CHEMISTRY ABBREVIATIONS.....	xxiii
CHAPTER	
1. INTRODUCTION.....	1
1.1 General.....	1
1.2 Objectives and Scope.....	3
2. THEORETICAL BACKGROUND AND LITERATURE REVIEW.....	5
2.1 Introduction.....	5
2.2 Natural Zeolites.....	5
2.3 Pozzolanic Reaction.....	8
2.3.1 Strength of lime-pozzolan mixes.....	12
2.4 Blended Portland Cements Containing Pozzolans.....	13
2.4.1 Hydration of pozzolan-containing cements.....	14
2.4.2 Microstructure of blended cement pastes.....	18
2.5 Cementitious Systems Containing Natural Zeolites.....	22

2.5.1 Pozzolanic activity of natural zeolites.....	23
2.5.2 Properties of blended cement pastes containing natural zeolites..	25
2.5.3 Properties of blended cement mortars containing natural zeolites	28
2.5.4 Properties of concretes containing natural zeolites.....	33
3. EXPERIMENTAL STUDY.....	35
3.1 Introduction.....	35
3.2. Materials.....	36
3.2.1 Portland cement.....	36
3.2.2 Natural zeolites.....	37
3.2.2.1 Chemical composition of the natural zeolites.....	39
3.2.2.2 Mineralogical/petrographical characterization of the natural zeolites.....	42
3.2.2.3 Morphology of the natural zeolites.....	44
3.2.2.4 Physical properties of the finely ground natural zeolites.....	45
3.2.3 Other pozzolanic materials used for comparison purposes.....	47
3.2.4 Superplasticizers.....	51
3.2.5 Hydrated limes.....	51
3.2.6 Aggregates.....	51
3.3 Experimental Methods.....	52
3.3.1 Test methods for pozzolanic activity evaluation.....	52
3.3.1.1 Thermal analysis of lime-pozzolan pastes.....	53
3.3.1.2 Electrical conductivity of lime-pozzolan-water suspensions..	54
3.3.1.3 Compressive strength of lime-pozzolan pastes.....	56
3.3.1.4 Mercury intrusion porosimetry on lime-pozzolan pastes.....	57
3.3.1.5 Strength activity index.....	57
3.3.2 Test on zeolite blended cement pastes and mortars.....	58
3.3.2.1 Normal consistency and setting time.....	60
3.3.2.2 Free Ca(OH) ₂ content of the pastes.....	60
3.3.2.3 XRD analysis of the hardened pastes.....	60
3.3.2.4 Mercury intrusion porosimetry of the hardened cement	61

pastes.....	
3.3.2.5 SEM/EDX.....	61
3.3.2.6 Superplasticizer requirement and compressive strength of mortars.....	62
3.3.3 Tests on zeolite concrete mixtures.....	63
3.3.3.1 Mixture proportions.....	63
3.3.3.2 Preparation and casting of test specimens.....	64
3.3.3.3 Tests on hardened concretes.....	65
4. RESULTS AND DISCUSSIONS.....	66
4.1. Pozzolanic Activity.....	66
4.1.1. Ca(OH) ₂ depletion in lime-pozzolan pastes.....	66
4.1.2. Electrical conductivity of lime-pozzolan-water suspensions....	71
4.1.3. Compressive strength of lime-pozzolan pastes.....	75
4.1.4. Pore size distribution of lime-pozzolan paste.....	79
4.1.5. Strength activity index.....	82
4.1.6. Overall evaluation on pozzolanic activity of the natural zeolites	84
4.2 Properties and Hydration of Zeolite Blended Cements.....	85
4.2.1 Normal consistency and setting time.....	85
4.2.2 Free Ca(OH) ₂ content of the hardened cement pastes.....	92
4.2.3 Pore size distribution of the hardened cement pastes.....	95
4.2.4 XRD examinations of hardened cement pastes.....	99
4.2.5 BS-SEM examinations of hardened cement pastes.....	106
4.2.6 Superplasticizer requirement and compressive strength of mortars.....	115
4.3 Properties of Zeolite Concrete Mixtures.....	126
4.3.1 Properties of fresh concrete.....	126
4.3.2 Compressive strength and splitting-tensile strength.....	128
4.3.3 Modulus of elasticity.....	131
4.3.4 Chloride-ion penetration resistance (ASTM C 1202).....	132

5. CONCLUSIONS AND RECOMMENDATIONS	134
REFERENCES.....	139
APPENDICES	
A. TGA PLOTS FOR LIME-POZZOLAN PASTES.....	147
B. TGA PLOTS FOR HARDENED CEMENT PASTES.....	158
CIRRICULUM VITAE.....	169

LIST OF TABLES

TABLES

Table 2.1 Annual natural zeolite production in some countries.....	7
Table 2.2 Porosity of cement pastes containing natural zeolite	28
Table 2.3 Compressive strength of zeolite/fly ash/bottom ash blended cement mortars	31
Table 3.1 Chemical composition and physical properties of PC	36
Table 3.2 Oxide composition of the natural zeolites determined by various techniques	39
Table 3.3 Trace element contents of the natural zeolites used in the study	40
Table 3.4 Reactive SiO ₂ content of the natural zeolites	42
Table 3.5 Summary of mineralogical-petrographical analysis report for the natural zeolites.....	43
Table 3.6 Physical properties of the finely ground natural zeolites.....	46
Table 3.7 Chemical composition and physical properties of the pozzolanic materials	48
Table 3.8 Reactive SiO ₂ content of the pozzolanic materials	49
Table 3.9 Gradation data of the aggregate groups.....	52
Table 3.10 Mixture proportions for strength activity test mortars	58
Table 3.11 Notation and composition of the cements	59
Table 3.12 Mixture proportions of the concrete mixtures.....	64
Table 4.1 Strength activity indices (SAI) of the pozzolanic materials.....	82
Table 4.2 Free Ca(OH) ₂ contents of the cement pastes	92
Table 4.3 Superplasticizer dosages of blended cement mortars for NS and MS.....	116
Table 4.4 Compressive strength of mortars	119

Table 4.5 Proportions of the concrete mixtures	126
Table 4.6 Properties of fresh concrete.....	127
Table 4.7 Compressive and splitting-tensile strengths of the hardened concrete mixtures.....	128

LIST OF FIGURES

FIGURES

Figure 2.1 Compressive strength versus combined calcium hydroxide for lime-pozzolan pastes	12
Figure 2.2 Compressive strength versus surface area of hydration products for lime-pozzolan pastes	13
Figure 2.3 X-ray diffractograms of hydrated blended cement pastes	17
Figure 2.4 Pore size distributions of hydrated cement pastes	20
Figure 2.5 BEI of blended cement paste cured for 1 year at (A) 10°C and (B) 60°C.....	21
Figure 2.6 Classification of pozzolans	23
Figure 2.7 Water demand of zeolitic and non-zeolitic pozzolans	26
Figure 2.8 Effect of metal nitrates on the setting time of zeolite-containing cementitious systems	26
Figure 2.9 Ca(OH) ₂ content of cement pastes in relation to zeolite addition and age	27
Figure 2.10 Effect of addition of mordenite and clinoptilolite types zeolites on compressive strength of blended cement mortars in relation to volcanic glass blended cements	30
Figure 2.11 Compressive strength of clinoptilolite blended cements for various replacement levels	32
Figure 3.1 Particle size distribution of PC as determined by laser diffraction...	37
Figure 3.2 Bulk form of Gördes zeolite (GZ).....	38
Figure 3.3 Bulk form of greenish fraction of Bigadiç zeolite (BZ-A).....	38

Figure 3.4 XRD diffraction pattern of Gördes zeolite and two fractions of Bigadiç zeolite	43
Figure 3.5 SEM micrographs of Gördes zeolite sample (bulk from before grinding) in different magnifications	44
Figure 3.6 SEM micrographs of Bigadiç zeolite sample (bulk form before grinding).....	45
Figure 3.7 Particle size distributions of the finely ground natural zeolites as determined by laser diffraction.....	46
Figure 3.8 Particle size distribution curves of the pozzolanic materials used for comparison purposes	49
Figure 3.9 XRD patterns and identified phases of the pozzolanic materials..	50
Figure 3.10 Conductivity measurement set-up	56
Figure 4.1 Amounts of reacted Ca(OH)_2 as percent of initially available Ca(OH)_2 content	68
Figure 4.2 Relationship between reactive SiO_2 content and Ca(OH)_2 consumption of the pozzolanic materials	70
Figure 4.3 Predicted vs. experimental 28-day lime consumption data plot...	71
Figure 4.4 Conductivity vs time and pH vs time plots for the pozzolan-water suspensions	72
Figure 4.5 Net relative losses in conductivity of lime-pozzolan-water suspensions	74
Figure 4.6 Compressive strength of lime-pozzolan pastes	76
Figure 4.7 Digital images of fractured surfaces of the lime-pozzolan pastes.	77
Figure 4.8 Relationship between the amount of reacted Ca(OH)_2 and compressive strength of lime-pozzolan pastes	78
Figure 4.9 Pore size distribution of lime-pozzolan pastes as determined by mercury intrusion porosimetry	79
Figure 4.10 Correlation between porosity and compressive strength of lime-pozzolan pastes (the paste with BZ excluded).....	81
Figure 4.11 Correlation between the amount of pores smaller than 100 nm and compressive strength (the paste with BZ excluded).....	81

Figure 4.12 Strength-to-percentage amount of reacted lime ratio for the lime-pozzolan pastes	85
Figure 4.13 Normal consistency and setting time of the cements	87
Figure 4.14 Relationship between surface area and water demand of the cements	88
Figure 4.15 Relationship between surface area and water demand of the cements	89
Figure 4.16 Relationship between surface area of blended cements their initial setting times for individual analyses of GZ and BZ blended cements.	90
Figure 4.17 Relationship between surface area of blended cements their final setting times for individual analyses of GZ and BZ blended cements ..	91
Figure 4.18 Ca(OH) ₂ content of GZ blended cements and PC (normalized to PC content).....	94
Figure 4.19 Ca(OH) ₂ content of BZ blended cements and PC (normalized to PC content).....	94
Figure 4.20 Pore size distributions of the cement pastes as determined by MIP.....	96
Figure 4.21 Effect of zeolite type and content on pore size distribution of the cement pastes at various ages	97
Figure 4.22 XRD pattern of hardened PC paste at 7 days and 28 days	100
Figure 4.23 XRD pattern of hardened GZ15 paste at 7 days and 28 days ...	101
Figure 4.24 XRD pattern of hardened GZ55 paste at 7 days and 28 days	102
Figure 4.25 XRD pattern of hardened BZ15 paste at 7 days and 28 days	103
Figure 4.26 XRD pattern of hardened BZ55 paste at 7 days and 28 days ...	104
Figure 4.27 BS- EM micrograph of 28-day old PC paste	107
Figure 4.28 EDX analysis and corresponding composition of unhydrated core of cement grain in PC paste	107
Figure 4.29 EDX spectrum and corresponding composition of the inner product surrounding the partially hydrated cement grain in PC paste	108
Figure 4.30 Back scattered SEM micrograph of 28-day old GZ15 paste	109

Figure 4.31 Partially reacted cement grain at 1500x magnification and its EDX analysis	109
Figure 4.32 Unreacted zeolite grain in GZ15 paste at 4000x magnification and its EDX analysis	111
Figure 4.33 BS-SEM image taken from 28-day old GZ55 paste at 500x magnification (Z: Unreacted zeolite grain).....	111
Figure 4.34 Unreacted zeolite particle in GZ55 paste at 4000x magnification.....	112
Figure 4.35 EDX spectrum and corresponding compositions of Point A and Point B.....	113
Figure 4.36 BS-SEM image taken from 28-day old BZ15 paste at 500x magnification.....	114
Figure 4.37 BS-SEM image taken from 28-day old BZ55 paste at 500x magnification.....	115
Figure 4.38 Effects of zeolite content and superplasticizer type on superplasticizer requirement of GZ and BZ blended cements	116
Figure 4.39 Effect of GZ content in blended cements on compressive strength of mortars (for LSWC).....	120
Figure 4.40 Effect of BZ content in blended cements on compressive strength of mortars (for LSWC).....	121
Figure 4.41 Strength performance of high-volume natural zeolite blended cements and high-volume non-zeolitic natural pozzolan blended cements ...	122
Figure 4.42 Compressive strength development of GZ and BZ blended cement mortars prepared with MS.....	124
Figure 4.43 Comparison of compressive strength development of zeolite blended cement mortars for LSWC and MC conditions.....	125
Figure 4.44 Compressive strength of the concrete mixtures.....	129
Figure 4.45 Modulus of elasticity of the concrete mixtures at 91 days.....	131
Figure 4.46 Total charged passed values as determined in accordance with ASTM C 1202.....	132

Figure A.1 TGA plot of the technical grade $\text{Ca}(\text{OH})_2$ used in pozzolanic activity studies.....	147
Figure A.2 TGA plot of Gördes zeolite (GZ).....	148
Figure A.3 TGA plot of Bigadiç zeolite (BZ).....	148
Figure A.4 TGA plot of the silica fume (SF).....	149
Figure A.5 TGA plot of the fly ash (FA).....	149
Figure A.6 TGA plot of the non-zeolitic natural pozzolan (NZP).....	150
Figure A.7 TGA plot of the GZ-lime paste at 3 days.....	150
Figure A.8 TGA plot of the GZ-lime paste at 7 days.....	151
Figure A.9 TGA plot of the GZ-lime paste at 28 days.....	151
Figure A.10 TGA plot of the BZ-lime paste at 3 days.....	152
Figure A.11 TGA plot of the BZ-lime paste at 7 days.....	152
Figure A.12 TGA plot of the BZ-lime paste at 28 days.....	153
Figure A.13 TGA plot of the SF-lime paste at 3 days.....	153
Figure A.14 TGA plot of the SF-lime paste at 7 days.....	154
Figure A.15 TGA plot of the SF-lime paste at 28 days.....	154
Figure A.16 TGA plot of the FA-lime paste at 3 days.....	155
Figure A.17 TGA plot of the FA-lime paste at 7 days.....	155
Figure A.18 TGA plot of the FA-lime paste at 28 days.....	156
Figure A.19 TGA plot of the NZP-lime paste at 3 days.....	156
Figure A.20 TGA plot of the NZP-lime paste at 7 days.....	157
Figure A.21 TGA plot of the NZP-lime paste at 28 days.....	157
Figure B.1 TGA plot of PC paste at 3 days.....	158
Figure B.2 TGA plot of PC paste at 7 days.....	159
Figure B.3 TGA plot of PC paste at 28 days.....	159
Figure B.4 TGA plot of GZ15 paste at 3 days.....	160
Figure B.5 TGA plot of GZ15 paste at 7 days.....	160
Figure B.6 TGA plot of GZ15 paste at 28 days.....	161
Figure B.7 TGA plot of GZ35 paste at 3 days.....	161
Figure B.8 TGA plot of GZ35 paste at 7 days.....	162
Figure B.9 TGA plot of GZ35 paste at 28 days.....	162

Figure B.10 TGA plot of GZ55 paste at 3 days.....	163
Figure B.11 TGA plot of GZ55 paste at 7 days.....	163
Figure B.12 TGA plot of GZ55 paste at 28 days.....	164
Figure B.13 TGA plot of BZ15 paste at 3 days.....	164
Figure B.14 TGA plot of BZ15 paste at 7 days.....	165
Figure B.15 TGA plot of BZ15 paste at 28 days.....	165
Figure B.16 TGA plot of BZ35 paste at 3 days.....	166
Figure B.17 TGA plot of BZ35 paste at 7 days.....	166
Figure B.18 TGA plot of BZ35 paste at 28 days.....	167
Figure B.19 TGA plot of BZ55 paste at 3 days.....	167
Figure B.20 TGA plot of BZ55 paste at 7 days.....	168
Figure B.21 TGA plot of BZ55 paste at 28 days.....	168

ABBREVIATIONS

ASTM	: American Society for Testing and Materials
BEI	: Backscatter electron image
BET	: Brunauer- Emmett- Teller method for surface area determination
BS-SEM	: Backscatter mode scanning electron microscopy
BZ	: Bigadiç zeolite
CEN	: The European Committee for Standardization
EDX	: Energy dispersive X-ray analysis
FA	: Fly Ash
FTIR	: Fourier Transform Infrared Spectroscopy
GZ	: Gördes zeolite
ICP	: Inductively Coupled Plasma
MIP	: Mercury intrusion porosimetry
NMR	: Nuclear Magnetic Resonance
NZP	: Non-zeolitic pozzolan
PC	: Portland cement
SAI	: Strength activity index
SBU	: Secondary building units
SCMs	: Supplementary cementing materials
SEM	: Scanning electron microscopy
SF	: Silica Fume
TGA	: Thermo-gravimetical analysis
TS EN	: Turkish Standards European Norms
w/c	: Water-to-cement ratio
w/cm	: Water-to-total cementitious materials ratio
XRD	: X-ray diffraction
XRF	: X-ray Fluorescence

CEMENT CHEMISTRY ABBREVIATIONS

C	: CaO
S	: SiO ₂
A	: Al ₂ O ₃
F	: Fe ₂ O ₃
H	: H ₂ O
\bar{S}	: SO ₃

CHAPTER 1

INTRODUCTION

1.1 General

The use of supplementary cementing materials (SCMs) such as fly ash, natural pozzolans, silica fume and ground granulated blast furnace slag in blended cements or in concrete has become unavoidable in recent years due to some benefits which are more important today than in the past. These benefits are energy saving and reduction in CO₂, which is a major greenhouse gas causing global warming, emitted during cement production. CO₂ emission related to portland cement production results from the calcination of raw materials and the fossil fuels used during clinker production. 1 ton of portland cement production results in the release of approximately 1 ton of CO₂ into atmosphere. The cement industry alone is responsible for about 7% of total CO₂ emission in the world [1].

Use of mineral admixtures to reduce the clinker content in portland cements results not only in an environment-friendly product but also provides many benefits to the properties of fresh and hardened concrete, such as improvement in workability, reduction in the heat of hydration, low permeability, high ultimate strength, and control of alkali-silica expansions, when compared to plain portland cement concrete.

The extent of the benefits provided by use of SCMs in cementitious systems increases as their percentage amounts in total binder increases. However, the percentage amount of SCMs in binders of cementitious systems is limited, especially for natural pozzolans, by some factors such as increase in water requirement and decrease in rate of strength development. The lower 28-day compressive strength of mortars made with blended cements containing large amounts of glassy-structure natural pozzolans, when compared to ordinary Portland cement, had been found to be a disadvantage of this kind of blended cements, although they show similar strength values at 91 days of age [2, 3, 4, 5]. Therefore further investigations are needed with relatively high reactive natural pozzolans to improve the properties of high-volume natural pozzolan blended cements.

Although fly ash, the by-product of thermal power plants, is a widely used SCM in concrete due to some advantages over other pozzolanic materials, natural pozzolans are still important alternatives as a SCM when a good quality fly ash is not readily available to use. Fly ashes produced by thermal power plants which are operated with old technologies are coarser and usually contain high carbon, and therefore they do not perform well in cementitious systems with respect to strength development, drying shrinkage and durability [6].

Natural zeolites are crystalline aluminosilicates which have a three dimensional framework consisting of silicon-oxygen (SiO_4) and aluminum-oxygen (AlO_4) tetrahedra [7]. They are considered as microporous adsorbent, ion exchanger, and catalyst and used in industrial, agricultural, and environmental applications [8]. Although it is known that they show considerable pozzolanic activity and they are commonly used as a SCM in some countries, especially in China, information on the properties and hydration of cementitious systems containing natural zeolites are limited [9-14]. Especially, published literature contains no reports on properties and hydration of cementitious systems containing large amounts (the amounts similar or higher than that of portland cement) of natural zeolites. One of the objectives of this dissertation study is to fulfill this need.

1.2 Objectives and Scope

The objective of the study was to investigate the pozzolanic activity of two Turkish natural zeolites, and properties of cementitious systems containing low, moderate and high amounts of them as a SCM. Specifically, properties and performance of blended cements and concrete mixtures containing high amounts of natural zeolites (the amount higher than that of portland cement) are the major concern of the study. The relatively high pozzolanic activity of natural zeolites, when compared to some other natural pozzolans, is one of the encouraging factors for studying on cementitious systems containing large volume of natural zeolites.

First of all, detailed characterization of natural zeolites obtained from two main zeolite deposits in Turkey, Manisa/Gördes and Balıkesir/Bigadiç, was done. Characterization of zeolite samples used in the study covers their chemical compositions including trace elements, mineralogical / petrographical analyses, and morphology as observed with scanning electron microscopy (SEM).

Pozzolanic activity of the natural zeolites ground to a certain fineness level was evaluated comparatively with respect to silica fume, fly ash and non-zeolitic natural pozzolan, which are mainly composed of glassy/amorphous phases. Activity of the materials was evaluated by various methods including; monitoring of calcium hydroxide depletion in lime-pozzolan pastes via thermal analysis of lime-pozzolan pastes, measurement of electrical conductivity change in lime-pozzolan-water systems, and compressive strength development of lime-pozzolan pastes. Water requirement and strength activity index (SAI) of the natural zeolites were also determined and compared to the other pozzolanic materials in order to evaluate the performance of zeolites for practical use.

So as to investigate the properties and hydration of blended cements containing low, moderate and high amounts of natural zeolites, blended cements were prepared with direct replacement of ordinary portland cement by 15%, 35%, and 55% finely

ground natural zeolites by weight. Totally six blended cements, three for each natural zeolite, were obtained as well as the reference portland cement and they were tested for their water demand, setting time, and free calcium hydroxide content of the hardened pastes. The hardened pastes of blended cements containing 15% and 55% natural zeolites were also examined for pore size distribution by mercury intrusion porosimetry (MIP), crystalline hydration products by X-ray diffraction analysis, and microstructure and chemistry of hydration products by backscatter scanning electron microscopy (BS-SEM) equipped with energy dispersive X-ray analysis (EDX). Compressive strengths of blended cement mortars were also determined for two different types of superplasticizer (a melamine-based and a naphthalene-based) and two different curing conditions (lime-saturated water curing and moist curing at 99% relative humidity).

Finally, the properties of concrete mixtures containing low (15% replacement), moderate (35% replacement), and high (55% replacement) amounts of natural zeolites as direct replacement for portland cement were determined. For 400 kg/m³ total cementitious materials dosage and 0.45 water-to-cementitious materials ratio (w/cm), the following properties of zeolite concrete mixtures were determined; superplasticizer requirement to provide a desired slump value, air content, setting time, compressive strength, splitting tensile strength, modulus of elasticity and resistance to chloride ion penetration. The results were evaluated comparatively with respect to two different ordinary concrete mixtures; a superplasticized mixture with a 0.45 water to cement ratio (w/c) and a non-superplasticized mixture made with a w/c required for providing a desired slump value.

CHAPTER 2

THEORETICAL BACKGROUND AND LITERATURE REVIEW

2.1 Introduction

In this chapter, theoretical background and literature review on pozzolanic activity of natural zeolites and their use in cementitious systems are presented. Firstly the definition and structure of natural zeolites as well as their types and classification are introduced. Thereafter, theoretical background on pozzolanic reaction and blended cements containing pozzolans are briefly presented from a general point of view. Finally a detailed literature review are made on the use of natural zeolites in cementitious systems, covering the topics on pozzolanic activity and properties of pastes, mortars and concretes containing natural zeolites.

2.2 Natural Zeolites

The first identification of zeolites was made by Cronstedt, a Swedish mineralogist, in 1756. The term “zeolite” created by Cronstedt from Greek words meaning “boiling stone” since zeolite minerals expel water when heated and hence seem to boil [15]. Zeolite group of minerals currently include more than 40 naturally occurring species, and is the largest group of silicate minerals [7]. Clinoptilolite, heulandite, analcime, chabazite, mordenite, and erionite are the most common types of natural zeolite minerals.

Zeolites are defined as natural or artificial crystalline aluminosilicates, which have a three dimensional framework consisted of silicion-oxygen (SiO_4) and aluminum-oxygen(AlO_4) tetrahedra. A zeolite is an aluminosilicate with a skeletal structure, containing voids occupied by ions and molecules of water having a considerable freedom of movement that leads to ion-exchange and reversible dehydration. The primary building unit of the zeolite framework is the tetrahedron, the center of which is occupied by a silicon or aluminum atom, with four oxygen atoms at the corners. Each oxygen atom is shared between two tetrahedra. Hence, the tetrahedra form a continuous framework. Substitution of Si^{4+} by Al^{3+} results in the negative charge on the framework, which is compensated my monovalent or divalent cations located together with water molecules in structural channels. Cations in the channels are easily substituted, and therefore they are termed “exchanged cations” unlike Si and Al which are not exchanged under ordinary conditions [7].

Currently, three different classification strategies are used for zeolites based upon the followings; a) framework topology, b) geometric arrangement of tetrahedra, c) properties (e.g. morphology) [16].

The first classification scheme is based on framework topology, which is indicated by a three-letter code. For instance, the framework for heulandite and clinoptilolite are identical, which are indicated by HEU three-letter code. Since heulandite was named before clinoptilolite, the priority is given for framework type naming. This kind of classification scheme is useful for those zeolite researchers whose major interests are in cation exchange and synthetic zeolites since these properties are related to framework topology [16].

The second method of classification for zeolites is based on geometric arrangement of tetrahedra, “secondary building units” (SBU). The primary building units for zeolites is the tetrahedron. SBUs are geometric arrangements of tetrahedra. According to this classification system, heulandite and clinoptilolite are in Group 7 minerals with $\text{T}_{10}\text{O}_{20}$, where T most commonly refers to Si or Al [16].

The third scheme of classification is similar to the SBU classification and based on morphology with the fact that SBUs tend to control the morphology of the zeolite. This scheme uses a combination of zeolite group names which have specific SBUs and is the most widely used by geologists [16].

Rock-forming zeolites such as clinoptilolite, analcime, mordenite, chabazite, heulandite are formed as a result of alteration of natural glass. Zeolitisation of porous ash-glass rocks (tuffs) is of regional importance [16].

Natural zeolite is a type of aluminosilicate mineral containing large quantities of reactive SiO₂ and Al₂O₃. General structural formula of zeolites is given as follows;



where M⁺ refers to a monovalent cation such as Na⁺ or K⁺, and M²⁺ refers to a divalent cation such as Mg²⁺, Ca²⁺, Ba²⁺ [8].

Zeolite-rich volcanic tuffs are widely distributed in almost every country of the world, where they are present in low-, medium-, or high-grade million-ton deposits. China, Japan, USA, Cuba, Turkey, Bulgaria are major countries in terms of deposits and/or annual production of natural zeolites [17]. Approximate amount of annual production of these countries are given in Table 2.1. The total worldwide natural zeolite production is approximately 3-3.5 million tons per year [18].

Table 2.1 Annual natural zeolite production in some countries [18]

Country	Annual Production
China	2,500,000 tons
Japan	450,000 tons
USA	46,000 tons
Cuba	38,000 tons
Greece	3,000 tons

Turkey has very rich natural zeolite deposits. It is estimated that the amount of total zeolite deposit in Turkey is approximately 50 billion tons. There is no detailed and reliable reserve information about natural zeolites covering all over the country. However, Manisa-Gördes region is a well-known clinoptilolite zeolite deposition area with approximately 2 billion tons of apparent reserve. Another natural zeolite deposit in Turkey is in Balıkesir-Bigadiç region with 500 million tons of reserve. Although Turkey has rich natural zeolite deposits, amount of production is very low with only 1000 tons when compared the worldwide values [19].

2.3 Pozzolanic Reaction

Pozzolans are inorganic materials, either natural or artificial, which have no cementitious value when contact with water, but harden in water when mixed with calcium hydroxide or with materials that can release calcium hydroxide (portland cement clinker). The term “pozzolanic activity” addresses all the reactions occurring in a lime-pozzolan-water system. In spite of the fact that this definition for pozzolanic activity seems to be cursory, it is acceptable from a technical and practical point of view. Since it is very difficult to observe the evolution of pozzolanic activity in terms of hydration products, the progress of pozzolanic reaction is commonly evaluated by depletion of the free calcium hydroxide in the system [20].

Pozzolanic activity refers not only the amount of lime fixed by a pozzolan but also the rate of lime fixation. Both factors are affected by quality and quantity of the active phases present in pozzolanic material. The heterogeneity of the materials and complexity of pozzolanic reaction do not allow modeling the pozzolanic activity, however, general agreements can be stated on the factors affecting the amount of combined lime in lime-pozzolan-water mixes. These are as follows [20];

1. the nature of the active phases,
2. content of active phases in pozzolan,

3. SiO₂ content of active phases,
4. the lime/pozzolan ratio of the mix,
5. curing time
6. the specific surface area (BET) of pozzolan
7. water/solid mix ratio
8. temperature

The last three ones are the factors governing the rate of lime fixation. These general factors are explicated in a detailed manner below [20].

1. Zeolitic pozzolans are regarded as more active than glassy ones. Within the zeolite minerals, harschelite and clinoptilolite are considered to be more reactive than analcime. The glasses of different pozzolans may exhibit different lime fixation ability.
2. The higher the amount of active phases and the lower the content of inert or crystalline phases, the larger the amount of combined lime.
3. The amount of reactive SiO₂ which varies between 45% and 75% in natural pozzolans and in fly ash whereas exceeds 95% in amorphous microsilica such as silica fume. In addition, the other chemical species are effective in determining pozzolanic activity.
4. Generally speaking, the amount of combined lime increases with the increasing lime/pozzolan ratio.
5. The amount of combined lime also depends on the age of lime-pozzolan mixtures.
6. The short term pozzolanic activity is essentially associated with the specific surface area (BET) of pozzolan, whereas the long-term activity seems to be attributed to the chemical and mineralogical composition of pozzolan. The reaction rate of pozzolanic materials is proportional to the square of the specific surface area.
7. The higher the content of water in mix, the higher the rate of lime fixation.
8. The rate of pozzolanic reaction increases with temperature

The reaction of pozzolan-lime mixes result in formation of compounds which are similar to products of Portland cement hydration, such as poorly crystalline calcium silicate hydrate (C-S-H)* gel. Generally, different types of pozzolans produce the same silicate and aluminate hydrates, but the amount rather than the nature of the hydrated phases varies depending on the type of pozzolan. By extending the duration of pozzolanic reaction, besides hexagonal calcium aluminate and calcium silicate hydrate, some other compounds are recognizable: carboaluminate, gehlenite hydrate and hydrogarnet [20].

The C/S ratio of C-S-H is variable and seems to depend on the type of pozzolan, the time and the temperature of curing as well as the lime/pozzolan ratio. For instance, C/S ratio of C-S-H varied between 0.75-0.87 for an opal-based pozzolan whereas it is significantly higher, between 1.35 and 1.75, for a glassy pozzolan. The variability of the C/S gel ratio can be attributed to the non-stoichiometry of the C-S-H, depending on chemical composition of the pore solution [20].

As a result of pozzolanic reaction of low-lime fly ashes, SO_4^- contained dissolves in lime water and after a certain period causes ettringite and gypsum to precipitate. In addition, C-S-H, C_4AH_{13} and C_2SH_8 and sometimes carboaluminate as well are formed. The presence of quartz (from fly ash) and calcite (by carbonation) in the mix can prevent the XRD determination of C-S-H [20].

Limited data on the pozzolanic reaction of silica fume with $\text{Ca}(\text{OH})_2$ is available on the published literature. The reaction is very rapid and causes a phase to precipitate on SiO_2 particles as a high-silica hydrated layer. This layer is unstable and turns into C-S-H very quickly. In pastes of normal consistency, due to the high reactivity of silica fume, free lime is almost completely consumed generally between 7 and 28 days and in some cases even sooner. Therefore it shows up earlier than in natural pozzolans and fly ashes. The resulted C-S-H is much more crystalline than in C-S-H formed from hydration of Portland cement [20].

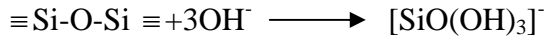
* see the list of cement chemistry abbreviations

The mechanism of pozzolanic reaction can be summarized briefly as follows [21] (see the cement chemistry abbreviations for abbreviated chemical formulas);

- When a lime-pozzolan blend is mixed with water, Ca(OH)_2 in the blend hydrolyses first and the solution reaches a high pH value very quickly:



- Under the attack of OH^- in such a high pH solution, network modifiers, such as Ca^{2+} , K^+ , Na^+ , etc., in the pozzolan are dissolved into the solution very quickly.
- Silicate or aluminosilicate network formers in the pozzolan are also depolymerized and dissolved into the solution. However, a larger fraction of network modifiers are dissolved into the solution than network formers due to the lower bond energy of network modifiers.
- Depolymerized monosilicate and aluminate species enter the solution as follows



- When Ca^{2+} ions contact these dissolved monosilicate and aluminate species, C-S-H and calcium aluminate hydrate C_4AH_{13} form
- In the presence of sulfate ions $\text{C}_6\text{A}\bar{\text{S}}_3\text{H}_{32}$ forms first. Since the SO_3 content of the natural pozzolan is low, $\text{C}_6\text{A}\bar{\text{S}}_3\text{H}_{32}$ transforms to $\text{C}_4\text{A}\bar{\text{S}}\text{H}_{12}$ very quickly.
- Since the dissolution of aluminosilicate glass is the slowest process during the initial pozzolanic reaction, it determines the total pozzolanic reaction rate.
- After a certain period, the surface of pozzolan particles is covered by precipitated hydration products, then the further reaction is controlled by the diffusion of OH^- and Ca^{2+} through the precipitated products and into the inner side of precipitated products. The later hydration is no longer a solution precipitation reaction but a topochemical reaction.
- A rise in curing temperature does not affect the hydration process, but the hydration rate.

2.3.1 Strength of lime-pozzolan mixes

The practical and technical evaluation of pozzolanic materials is commonly evaluated by measuring the strength of lime-pozzolan mix (or Portland cement-pozzolan mix), although depletion of $\text{Ca}(\text{OH})_2$ in lime-pozzolan pastes is a good measure monitoring the pozzolanic activity. Strength of a lime-pozzolan system increases as the amount of fixed lime increases. However, there is no general correlation between the two parameters, when considering different pozzolanic materials, as shown in Figure 2.1. The monitoring of lime depletion is only a useful tool in explaining the hardening process of pozzolanic systems. In this regard a typical example is the behavior of clay-based materials which, despite their ability to fix lime, do not harden appreciably [20].

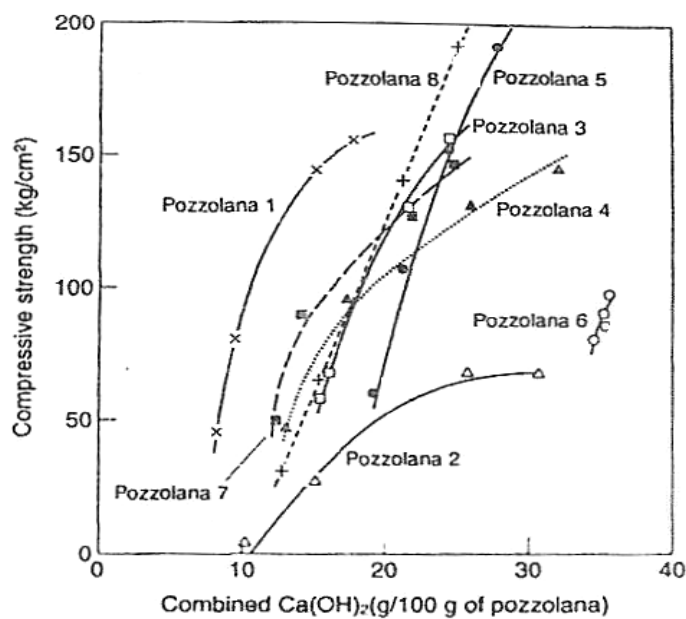


Figure 2.1 Compressive strength versus combined calcium hydroxide for lime-pozzolan pastes [20]

There is a general correlation between compressive strength and specific surface area of the hydration products as shown in Figure 2.2. Lime/pozzolan ratio and fineness of pozzolan are the other factors influencing the strength of lime-pozzolan pastes. Up to a certain limit, the strength increases with increasing lime/pozzolan

ratio, but beyond the limit, it decreases. A good linear correlation has been found between the Blaine fineness of a natural pozzolan and the compressive strength of 20:80 lime-pozzolan mix. The positive effect of the fineness on the strength is more distinct at early ages when compared to late ages [20].

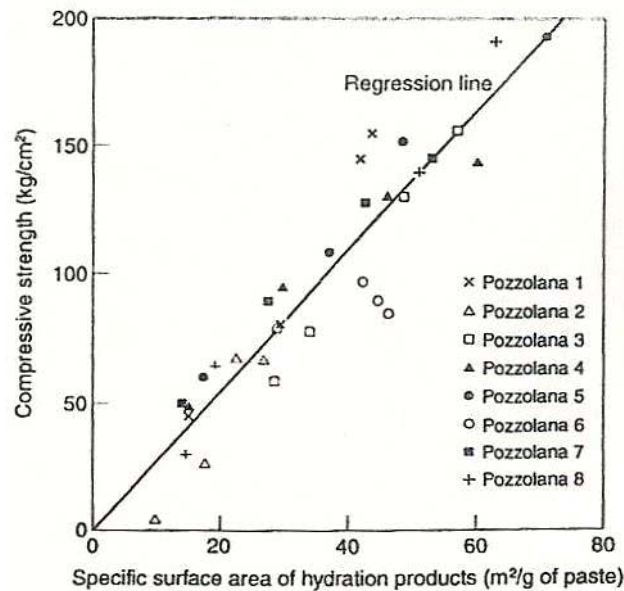


Figure 2.2 Compressive strength versus surface area of hydration products for lime-pozzolan pastes [20]

2.4 Blended Portland Cements Containing Pozzolans

Blended cements are the cements containing not only portland cement but also pozzolanic material(s) as well. Their production and use has been increased in recent years due to benefits such as low energy requirement during production and positive effects on properties of cementitious systems such as improvement in workability, reduction in the heat of hydration, low permeability, high ultimate strength, and increased durability.

Production of Portland cement is not only energy-intensive but also not environment-friendly process due to release of significant amount of CO₂ which is one of the major greenhouse gases. Therefore use of blended cements, instead of plain portland cement, provides reduction in greenhouse gas emission related to cement industry. The role of blended cements in the reduction of emission of greenhouse gases associated with cement industry have become crucial since the adverse effects of global warming on climatic change in the world are obviously observed in recent years.

In principle, pozzolan can be added to Portland cement either at the cement plant or at the building site. In the first case, pozzolan is interground together with clinker and gypsum or separate grinding followed by mixing and homogenization with suitable equipment. In the latter case, pozzolan is added with Portland cement into the concrete mixer [20].

2.4.1 Hydration of pozzolan-containing cements

The kinetics of Portland cement hydration is modified by pozzolan even at the first stages of the process and its influence is revealed by changes occurring in;

- heat of hydration
- Ca(OH)₂ content
- combined water content
- degree of hydration of alite
- degree of reaction of pozzolan [20] .

Some of the above are explained briefly below.

Heat of hydration: The determination of the rate of heat evolution is a sensitive method recording the changes induced by pozzolan in the early hydration of cement up to 3-7 days. The effect of pozzolan on the heat evolved by hydrating cement becomes clearer when the measured parameters are referred not to the whole

system formed by clinker + gypsum + pozzolan, but only to the Portland cement fraction [20].

In rate of heat evolution vs. time curve for the cements containing natural pozzolans, the dormant period is shortened and the height of the main peak is increased. This results in an accelerated rate of clinker hydration. The acceleration induced by natural pozzolans has not yet been exhaustively explained by experimental evidence [20].

The cumulative heat of hydration which is released by the blended cement accounts for the overall reactions occurring during hydration. It depends on the height and the width of the main peak of the heat evolution curve. The total heat released from blended cements in the first 2 days of hydration is always lower than that of the control Portland cement, but it is generally higher when referred to the amount of Portland cement fraction. This indicates that pozzolanic materials in blended cements accelerate the hydration of the Portland cement fraction [20].

Shannag and Yeginobali investigated the effects of natural pozzolan addition on the heat of hydration of blended cements (measured by heat of solution method) and they concluded that the pozzolanic addition caused almost linear reduction on the 7 days heat of hydration of pozzolanic portland cements [22].

Ca(OH)₂ content: The presence of pozzolan changes the ordinary course of the hydration of cements. Therefore the Ca(OH)₂ content depends not only on the degree of hydration of clinker, but also on the progress of the pozzolanic reaction, the composition of the hydrates and of the mix, the type of pozzolan, the temperature, the water/cement ratio, the pozzolan/clinker ratio, etc. The Ca(OH)₂ content of blended cements is lower when it is referred to the cement as a whole, but it is higher when it is referred to the Portland cement fraction for the blended cements containing various amounts of fly ash. [20].

Mehta reported that the 11, 20, and 25 percent of the available Ca(OH)_2 was consumed by the pozzolanic reactions in the 1-year old pastes of the blended cements containing 10, 20, 30% natural pozzolan (Santorin earth) , respectively. Mehta also showed that the depletion of Ca(OH)_2 in blended cement pastes can be observed clearly by their XRD patterns indicating reduced intensity of Ca(OH)_2 peaks as shown in Figure 2.3 [23].

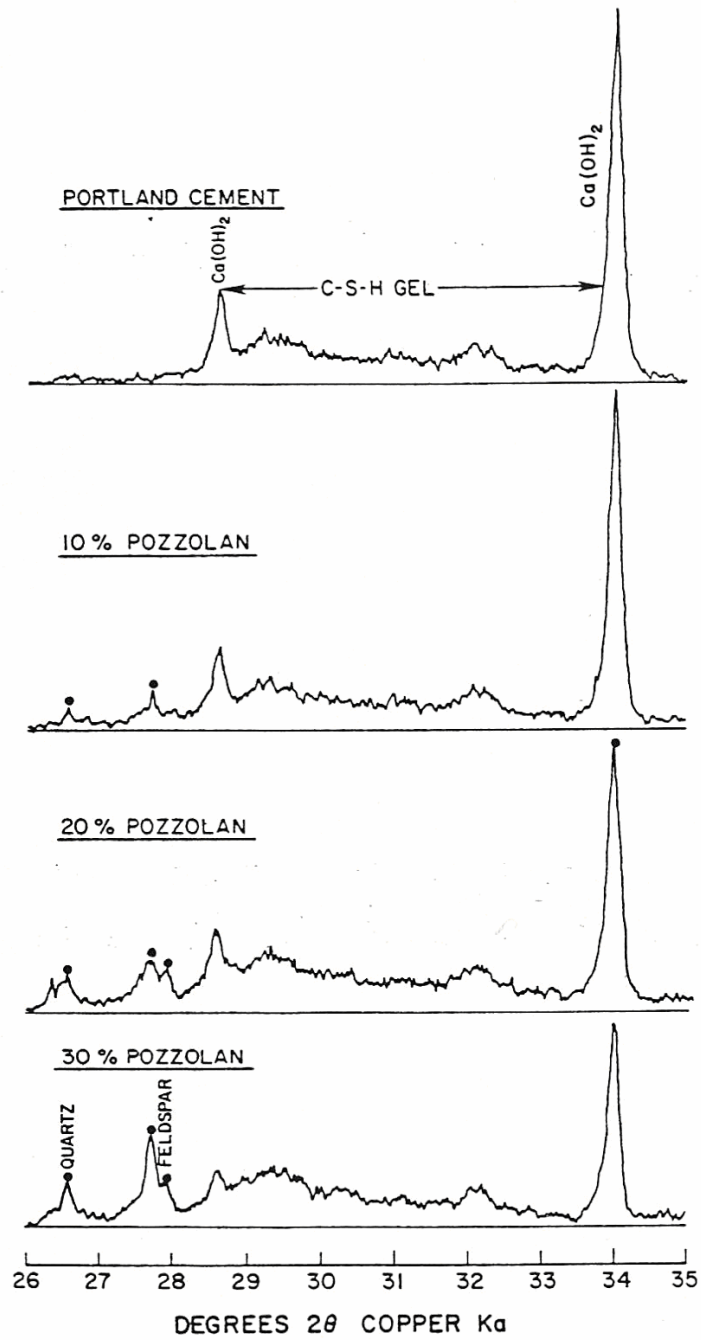


Figure 2.3 X-ray diffractograms of hydrated blended cement pastes [23]

Bound water: The degree of hydration of Portland cement is commonly estimated by determining the non-evaporable water content of the paste, that is, the weight

loss occurring in dried specimens heated between 105 and 1000 °C. Non-evaporable water includes inputs from all the products of hydration, and thus from calcium hydroxide too. By subtracting the water bound in Ca(OH)_2 from non-evaporable water, the content of water that is chemically combined in silicates and aluminates hydrates is obtained. Due to the modifications caused by pozzolanic materials in the amount of the different hydrates, as well as in their chemical composition, the determination of non-evaporable water is far from being useful in determining the degree of hydration of blended cements. Also, for the case of chemically combined water, the variability in composition of the phases does not allow a good estimate of the degree of hydration to be obtained. Nevertheless, comparison of the results obtained from the blended and the reference Portland cements indicates the differences in the hydration process of these two types of cement [20].

The contents of non-evaporable and bound water in fly ash cement pastes are lower than in the parent portland cement, but are higher if they are referred to the Portland cement fraction [20].

2.4.2 Microstructure of blended cement pastes

Morphology of the paste

The first microstructural outcome of hydration of blended cements is the early formation of shells of hydration products, typically $\sim 1\mu\text{m}$ thick and composed mainly of C-S-H, around the clinker grains. Ettringite as thin needles, monosulfate thin plates and Ca(OH)_2 crystals can also be observed. After a while, C-S-H fibers project outward, coating the shells and making them appear blurred. [20].

Mehta studied the microstructural morphology of the blended cement pastes by scanning electron microscopy (SEM) on the blended cements containing various amounts of natural pozzolan (Santorin earth). Scanning electron micrographs of the 28-days old specimens containing 20% and 30% pozzolan showed large areas

occupying aggregation of Ca(OH)_2 crystals, however, such areas were relatively small in the 1-year old specimens [23].

Porosity and pore size distribution of blended cement pastes

Porosity is an intrinsic property of cement paste which can be limited but not eliminated completely. It mainly influences the strength and permeability of cement pastes, mortars and concretes. The pore size distribution, not the total porosity, actually controls the strength, permeability, and volume changes in a hardened cement paste. Generally large pores influence mostly the compressive strength and permeability whereas small controls mostly the drying shrinkage and creep behavior of hardened cementitious systems [20].

The porosity of the pastes typically decreases by decreasing the water/cement ratio and increasing the curing period. Porosity also increases with increasing curing temperature; the difference mostly concerns the volume of large pores [20].

The correct determination of porosity and/or pore size distribution of cement-based materials is an important but difficult to achieve. Difficulties are mainly caused by structural changes occurring during sample preparation. The correct determination of porosity requires the complete removal of water from the pores before measurement. Water removal can be provided by different procedures such as oven drying, vacuum drying, freeze drying, and solvent replacement techniques [24].

Each drying technique may result in different pore size distribution data. Measuring technique is another factor influencing the measured data. Mercury intrusion porosimetry (MIP) is a commonly-used method for examination of hardened cementitious systems, especially for comparison studies, although there are many controversial issues related to its use in determination of pore size distribution of hardened pastes [24-32].

Total porosity of blended cement pastes is generally higher than that of the reference portland cement paste when the measurement is carried out by mercury intrusion porosimetry [20].

Mehta investigated the pore size distribution of natural pozzolan blended cement pastes by MIP technique for various amounts of pozzolan replacement, and he obtained the distribution data shown in Figure 2.4, which is divided into pore volumes $<45 \text{ \AA}$, $45\text{-}500 \text{ \AA}$, $500\text{-}1000 \text{ \AA}$, and $>1000 \text{ \AA}$. He found some evidence that only large pores (larger than 1000 \AA or perhaps 500 \AA) adversely affect the strength and permeability of the cement pastes, whereas the pores $< 500 \text{ \AA}$ may be associated with the microporous cementitious hydrates. He also concluded that monitoring of the pore refinement process, i.e. the conversion of $>1000 \text{ \AA}$ pores to $<1000 \text{ \AA}$ pores, in hydrating blended cements offers the most useful technique for direct evaluation of activity of a pozzolan and the potential improvement in performance characteristics associated with pozzolanic reaction [23].

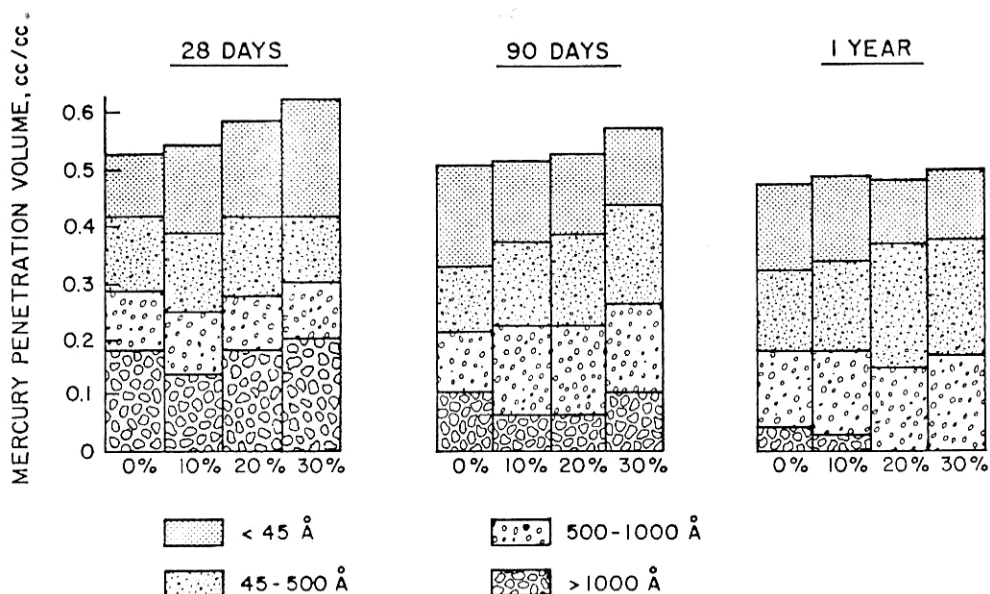


Figure 2.4 Pore size distributions of hydrated cement pastes [23]

Microstructure

Escalante-Garcia and Sharp investigated the chemical composition and microstructure of hydration products in blended cements for two different curing temperatures, 10°C and 60°C, by using SEM and EDX analysis techniques. They have reported that the composition of inner product C-S-H, product rim surrounding a partially hydrated cement grain, shifted towards higher Si and Al but lower Ca contents in blended cement pastes when compared to neat portland cement paste. They have also reported that the microstructure of the blended cement pastes cured at 60°C showed greater apparent porosity than those cured at 10°C (Figure 2.5) [33].

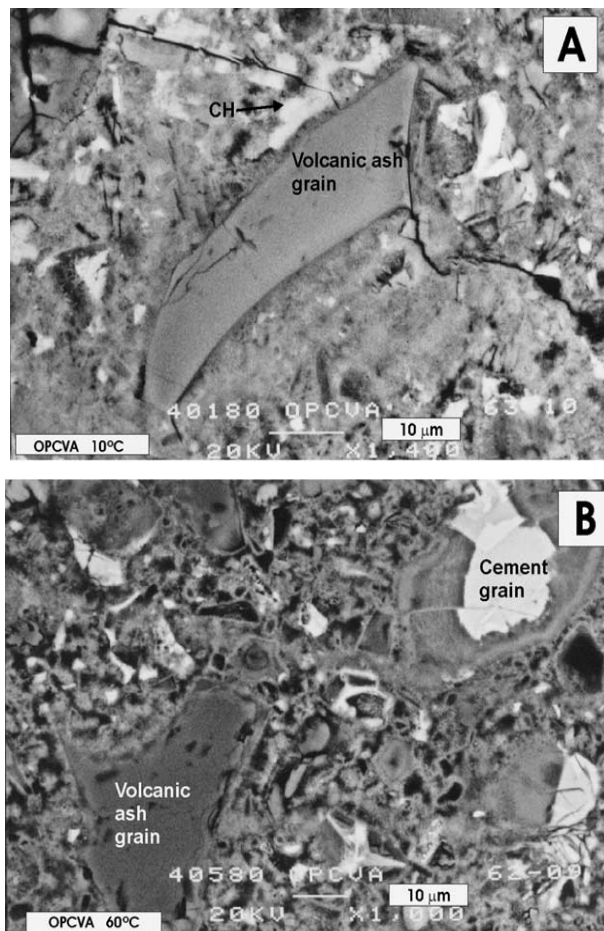


Figure 2.5 BEI of blended cement paste cured for 1 year at (A) 10°C and (B) 60°C [33]

2.5 Cementitious Systems Containing Natural Zeolites

Zeolitic tuffs have been utilized in construction industry since ancient times, mostly as dimension stone. However some other types of applications in construction industry have become popular, such lightweight aggregate or as blending component in cement industry.

Information is limited on the use of natural zeolites as addition to cement, because the utilization of zeolitic tuff as a pozzolanic material is rather recent and is widespread only in those locations in which other pozzolanic materials, such as natural pozzolan, fly ash, silica fume, etc., are not readily available [17].

It is interesting to note that the industry of the largest zeolite consumption in China is cement production. Zeolite has also been applied as a mineral admixture for concrete production during more than ten years in China. China Concrete Association has put forward a technical recommendation to promote the applications of natural zeolite in the construction industry. Presently, the annual consumption of natural zeolite in China is over 30 million tons [34].

According to Massazza's classification of pozzolans, zeolitized tuffs are categorized as coherent rocks (altered) in group of pyroclastic rocks (Figure 2.6). Pyroclastic rocks occurs as result of explosive volcanic eruptions which project minute particles of melted magma into the atmosphere. The deposits of volcanic pozzolans are often associated with compact layer (tuffs) which originate from weathering and cementation of loose particles by diagenetic or other natural processes. Weathering can cause zeolitization (transformation of glass of pozzolan into zeolitic minerals) or argillation (transformation of glass of pozzolan into clay minerals). The degree of transformation depends on the intensity of the diagenetic actions and on their duration as well. Zeolitization improves pozzolanic properties, whereas argillation reduces the pozzolanic activity. [20]. Mehta and Malhotra state that zeolitic minerals in finely ground condition show pozzolanic behavior since

they react with $\text{Ca}(\text{OH})_2$ by a base-exchange (cation exchange) process to form cementitious products [35].

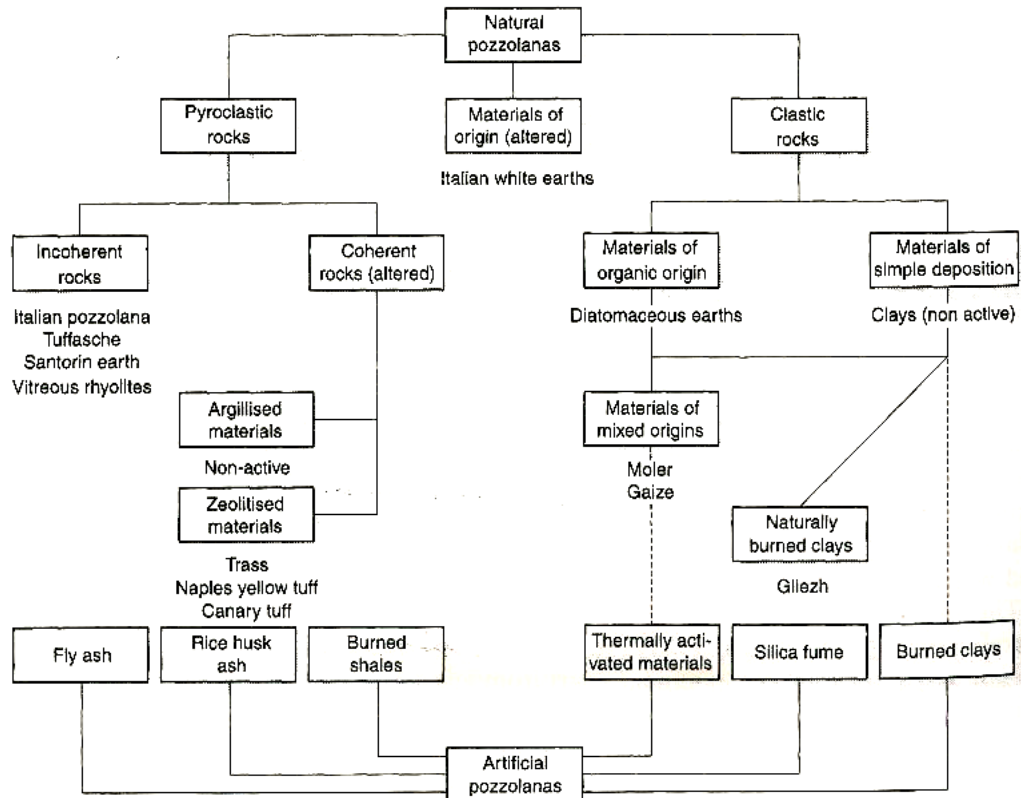


Figure 2.6 Classification of pozzolans [20]

2.5.1 Pozzolanic activity of natural zeolites

It is known that zeolitized tuff exhibits excellent pozzolanic activity. This behavior has been exploited, unconsciously, since at least the beginning of 1900s. Blended portland cements containing 25% of a natural pozzolan from Tehachapi, California, later recognized as a clinoptilolite-rich tuff, were used in 1912 for the construction of the 386-km-long Los Angeles aqueduct. Zeolitized tuffs have also been used, beginning in the first decades of the 20th century, for producing commercial blended cements, e.g. in USA, in the Canary Islands, and in Germany. At the end of 1950s, many tuffs were recognized to contain zeolites. Studies were then initiated on the pozzolanic properties of zeolites by Sersale in 1960 [17].

Drzaj et al. investigated the kinetics and mechanism of reaction between zeolitic tuff and lime in water solutions at increased temperature (65 °C), by means of X-Ray diffraction and SEM. They defined the reaction mechanism as consecutive diffusion-controlled topochemical reactions, and the initial period of reactions consist of diffusive dissolution of zeolite and portlandite ($\text{Ca}(\text{OH})_2$). They also concluded that the final product, tobermorite, is formed by heterogeneous nucleation on the solid (C-S-H)-liquid (solution) interface [9].

Sersale compared the zeolitic tuffs from Italy, Germany and Spain with a typical non-zeolitic pozzolan by a standard test method for measuring pozzolanic activity. According to this method, proposed by Fratini and then accepted as European Standard EN 196/5, mixtures of Portland cement clinker (65%) and pozzolanic material (35%) are mixed with distilled water (solid/liquid ratio=1/50) at 40 °C for 8 days. At the end of the experiment, Ca^{2+} and OH^- concentrations in the contact solution are measured and reported in a plot of the lime solubility vs. alkalinity. The lower the Ca^{2+} concentrations the higher the amount of lime fixed by the pozzolanic material. Sersale determined that all of the zeolitic tuffs tested displayed better pozzolanic behavior than the non-zeolitic pozzolan, which indicates that zeolitization of the original glassy pozzolan does not reduce its capacity to fix lime. On the contrary, it increases the reactivity of the aluminosilicate framework [10, 17].

Ortega et al. studied on $\text{Ca}(\text{OH})_2$ -clinoptilolite zeolite mixes as an alternative solidification binder system for treating industrial wastes, and they focused on the effects of $\text{Ca}(\text{OH})_2$ addition, clinoptilolite particle size, curing time and curing temperature on compressive strength and microstructure of the resulted binder. They reported that optimizing each of these factors produced compacted materials containing 20% $\text{Ca}(\text{OH})_2$ by weight with average compressive strength of 38.7 MPa. XRD analysis showed that $\text{Ca}(\text{OH})_2$ is consumed during curing and that is not present in high strength, fully cured materials. SEM analysis combined with energy-dispersive X-Ray (EDX) indicated the formation of hydration products with

Ca/Si ratio in the range 0.8-1.2 and that a significant amount of unreacted clinoptilolite remained in optimized materials [12].

Blanco Varela et al. recently investigated the characterization and pozzolanic activity of two different zeolitic tuffs from Cuban deposits and they showed that both rocks, which are characterized as clinoptilolite and faujasite type zeolitic tuffs, have pozzolanic activity. They reported that the reaction rate with $\text{Ca}(\text{OH})_2$ was found to be much higher for the clinoptilolite type zeolitic tuff than for the faujasite-type tuff. They related the results with particle size distribution and reactive SiO_2 content of the materials [11].

Martinez Ramirez et al. investigated the reaction products resulted from pozzolanic reaction of Cuban zeolites, as the second part of their study [9], and they reported that pozzolanic reaction of both zeolitic tuffs resulted in formation of C-S-H gel, whereas there was no indication of formation of hydrated calcium aluminates in the results of XRD (X-ray Diffraction), FTIR (Fourier Transform Infrared Spectroscopy), NMR (Nuclear Magnetic Resonance) analysis [36].

2.5.2 Properties of blended cement pastes containing natural zeolites

Faragoulis et al. investigated the effects of clinoptilolite and mordenite type zeolitic tuff additions on water demand and setting time of the blended cement pastes, and compared the results with those of a glassy natural pozzolan. They determined that the water demand of the clinoptilolite-type zeolitic tuff was higher than that of the mordenite-type, whereas the water demand of volcanic glass pozzolan is lower than the zeolitic tuffs (Figure 2.7). They associated the highest water demand of the clinoptilolite-type zeolitic tuff with porous structure of clinoptilolite mineral. For both types of natural zeolites, setting time of the blended cement pastes delayed with increasing zeolite content [37].

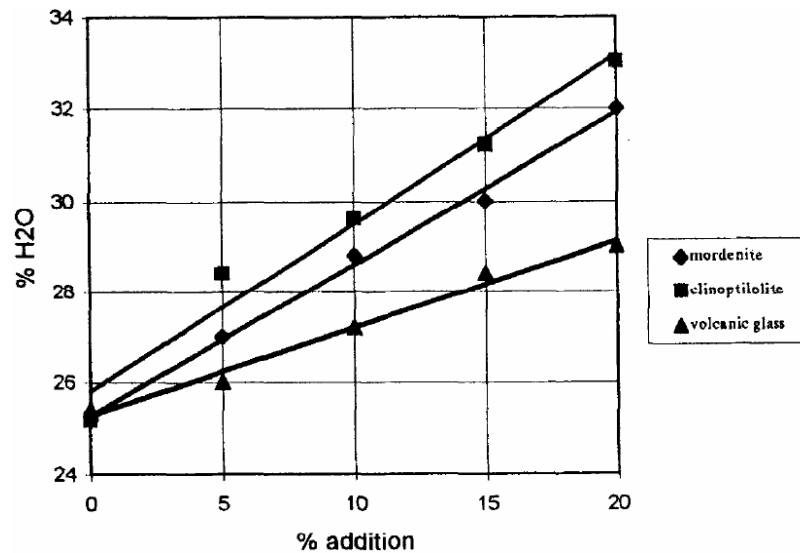


Figure 2.7 Water demand of zeolitic and non-zeolitic pozzolans [37]

Gervais and Ouki studied the effect of metal nitrate contaminants on the setting time of zeolite-containing cementitious systems for use in stabilization/solidification of wastes. It was reported that setting time was accelerated in presence of chromium, while in presence of manganese, lead and zinc it was delayed. However, for the last two contaminants, 10% replacement of portland cement by zeolite markedly accelerated the setting time compared to cement-only matrix (Figure 2.8) [38].

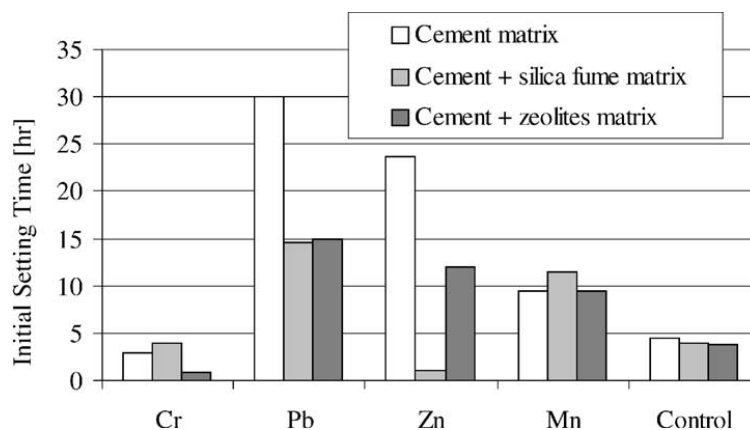


Figure 2.8 Effect of metal nitrates on the setting time of zeolite-containing cementitious systems [38]

Perraki et al. investigated the effect of incorporation of natural zeolite, which is characterized as heulandite, on the hydration rate and products in pastes samples. They reported that the examined zeolite has a good pozzolanic activity, and its incorporation in cement contributes to the consumption of $\text{Ca}(\text{OH})_2$ formed during the cement hydration and the formation of cement-like hydrated products. They also determined that the highest degree of $\text{Ca}(\text{OH})_2$ consumption was for 10% zeolite replacement by weight, and the increase of the zeolite content does not seem to promote the consumption of $\text{Ca}(\text{OH})_2$ for any further (Figure 2.9) [14].

Poon et al. studied the degree of pozzolanic reaction and porosity of natural zeolite blended cement pastes in comparison with silica fume and fly ash. They concluded that the clinoptilolite-type natural zeolite used in the study is a pozzolanic material, with a reactivity between that of silica fume and fly ash. They also reported that in the pastes with a higher water-to-cementitious materials ratio and lower cement replacement level it undergoes a higher degree of reaction. In addition, it was reported that 15% zeolite replacement resulted in lower porosity at all ages, when compared to reference Portland cement paste; however, the porosity of the paste was higher than that of the control sample for 25% replacement (Table 2.2) [13].

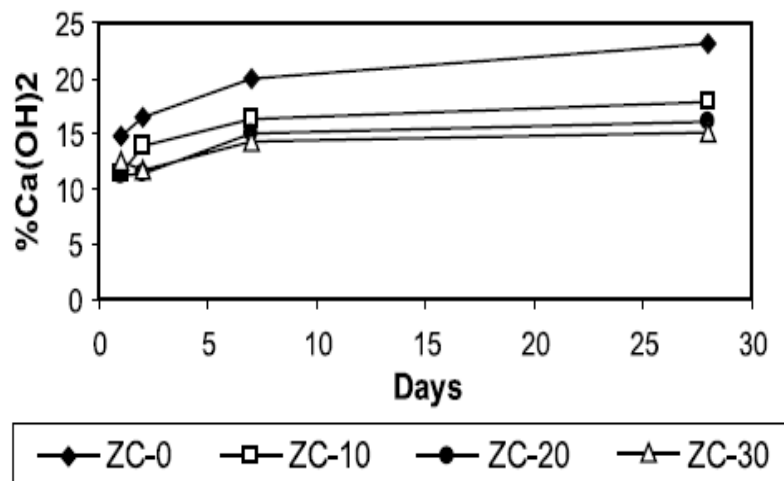


Figure 2.9 $\text{Ca}(\text{OH})_2$ content of cement pastes in relation to zeolite addition and age [14].

Table 2.2 Porosity of cement pastes containing natural zeolite [13]

Mix		Mercury porosity (%)				
W/CM	% zeolite	3 days	7 days	28 days	90 days	180 days
0.25	0	12.44	12.32	10.61	9.15	8.72
	15	12.21	12.19	10.10	9.03	8.15
	25	15.22	13.21	12.03	10.04	9.07
0.30	0	12.89	12.64	11.25	9.74	9.25
	15	12.62	12.34	10.45	9.36	8.42
	25	15.69	13.72	12.36	10.28	9.34

Relating to compressive strength of blended cement pastes, Poon et al. reported that zeolite in cement pastes with a lower water/cementitious materials ratio contributes more to the strength of the pastes when compared to relatively high w/cm (water-to-total cementitious materials ratio). Comparing the zeolite blended cement pastes with fly ash blended cements, it was reported that natural zeolite replacement resulted in less compressive strength reduction at early ages, however, lower strength improvement at the later ages [13].

2.5.3 Properties of blended cement mortars containing natural zeolites

Sersale investigated the compressive strength performance of natural zeolite blended cements on mortar specimens, comparatively with respect to a typical natural pozzolan, for various replacement levels ranged between 0% and 40%. Zeolite blended cement mortars exhibited higher compressive strength values when compared to the blended cement containing a typical natural pozzolan, especially at later ages [17].

Kasai et al. reported the compressive strength performance of blended cements containing clinoptilolite and mordenite type-zeolites comparatively with respect to fly ash and silica fume blended cements. Clinoptilolite-type zeolite exhibited higher

strength values than mordenite-type and required less water to obtain the same workability. In general, the strength of the clinoptilolite containing mortars was lower than that of the reference standard mortars at early ages but comparable at 28 days [17].

Fragoulis et al. compared the strength performance of blended cements containing clinoptilolite-type and mordenite-type natural zeolites as well as blended cements containing volcanic glass, for various replacement levels ranging between 0% and 20%. The results indicated that the addition of small quantities (5%) of these materials to cement improves early strength. On the contrary, when more than 10% is added, a significant reduction is observed on the 28-day compressive strength in all blended cement mortars. In general, cement containing mordenite tuff and volcanic glass resulted in better results than the blended cement containing clinoptilolite (Figure 2.10) [37].

Canpolat et al. investigated the effects of zeolite, coal bottom ash and fly ash replacements on the compressive strength of blended cement mortars. They concluded that the inclusion of zeolite up to level of 15% resulted in an increase in compressive strength at early ages, but resulted in a decrease in compressive strength when used in combination with fly ash (Table 2.3) [39].

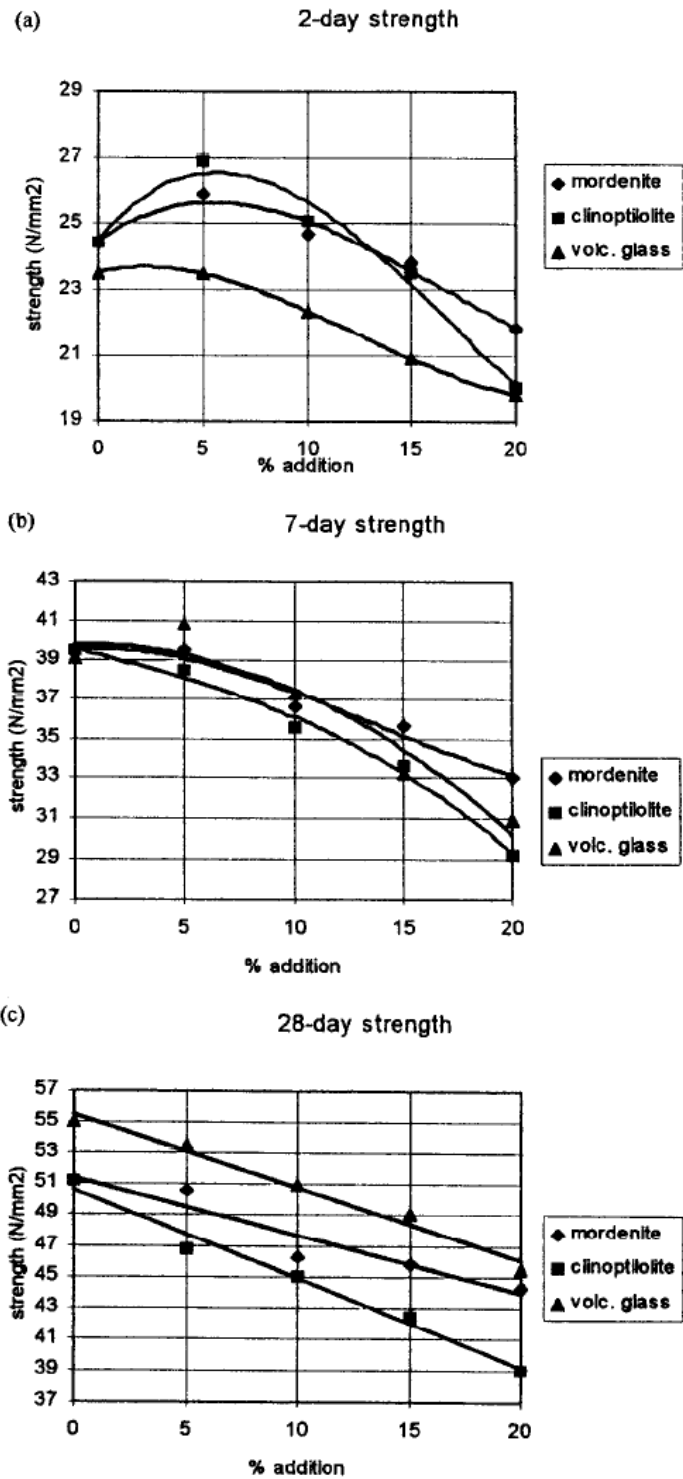


Figure 2.10 Effect of addition of mordenite and clinoptilolite types zeolites on compressive strength of blended cement mortars in relation to volcanic glass blended cements [37].

Table 2.3 Compressive strength of zeolite/fly ash/bottom ash blended cement mortars [39]

Symbol	Cement mixtures	Compressive strength (N/mm ²)			
		2 days	7 days	28 days	90 days
R	Reference mix	21.2	34.4	45.1	57.6
	PC 42.5	(47)	(76)	(100)	(128)
A ₁	5% Z+	25.2	38.6	52.5	55.7
	95% PC	(56)	(86)	(116)	(124)
A ₂	10% Z+	23.5	36.8	51.3	53.6
	90% PC	(52)	(82)	(114)	(119)
A ₃	15% Z+	22.1	33.5	52.8	56.8
	85% PC	(49)	(74)	(117)	(126)
A ₄	20% Z+	17.8	30.7	54.2	58.5
	80% PC	(39)	(68)	(120)	(130)
A ₅	25% Z+	14.2	25.6	49.8	57.2
	75% PC	(31)	(57)	(110)	(127)
A ₆	30% Z+	13.4	26.8	47.8	58.5
	70% PC	(30)	(59)	(106)	(130)
A ₇	35% Z+	11.7	22.2	46.2	53.5
	65% PC	(26)	(49)	(102)	(119)
B ₁	5% Z+5%	20.8	29.6	49.5	56.2
	FA+90% PC	(46)	(66)	(110)	(125)
B ₂	10% Z+5%	19.4	33.8	51.4	58.7
	FA+85% PC	(43)	(75)	(114)	(130)
B ₃	15% Z+5%	17.8	28.4	51	59.4
	FA+80% PC	(39)	(63)	(113)	(132)
B ₄	20% Z+5%	15.4	26.2	50.8	60.8
	FA+75% PC	(34)	(58)	(113)	(135)
B ₅	25% Z+5%	14.4	27.3	50.8	58.3
	FA+70% PC	(32)	(61)	(113)	(129)
B ₆	30% Z+5%	11.8	24.2	47.6	54.3
	FA+65% PC	(26)	(54)	(106)	(120)
B ₇	35% Z+5%	9.6	23.1	43.3	50.4
	FA+60% PC	(21)	(51)	(96)	(112)
C ₁	5% Z+5%	20.5	33.8	53.6	61.3
	BA+90% PC	(45)	(75)	(119)	(136)
C ₂	10% Z+5%	18.5	33.4	54.1	58.4
	BA+85% PC	(41)	(74)	(120)	(129)
C ₃	15% Z+5%	15.5	29.6	52.7	57.9
	BA+80% PC	(34)	(66)	(117)	(128)
C ₄	20% Z+5%	13.9	26.8	48.9	56.7
	BA+75% PC	(31)	(59)	(108)	(126)
C ₅	25% Z+5%	13.7	26.6	50.2	54.1
	BA+70% PC	(30)	(59)	(111)	(120)
C ₆	30% Z+5%	11.6	24.1	46.8	51.3
	BA+65% PC	(26)	(53)	(104)	(114)
C ₇	35% Z+5%	11.9	21.9	45.6	48.9
	BA+60% PC	(26)	(49)	(101)	(108)
	TS 12142-	≥ 10	-	42.5-	-
	TS 12144			62.5	
	TS 26-	≥ 10	>21.0	>32.5	-
	TS 10156				

Values inside parentheses show the percentages with respect to the 28-day compressive strength of PC 42.5.

More recently, Yilmaz et al. investigated the compressive strength of blended cements containing clinoptilolite-type natural zeolite in various levels ranging from 5% to 40% by weight. They reported that the 28-day strength values of mortars up to 20% replacement level were higher than the reference Portland cement; however 28-day strength of the mortar prepared with blended cement containing 40% zeolite was lower than that of the reference (Figure 2.11). They associated the reduction in strength with the lack of sufficient $\text{Ca}(\text{OH})_2$ in the medium despite an increase in zeolite content [40]

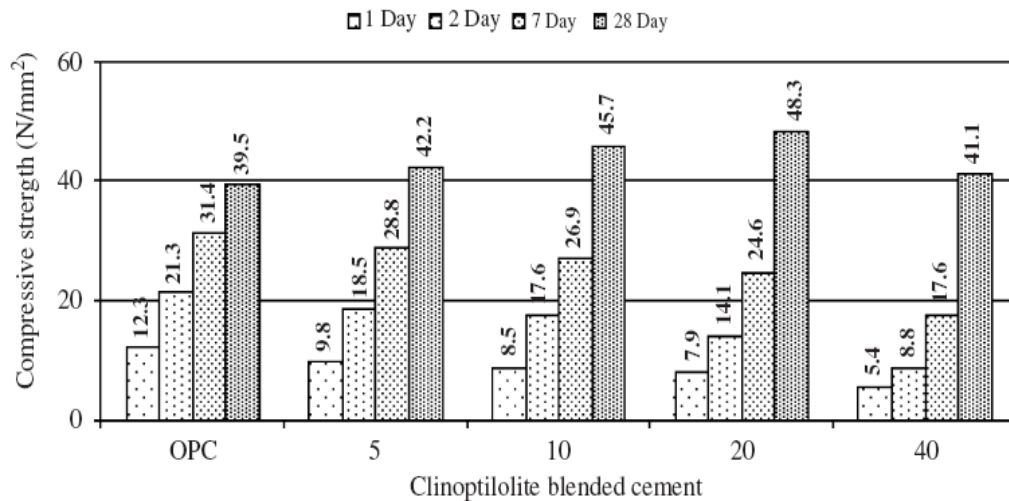


Figure 2.11 Compressive strength of clinoptilolite blended cements for various replacement levels [38]

Yilmaz et al. also investigated the microstructure of zeolite blended cement mortars by SEM/EDX. They observed that the microstructure of 7 days old mortar prepared with blended cement containing 20% zeolite consist of more complex shapes and voids than reference Portland cement paste, and this resulted in crystal structures to grow in every direction, which explains the strength performance of 20% zeolite blended cement [40].

2.5.4 Properties of concrete containing natural zeolites

The published literature contains very limited data on properties of concrete mixtures containing natural zeolites.

Feng et al. [32] reported the effect of zeolite as a strength increasing admixture for concrete. They used a Japanese natural zeolite characterized as containing 60% clinoptilolite, and reported that concrete replaced by 10% zeolite showed 10-15% higher compressive strength at 28 days when compared to the reference concrete. They also reported the following conclusions;

- Increasing the fineness of zeolite powder was considered to be ineffective to improve the compressive strength of concrete. Therefore the optimum average particle size of zeolite powder seems to be 6 μm .
- The highest compressive strength value was determined for 10% replacement. 15% and 20% replacement levels were considered to be ineffective to improve the strength performance of concrete [41].

Chan and Ji investigated the initial surface absorption and chloride diffusion of high performance concrete mixtures containing natural zeolite, comparatively with silica fume and fly ash concrete mixtures. They reported that zeolite addition decreased bleeding and increased marginally the viscosity of concrete without significantly compromising the slump. At 15% replacement level, it resulted in 14% increase in 28-day compressive strength when compared to the control concrete. The results also showed that there existed an optimum replacement level for zeolite to provide reduction in initial surface adsorption and in chloride diffusion of concrete. The natural zeolite performed better than fly ash but was inferior to silica fume in terms of increasing strength, decreasing initial surface adsorption and chloride diffusion [42].

Feng et al. studied on the chloride permeability of concrete containing ultrafine mineral powders of silica fume, natural zeolite and granulated blast furnace slag by

using ASTM C 1202 standard method. They concluded that the charge passed of concrete with ultrafine mineral powders is obviously lower than that of the reference concrete, and the order of reducing the charge passes is silica fume > fly ash > natural zeolite > ground blast furnace slag [43].

In published literature, there are a lot of papers on suppression effect of natural zeolite addition on alkali-silica reaction in concrete [44, 48]. Feng and Hao explained the mechanism of zeolite powder in preventing alkali-silica reaction as decreasing the alkaline ion concentration in pore solution of concrete through ion-exchange, adsorption and pozzolanic reaction of zeolite powder, so the formation of alkali-silica gel is prevented [49].

CHAPTER 3

EXPERIMENTAL STUDY

3.1 Introduction

The objective of the study is to evaluate the pozzolanic activity of natural zeolites from two main deposits in Turkey, and to determine the properties and hydration characteristics of zeolite containing systems; pastes, mortars and concrete mixtures. In order to attain these objectives, the experimental study was organized in three main parts;

- a) Pozzolanic activity of the zeolites,
- b) Properties and hydration characteristics of zeolite blended cements containing low, moderate and high volume of natural zeolites,
- c) Properties of concrete mixtures containing low, moderate and high volume of the natural zeolites.

In this chapter, materials and experimental methods used in the study are presented.

3.2 Materials

3.2.1 Portland cement

An ordinary portland cement CEM I 42.5R was used in all blended cements and concrete mixtures prepared in the study. Chemical composition and physical properties of the portland cement (PC) are given in Table 3.1. In addition, its particle size distribution was also determined by laser diffraction technique using Malvern Mastersizer 2000 analyzer and shown in Figure 3.1.

Table 3.1 Chemical composition and physical properties of PC

Chemical Composition		
SiO ₂ , %	19.94	
Al ₂ O ₃ , %	5.34	
Fe ₂ O ₃ , %	3.72	
CaO, %	63.02	
MgO, %	2.44	
SO ₃ , %	2.95	
Na ₂ O, %	0.52	
K ₂ O, %	0.81	
Loss on ignition, %	1.02	
Insoluble residue, %	0.51	
Physical Properties		
Specific gravity	3.03	
Blaine fineness, m ² /kg	313	
Initial setting time, min	140	
Final setting time, min	205	
Compressive strength, MPa		
	3 days	26.8
	7 days	33.5
	28 days	51.1

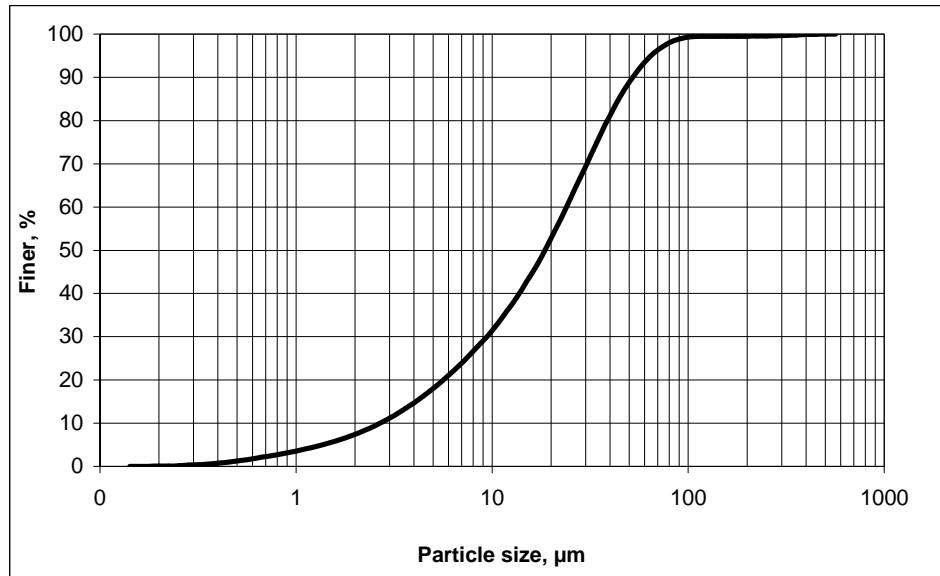


Figure 3.1 Particle size distribution of PC as determined by laser diffraction

3.2.2 Natural zeolites

The natural zeolites were obtained from two main deposits in Turkey, Manisa/Gördes and Balıkesir/Bigadiç.

Gördes zeolite was obtained as two batches in particle sizes of 0-1 mm, 1-4mm, 4-7 mm and 15-80 mm. The batch in 0-1 mm size range was used for obtaining finely ground zeolite powders whereas the batch in 15-80 mm size range was used for geological characterization studies. Preliminary analysis showed that there is no considerable difference between chemical compositions of two batches.

Bigadiç zeolite was obtained in a bulk form consisting of a wide range of particle sizes in 15-150 mm. In order to obtain finely ground form of Bigadiç zeolite for use in the study, representative samples taken from the main batch was crushed, and the particles smaller than 1.6 mm were used in grinding process.

Visual inspection of the zeolites indicated that Gördes zeolite is uniform in color (white) whereas Bigadiç zeolite has different color fractions; mainly greenish and

whitish (Figure 3.2 and Figure 3.3). Therefore BZ was sampled for geological characterization as two different fractions, greenish (notated as Bigadiç zeolite-A) and whitish (Bigadiç zeolite-B) in order to observe possible differences in their characterizations. Visual inspection of the Bigadiç zeolite batch indicated that percentage ratio of greenish: whitish fraction is approximately 85:15.



Figure 3.2 Bulk form of Gördes zeolite (GZ)



Figure 3.3 Bulk form of greenish fraction of Bigadiç zeolite (Bigadiç zeolite-A)

Detailed characterization of the zeolites was made by different techniques, mineralogy/petrography, and microstructure inspected by scanning electron microscopy (SEM).

3.2.2.1 Chemical composition of the natural zeolites

Chemical composition of the natural zeolites was determined by three different techniques, namely wet chemical analysis (WCA), X-ray fluorescence (XRF) and Inductively Coupled Plasma (ICP), for cross-checking. Major oxide compositions of the natural zeolites are given in Table 3.2 for each analysis technique. For detailed characterization of the natural zeolites used in the study, trace element composition of the natural zeolites was also determined by ICP technique and the results are given in Table 3.3. It should be noted that chemical composition of two color fractions of Bigadiç zeolite seems to be similar.

Table 3.2 Oxide composition of the natural zeolites determined by various techniques

<i>Compound</i>	Gördes Zeolite			Bigadiç Zeolite-A			Bigadiç Zeolite-B		
	WCA	XRF	ICP	WCA	XRF	ICP	WCA	XRF	ICP
SiO ₂	68.88	71.7	69.32	70.92	70.1	66.05	68.08	70.2	64.47
Al ₂ O ₃	12.82	11.9	11.35	11.31	11.2	11.04	11.40	11.9	11.23
Fe ₂ O ₃	1.43	2.5	1.28	3.04	2.3	1.08	1.06	1.9	1.19
CaO	2.71	1.9	1.72	4.96	3.5	3.71	4.72	3.3	3.56
MgO	0.73	n.a.	0.82	1.08	n.a.	0.96	2.88	n.a.	1.40
SO ₃	0.09	n.a.	n.a.	0.19	n.a.	n.a.	0.24	n.a.	n.a.
Na ₂ O	0.53	0.8	0.95	0.18	0.2	0.19	0.15	0.2	0.13
K ₂ O	3.71	4.4	3.96	1.88	2.6	1.75	1.76	2.7	2.24
TiO ₂	n.a.	n.a.	0.09	n.a.	n.a.	0.06	n.a.	n.a.	0.07
LOI	8.9			11.0			10.4		

n.a.: not analyzed

Table 3.3 Trace element contents of the natural zeolites used in the study

Element	Content, ppm		
	Gördes Zeolite	Bigadiç Zeolite-A	Bigadiç Zeolite-B
Ba	170.9	276.8	322.9
Be	3	3	3
Co	1.1	<.5	<.5
Cs	23.1	41.2	35.3
Ga	11.6	12.9	13.3
Hf	3.5	4.1	3.8
Nb	12.1	13	15
Rb	146.6	111.9	149.9
Sn	3	4	4
Sr	259.4	4595	7346.8
Ta	1.2	1.4	1.5
Th	31	31.3	33.3
U	6	5.8	8.2
V	14	8	10
W	1.3	0.3	0.8
Zr	92.2	88.7	81.5
Y	15.6	17.3	11.3
La	28.3	23.5	21.2
Ce	56.8	44.6	40.4
Pr	6.37	5.33	5.03
Nd	22.8	20.8	18.9
Sm	4.2	4	3.7
Eu	0.35	0.23	0.19
Gd	3.05	3.37	3.02
Tb	0.59	0.66	0.51
Dy	3.08	3.53	2.7
Ho	0.56	0.61	0.49

Table 3.3 Trace element contents of the natural zeolites
used in the study (Continued)

Element	Content, ppm		
	Gördes Zeolite	Bigadiç Zeolite-A	Bigadiç Zeolite-B
Er	1.57	1.71	1.33
Tm	0.25	0.27	0.21
Yb	1.67	1.88	1.4
Lu	0.28	0.27	0.18
Mo	2.1	0.1	<.1
Cu	4	1.6	2.2
Pb	40.8	17.3	7.9
Zn	26	28	33
Ni	7.1	1	4.9
As	10.4	19.9	2.7
Cd	0.1	0.1	<.1
Sb	0.3	0.9	0.2
Bi	0.3	0.3	0.3
Ag	<.1	<.1	<.1
Au	1	0.8	0.7
Hg	<.01	<.01	0
Tl	0.4	0.7	0.8
Se	<.5	<.5	<.5

In addition to total SiO₂ content, reactive SiO₂ content of the natural zeolites were also determined. Since there is no considerable difference between chemical compositions of two fractions of Bigadiç zeolite, a sample representing the whole of Bigadiç zeolite batch was tested for reactive SiO₂ content. According to TS EN 197-1 [50], reactive SiO₂ is defined as the soluble part of the total SiO₂ in potassium hydroxide solution after processing with hydrochloric acid, and it is associated with the reactive part of the total SiO₂ in pozzolanic reaction. Reactive

SiO₂ content of the natural zeolites were determined in accordance with TS EN 196-2 [51] and the results are given in Table 3.4.

Table 3.4 Reactive SiO₂ content of the natural zeolites

	Gördes zeolite	Bigadiç zeolite
Total SiO ₂ , %	69.32	66.05
Reactive SiO ₂ , %	51.29	54.93

3.2.2.2 Mineralogical/petrographical characterization of the natural zeolites

Mineralogical and petrographical characterizations of the natural zeolites were made by Geological Engineering Department of METU, and the results in the analysis report were presented below.

Powder X-ray diffraction patterns and identified phases of the Gördes zeolite and two fractions of Bigadiç zeolite are given in Figure 3.4. As seen from the patterns, clinoptilolite being a common zeolite mineral is the major crystalline phase in the samples. Quartz is another crystalline phase detected in both fractions of Bigadiç zeolite. Similarly to chemical composition, XRD patterns of two fractions of Bigadiç zeolite also appear to be almost the same. Mineralogical-petrographical analysis report covering polarized-light microscopy inspections of thin-sections prepared from bulk forms of the zeolites as well as XRD analyses indicated the facts summarized in Table 3.5.

It can be noted from Table 3.5 that Gördes and Bigadiç zeolites samples have similar purity level in terms of zeolite mineral content (75%-80%) and Gördes zeolite contains a little amount of un-zeolitized glassy phase.

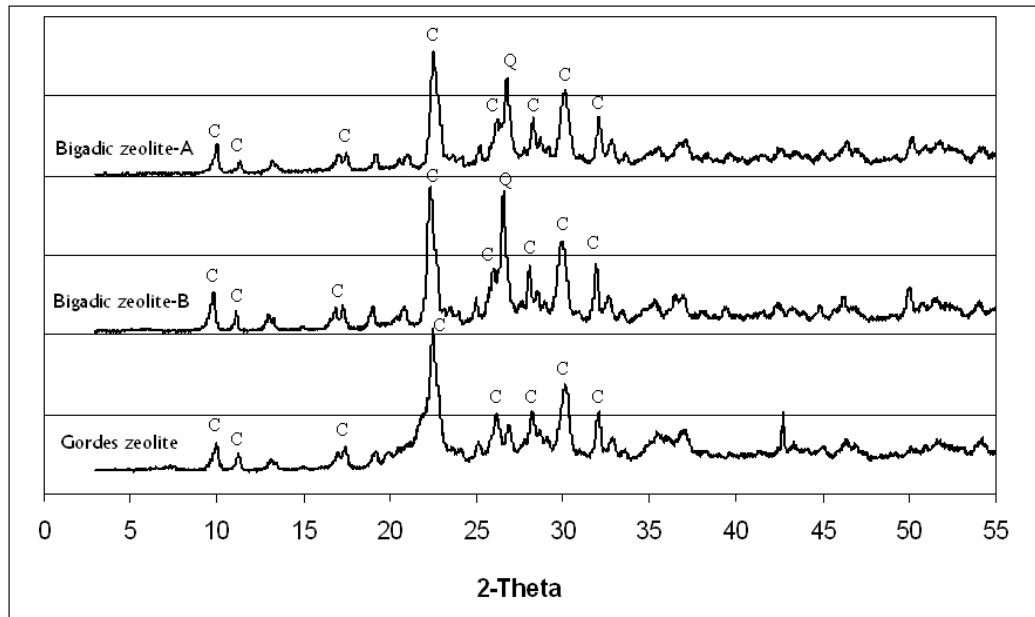


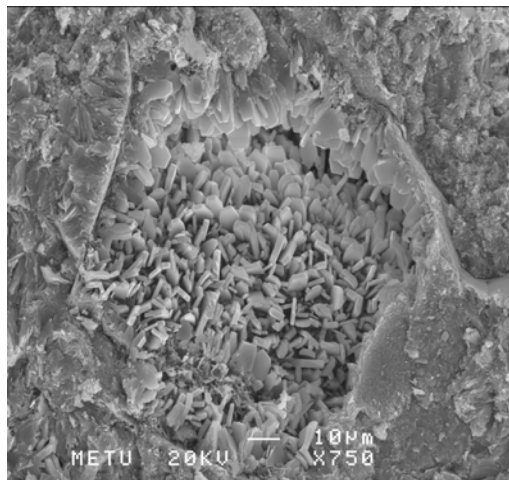
Figure 3.4 XRD diffraction patterns of Gördes zeolite and two fractions of Bigadiç zeolite (C: Clinoptilolite, Q:Quartz) (X-ray: Cu/Alpha-1/ 40kV/ 40 mA)

Table 3.5 Summary of mineralogical-petrographical analysis report for the natural zeolites

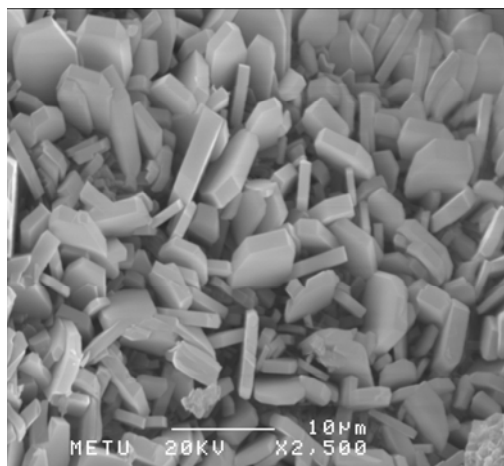
Gördes zeolite	Bigadiç zeolite-A	Bigadiç zeolite-B
<ul style="list-style-type: none"> • 75±5% zeolite content • Quartz, Sanidine, and Biotite are the minerals observed • Zeolitized glass chards are observed • A small amount of un-zeolitized glassy phase is also observed 	<ul style="list-style-type: none"> • 80±5% zeolite content • Biotite, Quartz and clay minerals are observed • Zeolitized glass chards are observed 	<ul style="list-style-type: none"> • 75±5% zeolite content • Biotite, Quartz and clay minerals are observed • No glass chards observed

3.2.2.3 Morphology of the natural zeolites

The zeolite samples were examined by SEM to observe their microstructure, and the micrographs are given in Figure 3.5 and Figure 3.6 for Gördes zeolite and Bigadiç zeolite samples, respectively, with some electron dispersive X-ray (EDX) analysis results. Clinoptilolite crystals in prismatic form were clearly observed in Gördes zeolite (Figure 3.5). However, in Bigadiç sample, zeolite crystals in flaky form were also observed as well as the prismatic ones (Figure 3.6).



a) x750 magnification

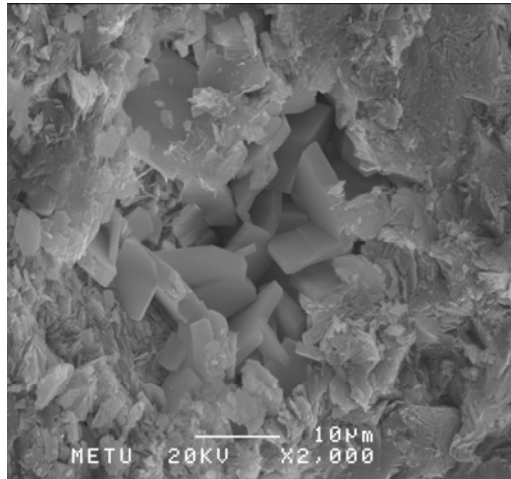


Oxide Composition (EDX analysis)

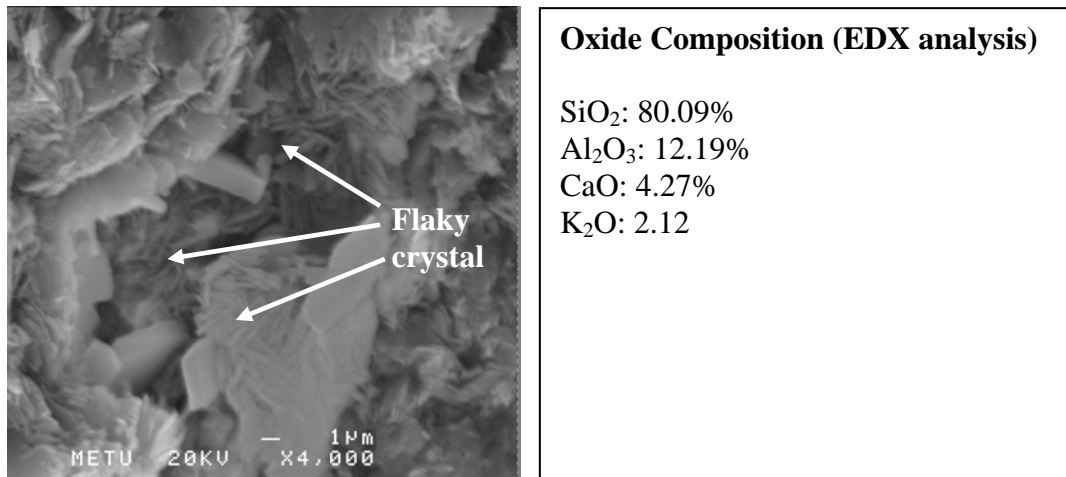
SiO₂: 78.85%
Al₂O₃: 12.99%
CaO: 3.52%
K₂O: 4.64%

b) x2500 magnification

Figure 3.5 SEM micrographs of Gördes zeolite sample (bulk from before grinding) in different magnifications



a) Clinoptilolite crystals in prismatic form



b) Flaky crystals of clinoptilolite

Figure 3.6 SEM micrographs of Bigadiç zeolite sample (bulk form before grinding)

3.2.2.4 Physical properties of the finely ground natural zeolites

In order to obtain zeolite powders to be used in studies, both natural zeolites were ground by a ball mill, after drying overnight at 105 °C to prevent agglomeration in mill, so as to have approximately 80% passing through 45-µm sieve after wet-sieving. The resultant finely ground forms of Gördes and Bigadiç zeolites were coded as GZ and BZ, respectively. Their physical properties and particle size

distribution as determined by laser diffraction by using Malvern Mastersizer 2000 analyzer were determined and given in Table 3.6 and Figure 3.7, respectively. Blaine surface area was determined in accordance with ASTM C 204 standard method, and BET surface area was determined after drying of the samples at 300 °C.

Table 3.6 Physical properties of the finely ground natural zeolites

	GZ	BZ
Specific gravity	2.16	2.19
Fineness		
Passing 45- μm , %	80	80
Blaine surface area, m^2/kg	995	1287
BET surface area, m^2/kg	35500	26870
Median particle size, μm	13.9	8.2

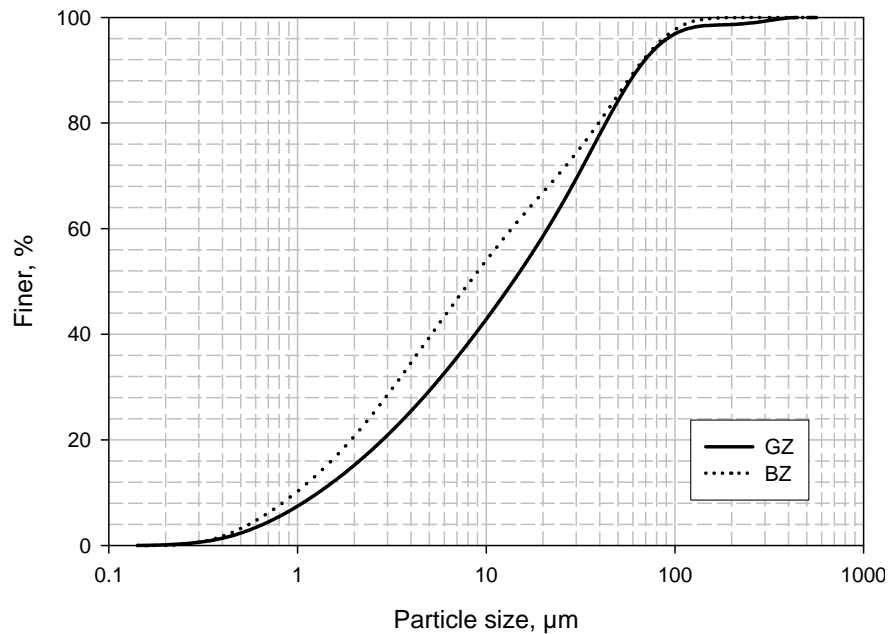


Figure 3.7 Particle size distributions of the finely ground natural zeolites as determined by laser diffraction

Regarding the physical properties of the finely ground natural zeolites used throughout the study, the following facts should be noted;

- They have similar specific gravity
- Their 45- μm passing values after wet-sieving are equal
- Although BZ seems to be finer than GZ in terms of Blain fineness and particle size distribution, BET surface area of GZ is higher than that of BZ.

3.2.3 Other pozzolanic materials used for comparison purposes

Three different types of pozzolanic materials were used for comparison purposes in studies aiming to evaluate pozzolanic activity of the natural zeolites. An undensified silica fume, a low calcium fly ash and a non-zeolitic natural pozzolan were used and they are notated as SF, FA, and NZP, respectively.

SF was a commercially available product whereas FA was obtained by Sugozy Thermal Power Plant in Iskenderun, Turkey. NZP was obtained from Bursa region and it was crushed and finely ground by a ball mill so as to have approximately 80% passing through 45- μm sieve after wet-sieving.

Chemical composition determined by ICP technique and physical properties of SF, FA, and NZP are given in Table 3.7 and their particle size distribution curves as determined by laser diffraction are presented in Figure 3.8. In addition, their reactive SiO_2 content were determined in accordance with TS EN 196-2 [51] and the results are given in Table 3.8.

Table 3.7 Chemical composition and physical properties of the pozzolanic materials

Definition	Silica Fume	Sugozu Fly Ash	Non-Zeolitic Natural Pozzolan
Notation	SF	FA	NZP
Chemical compositions (%)			
SiO ₂	95.2	57.86	61.56
Al ₂ O ₃	0.55	22.67	11.46
Fe ₂ O ₃	0.17	6.88	2.96
CaO	0.21	4.08	2.90
MgO	0.55	4.32	1.42
Na ₂ O	0.17	0.77	3.76
K ₂ O	1.03	1.82	2.39
Loss on ignition (105°C-750°C)	1.11	1.12	4.98
Physical properties			
Specific gravity	2.18	2.37	2.36
Fineness			
Passing 45- μ m (%)	100	84	79
Blaine fineness (m ² /kg)	5684	388	615
Median particle size, μ m	0.4	13	15
BET Surface area, m ² /kg	18780	3380	24650

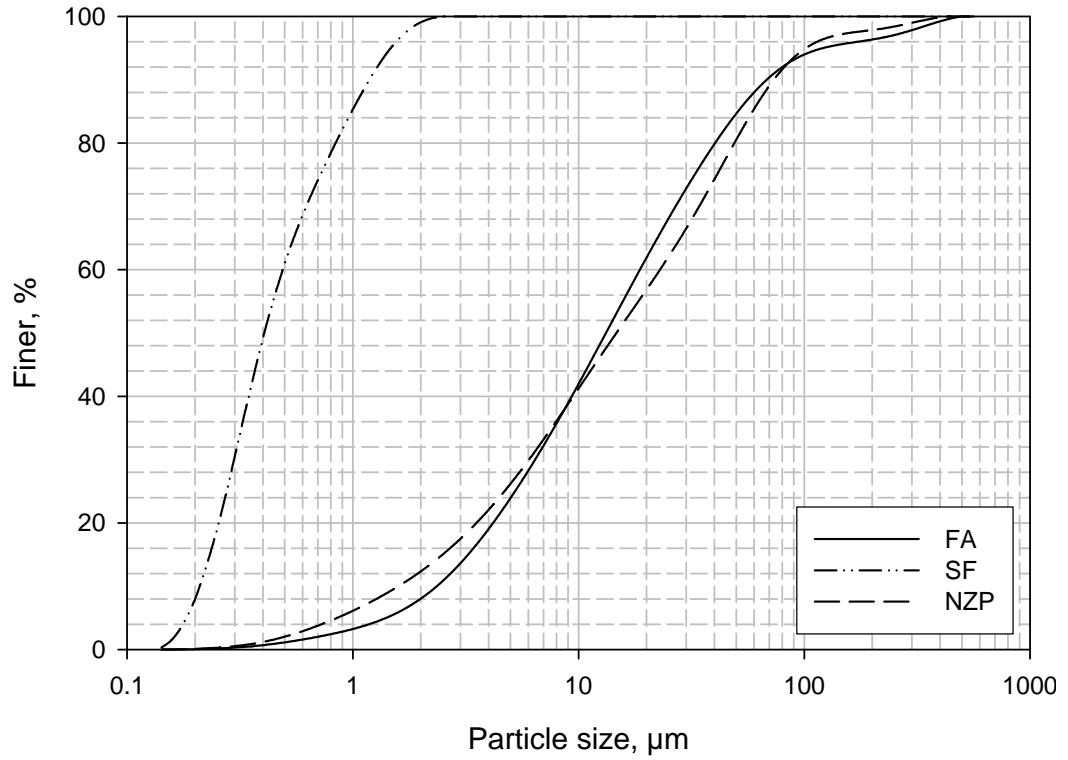


Figure 3.8 Particle size distribution curves of the pozzolanic materials used for comparison purposes

Table 3.8 Reactive SiO₂ content of the pozzolanic materials

	SF	FA	NZP
Total SiO ₂ , %	95.25	57.86	61.56
Reactive SiO ₂ , %	94.26	41.15	45.63

X-Ray diffraction pattern of SF, FA, and NZP are shown in Figure 3.9 with identified phases.

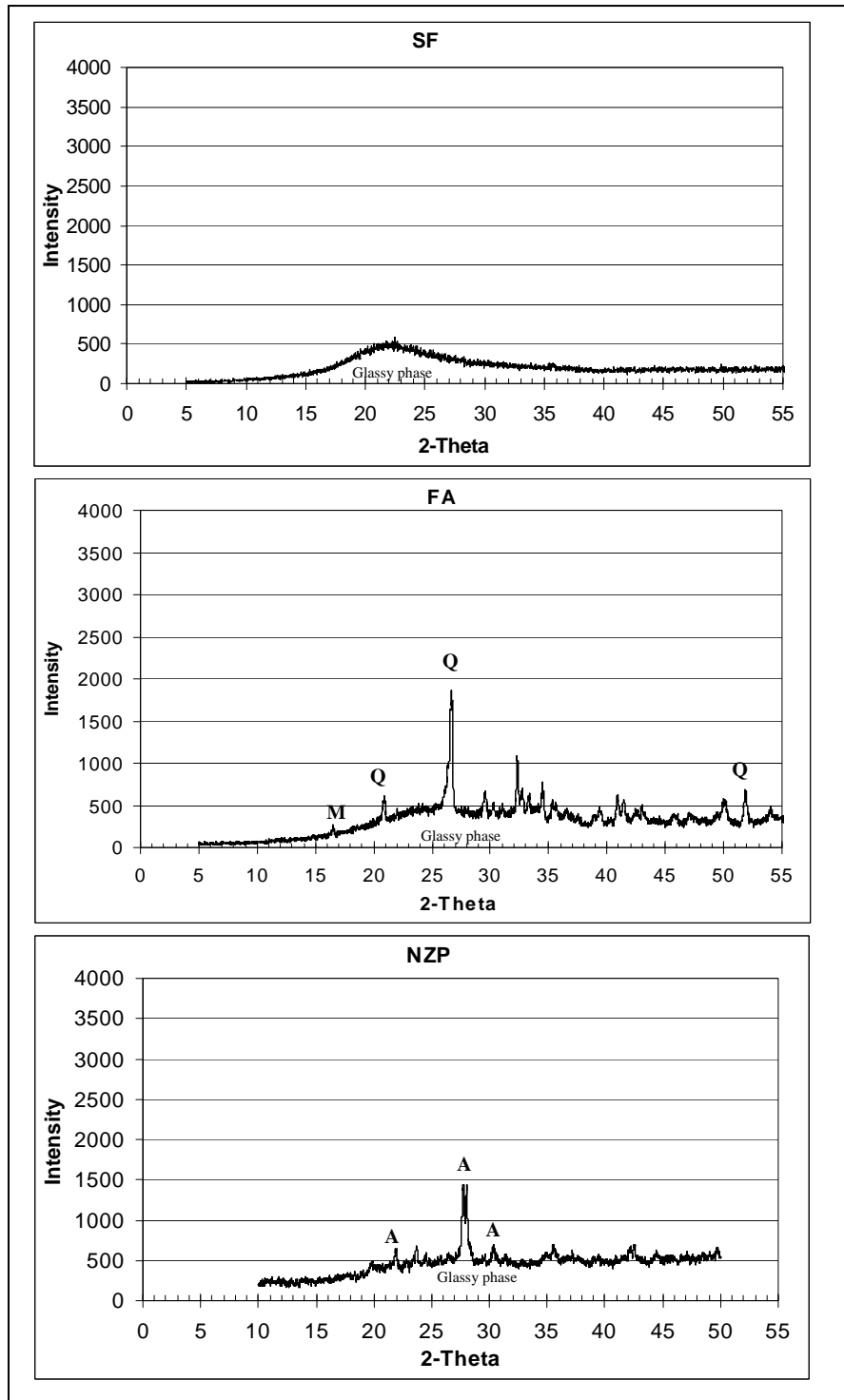


Figure 3.9 XRD patterns and identified phases of the pozzolanic materials (Q:Quartz, M: Mullite, A: Albite)

3.2.4 Superplasticizers

Two different types of superplasticizers, a sulfonated melamine condensate and a sulfonated naphthalene formaldehyde, were used to test their efficiencies in zeolite blended cements. Both superplasticizers were in a dry-powder form. A selected one of two kinds of superplasticizer according to the performance data in blended cement mortars was also used in zeolite containing concrete mixtures.

3.2.5 Hydrated limes

For the studies on pozzolanic activity of the natural zeolites, a technical-grade Ca(OH)_2 was used to prepare lime-pozzolan pastes, and its calcium hydroxide content was found to be 84% by weight of ignited sample as a result of thermogravimetric analysis. In addition, an analytical-grade Ca(OH)_2 was used in pozzolanic activity measurements based on electrical conductivity of lime-pozzolan-water mixtures.

3.2.6 Aggregates

A crushed limestone aggregate with nominal maximum size of 20 mm was used in concrete mixtures. The aggregate was obtained in three different size groups as nominally 0-4 mm, 4-12 mm, and 12-20 mm. These size groups were combined to obtain a well-graded aggregate. Grading data of the size groups are given in Table 3.9.

Table 3.9 Gradation data of the aggregate groups

Sieve size, mm	Cumulative Passing, %		
	0-4 mm	4-12 mm	12-20 mm
19.1	100.0	100.0	100.0
12.7	100.0	100.0	31.2
9.5	100.0	91.4	1.2
4.75	100.0	17.0	-
2.36	71.4	1.4	-
1.19	45.5	-	-
0.60	29.6	-	-
0.30	20.0	-	-
0.15	10.7	-	-

3.3 Experimental Methods

3.3.1 Test methods for pozzolanic activity evaluation

In order to evaluate the pozzolanic activity of the finely ground natural zeolites, three different approaches were used; i) direct measurement of $\text{Ca}(\text{OH})_2$ consumption in lime-pozzolan pastes, ii) measurement of electrical conductivity change in lime-pozzolan-water suspensions, iii) determination of compressive strengths of lime-pozzolan pastes. In addition, for a practical performance evaluation, strength activity indices of the natural zeolites were determined in accordance with ASTM C 311 [52]. The results for the natural zeolites were evaluated in comparison with the results for SF (silica fume), FA (fly ash) and NZP (non-zeolitic pozzolan). Experimental procedures for each evaluation approach for pozzolanic activity are presented below.

3.3.1.1 Thermal analysis of lime-pozzolan pastes

In order to evaluate the direct pozzolanic activity of natural zeolites and the other pozzolanic materials, Ca(OH)_2 depletion in the lime-pozzolan pastes was monitored by thermal analysis (TGA) conducted at various ages. Lime-pozzolan pastes were prepared by using a technical grade Ca(OH)_2 , with 1:1 lime:pozzolan ratio and 0.55 water-to-solid ratio. Fresh pastes were filled into plastic syringes to prevent moisture loss and carbonation, and then the pastes in syringes were cured at $50\pm 1^\circ\text{C}$ to accelerate the pozzolanic reaction.

The amount of reacted lime in the lime-pozzolan pastes was calculated by thermogravimetric analysis (TGA) of the hardened pastes at 3, 7, and 28 days of age. Perkin Elmer Pyris TGA&FTIR thermal analyzer system was utilized for temperature range between room temperature and 950°C at the heating rate of $10^\circ\text{C}/\text{min}$.

TGA allow measuring the changes in weight of a sample as a function of increasing temperature. The amount of Ca(OH)_2 in an hardened cementitious system can be calculated from the amount of weight loss occurring at around 450°C , resulting from decomposition of Ca(OH)_2 and evaporation of water in its structure. The amount of Ca(OH)_2 was calculated based on molar weight ratio between evaporated H_2O and Ca(OH)_2 .

First of all, the initial amount of Ca(OH)_2 for each lime-pozzolan mixture was calculated from the TGA data of the original lime and the pozzolanic material as percent by total ignited weight of the components. The amount free lime in hardened lime-pozzolan pastes for the specified test ages was determined by TGA as percent by the ignited weight of the paste. The amount of reacted lime, for a specific age, was calculated from the difference between initial and final amounts of free lime, and expressed as percentage of the initial amount.

3.3.1.2 Electrical conductivity of lime-pozzolan-water suspensions

Evaluation of pozzolanic activity of finely divided materials by electrical conductivity measurement of lime-pozzolan-water suspension is a rapid method which is firstly proposed by Luxan et al. [53]. The method covers the determination of decrease in electrical conductivity of lime-water solution after addition of finely ground pozzolanic material to provide a rapid indication of its pozzolanic activity. The reaction between Ca(OH)_2 and pozzolanic material results in a reduction in electrical conductivity of aqueous suspension, which is attributed to fixation of dissolved Ca(OH)_2 by pozzolan particles. Therefore the amount of reduction in conductivity can be used as a measure of pozzolanic activity. However the method proposed by Luxan et al. [53] is not useful for the pozzolanic materials which contain soluble ions, such as fly ash, since they contribute to conductivity value of the aqueous solution, hence cause incorrect results. In order to overcome this issue, Paya et al. improved the method proposed by Luxan et al. and they suggested an enhanced conductivity technique including a correction procedure considering the effect of soluble ions in pozzolanic materials on conductivity value [54].

The enhanced conductivity measurement technique proposed by Paya et al. [54] was used for comparative evaluation of pozzolanic activity of natural zeolites with respect to the other pozzolanic materials.

The following procedure was applied for each pozzolanic material in the experimental program;

- An unsaturated Ca(OH)_2 solution was prepared in a beaker with solution of 200 mg of analytical-grade Ca(OH)_2 in 250 ml of deionized water.
- The beaker was then placed in a constant-temperature water bath to hold the temperature of the solution at 40 ± 1 °C. The solution was continuously mixed by a small electrical mixer. The electrical conductivity and the temperature of the solution are continuously measured by a digital conductivity-meter. pH value of the solution is also measured continuously.

- After the lime-water system reached a constant conductivity, 5 grams of pozzolanic material is added into the beaker. Conductivity and pH values of the solution are recorded for certain time intervals after adding the pozzolanic material, and conductivity vs. time curve is obtained for the lime-pozzolan-water system.
- The same procedure was repeated for the pozzolan-water systems at 40 ± 1 °C. For this purpose, 5 grams of pozzolanic material is added into 250 ml of deionized water, and conductivity vs. time curve and pH vs. time curves were obtained. This was done because the contribution of the pozzolanic material to conductivity should be subtracted from the conductivity of lime-pozzolan-water system.
- Corrected conductivity-time curves for each lime-pozzolan-water system were obtained by subtracting the contribution of pozzolanic material to conductivity of lime-pozzolan-water suspension. Finally, for an effective comparison, relative loss in conductivity was calculated as percentage with respect to initial conductivity of lime-water solution before addition of pozzolanic material. A higher loss in conductivity is attributed to a higher amount of lime fixation by the pozzolanic material.

The measurement set-up in a constant-temperature water-bath is shown in Figure 3.10

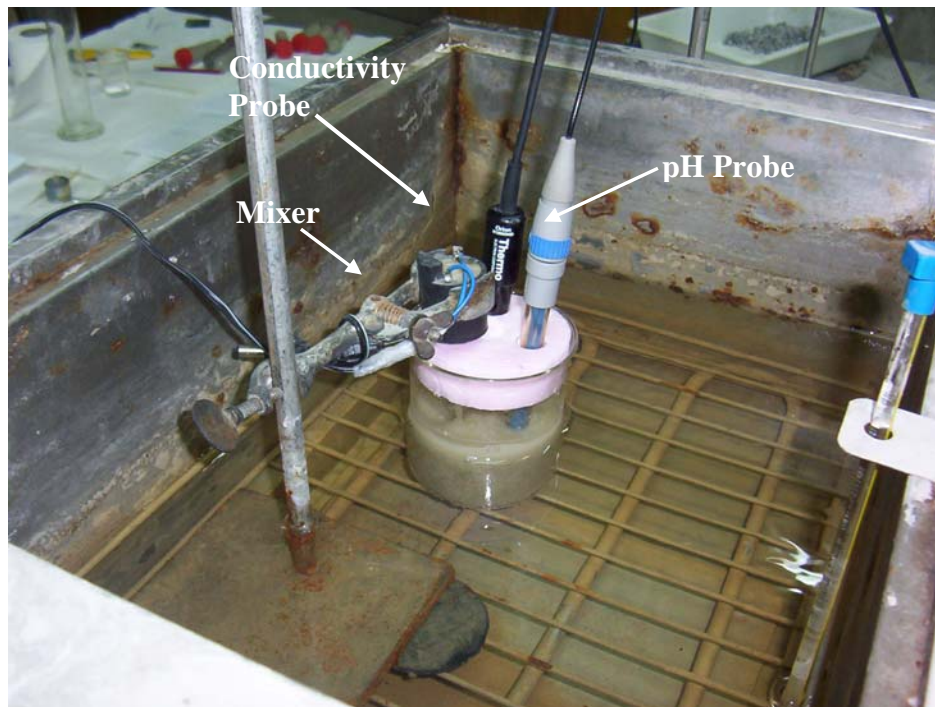


Figure 3.10 Conductivity measurement set-up

3.3.1.3 Compressive strength of lime-pozzolan pastes

Measuring the compressive strength of lime-pozzolan pastes is another test method which reflects the pozzolanic activity in terms of strength contribution. In order to evaluate the pozzolanic activity of natural zeolites from the strength contribution point of view, lime-pozzolan pastes were prepared with natural zeolites and the other pozzolanic materials by using 1:1 lime:pozzolan ratio and 0.55 water-to-powder ratio. A technical-grade $\text{Ca}(\text{OH})_2$ was used in the mixtures. Fresh pastes were cast into 2.5 cm cubic molds, sealed with stretched-film to prevent moisture loss and carbonation, then allowed to cure at 50 ± 1 °C until test age. Compressive strengths of hardened lime-pozzolan pastes were determined at 3, 7, and 28 days after casting.

3.3.1.4 Mercury intrusion porosimetry of lime-pozzolan pastes

Pore size distributions of hardened lime-pozzolan pastes were determined at their 28 days of age. The hardened lime-pozzolan pastes which were prepared and used for thermal analyses and compressive strength tests were also used for mercury intrusion porosimetry analyses in order to determine their pore size distributions.

Determination of pore size distribution of hardened cementitious systems requires the complete removal of free water in specimens. Since oven-drying at 100-105°C may cause damage to microstructure and pore system of the hardened pastes, some special drying procedures are commonly applied before mercury intrusion porosimetry such as vacuum drying at relatively low temperatures, freeze drying, and methanol replacement [24]. A drying procedure consisting of methanol replacement followed by vacuum drying at 55 °C was applied in the study.

The hardened pastes were crushed to particle size range of approximately 3-5 mm and then immersed in acetone for 24 hours to replace free water. The samples were then subjected to vacuum drying at 55 °C in a vacuum oven for 24 hours. The pretreated samples were analyzed by Quantachrome Corporation Poremaster 60 mercury intrusion porosimeter with a maximum 55000 psi injection pressure for pore size range between 3-10000 nm (0.003- 10 μm). In calculations for pore size distribution from mercury intrusion data, the contact angle was taken as 142°. For all the samples, a completely identical sample preparation procedure was applied.

3.3.1.5 Strength activity index

Strength activity indices of the finely ground natural zeolites GZ and BZ as well as SF, FA and NZP were determined in accordance with ASTM C 311 [52] to evaluate the performance of the natural zeolites in terms of practical usage, in comparison with the other pozzolanic materials used in the study. The method covers the determination of relative compressive strength of mortar prepared with blended

portland cement consisting of 80% portland cement and 20% pozzolanic material (by weight) with respect to the control mortar prepared with 100% portland cement. Control mortar mixture is prepared with 0.485 water-to cement ratio whereas the amount of water for test mixture is adjusted so as to provide a flow $\pm 5\%$ of control mixture. Mixture proportions for the control mixture and the test mixture are given in Table 3.10.

Since water-to-cementitious materials ratio of test mixtures depends on water requirement of the pozzolanic material, strength activity index reflects the general performance of pozzolanic material including strength contribution of its pozzolanic reaction together with its water requirement. In addition, strength contribution caused by filler effect of fine pozzolanic material is another factor effecting strength activity index value.

Table 3.10 Mixture proportions for strength activity test mortars

Material	Control Mix, grams	Test Mix, grams
Portland cement	500	400
Pozzolan	-	100
Standard sand	1375	1375
Water	242	The amount required to provide the same flow as the control mix*

*Flow of fresh mortar is measured in accordance with ASTM C 109 [55].

3.3.2 Tests on zeolite blended cement pastes and mortars

This part of the experimental program aims to investigate the properties and hydration of blended cements containing low, moderate and high amounts of natural zeolites. The ordinary portland cement (PC) was directly replaced by each of finely ground natural zeolites namely GZ and BZ in amounts of 15% (low), 35% (moderate), and 55% (high) by weight. The blended cements were prepared by direct replacement method instead of intergrinding of raw materials (clinker,

pozzolan and gypsum) together in order to control the fineness of the blending components. Because it is known that intergrinding of natural pozzolan, clinker and gypsum may result in a relatively coarse clinker phase when compared to natural pozzolan phase, and this is disadvantageous in terms of strength development rate of the end product [3, 56]. The notations and compositions of the blended cements prepared with direct replacement are given in Table 3.11.

Table 3.11 Notation and composition of the cements

Cement notation	Portland cement content	Natural zeolite content
PC	100%	0%
GZ15	85%	15% GZ
GZ35	65%	35% GZ
GZ55	45%	55% GZ
BZ15	85%	15% BZ
BZ35	65%	35% BZ
BZ55	45%	55% BZ

Blended cement pastes were tested at various ages for water demand and setting time determined by standard methods; free Ca(OH)_2 content determined by TGA; crystalline hydration products examined by XRD, pore size distribution determined by mercury intrusion porosimetry (MIP), microstructure examined by SEM/EDX in comparison with the reference portland cement paste.

Compressive strength of blended cement mortars were determined for two different types of superplasticizers namely a naphthalene-based product and a melamine-based product, in order to test their efficacy for and compatibility with zeolite blended cements.

The experimental procedures applied on blended cements are described below.

3.3.2.1 Normal consistency and setting time

Blended cements containing various amounts of natural zeolites and the reference portland cement were tested for normal consistency water demand and setting time of the pastes in accordance with ASTM C 187 [57] and ASTM C 191 [58], respectively.

3.3.2.2 Free Ca(OH)₂ content of the pastes

The free Ca(OH)₂ content of the hardened cement pastes prepared with 0.5 water-to-cementitious materials ratio by using deionized water was determined at 3, 7, 28 and 91 days of age by thermogravimetry analysis (TGA). The pastes were prepared by using an electrical mixer and immediately placed into plastic syringes and the lids were sealed to prevent moisture loss and carbonation, then the samples were cured in temperature of 23 ±1 °C till the test ages.

At a specified test age, the hardened pastes were crushed and sieved to obtain particles smaller than 800-µm, and then immediately analyzed by Perkin Elmer Pyris TGA&FTIR thermal analyzer system in temperature range between room temperature and 1000 °C at heating rate of 10°C/min. The amount of Ca(OH)₂ was calculated from the weight loss occurred approximately at 450°C as percent by ignited weight of the paste.

3.3.2.3 XRD analysis of the hardened pastes

In order to examine crystalline hydration products qualitatively and to observe some possible similarities and differences depending on zeolite type and amount, the crushed and sieved samples of hardened cement pastes prepared with the procedure described above in Section 3.3.2.2 were also used for XRD analyses.

XRD examinations were carried out for blended cements containing 15% and 55% natural zeolites as well as the reference portland cement at 7 days and 28 days of age. XRD patterns of the hardened pastes were obtained by using a Cu- α 1 radiation /40 kV x-ray diffractometer between 2-theta angles of 5° and 65°.

3.3.2.4 Mercury intrusion porosimetry of hardened cement pastes

Pore size distribution of hardened cement pastes were determined for the blended cements containing 15% and 55% natural zeolites as well as the reference portland cement at 28, and 91 days of age. The hardened cement pastes whose preparation described in thermal analyses part above were tested for pore size distribution after a specific pretreatment process.

Determination of pore size distribution of hardened cementitious systems were made by following the procedure described in the part of mercury intrusion porosimetry of lime-pozzolan pastes, Section 3.3.1.4.

3.3.2.5 SEM/EDX

Microstructure and hydration products of the hardened cement pastes were examined for the blended cements containing 15% and 55% natural zeolites as well as the reference portland cement at 28 days of age. The hardened cement pastes whose preparation described in Section 3.3.2.2 were examined by JEOL JSM-6400 scanning electron microscope (SEM) equipped with NORAN System 6 energy dispersive X-ray analysis (EDX), in backscattered mode electron microscopy.

28 days old hardened cement pastes were crushed to size of approximately 15-20 mm and immersed in methanol for 48 hours in order to remove free water and to stop hydration. Since backscattered-mode SEM requires polished samples, hardened cement paste specimens were then immersed in epoxy resin and finally the polished surfaces were prepared. The polished surfaces were coated with gold-

palladium alloy to provide conductive surface. The polished surfaces of pastes were examined qualitatively to observe the microstructure of the pastes as seen in backscattered SEM.

Backscattered-mode SEM, which is one of various SEM imaging techniques, allows a clear assessment of the “internal architecture” of the hydrated cement system. Backscattered-mode SEM provides images based on variations in electron backscatter coefficient of different areas. Differences in backscatter coefficients primarily reflect differences in chemical composition. Chemical components of high electron density have high backscatter coefficients, and appear bright in the backscattered images. Conversely, components of lower electron density, such as most cement hydration products, have lower backscatter coefficients, and appear less bright. EDX system additionally provides chemical compositional data on any desired point or area of image observed [59].

3.3.2.6 Superplasticizer requirement and compressive strength of mortars

Compressive strength performance of blended cements containing low, moderate and high amount of the natural zeolites, which are listed in Table 3.11, were tested on mortar specimens prepared with 0.5 water-to-cementitious materials ratio (w/cm) and 2.75 sand-to-cement ratio. The CEN (the European Committee for Standardization) standard sand in accordance with TS EN 196-1 [60] was used in mortar mixtures.

Two different types of superplasticizers, a naphthalene-based and a melamine-based, were used for preparation of blended cement mortars so as to provide a flow value similar to that of the reference portland cement mortar. Flow value of fresh mortars was determined in accordance with ASTM C 109 [55] as a measure of workability. Thus superplasticizer requirements of the blended cements and their effects on compressive strength of mortar were determined for both types of superplasticizers.

Mortar mixtures were prepared by applying the standard mixing and molding procedures stated in ASTM C 109 [55]. Fresh mortars were placed into 5 cm cubic molds and allowed to moist curing for the first 24 hours under wet burlap. Two different curing regimes, curing in lime-saturated water and curing in 99% relative humidity cabinet, were applied to determine their effects on compressive strength development of blended cement mortars. Compressive strength of the hardened mortars was determined at 3, 7, 28, 91, 180 and 360 days of age, with a constant loading rate of 90 kgf/second.

3.3.3 Tests on zeolite concrete mixtures

Properties of high-performance concrete mixtures containing low (15% replacement), moderate (35% replacement), and high (55% replacement) amount of natural zeolites were determined for the finely ground natural zeolites GZ and BZ. For 400 kg/m³ total cementitious materials content and 0.45 water-to-cementitious materials ratio (w/cm), the following properties of zeolite-containing concrete mixtures were determined; superplasticizer requirement to provide a desired slump value, air content, setting time, compressive strength, splitting tensile strength, modulus of elasticity, and resistance to chloride ion penetration (ASTM C 1202). In addition two different plain portland cement concrete mixtures without any replacement were prepared for control purposes. One of them was prepared with 0.45 w/c ratio and superplasticizer addition in an amount required to provide a similar slump value with those of zeolite concrete mixtures. The other control mixture was prepared without superplasticizer addition and with w/c required to provide a similar slump value with those of the other mixtures.

3.3.3.1 Mixture proportions

The proportions of the mixtures are given in Table 3.12 for saturated surface-dry condition of the aggregates. For all the mixtures, the total amount of cementitious materials (PC+zeolite) was kept constant. A melamine-based superplasticizer in a

dry powder form was used in the mixtures, except C1 mix, in an amount required to provide approximately 150 mm slump value for 0.45 w/cm. For C1, 150 mm slump value was provided by increasing w/c instead of adding superplasticizer. Thus C1 mix represents a traditional plain portland cement concrete whereas C2 corresponds to the control mix having the same water-to-binder ratio and similar slump value as zeolite concrete mixtures. In addition to two control mixtures, totally six zeolite concrete mixtures were prepared by 15%, 35%, and 55% weight replacement by the finely ground natural zeolites GZ and BZ.

Table 3.12 Mixture proportions of the concrete mixtures

Mix Label	Portland cement kg/m ³	Natural zeolite kg/m ³	Water kg/m ³	Aggregates			SP kg/m ³
				0-4mm kg/m ³	4-12 mm kg/m ³	12-20 mm kg/m ³	
C1	400	-	212	847	425	425	-
C2	400	-	180	890	447	447	2.8
ZC-GZ15	340	60 (GZ)	180	882	442	442	4.4
ZC-GZ35	260	140 (GZ)	180	875	439	439	6.0
ZC-GZ55	180	220 (GZ)	180	861	432	432	10.0
ZC-BZ15	340	60 (BZ)	180	882	442	442	3.6
ZC-BZ35	260	140 (BZ)	180	875	439	439	4.8
ZC-BZ55	180	220 (BZ)	180	861	432	432	4.9

3.3.3.2 Preparation and casting of test specimens

The concrete mixtures were prepared by using a rotating planetary concrete mixer with approximately 5 minutes of mixing. The fine and coarse aggregates were added firstly into the mixer and then a small part of mixing water was included in order to dampen the surfaces of aggregate particles. After that, the binder (PC or

PC+zeolite) was added into the mixer and finally the remaining part of the mixing water containing dissolved superplasticizer was introduced.

The slump, unit weight and air content of the fresh concretes were determined immediately after mixing in accordance with ASTM C 143 [61], ASTM C 138 [62] and ASTM C 231 [63], respectively. A cubic specimen was cast for each mixture to determine the initial and final setting time of concrete in accordance with ASTM C 403 [64]. Cylindrical specimens of 100x200 mm in size were cast for determination of compressive and splitting tensile strength, modulus of elasticity and resistance to the chloride-ion penetration of concretes. The specimens were demolded after 24 h and cured in lime-saturated water until the test ages.

3.3.3.3 Test on hardened concretes

Compressive strength and splitting tensile strength of the hardened cylindrical specimens were determined in accordance with ASTM C 39 [65] and ASTM C 496 [66], respectively, using ELE 300 hydraulic compression machine at 3, 7, 28, and 90 days of age. The compressive and splitting tensile strength values were computed from the average of three cylinders for each test age.

Modulus of elasticity of the hardened concretes in compression was determined on cylindrical specimens at 91 days of age in accordance with ASTM C 469 [67]. Modulus of elasticity value for a mixture was calculated as average of three specimens.

The resistance of the concrete specimens to the chloride-ion penetration was determined at 28 days and 91 days on 50 mm thick slices of cylindrical specimens in accordance with ASTM C 1202 [68].

CHAPTER 4

RESULTS AND DISCUSSION

4.1 Pozzolanic Activity

Activity of the finely ground natural zeolites GZ and BZ with $\text{Ca}(\text{OH})_2$ were evaluated by different techniques in comparison with a silica fume (SF), a low-calcium fly ash (FA) and a non-zeolitic natural pozzolan (NZP). $\text{Ca}(\text{OH})_2$ depletion in lime-pozzolan pastes, reduction in electrical conductivity of lime-pozzolan-water suspensions, and compressive strength of lime-pozzolan pastes were used as indicators for pozzolanic activity. In addition, strength activity index determined in accordance with ASTM C 311 was also used as a performance indicator for comparative evaluation of the natural zeolites with the other more popular pozzolanic materials. Results of these evaluations are presented below.

4.1.1 $\text{Ca}(\text{OH})_2$ depletion in lime-pozzolan pates

The amounts of reacted $\text{Ca}(\text{OH})_2$ in lime-pozzolan pastes as percent of the initially available $\text{Ca}(\text{OH})_2$ are illustrated in Figure 4.1. TGA plots of the lime-pozzolan pastes are presented in Appendix A.

The data in Figure 4.1 indicated that finely ground natural zeolites GZ and BZ consumed higher amounts of $\text{Ca}(\text{OH})_2$ than the fly ash and the non-zeolitic natural pozzolan, but lower than the silica fume, for all test ages. The natural zeolites

consumed approximately 75% of available Ca(OH)_2 at the end of 28 days, whereas the consumption values were 83%, 53%, and 46% for the silica fume, the fly ash, and the non-zeolitic pozzolan, respectively.

Although BZ consumed slightly higher amount of Ca(OH)_2 at early ages when compared to GZ, they reacted with the similar amount of Ca(OH)_2 at the end of 28 days. The relatively higher reactivity of BZ with Ca(OH)_2 at early ages when compared to GZ is probably due to the finer particle size distribution of BZ (Figure 3.7).

Reactivity of the natural zeolites (GZ and BZ) was found to be significantly higher than those of NZP and FA. The higher reactivity of the zeolites can be attributed to their high reactive SiO_2 content and the high BET surface area (Table 3.4 and Table 3.6).

In addition, it should be noted from Figure 4.1 that the rate of Ca(OH)_2 consumption of FA between the ages of 3 days and 28 days (slope of the line) was higher than those of the natural zeolites and the other pozzolanic materials. This result confirms the phenomenon of delayed pozzolanic activity of fly ash, when compared to other pozzolanic materials, which has been reported by some authors. The phenomenon is explained by slow superficial reaction on fly ash particles at initial stages, and more efficient reaction of inner glassy phase of ash particles at later stages [20, 54].

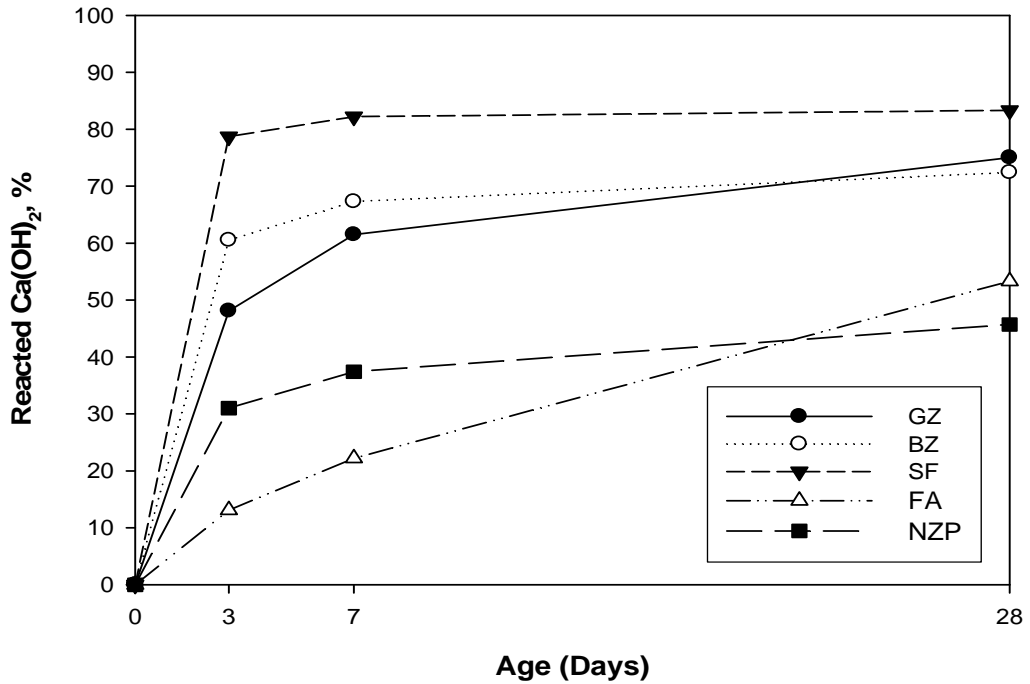
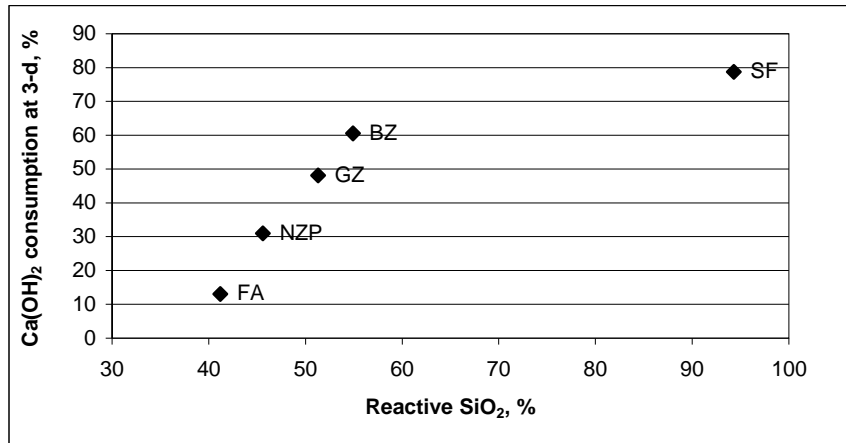


Figure 4.1 Amounts of reacted Ca(OH)_2 as percent of initially available Ca(OH)_2 content

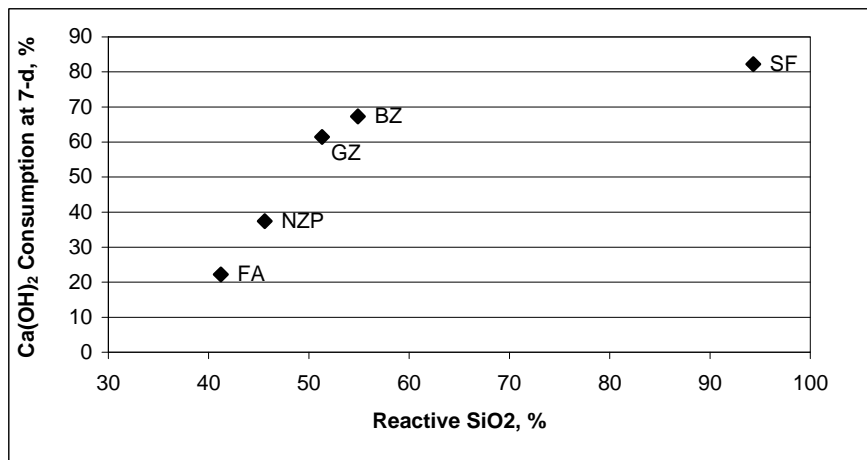
Focusing on relationships between properties of pozzolanic materials and their ability to fix Ca(OH)_2 , it was revealed out that there is a clear relationship between reactive SiO_2 content of the materials (Table 3.4 and Table 3.8) and the amount of Ca(OH)_2 which they consumed in lime-pozzolan pastes at early periods (3 days and 7 days) as shown in Figure 4.2a and Figure 4.2b. However, it was observed no such a correlation between them for 28-day data (Figure 4.2c). Thus, it can be concluded that relatively high content of reactive SiO_2 of the natural zeolites is responsible for their higher early-age performance of lime-fixation when compared to those of FA and NZP. A linear multiple-variable regression analysis indicated that the amount of lime consumed by the pozzolanic materials at the end of 28 days is not only a function of reactive SiO_2 content but also BET surface area. As a result of the regression analysis, the expression referring to 28-day lime consumption of a pozzolanic material as a function of its reactive SiO_2 content and BET surface area was determined as follows;

$$\text{28-days lime consumption, \%} = 0.4361 \text{ R-SiO}_2 + 0.7025 \text{ BET} + 28.6448 \quad (1)$$

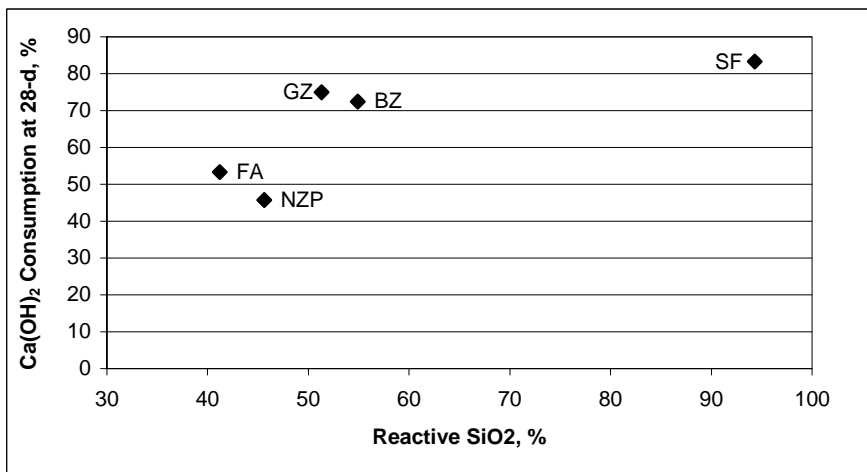
where R-SiO₂ is reactive SiO₂ content as percent, and BET refers to BET surface area of the pozzolanic material as m²/g. The plot of experimental values vs. predicted values calculated from Eq. 1 showed that the regression equation satisfactorily represents the 28-days lime consumption as a function of reactive SiO₂ and BET surface area, as shown in Figure 4.3. Such a good predictability of amount of Ca(OH)₂ consumption in lime-pozzolan pastes at 28 days indicated that combined effects of reactive SiO₂ and BET surface area mainly determines the amount of lime consumed by pozzolanic materials at late ages. This judgement clearly explains why GZ consumed a little bit more Ca(OH)₂ than BZ at 28 days, although the reverse is true for 3 days and 7 days.



a) 3-day



b) 7-day



c) 28-day

Figure 4.2 Relationship between reactive SiO₂ content and Ca(OH)₂ consumption of the pozzolanic materials

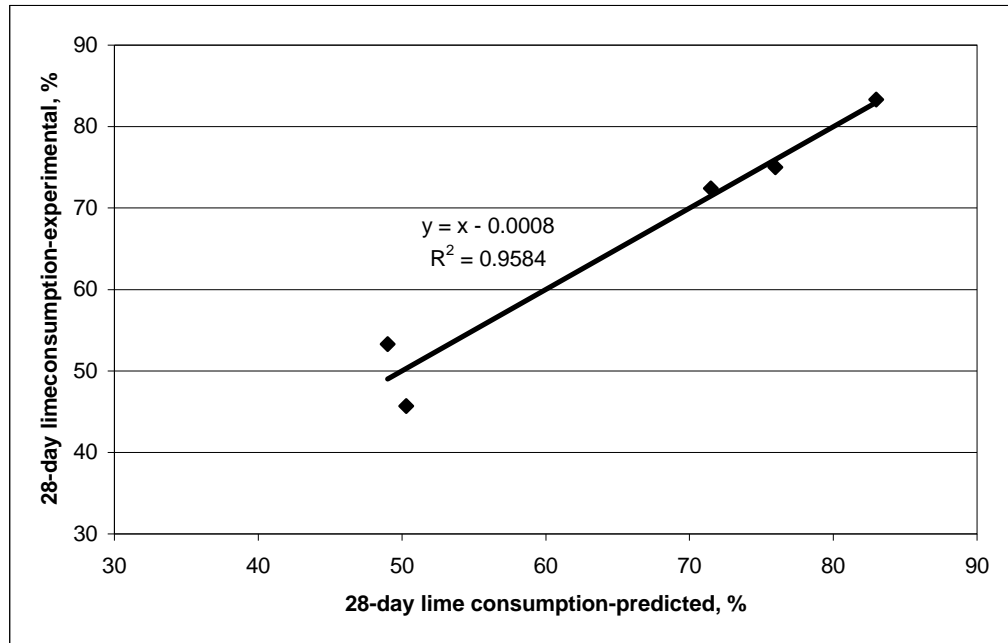


Figure 4.3 Predicted vs. experimental 28-day lime consumption data plot

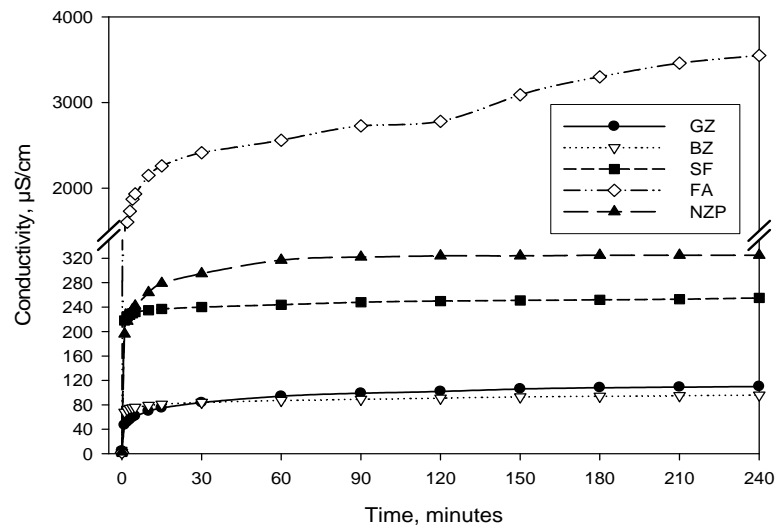
Consequently, it was experimentally shown that the natural zeolites (GZ and BZ) are more active than the fly ash and the non-zeolitic natural pozzolan in terms of reactivity with $\text{Ca}(\text{OH})_2$. The reactivity of the zeolites at early ages was associated with their reactive SiO_2 content whereas the reactivity at late ages was attributed to their BET surface area as well as reactive SiO_2 content.

4.1.2 Electrical conductivity of lime-pozzolan-water suspensions

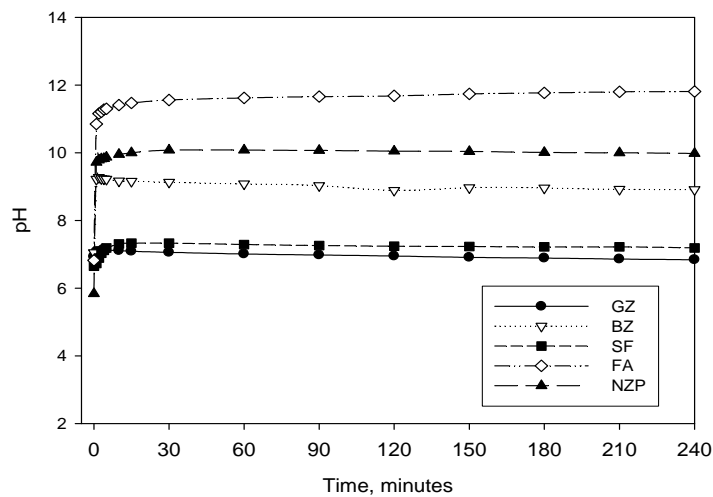
In order to evaluate the activity of the natural zeolites with $\text{Ca}(\text{OH})_2$ at very early periods of pozzolanic reaction, the reduction in electrical conductivity of lime-pozzolan-water suspensions was determined as a measure of lime fixation. For this purpose, electrical conductivity of continuously-stirred lime-pozzolan-water suspensions and pozzolan-water suspensions were measured as a function time. To exclude the contribution of the pozzolanic material to the electrical conductivity of lime-pozzolan-water suspension, the conductivity vs. time graph of pozzolan-water suspension was subtracted from the graph of lime-pozzolan-water suspension.

Conductivity vs. time graphs of pozzolan-water suspensions are also useful for observing and comparing the behavior of pozzolanic materials with each other in terms of soluble-ion release.

Conductivity and pH of the pozzolan-water suspensions at 40 ± 1 °C were determined as a function of time for the natural zeolites and the other pozzolanic materials and the results are given in Figure 4.4.



a) Conductivity vs. time curves of the pozzolan-water suspensions



b) pH vs. time curves of the pozzolan-water suspensions

Figure 4.4 Conductivity vs time and pH vs time plots for the pozzolan-water suspensions

As can be seen from Figure 4.4a, addition of the pozzolanic materials into deionized water resulted in an increase in conductivity of the suspensions due to incorporation of some ions into water from pozzolanic materials. Conductivity of suspensions of GZ and BZ were similar and approximately 85-90 $\mu\text{S}/\text{cm}$ at the end of 240 minutes of stirring, and lower than those of the other pozzolanic materials. The increase in conductivity of zeolite-water suspensions can be associated with release of cations such as Na^+ , K^+ and/or Ca^{+2} as a result of cation exchange with H^+ ions in water, as experimentally showed by Rivera et al [69]. The fly ash-water system showed extremely higher conductivity than the other suspensions even at early seconds and this indicated that the fly ash clearly differ from the other pozzolans by its significantly high content of water-soluble ions.

Comparing GZ and BZ in terms of influence on pH of their water suspensions (Figure 4.4b), it is clearly observed that BZ behaved to increase pH of the water suspension considerably whereas GZ was not so highly effective on pH. The increase in pH is due to decrease in concentration of H^+ ions captured by zeolite particles as a result of cation exchange, as showed by Rivera et al. [69]. Increase in pH of the SF, FA and NZP suspensions would be attributed to leaching of Na, K and or Ca from vitreous aluminosilicate fractions and the hydrolysis of these aluminosilicates would increase (OH^-) concentration in solution [54].

The net relative losses in conductivity of the lime-pozzolan-water suspensions, that is a measure of lime fixation by the pozzolanic material, are calculated by subtracting the conductivity vs. time curve of pozzolan-water system from the curve of corresponding lime-pozzolan-water system and are shown in Figure 4.5 for each pozzolanic material.

Loss in conductivity of all the suspensions increased with time due to lime fixation as a result of pozzolanic reactivity. GZ exhibited a considerably higher reactivity than BZ and the other pozzolanic materials at early times of testing, which is attributed to relatively high BET surface area of GZ (Table 3.4 and Table 3.8). By

the end of 240-minutes testing period, it was observed that reactivity of GZ is similar to SF but higher than BZ, FA and NZP. From the slope of the curve belonging SF suspension, it can be expected that SF may show higher reactivity than GZ for longer testing durations than 240 minutes. The higher reactivity of SF for longer testing periods can be attributed to its higher reactive SiO₂ content (Table 3.8) when compared to the natural zeolites and the other pozzolanic materials as well.

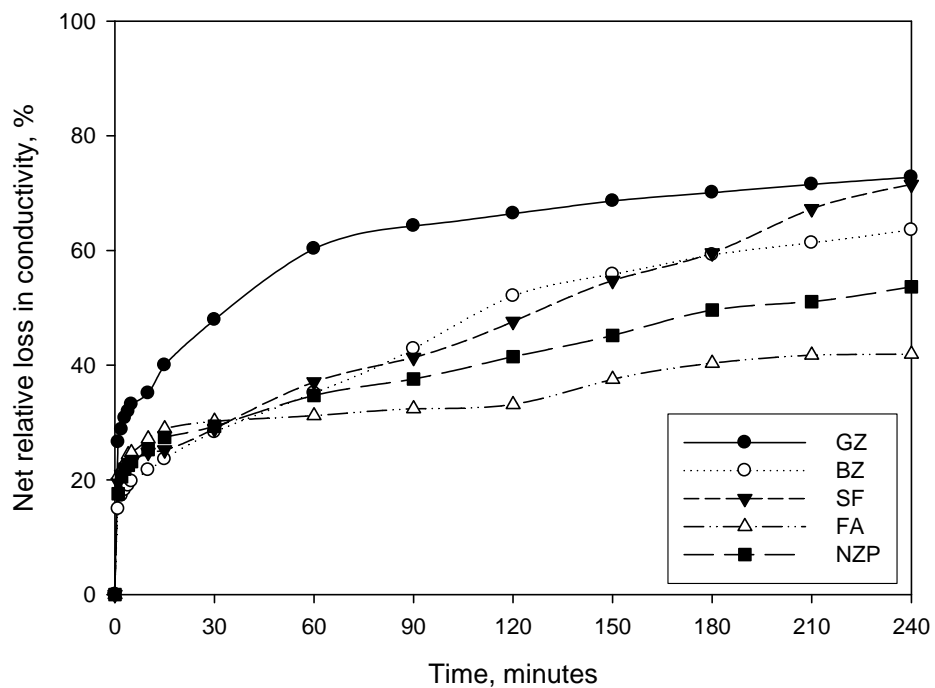


Figure 4.5 Net relative losses in conductivity of lime-pozzolan-water suspensions

Consequently, pozzolanic activity of the natural zeolites, measured by electrical conductivity technique, was found to be comparable to or lower than the silica fume and higher than the fly ash as well as the non-zeolitic pozzolan. This outcome is consistent with the results obtained by measuring the amount of reacted Ca(OH)₂ in lime-pozzolan pastes (Figure 4.1). For the early periods of conductivity measurements, it was observed that the specific surface area, which is higher for

natural zeolites than the others, is the governing parameter for the lime fixation ability of the materials. However, for the later periods of testing, the amount of active phases in the pozzolanic material (such as reactive SiO₂ content) becomes dominant parameter. Thus, the pozzolanic activity of natural zeolites, which is higher than those of the fly ash and the non-zeolitic pozzolan, can be attributed to the combined effects of relatively high BET surface area and reactive SiO₂ contents of the zeolites. BET surface area of the natural zeolites is found to be more influential on the very short-term activity whereas reactive SiO₂ content is another determining factor for later periods.

4.1.3 Compressive strength of lime-pozzolan pastes

Determination of compressive strength of lime-pozzolan mixes is generally used for the technical evaluation of pozzolanic materials. Although strength of lime-pozzolan paste increases as the amount of reacted lime increases for a pozzolanic material, there is no general correlation between the two parameters for different pozzolanic materials [20]. Therefore the evaluation of pozzolanic activity by strength point of view is more useful approach in terms of technical assessments, especially for using the pozzolanic materials as supplementary cementing material.

Compressive strength of the lime-pozzolan pozzolan pastes at 3, 7, and 28 days of age are shown in Figure 4.6. The natural zeolites, GZ and BZ, exhibited a completely different behavior in compressive strength of lime-pozzolan pastes. Compressive strength of the paste made with BZ was significantly lower than that of the paste with GZ for all the testing ages, although they showed comparable behavior in terms of Ca(OH)₂ consumption and conductivity of lime-pozzolan suspensions. The air voids which can be observed by a naked eye and seen on the digital images of fractured surface of the paste with BZ are probably the major cause of its lower compressive strength when compared to the paste with GZ (Figure 4.7). As seen from Figure 4.7b, the lime-pozzolan paste prepared with BZ contains large air voids which are in range of 0.1-0.5 mm in diameters whereas the

paste with GZ seems to be free of such kind of air voids (Figure 4.7a). Formation of air voids in BZ paste may be related with gas forming property of thermally treated natural zeolites. Although this ability is provided in a great extent by thermal treatment of the zeolites at temperatures higher than 300-400°C, it can be expected that the finely ground natural zeolites which were oven dried at 105°C before grinding may show this kind behavior in a limited extent. A question arising here is why BZ behaved to form air voids whereas GZ did not. The author is unable to explain this behavior of BZ with the data available in scope of the study. However it is clear that the air voids formed into BZ-lime paste is directly responsible for its relatively low strength.

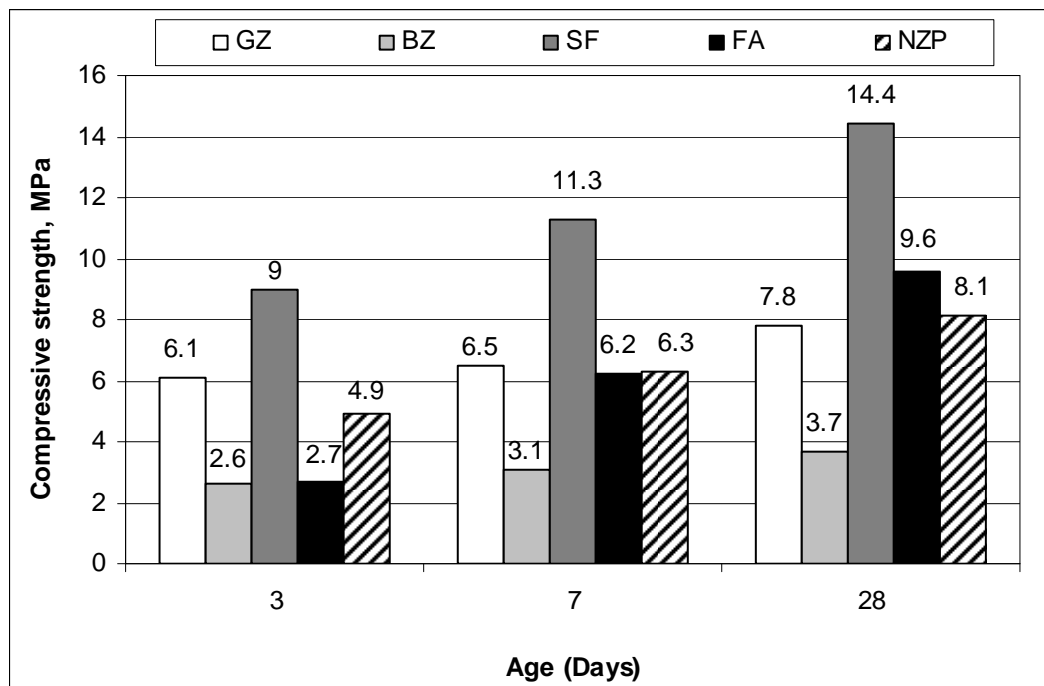
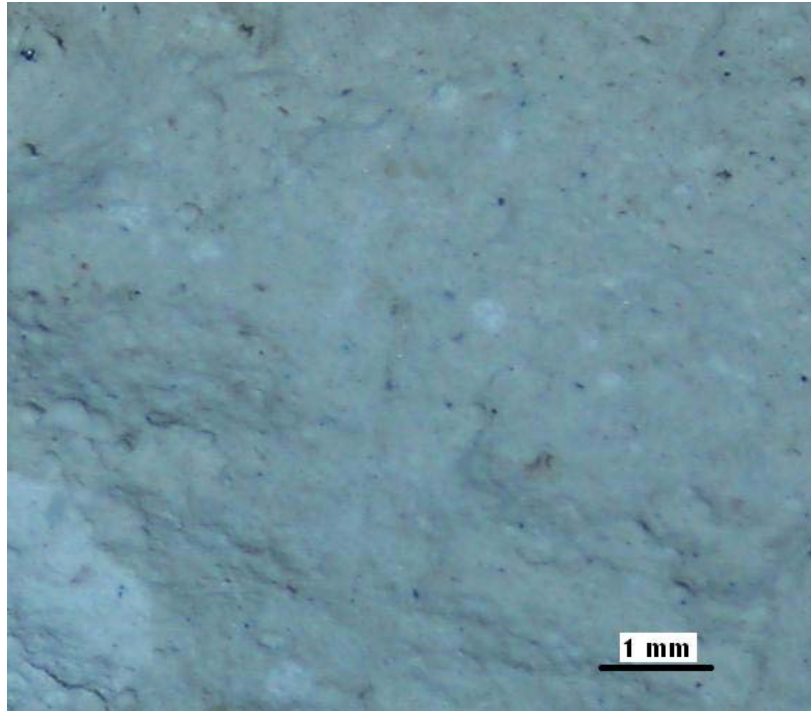
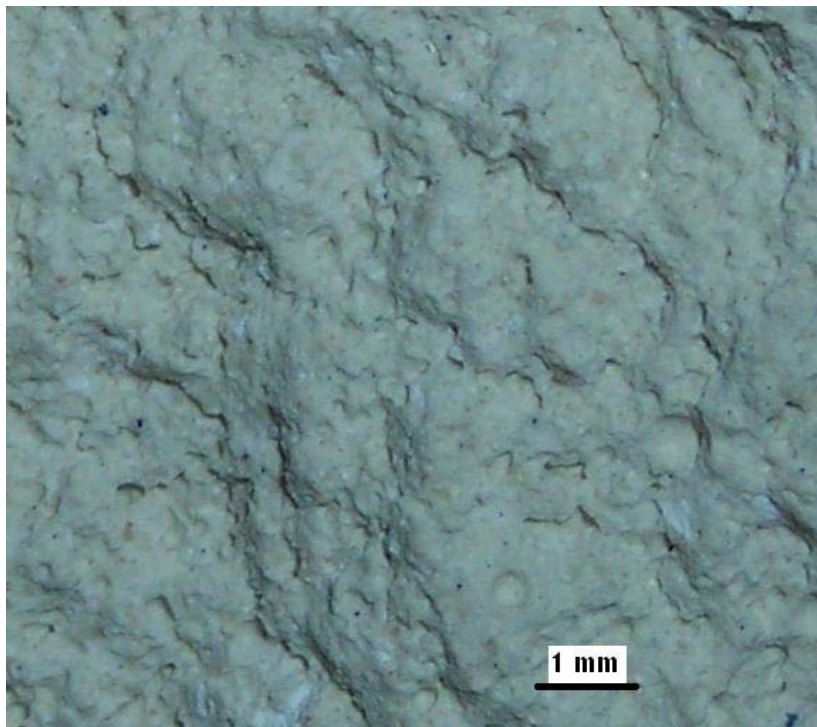


Figure 4.6 Compressive strength of lime-pozzolan pastes



a) Paste with GZ



b) Paste with BZ

Figure 4.7 Digital images of fractured surfaces of the lime-pozzolan pastes

Compressive strength of lime-pozzolan pastes prepared with SF was considerably higher than those of the pastes with the natural zeolites, fly ash and non-zeolitic pozzolan for all the test ages, likely as a result of its highest SiO₂ content among the others. At 3 days of age, lime-pozzolan paste with GZ exhibited higher strength than the pastes with FA and NZP whereas they showed similar strength values at 7 days. The higher strength performance of GZ at 3 days is probably due to its relatively high BET surface area being a dominant parameter for early stages of pozzolanic reaction, as clearly indicated by the electrical conductivity measurements on lime-pozzolan-water systems. At 28 days of age, the paste with GZ showed a compressive strength slightly lower than the paste with FA and similar to the paste with NZP, although the amounts of reacted lime in FA and NZP pastes were considerably lower than that in GZ paste (Figure 4.1). The lack of correlation between the amount of reacted Ca(OH)₂ and compressive strength of lime-pozzolan pastes when comparing pozzolanic materials, despite the correlation for a specific material, is illustrated in Figure 4.8 with 3-day, 7-day, and 28-day values for each material. This is a general case according to data in published literature on lime-pozzolan pastes as indicated in Figure 2.1.

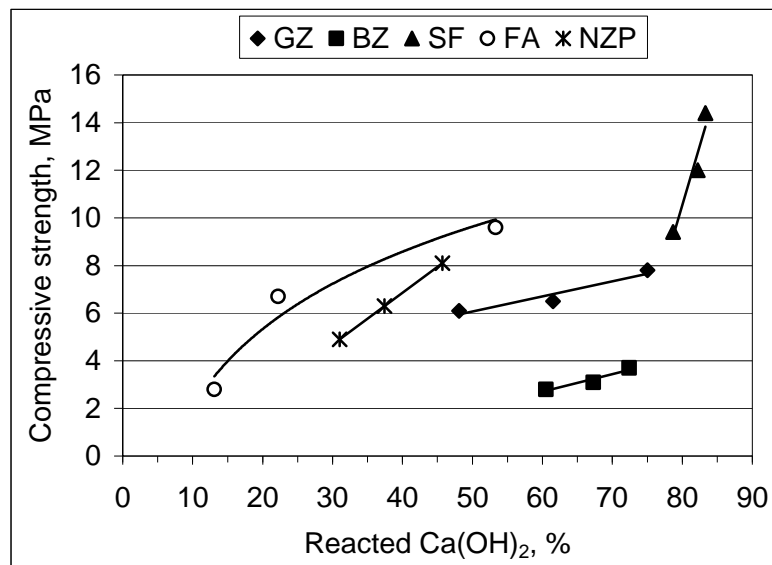
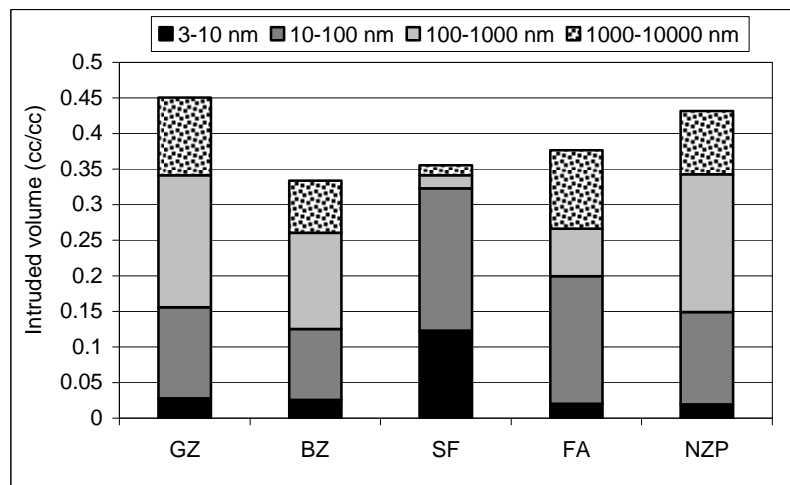


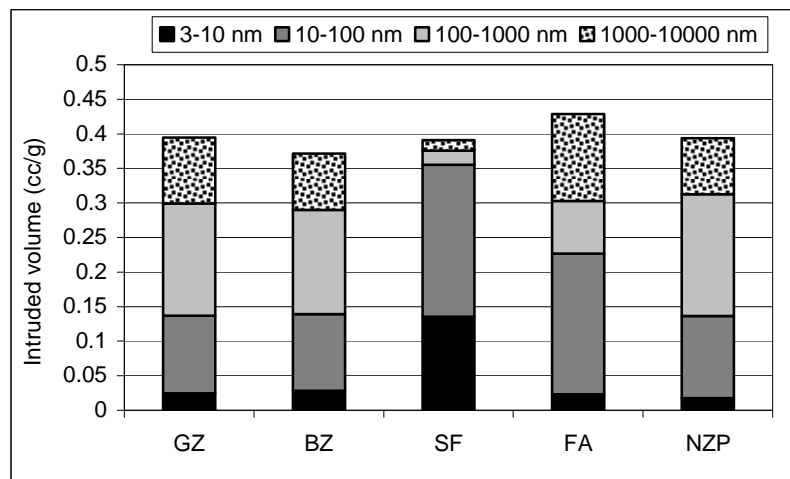
Figure 4.8 Relationship between the amount of reacted Ca(OH)₂ and compressive strength of lime-pozzolan pastes

4.1.4 Pore size distribution of the lime-pozzolan pastes

Pore size distributions of the lime-pozzolan pastes as determined by mercury intrusion porosimetry (MIP) are illustrated in Figure 4.9 for certain ranges of pore diameters. This kind of illustration gives an opportunity to compare the pastes with respect to the amounts of gel pores (< 100 nm) and capillary pores (> 100 nm) separately. Bulk density of the hardened pastes was measured and used to convert the pore volumes from cc/g to cc/cc and distributions are illustrated for both units.



a) distribution based on unit volume of the pastes (cc/cc)



b) distribution based on unit mass of the pastes (cc/g)

Figure 4.9 Pore size distribution of lime-pozzolan pastes as determined by MIP

As seen from the Figure 4.9, total porosity of the paste with BZ was lower than that of the paste with GZ. It seems that the formation of air voids which can be observed on fractured surface of the BZ paste by a naked eye are only limited for large voids and these voids did not effect the size distribution of pores smaller than 10000 nm (10 μm) as determined by MIP. Some reports on published literature already concluded that air voids are not generally recognized in the MIP plots [27] and more specifically entrained air voids only introduces the large air voids observable by a naked eye, and does not alter the characteristic fine pore structure of hydrated cementitious systems appreciably [70]. The lower total porosity of BZ paste than that of GZ paste when the porosity expressed as cc/cc is directly related to lower bulk density of BZ paste caused from the large air voids observable by a naked eye.

Regarding the relationship between total porosity and compressive strength of lime-pozzolan pastes, a weak linear correlation was observed between two parameters for 28 days of age as shown in Figure 4.10, when the paste with BZ was excluded due to its low compressive strength caused by the formation of air voids in macro scale. As seen from the figure, the lower the total porosity, the higher the compressive strength. On the other hand, it is well known that the pore size distribution, not the total porosity, actually controls the strength and relatively small pores (< 50 or 100 nm) do not adversely influence the mechanical strength of the hardened cementitious systems. Accordingly, a perfect correlation was observed between the amounts of pores smaller than 100 nm and compressive strength of pastes when BZ paste excluded again as shown in Figure 4.11. When it is assumed that the pores smaller than 100 nm are the gel pores, their amounts can be directly associated with the amounts of binding gel formed as a result of pozzolanic reaction. The data in Figure 4.11 supports this assumption since it is reasonable that the compressive strength of the lime-pozzolan pastes is mainly determined by the amount of the binding gel formed. Thus, it can be concluded that the amount of binding gel in GZ and BZ pastes was lower than those in SF and FA pastes whereas similar to that in NZP. It can also be concluded from the amount of pores smaller than 100 nm (Figure 4.11) that strength contribution directly originated from

pozzolanic reaction of BZ is slightly lower than that of GZ when the negative effect caused from formation of air voids ignored. This conclusion is already consistent with slightly lower lime fixation ability of BZ when compared to GZ.

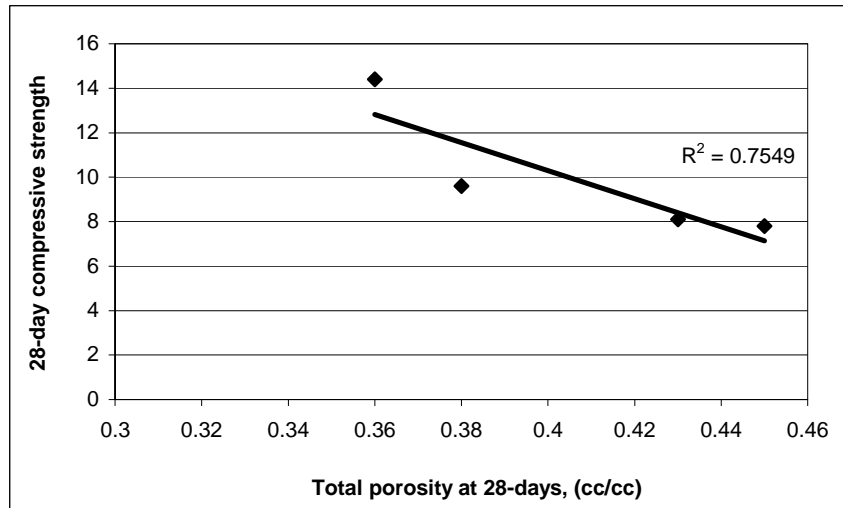


Figure 4.10 Correlation between porosity and compressive strength of lime-pozzolan pastes (the paste with BZ excluded)

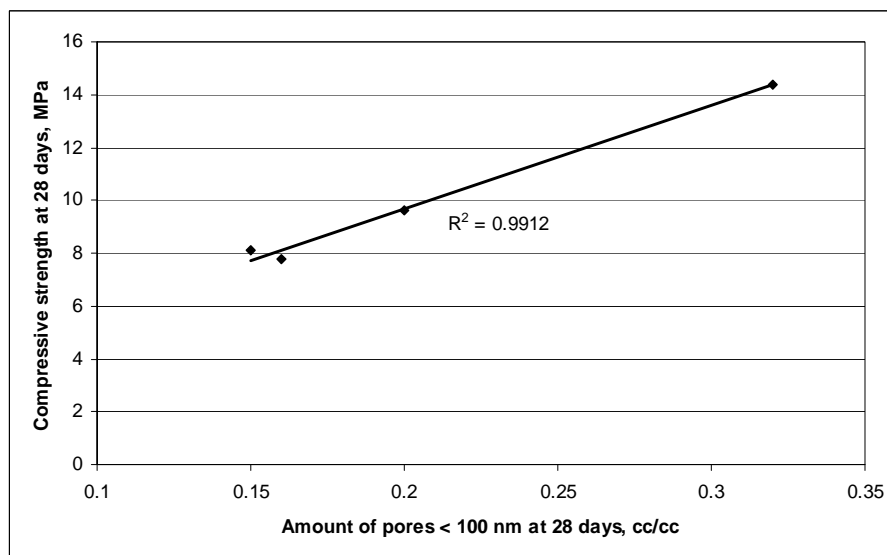


Figure 4.11 Correlation between the amount of pores smaller than 100 nm and compressive strength (the paste with BZ excluded)

4.1.5 Strength activity index (SAI)

Water requirements and strength activity indices of the pozzolanic materials were determined in accordance with ASTM C 311 and given in Table 4.1 together with the amounts of water used in preparation of the mortars.

Table 4.1 Strength activity indices (SAI) of the pozzolanic materials
(ASTM C 311 [52])

	GZ	BZ	SF	FA	NZP
w/cem	0.56	0.54	0.70 [*]	0.51	0.55
Water requirement, %	116	112	145	105	114
Strength activity index, %					
7-days	71	78	73 [*]	86	71
28-days	91	98	96 [*]	93	81

^{*}Although ASTM proposed a different test method for the strength activity of silica fume (ASTM C 1240 [71]), ASTM C 311 [52] method was applied for an identical comparison.

Regarding to water requirement of the pozzolanic materials, it was observed that water requirement of GZ is slightly higher than the maximum limit value, 115%, proposed by ASTM C 618 [72] whereas BZ satisfy the proposed limit. Water requirement of the natural zeolites was lower than that of SF, higher than that of FA, and similar to that of NZP. Although this case seems to be related to specific surface area of the materials when the natural zeolites, FA and NZP considered, the significantly higher water requirement of SF indicated that particle size distribution and/or median particle size is also an influencing factor. Because water requirement of SF is higher than those of the natural zeolites in spite of the fact that BET surface area of SF is lower than those of the natural zeolites. Therefore the higher water requirement of SF could be attributed to its finer particle size distribution.

Before discussion on strength activity index of the materials, it should be noted that strength activity index is a parameter reflecting not only strength contribution caused by pozzolanic activity of the materials but also their strength contribution originated from filler effect in microstructure of paste matrix and aggregate-cement paste transition zone in mortar specimens. In addition water requirement of the pozzolanic materials is another factor influencing its strength activity index because it is well known that the higher the w/cm the lower the mechanical strength of cementitious systems.

ASTM C 618 specifies the strength activity index of at least 75% for 7 days or 28 days. Based on this limitation, it was determined that GZ and BZ satisfy the strength activity requirement of ASTM C 618. BZ exhibited higher strength activity than GZ at both ages. As concluded in previous section, strength contribution directly originated from pozzolanic reaction of BZ is slightly lower than that of GZ, if the negative effect caused from formation of air voids ignored. It was observed no air voids in visual inspection of fractured surface of hardened mortars prepared with BZ for strength activity test. Therefore strength contribution caused from pozzolanic reaction of BZ is lower than that of GZ in strength activity index test mortars. Thus, the higher strength activity of BZ can be mainly attributed to combined effects of its finer particle size distribution increasing the strength contribution originated from filler effect, and slightly lower water-to-cementitious materials ratio of BZ test mortar.

Strength activity index of BZ was higher than that of SF for both test age, however the reverse is true for GZ. The lower strength activity of SF despite its extremely high pozzolanic activity is probably due to significantly high w/cm of its mortar.

GZ exhibited lower SAI when compared to FA for 7 and 28 days of age. BZ showed lower SAI than FA at 7 days, however, the reverse was true at 28 days. The higher 7-days SAI of FA is probably due to lower w/cm of FA test mortar whereas the reverse case for BZ at 28 days can be associated with combined

influences of strength contributions originated from pozzolanic reaction and filler effect of BZ.

Comparing SAIs of natural zeolites and NZP, it was observed that SAI of GZ was similar to that of NZP at 7 days, however at 28 days SAI of GZ was significantly higher than that of NZP, which is clearly attributed to higher pozzolanic activity of GZ between 7 days and 28 days of age. BZ exhibited higher SAI values than NZP at both ages due to more efficient filler effect of BZ, in addition to its pozzolanic activity, as mentioned before.

4.1.6 Overall evaluation on pozzolanic activity of the natural zeolites

The term “pozzolanic activity” consists of two main concerns; reactivity with lime and strength gaining as a result of this reactivity.

The natural zeolites tested were found to be highly reactive in terms of ability to consume the available lime in medium, that is, more reactive than FA and NZP but slightly less reactive than SF. In addition, GZ-lime paste exhibited a better performance in 3-day compressive strength than FA-lime and NZP-lime pastes whereas BZ-lime paste performed weakly in terms of strength at all the test ages due to air voids on its macro structure. However, when 28-day strength considered, GZ remained behind of FA while it is equivalent to NZP.

Considering 28-day compressive strength and Ca(OH)_2 consumption data of the pozzolanic materials in the experimental program, the natural zeolites, which have a crystalline structure, are distinguished from the glassy pozzolanic materials by relatively low ratio of compressive strength to the amount of reacted lime, as shown in Figure 4.12.

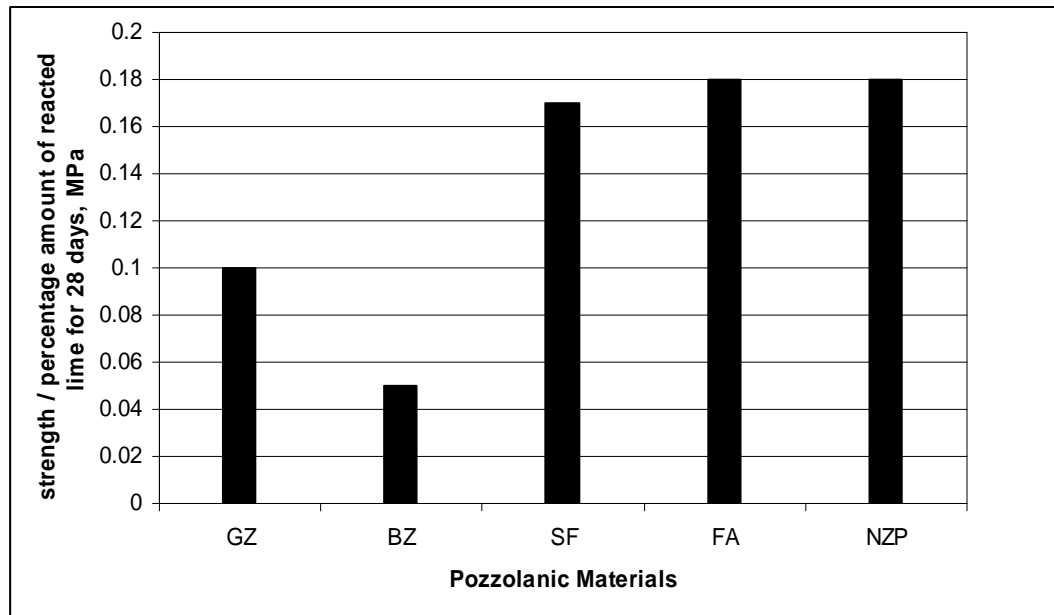


Figure 4.12 Strength-to-percentage amount of reacted lime ratio for the lime-pozzolan pastes

In terms of strength activity index which is a useful and widely-used parameter for practical evaluation of finely ground mineral admixtures, the natural zeolites showed a considerable performance when compared to the other materials. Especially BZ exhibited higher 28-day SAI value than all the other materials, even than SF, due to its more efficient filler effect in addition to its high pozzolanic reactivity.

4.2 Properties and Hydration of Zeolite Blended Cements

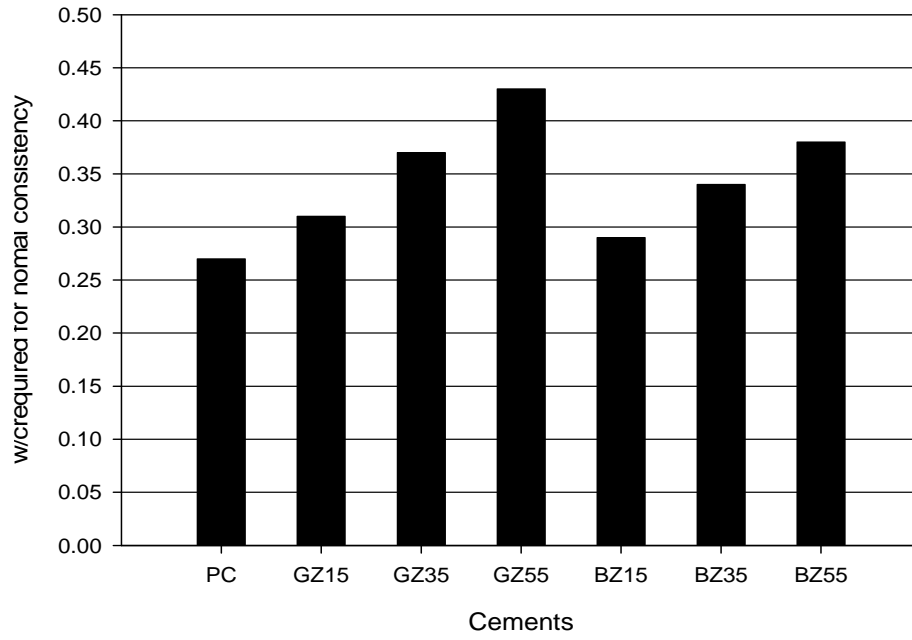
4.2.1 Normal consistency and setting time

The amount of water required for normal consistency and initial/final setting time of the zeolite blended cements and the reference Portland cement were determined and given in Figure 4.13.

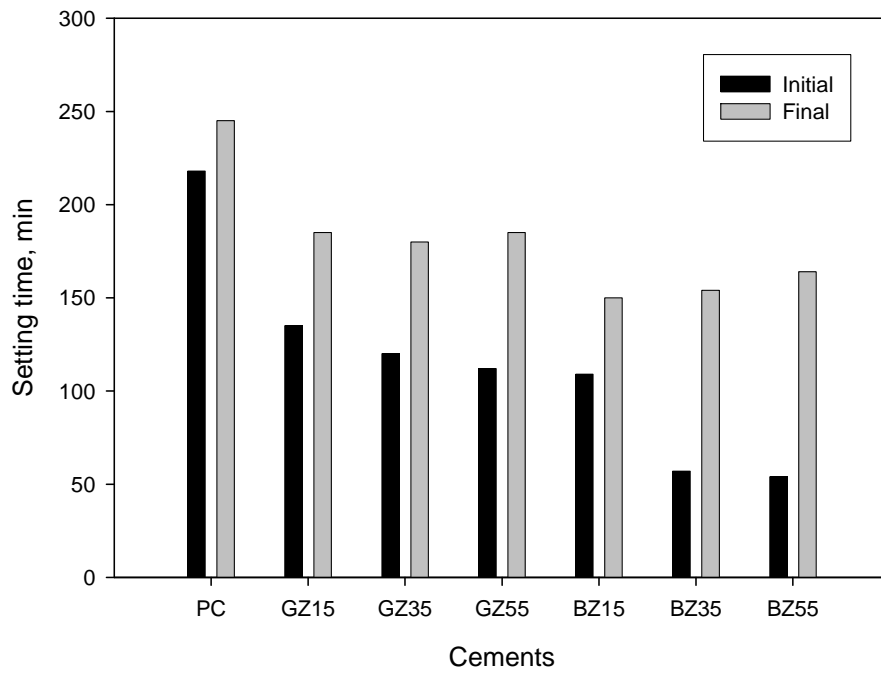
As seen from Figure 4.13a, w/c corresponding to normal consistency increased with increasing amount of natural zeolite in blended cements, due to water adsorption

property of the zeolites. Blended cements with GZ required more water for normal consistency when compared to the blended cements with BZ for the same level of zeolite replacement, which is due to lower BET surface area of BZ when compared to that of GZ. A perfectly linear correlation between specific surface area of the cements and their water demands for normal consistency was determined, as shown in Figure 4.14. Specific surface area values of the blended cements used in Figure 4.14 was calculated via the mixture rule based on Blaine surface area value for the portland cement and BET surface area values for the ground natural zeolites.

Initial and final setting times of all the blended cements were shorter than that of the reference portland cement, and initial setting time of the blended cements shortened as their zeolite contents increased (Figure 4.13b). It is usually expected that increasing amount of mineral replacement materials and decreasing amount of portland cement in blended systems results in longer setting times. The reverse case observed for initial setting times of the zeolite blended cements is probably due to decrease in consistency of the pastes caused by continuous water adsorption of zeolite particles after preparation of the paste and thus decrease in consistency of the pastes results in shorter initial setting time measurements. It is observed from Figure 4.13b that this kind of mechanism is not so effective on final setting time values, however final setting times of the zeolite blended cements are still shorter than that of the reference portland cement. Such kind of behavior of natural pozzolan blended systems was also reported in published literature [3, 4, 5].



a) water-to-cement ratio for normal consistency



b) Initial and final setting time of the cements

Figure 4.13 Normal consistency and setting time of the cements

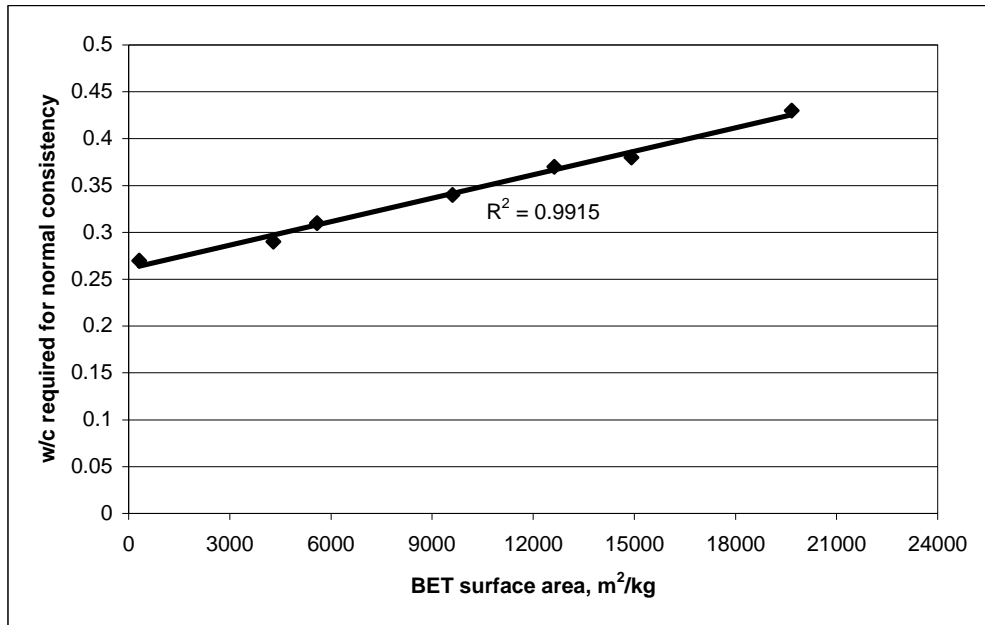
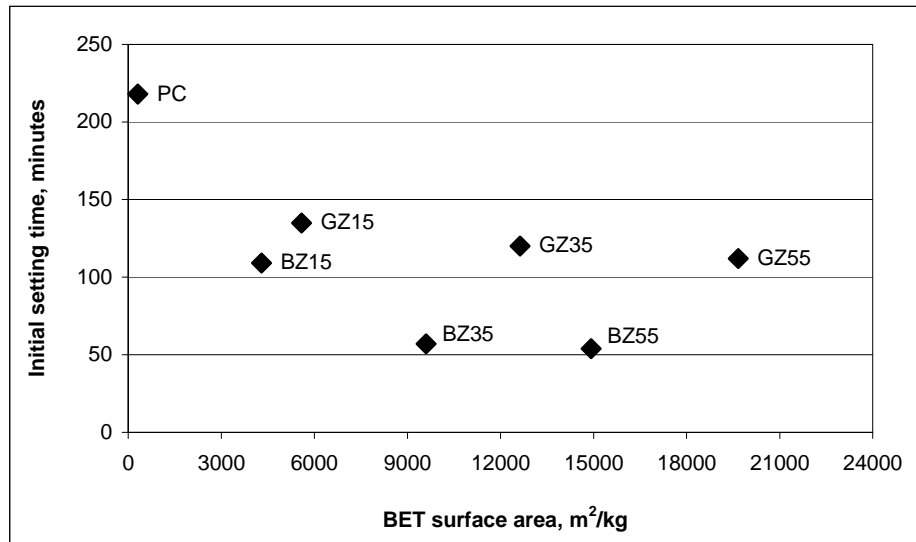


Figure 4.14 Relationship between BET surface area and water demand of the cements

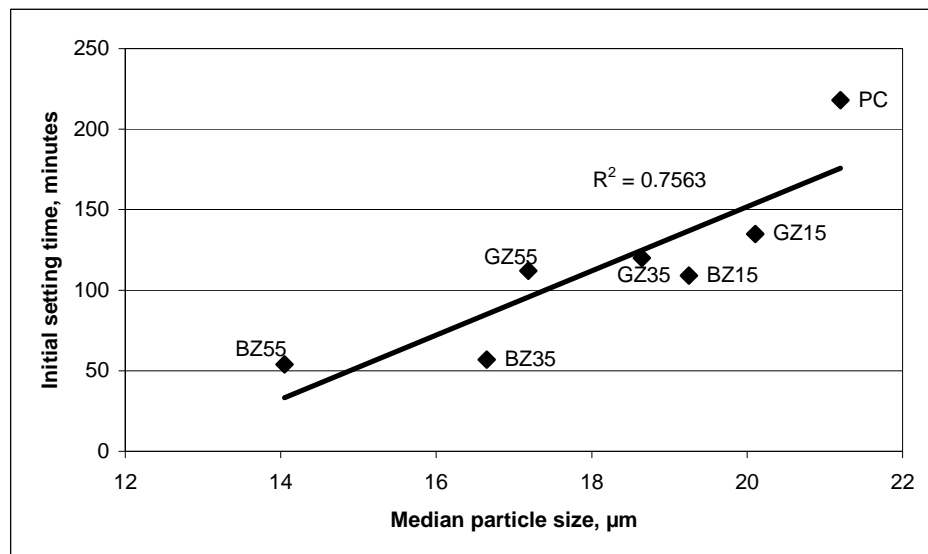
The blended cements with BZ exhibited shorter initial and final setting times than those with GZ for a given zeolite content, especially when initial setting time of the blended cements containing 35% and 55% zeolite considered. In order to find reasonable explanations for faster initial setting of BZ blended cements, possible correlations between physical properties and initial setting time of the cements were examined. For this purpose, physical properties of the blended cements such as median particle size and specific surface area were calculated via the rule of mixture from the parameters corresponding to each component; portland cement and finely ground zeolite.

The plots of surface area versus initial setting time and median particle size versus initial setting time are shown in Figure 4.15. As seen, there is no correlation between BET surface area of the cements and their initial setting times whereas a correlation with an acceptable R^2 value exists between median particle size and initial setting time of the cements. Therefore smaller particle size distribution of BZ

could be described as one of the factors responsible for faster initial setting of blended cements containing BZ than those containing GZ.



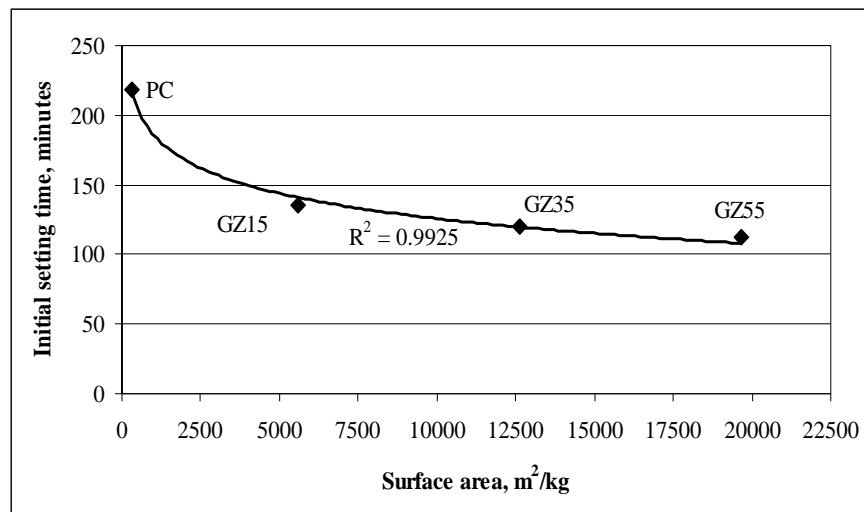
a) BET surface area vs. initial setting time plot for the cements



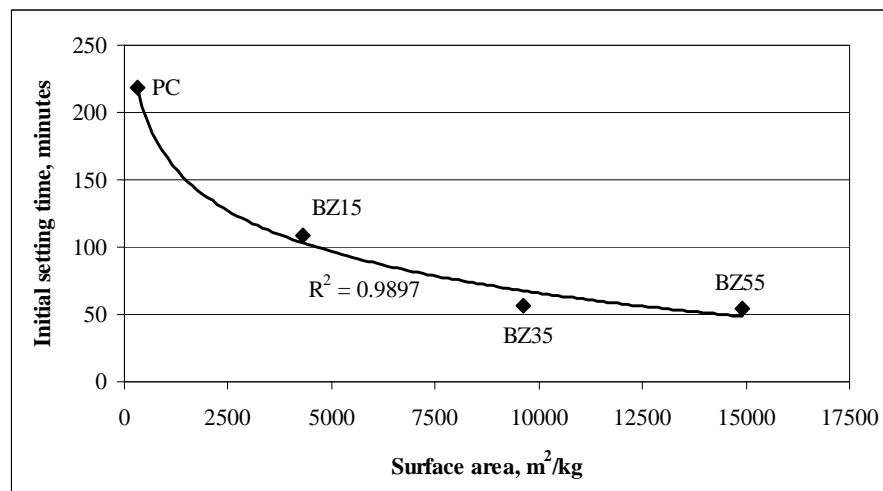
b) Median particle size vs. initial setting plot

Figure 4.15 Relationships between surface area and initial setting time; median particle size and initial setting time of the cements

Despite the lack of a general correlation between physical parameters of the natural zeolite blended cements and their initial setting times, a good logarithmic correlation was observed between surface area and initial setting time of the blended cements when only the blended cements containing GZ or BZ considered separately (Figure 4.16). These kinds of correlations were also observed for final setting time of the cements (Figure 4.17).

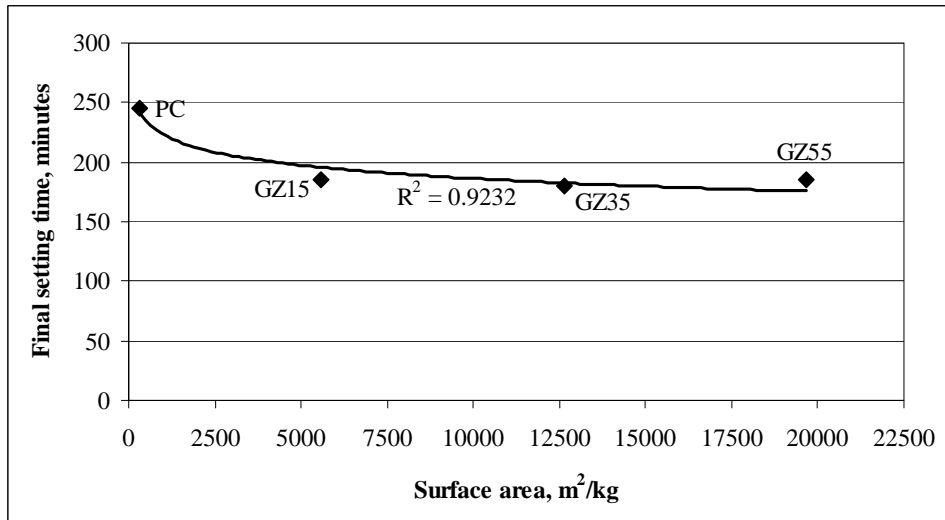


a) GZ blended cements and PC

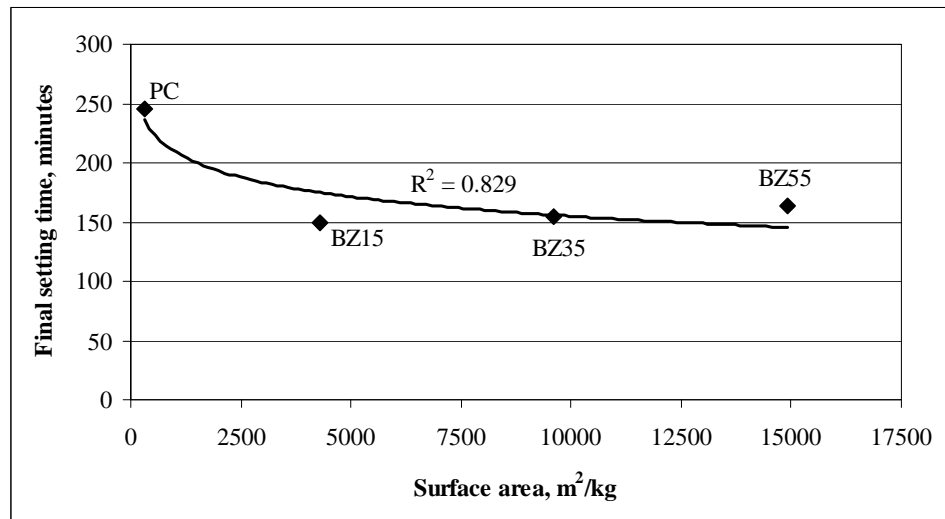


b) BZ blended cements and PC

Figure 4.16 Relationship between BET surface area of blended cements their initial setting times for individual analyses of GZ and BZ blended cements



a) GZ blended cements and PC



b) BZ blended cements and PC

Figure 4.17 Relationship between BET surface area of blended cements their final setting times for individual analyses of GZ and BZ blended cements

From all the evaluation above, it can be concluded that faster initial and final setting time of zeolite blended cements when compared to reference PC is directly related to high BET surface area of the finely ground natural zeolites. Comparing the influence of GZ and BZ addition on initial setting time of blended cements, the correlation between median particle size of the cements and their initial setting times (Figure 4.15b) revealed that the finer particle size distribution (smaller

median particle size) of BZ is responsible for the faster initial setting time of BZ incorporated blended cements than that of GZ blended cements for an equal replacement level.

4.2.2 Free Ca(OH)₂ content of the cement pastes

Amounts of free Ca(OH)₂ in cement pastes were determined by thermal analysis, and the results were expressed as percent by ignited weight of the paste. TGA plots of the cement pastes are given in Appendix B. Free Ca(OH)₂ contents of the hardened cement pastes and their normalized values to PC content in cements are given in Table 4.2. In blended systems, as replacement level increases, Ca(OH)₂ consumption increases due to increased amount of pozzolanic material, and also its production decreases due to decreased amount of PC. Therefore free Ca(OH)₂ contents are also expressed as normalized to PC content in order to evaluate Ca(OH)₂ consumption process effectively. For this purpose, free Ca(OH)₂ content values were divided by PC fraction value in cements. For instance, free Ca(OH)₂ content value of paste of blended cement containing 35% natural zeolite was divided by 0.65 whereas the dividing value was 1.00 for the reference PC paste.

Table 4.2 Free Ca(OH)₂ contents of the cement pastes
(% by weight of ignited paste)

Cement	% Ca(OH) ₂			% Ca(OH) ₂ (normalized to PC content)		
	3-day	7-day	28-day	3-day	7-day	28-day
PC	18.1	18.9	21.6	18.1	18.9	21.6
GZ15	13.0	15.7	16.0	15.3	18.5	18.8
GZ35	4.6	9.7	8.9	7.1	14.9	13.7
GZ55	4.2	5.3	0.8	9.3	11.8	1.7
BZ15	15.6	16.2	17.4	18.4	19.1	20.5
BZ35	12.0	12.1	9.1	18.5	18.6	14.0
BZ55	6.9	7.1	2.8	15.3	15.8	6.2

Ca(OH)_2 content of all the blended cement pastes was lower than that of the reference PC paste at all test ages, and Ca(OH)_2 content decreased as the zeolite content increased in blended cements (Table 4.2). This case is not only due to decreasing lime production with decreasing PC content but also due to increasing lime consumption with increasing zeolite content. Ca(OH)_2 content of the blended cements containing GZ was lower than that of blended cements with BZ for a given zeolite content, which clearly indicated that GZ has a higher potential to consume Ca(OH)_2 when compared to BZ. This is in line with the experimental results obtained for lime-pozzolan pastes.

At the end of 28 days, it was observed that Ca(OH)_2 in GZ55 blended cement paste is almost completely consumed, i.e. only 0.8% remained, whereas 2.8% Ca(OH)_2 is still available in BZ55 paste.

Focusing on normalized amount of Ca(OH)_2 with respect to the amount of portland cement fraction in blended cements, consumption process of available lime was indicated graphically for GZ and BZ blended cements as shown in Figure 4.18 and Figure 4.19, respectively.

As seen from Figure 4.18, for 7 days and 28 days of age, increasing amount of GZ content in blended cements resulted in decreasing normalized Ca(OH)_2 contents. However, for 3 days, it was observed that normalized amount of Ca(OH)_2 in GZ55 is lower than that in GZ35. Since it is theoretically impossible that consumption of Ca(OH)_2 decreasing with increasing pozzolan content, relatively high amount of Ca(OH)_2 in GZ55 paste could be attributed to increasing Ca(OH)_2 production probably due to nucleation effect enhancing the hydration of portland cement phase in blended system. Published literature contains many reports on nucleation effect of ultrafine materials on hydration of portland cement phase by providing nucleation sites for more effective growth of hydration products [73, 74, 75, 76].

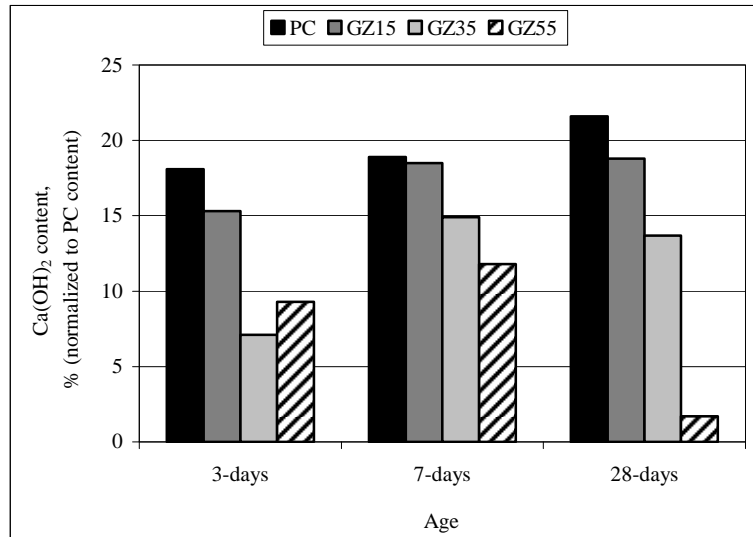


Figure 4.18 Ca(OH)₂ content of GZ blended cements and PC (normalized to PC content)

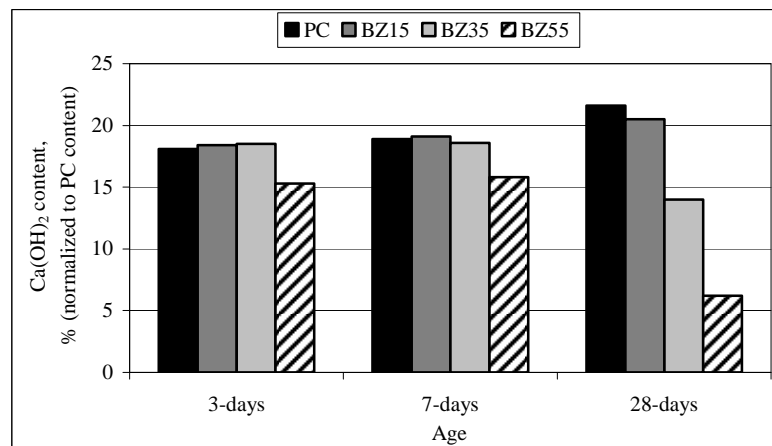


Figure 4.19 Ca(OH)₂ content of BZ blended cements and PC (normalized to PC content)

The nucleation effect providing enhancement of hydration of portland cement phase was observed more clearly on BZ blended cement pastes at 3 days and 7 days of age, as seen from Figure 4.19. Normalized Ca(OH)₂ contents of pastes of blended cements containing 15% and 35% BZ at 3 days and 7 days were higher or similar than that of reference PC paste. The higher or similar normalized Ca(OH)₂ content in blended cements despite the lower portion of PC and higher portion of the pozzolanic material indicates an enhancement in hydration of PC phase resulting in

higher amount of Ca(OH)_2 production. The more obvious nucleation effect of BZ replacement when compared to the effect of GZ could be attributed to the finer particle size distribution of BZ, providing more numbers of fine particles as nuclei for a specific volume of paste.

4.2.3 Pore-size distribution of the cement pastes

Pore-size distribution of zeolite blended cement pastes was determined for 15% and 55% replacement levels at 28 and 91 days of age by Mercury Intrusion Porosimetry (MIP), and evaluated comparatively with each other and with the reference portland cement paste. All the test results are given in Figure 4.20. Since total porosity is a parameter which is not able to monitor pore refinement process in blended cement systems, it was focused on pore-size distribution referring to various pore-size ranges for evaluation of hydration process in terms of pore refinement. In addition, it is known that the pore size distribution, not the total porosity, is a better criterion for evaluating the characteristics of a hydrated cement paste. Because it is not the total porosity, but the pore size distribution that actually controls the strength, permeability, and volume changes in a hardened cement paste [6].

In published literature, the pores smaller than 50 nm are associated with microporous cementitious hydrates and the high proportion of these pores means a large proportion of binding material present. The pores bigger than 50 nm and smaller than 100 nm are associated with capillary voids representing the space not filled by the solid components of the hydrated cement paste. Capillary voids larger than 50 nm, referred to as macropores in modern literature, are probably more influential on strength and impermeability characteristics, whereas pores smaller than 50 nm, referred to as micropores, play an important role in drying shrinkage and creep [6, 23].

In order to evaluate the effect of zeolite content on pore-size distribution of the cements, the MIP data are illustrated in Figure 4.21 for different ages separately.

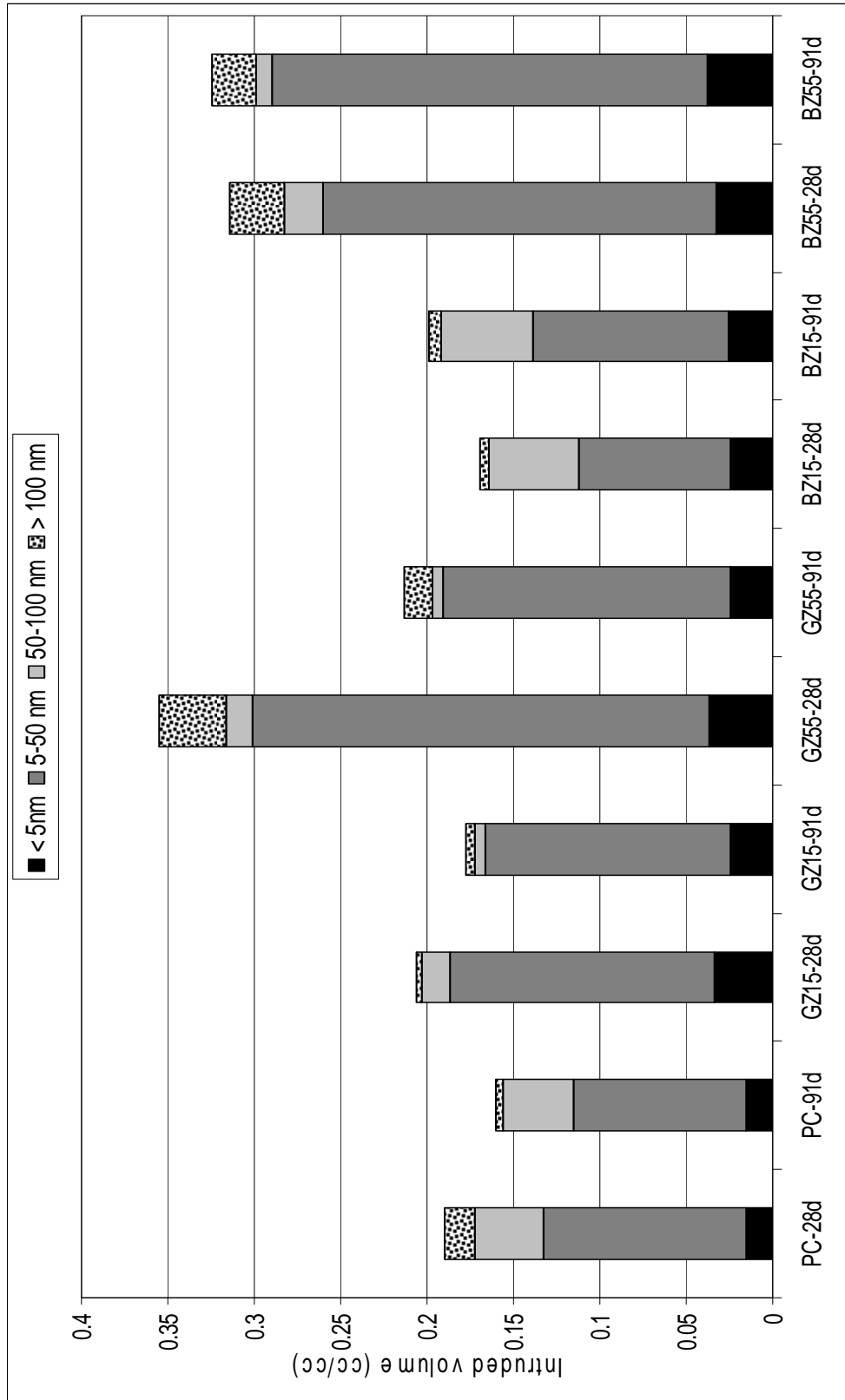
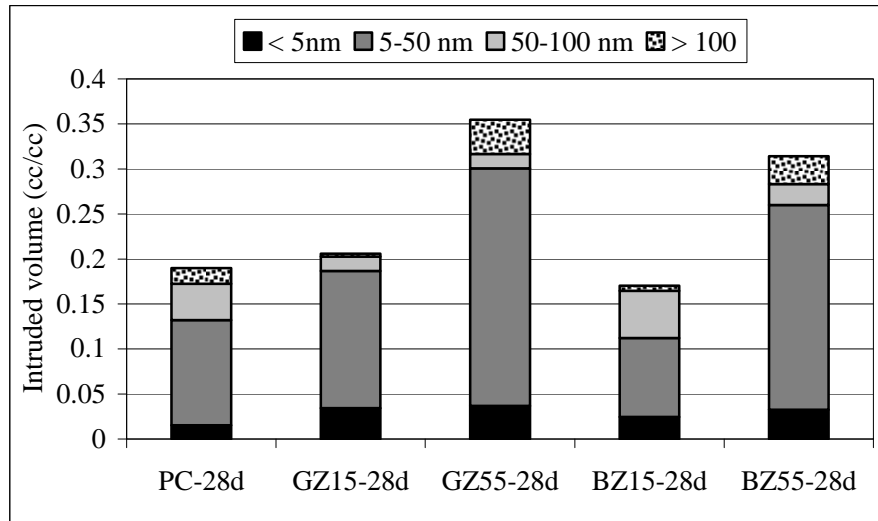
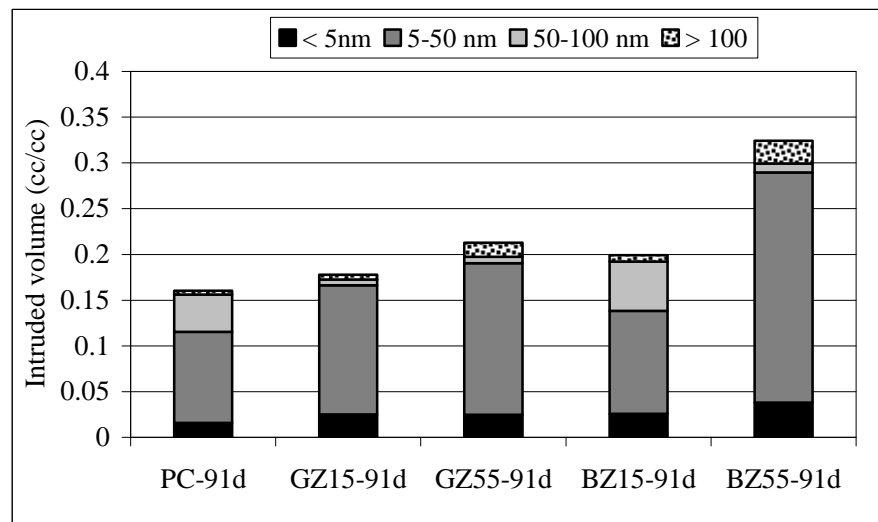


Figure 4.20 Pore size distributions of the cement pastes as determined by MIP



a) Pore size distribution of the cements at 28 days of age



b) Pore size distribution of the cements at 91 days of age

Figure 4.21 Effect of zeolite type and content on pore size distribution of the cement pastes at 28 days and 91 days of age

As seen from Figure 4.21a, at 28 days of age, 15% replacement of portland cement by GZ resulted in a lower amount of capillary pores larger than 50 nm and higher amount of pores smaller 50 nm in blended cement paste when compared to PC paste. This case was also observed for the same amount of BZ replacement but in a lower degree. These results clearly indicate a pore refinement process caused by

pozzolanic reaction of the natural zeolites, i.e. transformation of larger pores into smaller ones by formation of additional pozzolanic gels. Relatively high amount of pores < 50 nm, which are generally associated with cementitious hydrates, in GZ15 paste, when compared to BZ15 paste, confirms relatively high pozzolanic activity of GZ, which is already known from the data in previous sections.

For 55% replacement level, although total porosity of the blended cement pastes, at 28 days, was higher than that of the reference portland cement paste, the difference is mainly originated from the pores smaller than 50 nm which do not negatively affect the strength and permeability characteristics of hardened cement pastes as mentioned above. Since the pores < 50 nm are associated with cementitious hydrates, high amount of these pores in GZ55 and BZ55 pastes could result in high strength and low permeability.

At 91 days of age, capillary pores larger than 100 nm in PC paste disappeared as a result of further hydration continued after 28 days, as seen from Figure 4.21b, whereas the volume of the pores smaller than 100 nm was remained about unchanged. No drastic changes was observed in pore size distribution of GZ15, BZ15 and BZ55 blended cement pastes between 28 days and 91 days of age. However, a considerable decrease in total porosity of GZ55 paste occurred mainly due to decreasing in volume of 5-50 nm pores, which is probably due to progressive formation of pozzolanic reaction and hydration products in blended system. The relatively low pozzolanic activity of BZ paste may be responsible for only slight change in pore size distribution of BZ55 paste between 28 days and 91 days of age.

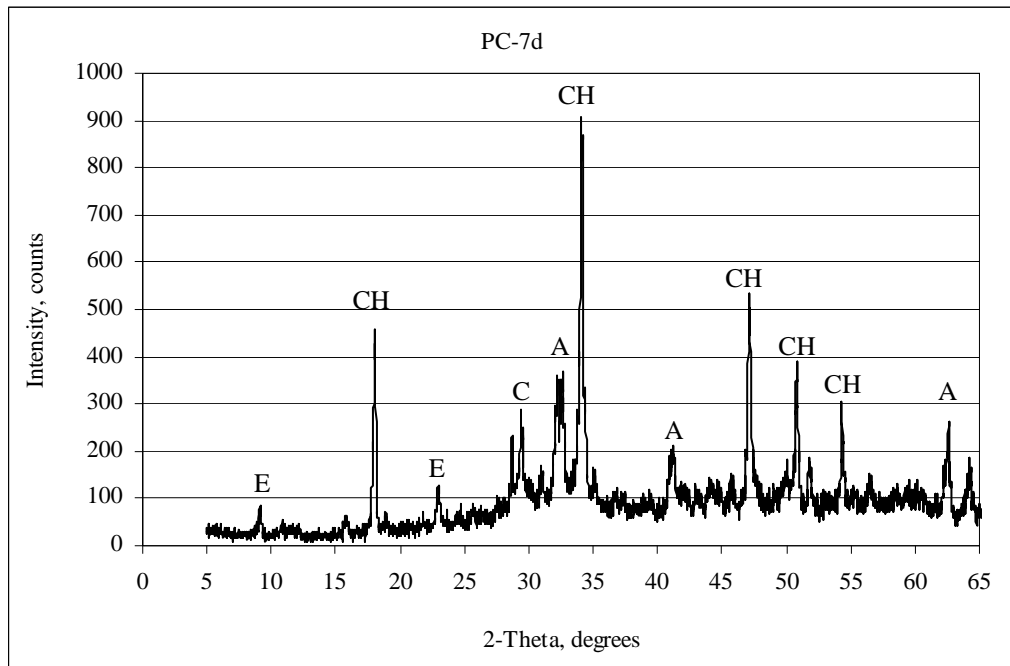
Consequently, it was experimentally shown that incorporation of GZ and BZ natural zeolites into blended cements provides refinement of pore size distribution of the pastes, i.e. transformation of larger pores into smaller ones. At 28 days and especially at 91 days of age, the volume fraction of pores larger than 50 nm in pastes of blended cements containing 15% and 55% natural zeolites was lower than that in reference PC paste, which is very beneficial when it is considered that

capillary pores larger than 50 nm are more influential in determining the strength and impermeability of the pastes. The lower the volume fraction of the pores smaller than 50 nm, the higher the strength and the lower the permeability of the paste. In addition, it should be noted that volume fraction of pores <50 nm in zeolite blended cement pastes is higher than that of reference PC paste and these pores associated with cementitious hydrates, which are mainly influential on drying shrinkage and creep behavior of the pastes.

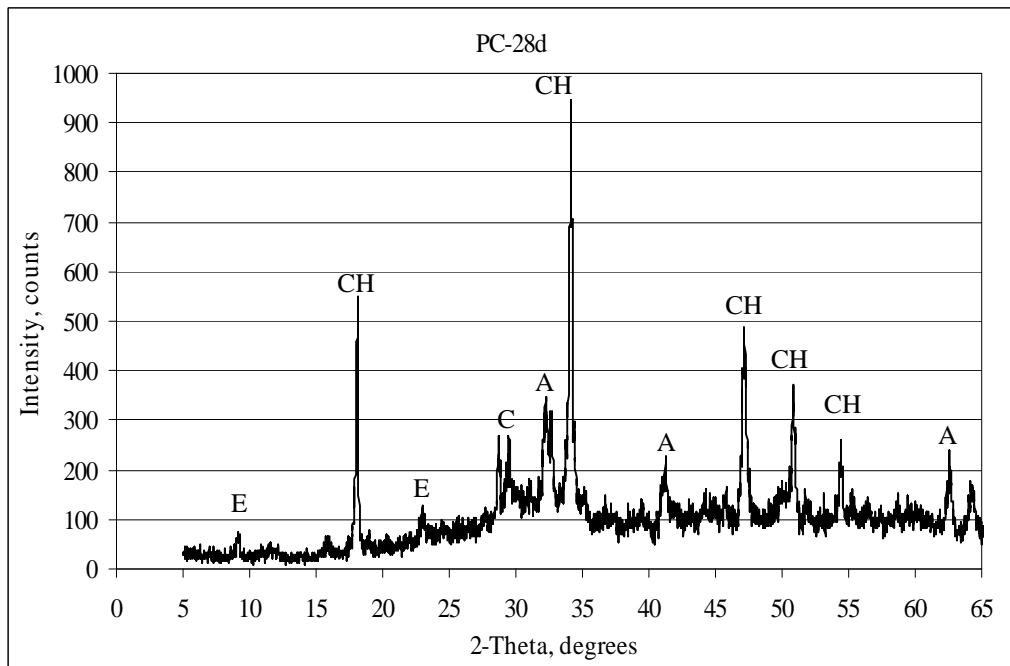
4.2.4 XRD examinations of hardened cement pastes

XRD patterns of the hardened cement pastes are given in Figure 4.22-Figure 4.26 with identified phases for PC, GZ15, GZ55, BZ15, and BZ55 cements, respectively.

As seen from Figure 4.22, crystalline species identified on XRD pattern of hardened PC paste are calcium hydroxide, ettringite, unreacted alite (impure form of $3\text{CaO}\cdot\text{SiO}_2$) as well as calcite which is probably formed as a result of carbonation. Slight increases in intensity of CH peaks at 28-day pattern (Figure 4.22b), when compared to 7-day pattern (Figure 4.22a), confirmed the results on the amount of CH determined by TGA and given in Table 4.2. Alite peaks observed for PC paste at 28 days of age indicated that some part of PC remains unreacted even at 28 days, which is probably associated with large particles of PC.

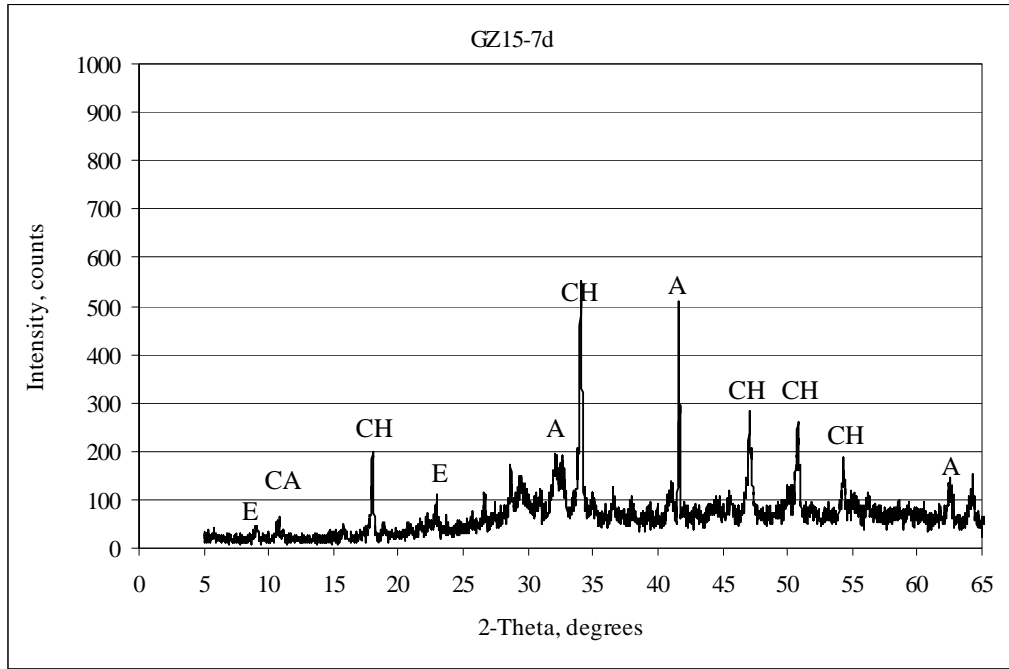


a) 7-day

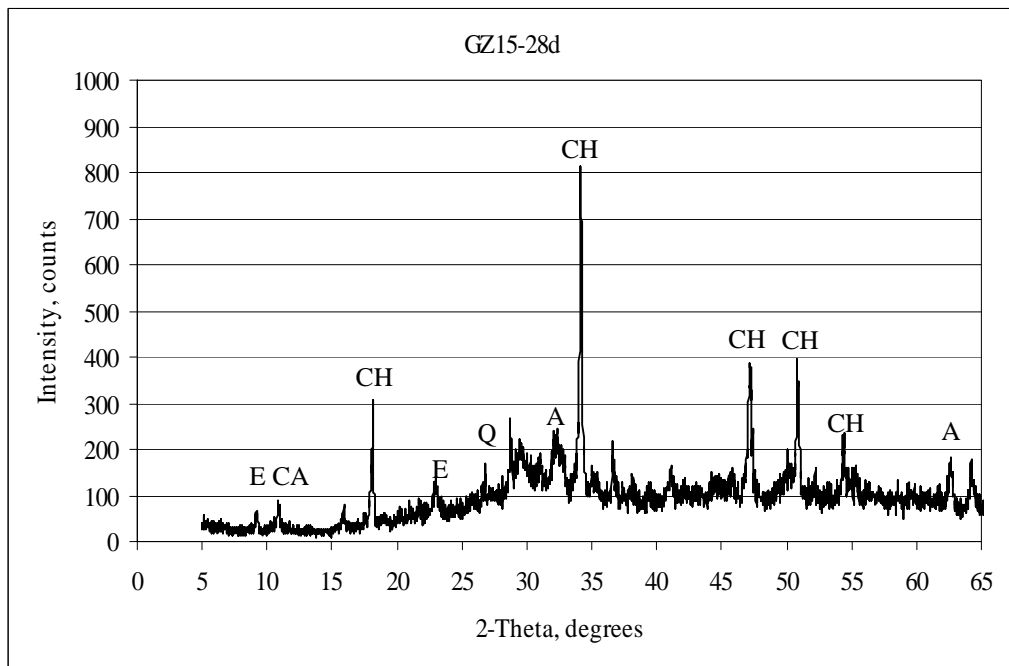


b) 28-day

Figure 4.22 XRD pattern of hardened PC paste at 7 days and 28 days
(A: Alite, C: Calcite, CH: Calcium hydroxide, E: Ettringite)



a) 7-day

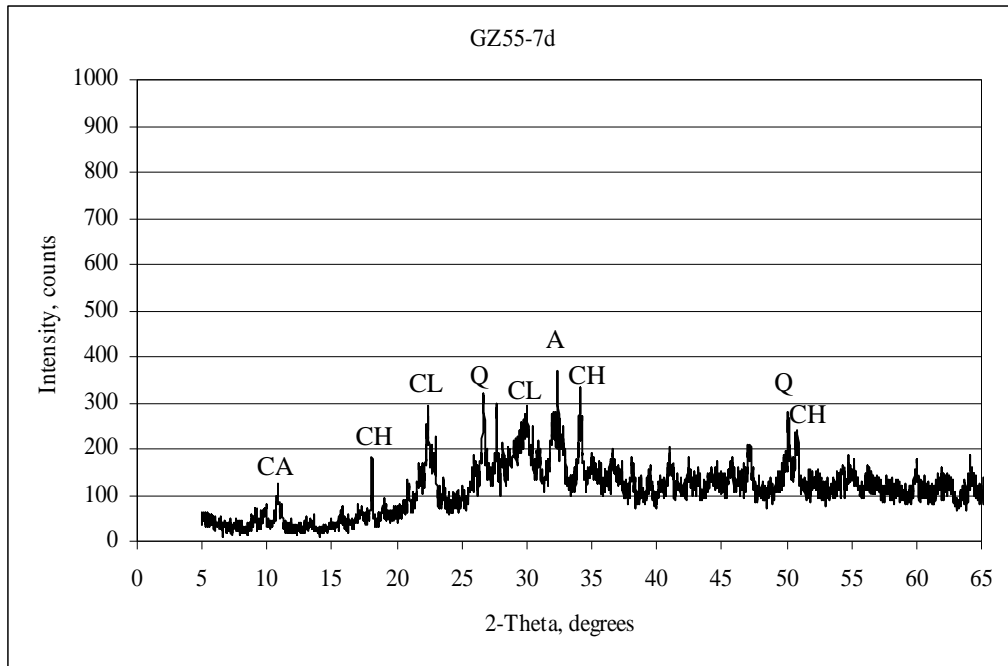


b) 28-day

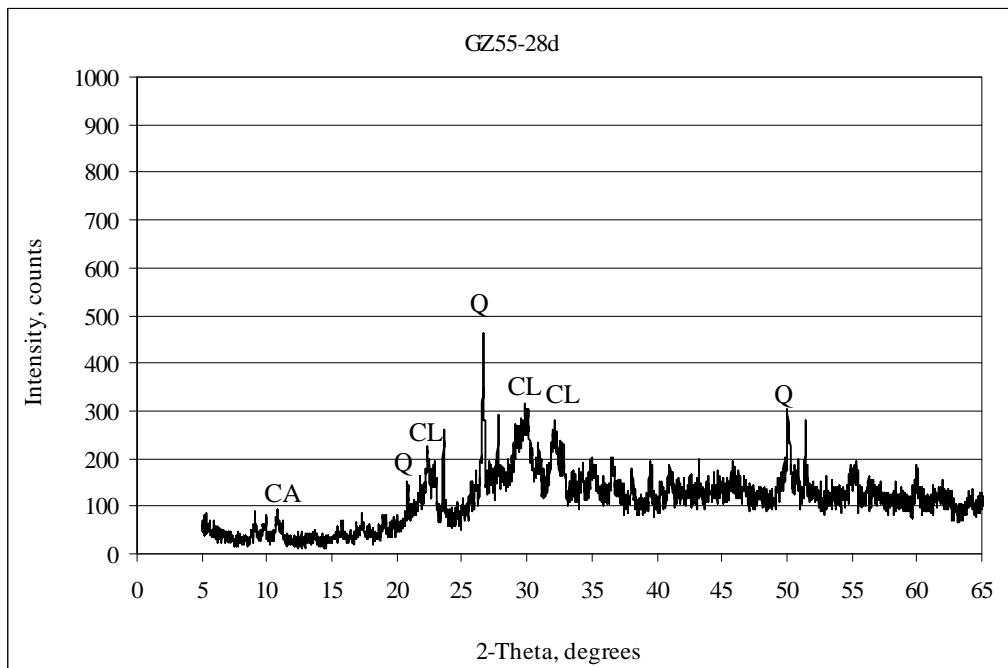
Figure 4.23 XRD pattern of hardened GZ15 paste at 7 days and 28 days

(A: Alite, C: Calcite, CA: Calcium aluminate hydrate (C_4AH_{13}),

CH: Calcium hydroxide, E: Ettringite, Q: Quartz)

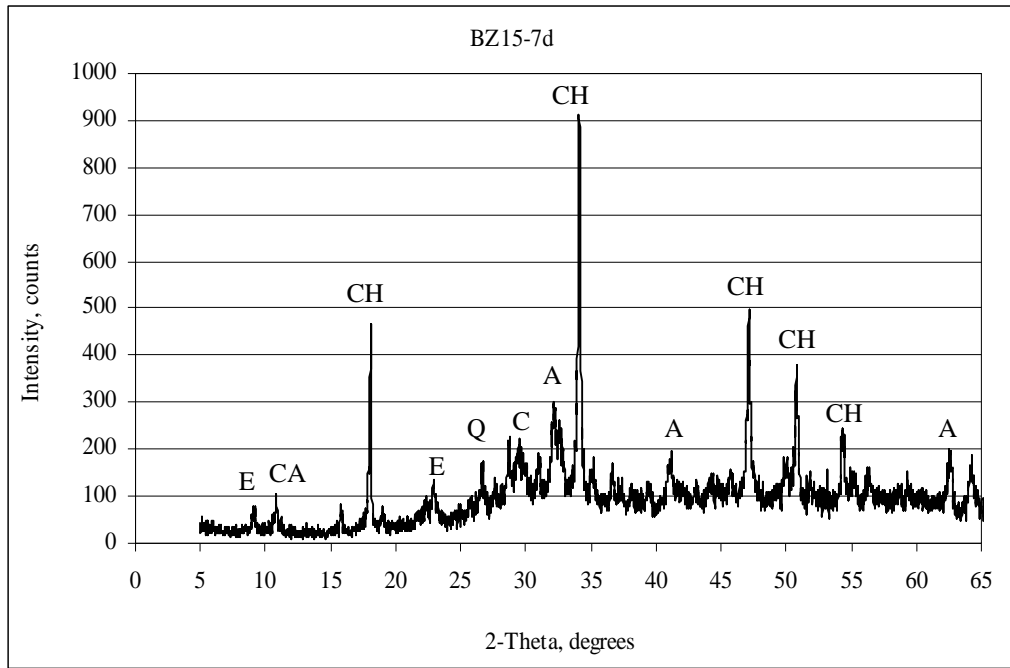


a) 7-day

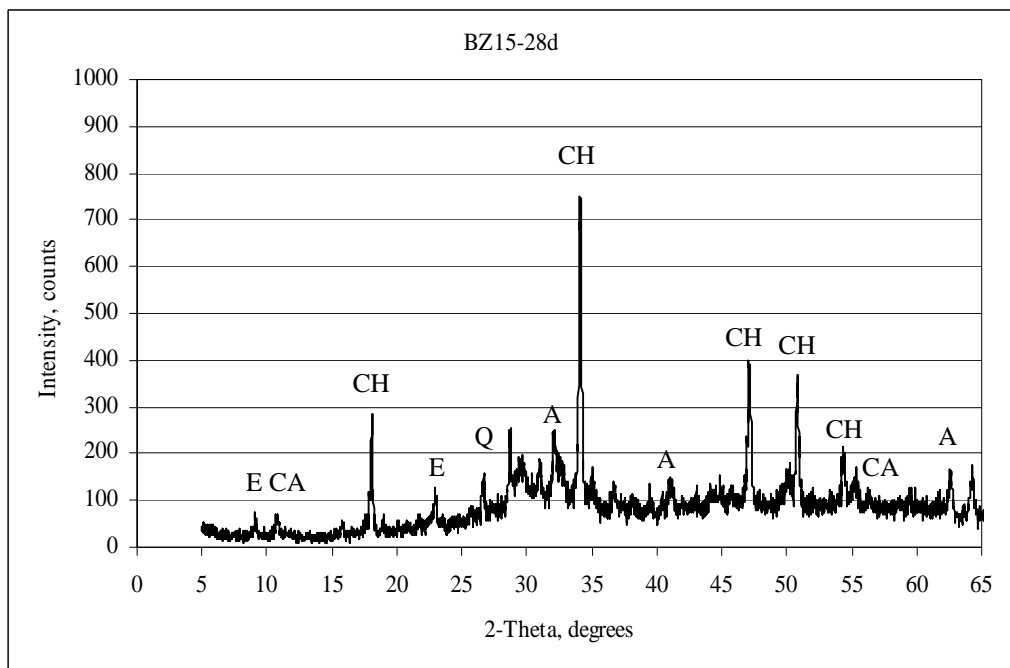


b) 28-day

Figure 4.24 XRD pattern of hardened GZ55 paste at 7 days and 28 days
 (A: Alite, CA: Calcium aluminate hydrate (C_4AH_{13}), CH: Calcium hydroxide,
 CL: Clinoptilolite, Q: Quartz)

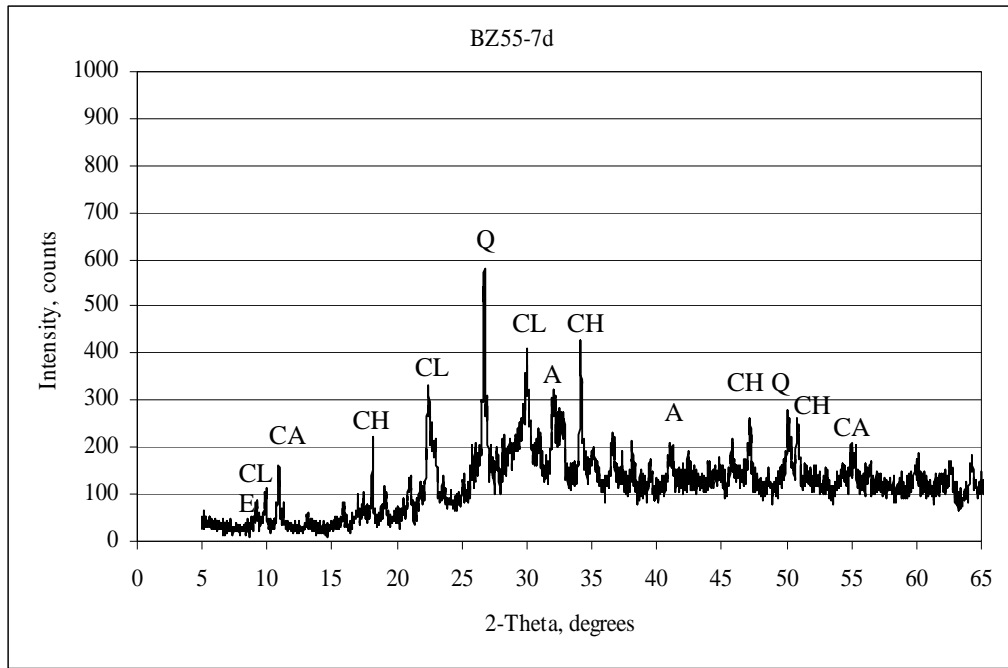


a) 7-day

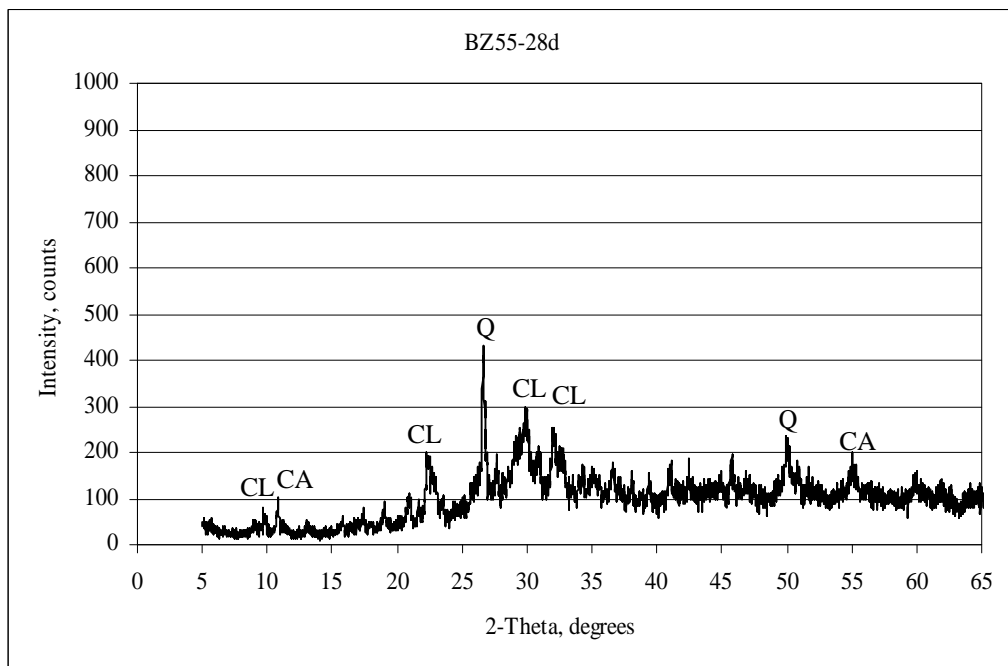


b) 28-day

Figure 4.25 XRD pattern of hardened BZ15 paste at 7 days and 28 days
 (A: Alite, CA: Calcium aluminate hydrate (C_4AH_{13}), CH: Calcium hydroxide,
 E: Ettringite, Q: Quartz)



a) 7-day



b) 28-day

Figure 4.26 XRD pattern of hardened BZ55 paste at 7 days and 28 days
(A: Alite, CA: Calcium aluminate hydrate (C_4AH_{13}), CH: Calcium hydroxide,
CL: Clinoptilolite, E: Ettringite, Q: Quartz)

On XRD patterns of hardened pastes of GZ15, as shown in Figure 4.23, it was observed that tetra calcium aluminate hydrate ($4\text{CaO}\cdot\text{Al}_2\text{O}_3\cdot 13\text{H}_2\text{O}$) exist as an additional compound which is a common product of pozzolanic reaction as well as the phases observed in PC paste. Quartz was another phase detected in GZ15 pastes as one of the crystalline phases in blending component GZ. The lower intensities of peaks corresponding to calcium hydroxide on XRD patterns of GZ15 paste, when compared to the intensities on patterns of PC paste, confirmed the lower amount of calcium hydroxide in GZ15 paste. It was observed no clinoptilolite peaks on patterns of GZ15 paste for 7 days and 28 days of age, probably due to low amount of zeolite content in blended system and/or dissolution of clinoptilolite crystals during pozzolanic activity process.

As seen from Figure 4.24, clinoptilolite and quartz phases were identified in GZ55 paste at both analysis ages in addition to pozzolanic reaction product tetra calcium aluminate hydrate ($4\text{CaO}\cdot\text{Al}_2\text{O}_3\cdot 13\text{H}_2\text{O}$) and the other phases coming from hydration of PC. Although calcium hydroxide peaks were observed with low intensities on 7-day patterns of GZ55 paste, it was observed that these peaks disappeared at 28-day pattern since the amount of calcium hydroxide probably reduced under detectable limit of XRD as a result of depletion of calcium hydroxide by pozzolanic reaction of GZ. Peaks corresponding to clinoptilolite got smaller in intensity at 28 days and their sharpness reduced when compared to the peaks observed at 7 days of age, which could be attributed to dissolution of clinoptilolite crystals as pozzolanic reaction develops with age. On the other hand, it was observed no reduction in intensities of quartz peaks between 7 days and 28 days since quartz is an inert mineral in terms of pozzolanic reaction. On the contrary, slight increases occurred in intensities of quartz peaks and this is probably due to becoming quartz phase more pronounced after decomposition of major crystal phase in GZ, namely clinoptilolite.

The observations from XRD analysis of BZ15 and BZ55 were generally similar in qualitative manner to those made for GZ15 and BZ55 as seen from Figure 4.25 and

Figure 4.26, respectively. Calcium hydroxide peaks on XRD pattern of BZ blended cement pastes had lower intensities than those of GZ blended cements, that confirms presence of higher amount of calcium hydroxide in BZ blended cements when compared to blended cements containing GZ for a given replacement level and a given age.

Consequently, from XRD analysis of hardened cement pastes, tetra calcium aluminate hydrate ($4\text{CaO}\cdot\text{Al}_2\text{O}_3\cdot 13\text{H}_2\text{O}$) was found to be a common crystalline product of pozzolanic reaction in GZ and BZ blended cements. It was observed no considerable difference between GZ and BZ blended cements in terms of crystalline phases in their hardened pastes. Clinoptilolite peaks which got smaller in intensity during hydration process of blended cements indicated decomposition of clinoptilolite at a high alkaline medium caused from presence of calcium hydroxide at early days of hydration. This outcome supports the hypothesis on pozzolanic reaction mechanism of the natural zeolites based on their dissolution, as mentioned in Section 4.1.

4.2.5 BS-SEM examinations of hardened cement pastes

28-day old hardened cement pastes were examined with backscatter mode SEM (BS-SEM) equipped with EDX (energy dispersive X-ray spectroscopy).

Figure 4.27 was taken from PC paste at a relatively low magnification (x500), and it displays the general microstructural architecture of hardened PC paste. In addition to micro cracks which are probably induced by drying shrinkage of the paste during sample preparation, partially hydrated individual cement grains were clearly observed with a relatively bright unhydrated core and surrounding shell of hydration products in relatively dark color. EDX spectrum of the unhydrated core and corresponding chemical compositions shown in Figure 4.28 reflected the typical oxide composition of Alite (impure form of C_3S) proposed by Taylor [78]. Thus existence of unhydrated Alite phase in hydrated cement paste which was previously indicated by XRD analyses was confirmed with EDX analyses.

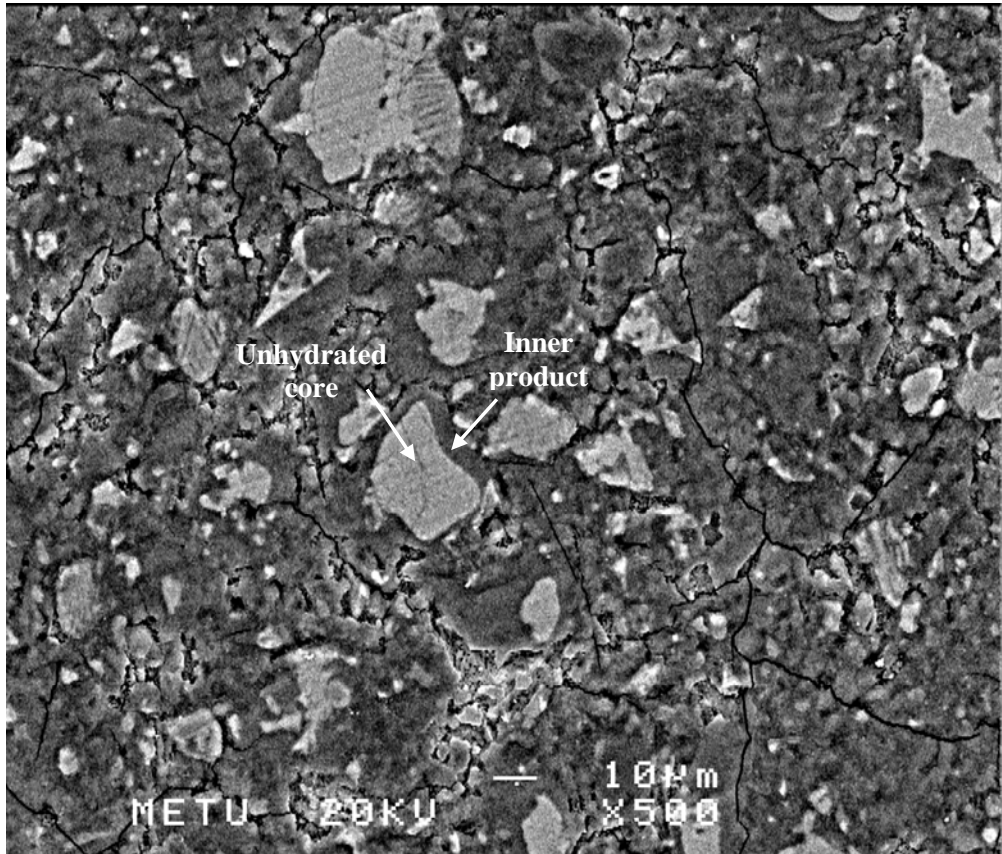


Figure 4.27 BS- EM micrograph of 28-day old PC paste

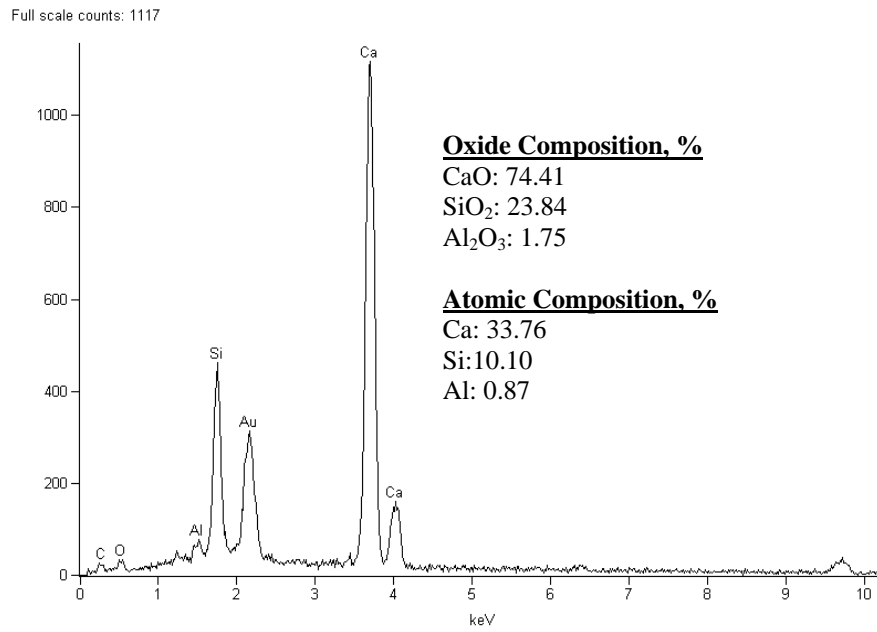


Figure 4.28 EDX analysis and corresponding composition of unhydrated core of cement grain in PC paste

EDX spectrum and corresponding composition of the inner product rim surrounding unhydrated core of the cement particle was given in Figure 4.29. Ca/Si ratio for inner products was determined as 1.93 which is a typical value for inner product of ordinary portland cements in accordance with published literature [20, 33, 78].

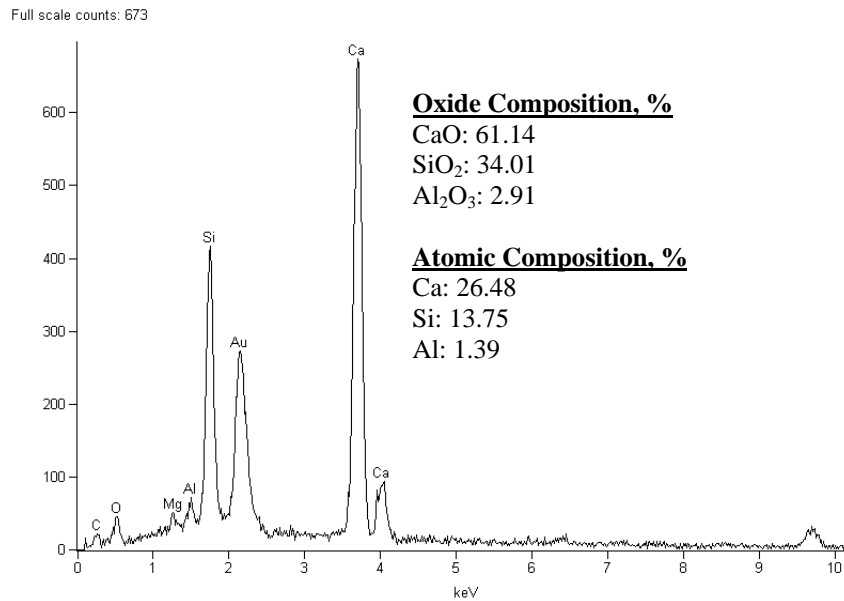


Figure 4.29 EDX spectrum and corresponding composition of the inner product surrounding the partially hydrated cement grain in PC paste

BS-SEM image taken from GZ15 paste at 500x magnification is shown in Figure 4.30. Compared the general architecture of GZ15 paste to that of PC paste shown in Figure 4.27, it was observed that GZ 15 paste has a denser structure and contains lower amount of partially reacted cement grains. Some unreacted zeolite particles which display a relatively dark color in BS-SEM image were also observed. The partially hydrated cement grain indicated in Figure 4.30 were imaged at relatively high magnification of 1500x and shown in Figure 4.31 with its EDX analysis results.

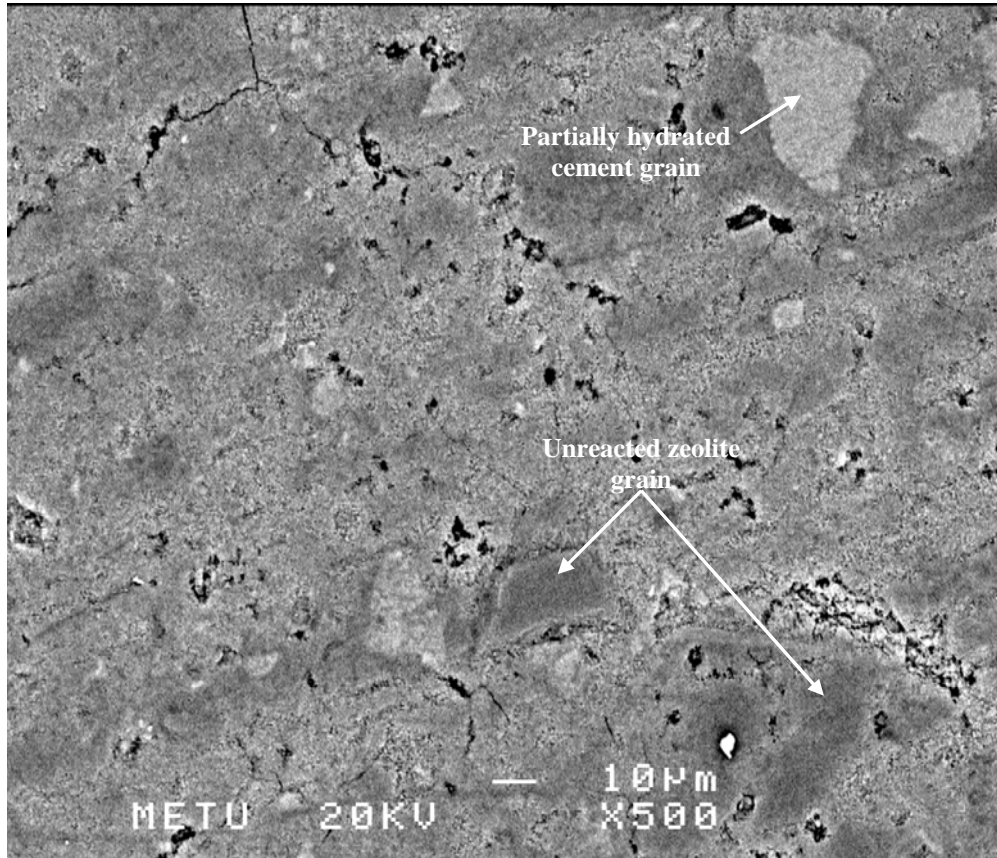


Figure 4.30 Back scattered SEM micrograph of 28-day old GZ15 paste

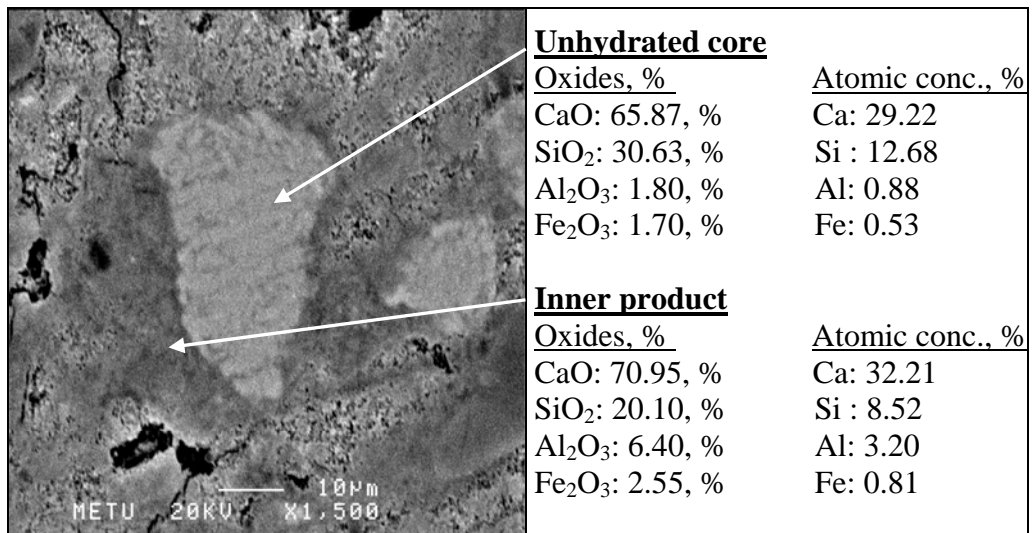


Figure 4.31 Partially reacted cement grain at 1500x magnification and its EDX analysis

As shown in Figure 4.31, unhydrated core of the partially hydrated cement grain exhibited a typical oxide composition of Belite (impure form of C_2S) which is one of the major compounds in portland cement clinker. Ca/Si ratio of the inner product surrounding the unhydrated core was determined as 3.78, and this value was almost 2 times higher than the value determined for the inner product in PC paste. This is an unexpected result because Escalante-Garcia and Sharp reported that Ca/Si ratio of inner products in pastes of fly ash, volcanic ash, and blast furnace slag blended portland cements (between 1.72-1.76) is considerably lower than that in neat portland cement paste (2.12) [33]. They associated this behavior of blended portland cements with pozzolanic activity involving uptake of Ca^{2+} ions by replacement materials for the formation of additional C-S-H. The relatively high Ca/Si ratio of the inner product in GZ15 paste seems to be an indirect result of its relatively high Al and low Si contents indicating a probable Al-rich inner product C-S-H formation. This is in line with outcomes published by Drzaj et. al. reporting that zeolite-CaO-H₂O system produces an Al-rich tobermorite (a poorly crystalline form of CSH) [9].

An unreacted zeolite particle in GZ15 paste imaged at 4000x magnification is shown in Figure 4.32 with results of its EDX analysis carried out at the center of the particle. The oxide analysis of the particle reflected a composition similar to that of GZ 15 and confirmed that the particle is an unreacted zeolite. It was observed that the edge of the particle is surrounded by a relatively bright line and this may be an evidence for zeolite dissolution in a high alkaline medium, which enables pozzolanic reaction of crystalline structure, mentioned in previous sections.

BS-SEM image taken from GZ55 paste at 500x magnification, shown in Figure 4.33, displayed a completely different microstructural architecture when compared to PC paste and GZ15 paste. Unreacted zeolite grains in a wide particle size range were clearly observed in a relatively more porous matrix than that of GZ15 paste which resulted from low amount of portland cement present in GZ55 blended cement. It should be note that no any distinct cement particle hydrated partially was observed on general view of GZ55 paste.

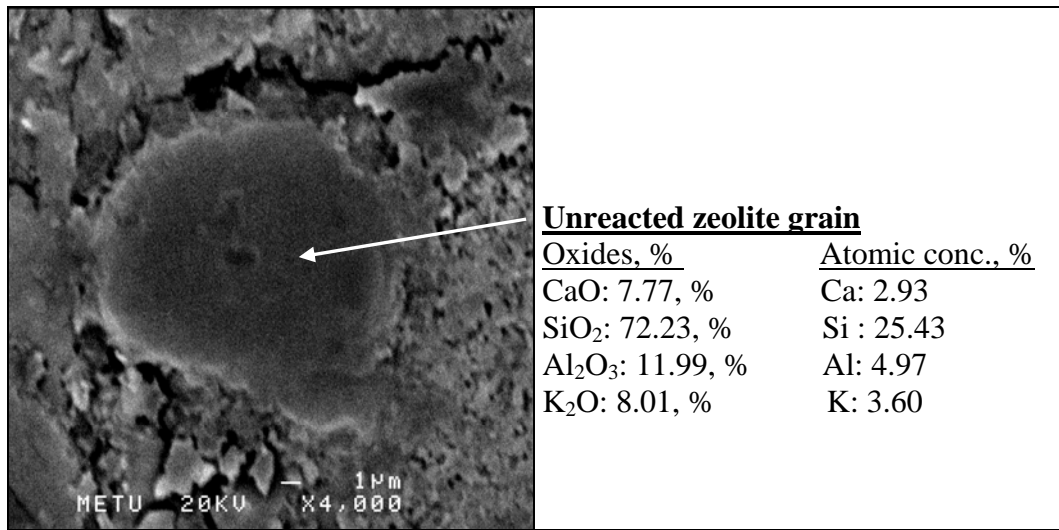


Figure 4.32 Unreacted zeolite grain in GZ15 paste at 4000x magnification and its EDX analysis

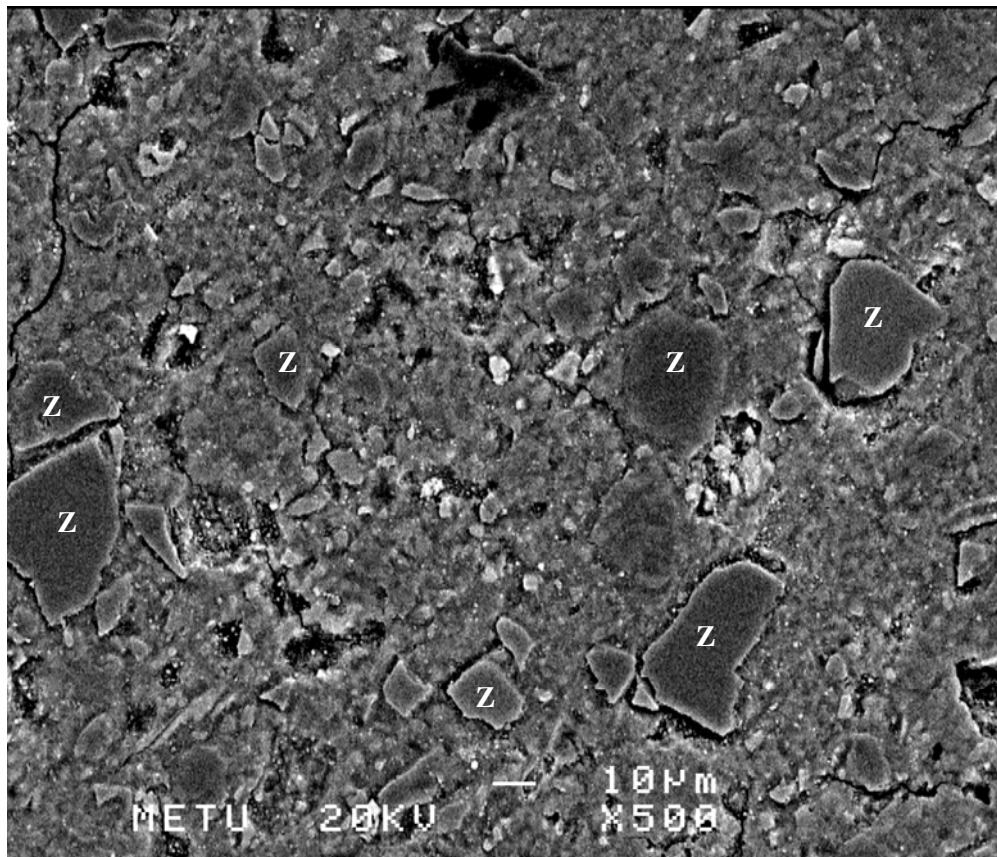


Figure 4.33 BS-SEM image taken from 28-day old GZ55 paste at 500x magnification (Z: Unreacted zeolite grain)

Relatively bright lines surrounding unreacted zeolite grains were more clearly observed in GZ55 paste. This kind of particle was imaged at 4000x magnification and shown in Figure 4.34. Chemical compositions of relatively dark center and bright edge of the particle were determined by EDX analysis taken from the points marked with A and B, and given in Figure 4.35. It was determined from EDX analyses that the surrounding rim (Point B) contains more Ca and less Si when compared to the center of the particle (Point A), and this implies zeolite dissolution and pozzolanic reaction with Ca^{2+} ions on the surface of the particle.

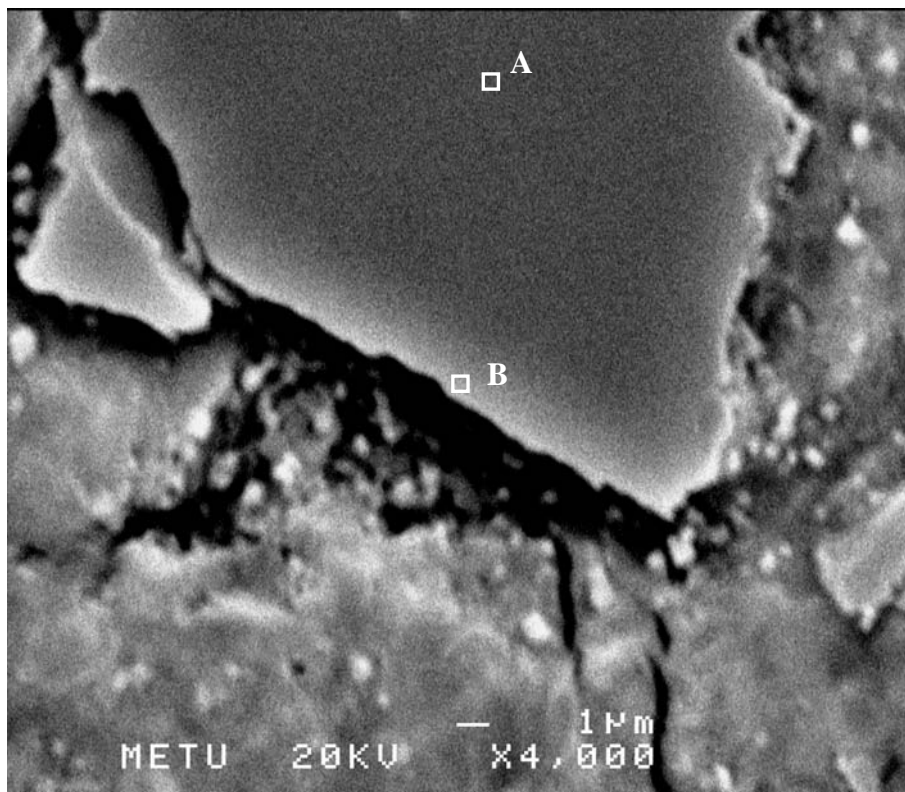
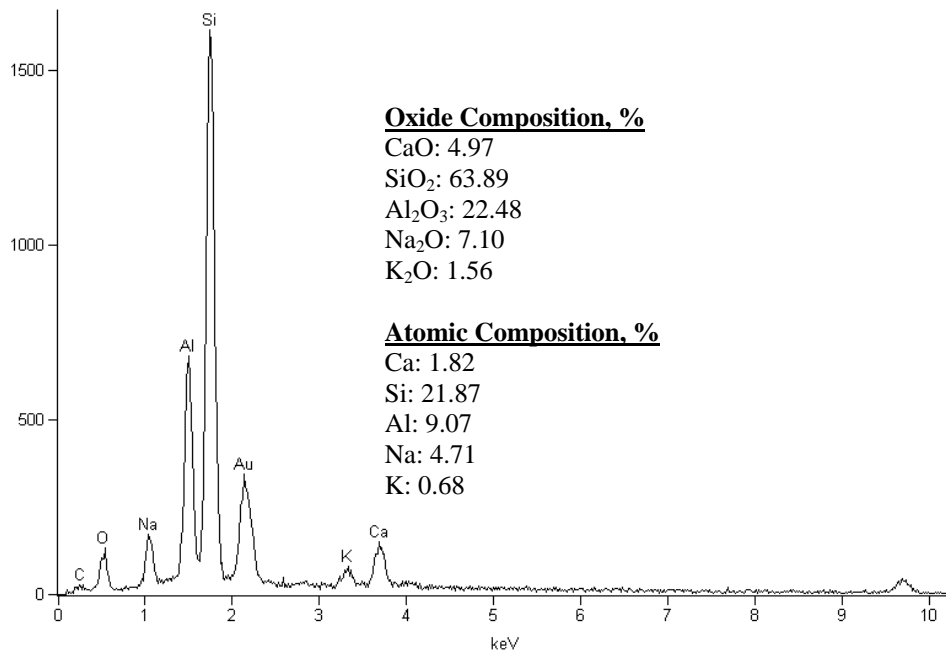


Figure 4.34 Unreacted zeolite particle in GZ55 paste at 4000x magnification

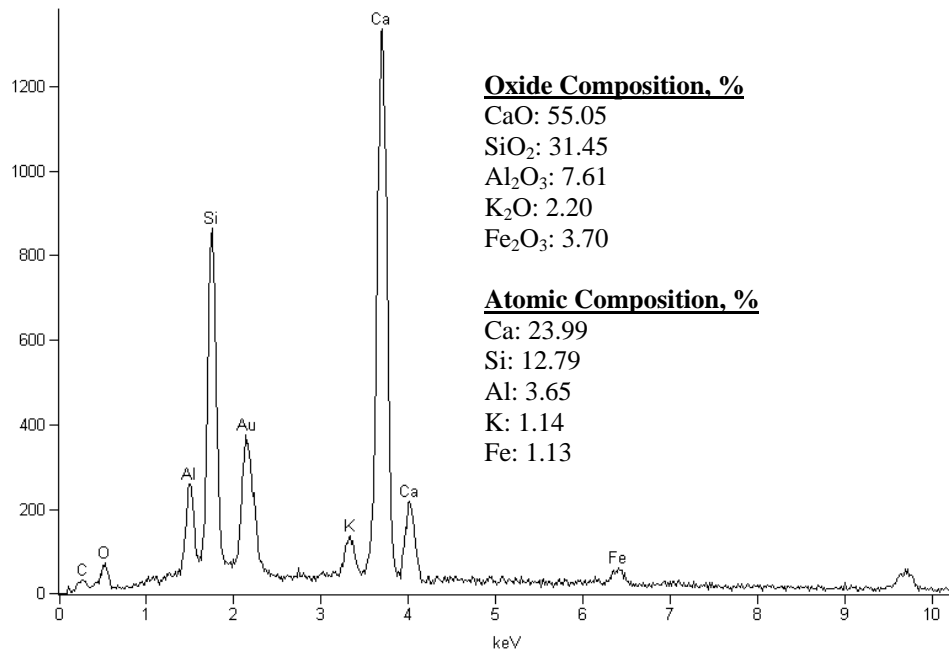
Full scale counts: 1615

iz10



a) Point A

Full scale counts: 1335



b) Point B

Figure 4.35 EDX spectrum and corresponding compositions of Point A and B

BS-SEM image taken from BZ15 paste at 500x magnification is shown in Figure 4.36. Unreacted zeolite grains and unreacted cement grains were observed in BZ15 paste similarly to GZ15 paste. However, BZ15 paste appears to be looser than GZ15 paste shown in Figure 4.30, which can be attributed to relatively low pozzolanic activity of BZ, as discussed in previous sections, resulted in low amount of additional C-S-H gel.

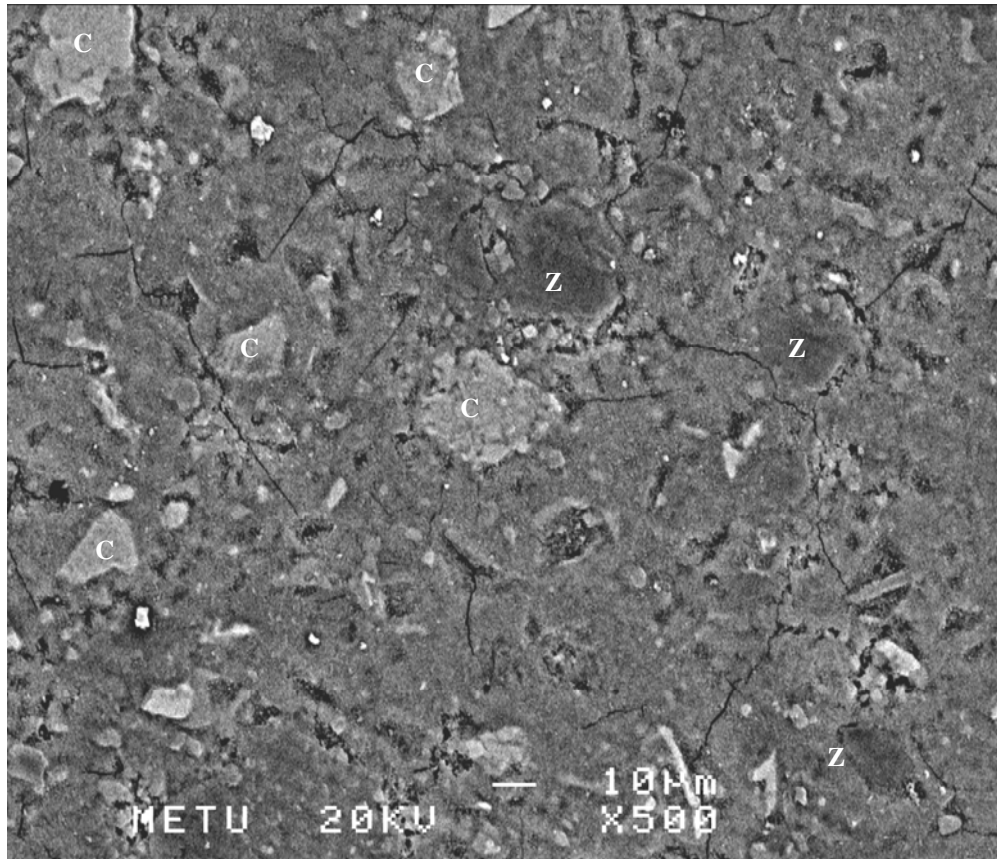


Figure 4.36 BS-SEM image taken from 28-day old BZ15 paste at 500x magnification (C: unreacted cement grains, Z: unreacted zeolite grains)

BS-SEM image of BZ55 paste shown in Figure 4.37 exhibited a similar architecture to GZ55 paste. Since BZ has a finer particle size distribution than GZ, relatively small unreacted zeolite grains were generally observed in hardened BZ55 paste.

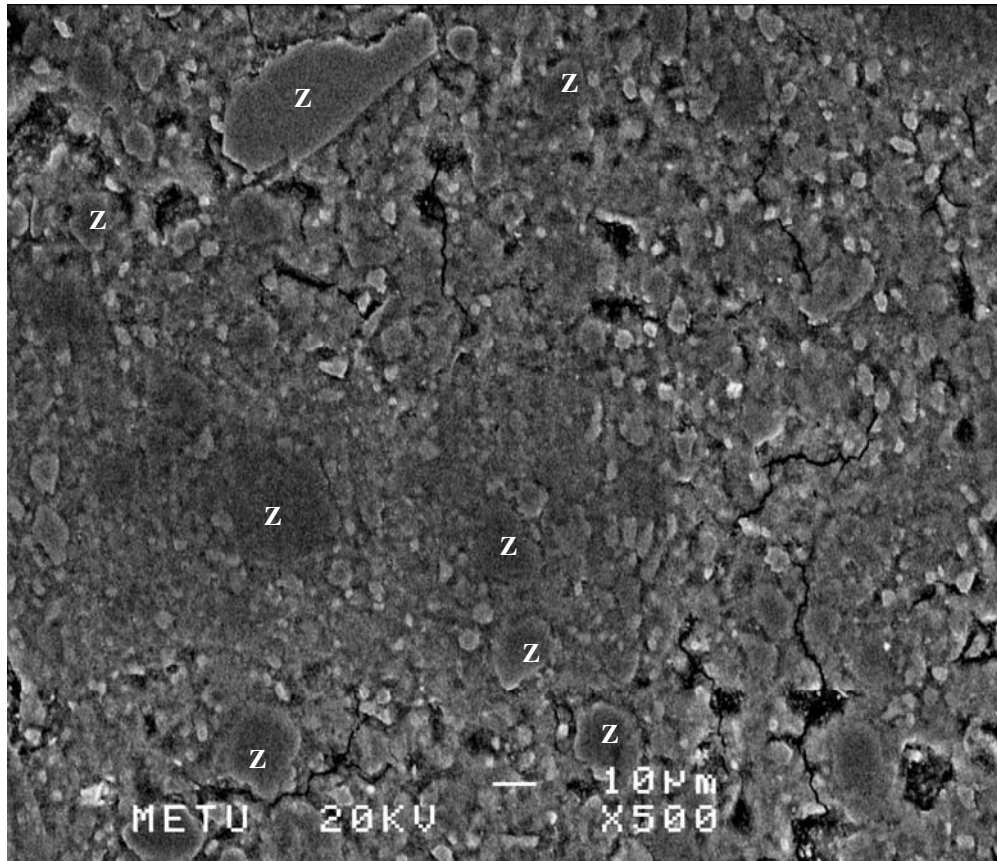


Figure 4.37 BS-SEM image taken from 28-day old BZ55 paste at 500x magnification (Z: Unreacted zeolite grains)

4.2.6 Superplasticizer requirement and compressive strength of mortars

Two different types of superplasticizers, a naphthalene-based superplasticizer (NS) and a melamine-based superplasticizer (MS), were used for preparation of blended cement mortars so as to provide a flow value similar to that of the reference portland cement mortar. The reference mortar mixture prepared with PC by using 0.5 w/c exhibited 98% flow value. Superplasticizer dosage used in blended cement mortars to provide a flow value which is similar to that of reference portland cement mortar are given in Table 4.3 for NS and MS as weight percent of blended cement. For comparative purposes, effects of zeolite content and type of

superplasticizer on superplasticizer requirements of GZ and BZ blended cement mortars are illustrated in Figure 4.38 as a function of zeolite contents.

Table 4.3 Superplasticizer dosages of blended cement mortars for NS and MS

Cement	w/c	NS		MS	
		Dosage, %	Flow, %	Dosage, %	Flow, %
GZ15	0.5	0.54	97	0.40	95
GZ35	0.5	1.20	97	1.10	95
GZ55	0.5	2.95	98	2.50	98
BZ15	0.5	0.42	96	0.32	98
BZ35	0.5	0.64	98	0.75	97
BZ55	0.5	1.00	97	1.2	97

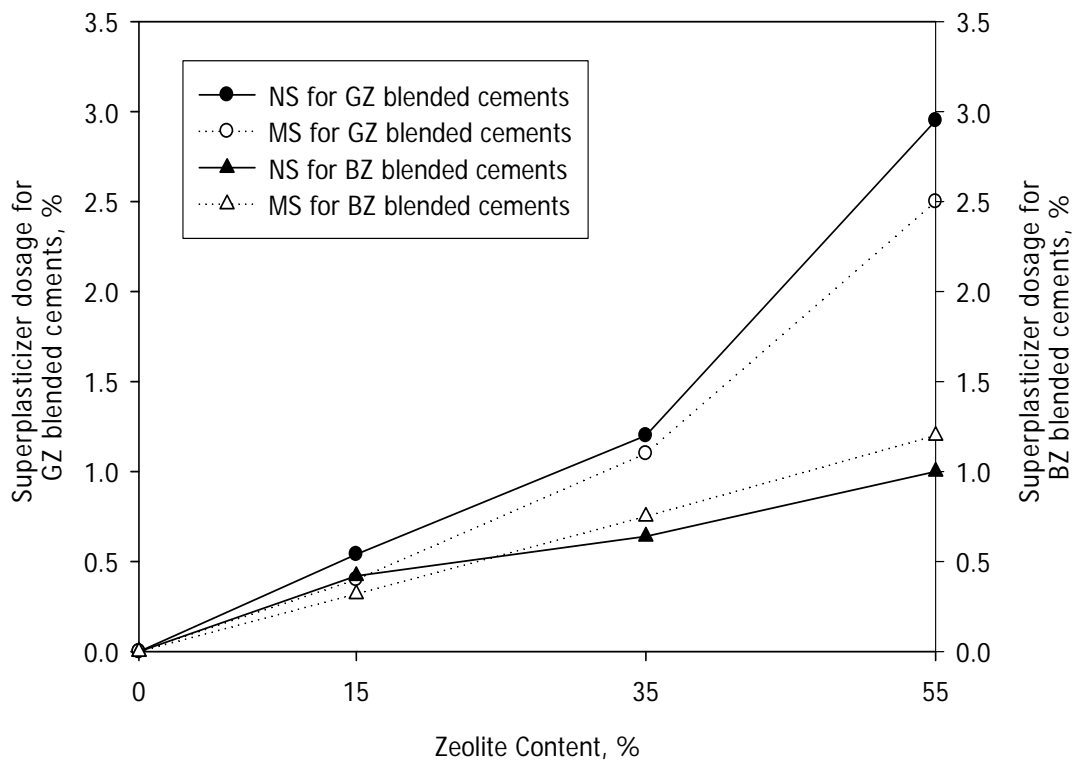


Figure 4.38 Effects of zeolite content and superplasticizer type on superplasticizer requirement of GZ and BZ blended cements

As seen from data on Table 4.3 or Figure 4.38, superplasticizer requirement of the blended cements increased as the zeolite content in blended cement increases, and BZ blended cements required less amounts of NS and MS than GZ blended cements for a given zeolite content. The difference between superplasticizer requirement of GZ and BZ blended cements increased with increasing zeolite content, and GZ55 blended cement required three times higher amount of NS than BZ55. It was also observed that MS is more effective than NS for the zeolite blended cements except BZ35 and BZ55 blended cements. For instance, required dosage of NS was 2.95% for GZ55 blended cement whereas 2.5% MS dosage was adequate for the same blended cement.

Compressive strength of blended cement mortars prepared with 0.5 w/cem were determined at 3, 7, 28, 91, 180, and 360 days of age for two different superplasticizer types used (NS and MS) and two different curing conditions, namely as lime-saturated water curing (LSWC) at 23 ± 2 °C and moist curing (MC) at 99% relative humidity (R.H.) and 23 ± 2 °C. The results are given in Table 4.4.

The evaluations on compressive strength performance of zeolite blended cements are made based on the values determined for LSWC since it is the standard curing condition according to ASTM C 109. However, a brief discussion on strength performance of zeolite blended cement mortars under moist curing conditions are done at the end of this section.

Effects of zeolite contents of blended cements on their compressive strengths are graphically illustrated for GZ and BZ blended cements in Figure 4.39 and Figure 4.40, respectively.

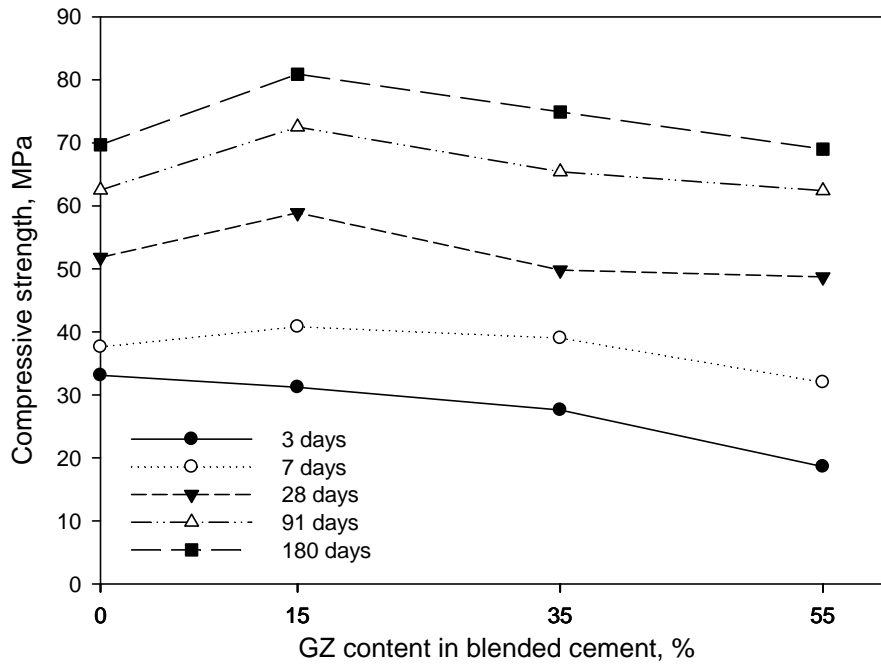
3-day compressive strength of GZ and BZ blended cement mortars decreased linearly with increasing zeolite content for both types of superplasticizer. GZ15 and BZ15 blended cement mortars exhibited slightly higher 7-day strength than the reference PC mortar. GZ15 and BZ15 mortars prepared with MS showed

considerably higher strengths than PC mortar at 28 days and later ages whereas this was not true for GZ15 mortar prepared with NS.

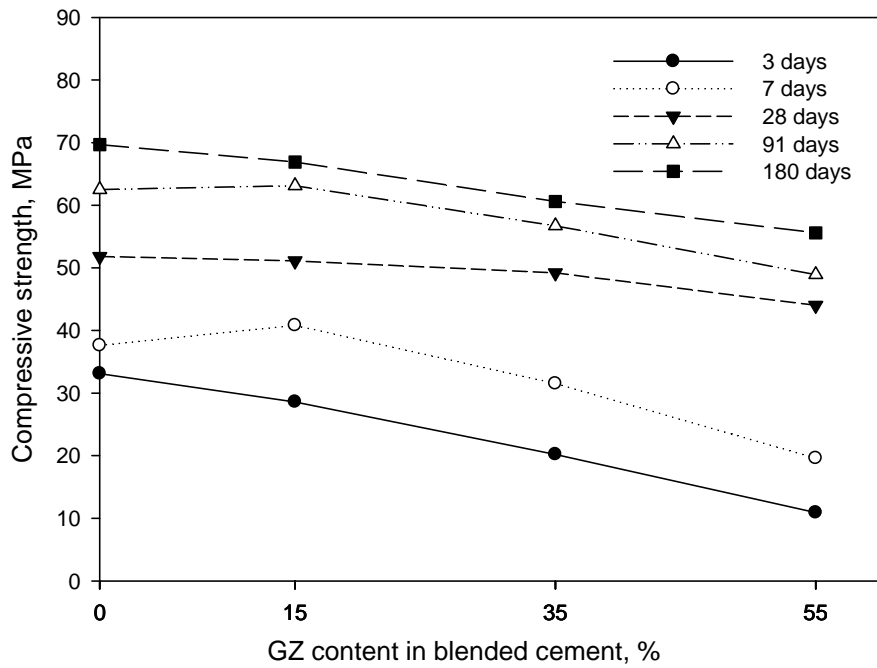
Table 4.4 Compressive strength of mortars

SP* Type	Cement	LSWC					MC				
		3 days	7 days	28 days	91 days	180 days	3 days	7 days	28 days	91 days	180 days
-	PC	33.1	37.6	51.8	62.5	69.7	32.6	40.9	56.1	67.1	71.1
NS	GZ15	28.6	40.8	51.1	63.1	66.9	25.1	32.1	52.2	63.5	68.1
	GZ35	20.2	31.5	49.2	56.7	60.6	21.1	30.7	50.7	58.5	59.1
	GZ55	10.9	19.6	44.0	48.9	55.6	13.4	24.8	42.8	45.9	47.5
	BZ15	28.3	38.8	61.2	66.6	67.6	26.0	35.5	45.7	61.6	63.6
	BZ35	19.5	31.9	54.7	60.7	63.7	15.7	24.9	34.8	37.5	40.2
	BZ55	11.7	24.8	39.1	54.1	56.7	11.2	19.9	27.6	28.1	33.6
MS	GZ15	31.2	40.8	58.9	72.5	80.9	30.7	41.4	50.6	61.4	67.5
	GZ35	27.6	39.0	49.8	65.4	74.9	24.2	32.7	42.1	52.4	57.9
	GZ55	18.6	32.0	48.7	62.4	69.0	16.8	26.8	35.5	52.6	66.2
	BZ15	36.5	43.7	65.2	72.7	83.6	33.0	42.5	61.0	73.3	76.2
	BZ35	23.8	34.4	54.3	64.1	65.7	21.8	34.9	49.9	58.2	66.4
	BZ55	17.6	28.6	51.5	60.7	64.3	13.8	25.0	31.5	43.6	53.4

*SP: Superplasticizer

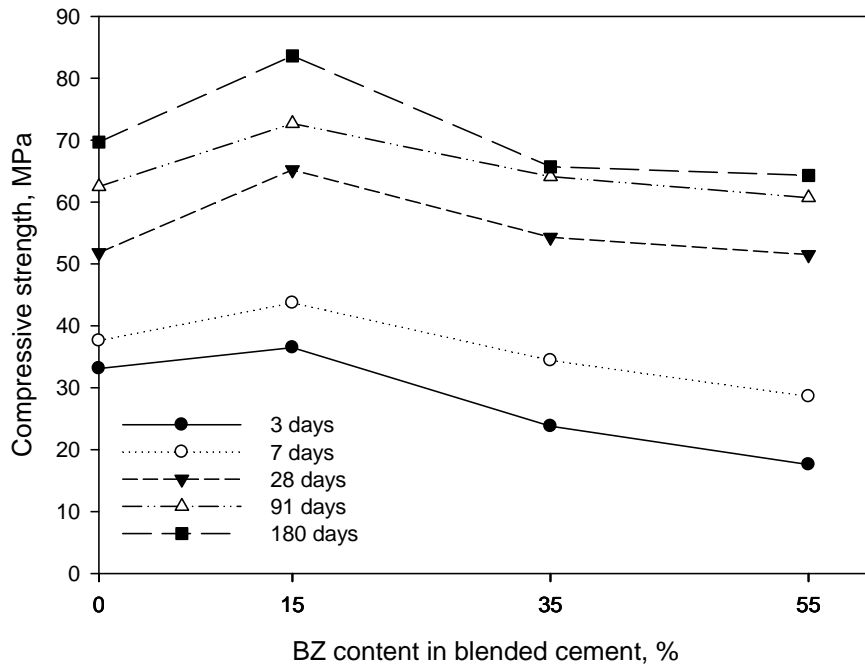


a) Mortars prepared with MS

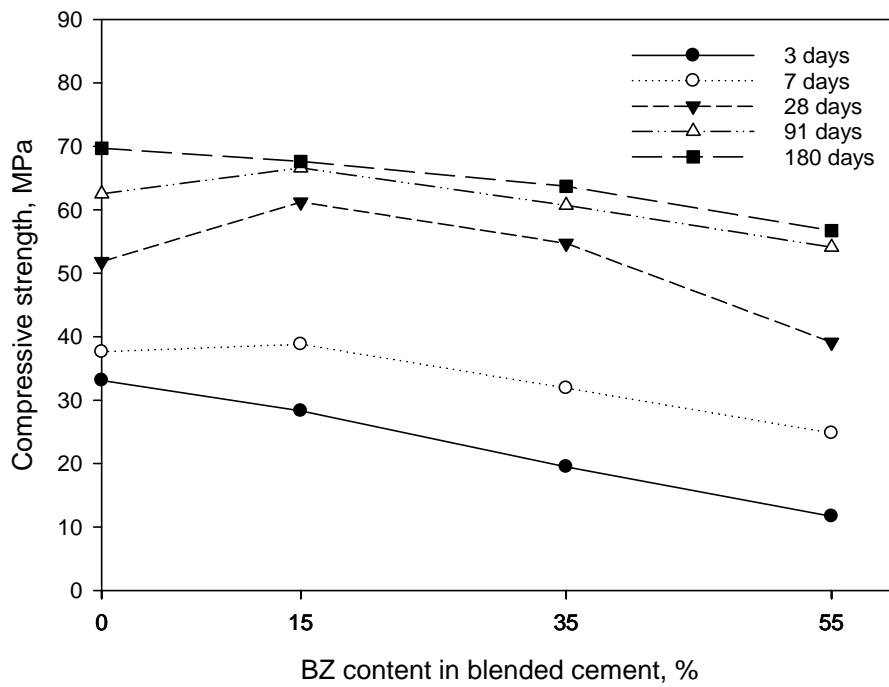


b) Mortars prepared with NS

Figure 4.39 Effect of GZ content in blended cements on compressive strength of mortars (for LSWC)



a) Mortars prepared with MS



b) Mortars prepared with NS

Figure 4.40 Effect of BZ content in blended cements on compressive strength of mortars (for LSWC)

Zeolite blended cements containing 55% natural zeolites, GZ55 and BZ55, performed 28-day compressive strengths of 94% and 99%, respectively, when normalized to the strength of reference PC mortar for the mixtures prepared with MS whereas these values were 85% and 75% for NS. It was revealed from these experimental data that high-volume zeolite blended cements (GZ55 and BZ55) perform similar 28-day strength when used with a melamine-based superplasticizer. This is a superior strength performance for 3, 7, and 28 days of age when compared to strength development of mortars of blended cements containing 55% non-zeolitic natural pozzolan (prepared with NS) investigated in previous studies [2, 3, 4, 5]. Comparative data are presented in Figure 4.41.

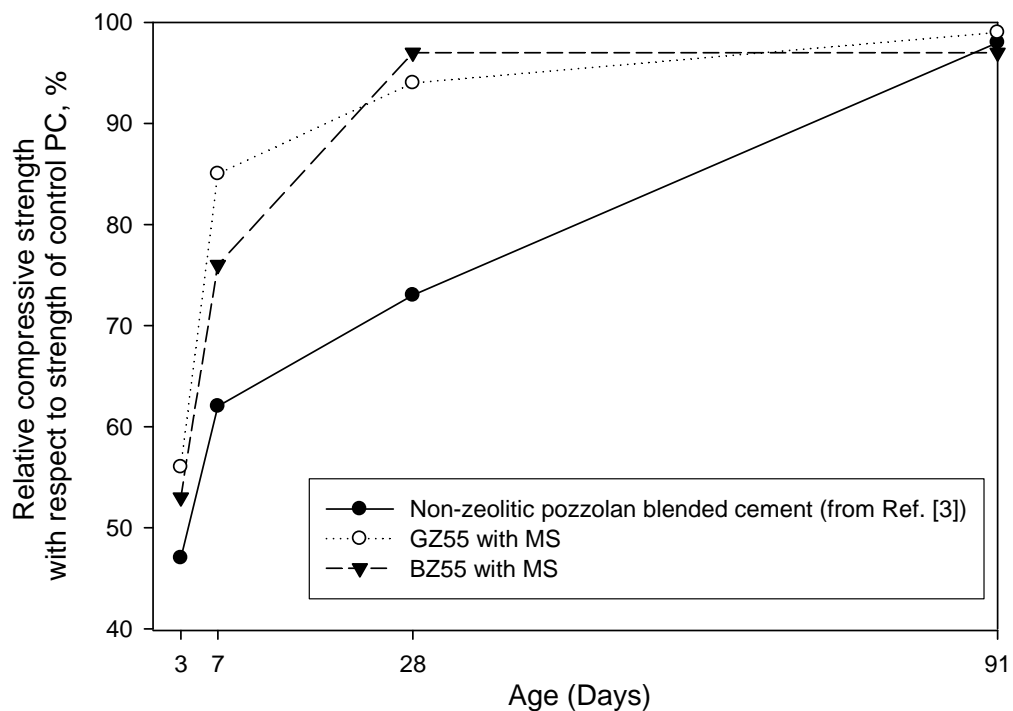


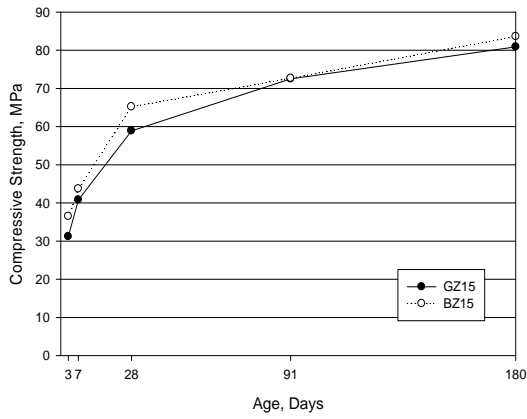
Figure 4.41 Strength performance of high-volume natural zeolite blended cements and high-volume non-zeolitic natural pozzolan blended cements from Ref. [3]

Strength performance of zeolite blended cement was generally lower for the mortars prepared with NS than those prepared with MS. It could be concluded that the melamine-based superplasticizer used in this study is more compatible with

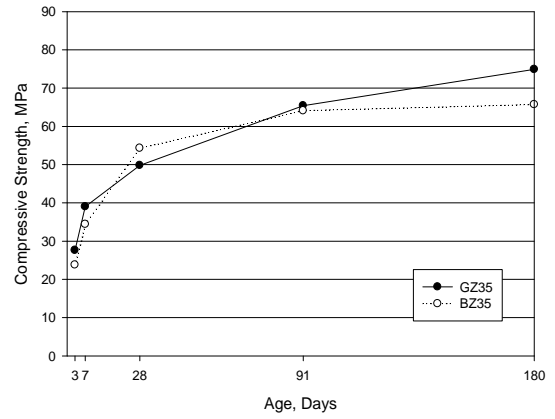
zeolite blended cements than the naphthalene-based superplasticizer due to not only strength point of view but also in terms of superplasticizer requirements indicated in Figure 4.38.

Compared the GZ and BZ blended in terms of compressive strength of mortars prepared with MS, shown in Figure 4.42, it was observed that compressive strengths of GZ and BZ blended cement mortars compete with each other. 28-day strength of BZ blended cement mortars are a little bit higher than that of GZ blended cements for a given zeolite content, which could be attributed to finer particle size distribution of BZ increasing the strength contribution originated from filler effect. This judgement is consistent with relatively high strength activity index (SAI) of BZ as discussed before in Section 4.1.5.

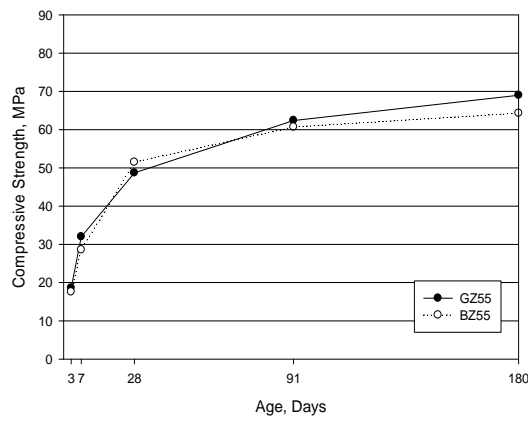
Finally, effect of moist curing (MC), instead of standard lime-saturated water curing (LSWC), on compressive strength of zeolite blended cement mortars are graphically illustrated in Figure 4.43 for the mixtures prepared with MS. For GZ blended cements, MC resulted in lower strength values when compared to LSWC for all contents of zeolite. The gap between strength development graphs corresponding to LSWC and MC got wider with age for GZ15 and GZ35 blended cement mortars whereas this was true for GZ55 mortar up to 28 days of age but thereafter the gap got closer. Lower strength values determined for MC are probably due to deficient curing of mortars in terms of providing additional water required for long-term pozzolanic activity when compared to LSWC. It is already known that cementitious systems containing mineral admixtures are more vulnerable to insufficient water curing since long-term pozzolanic reactions requires more water to produce additional binding components. Additional lime support from lime-saturated water into hardened blended cement mortars may be another cause for relatively high strength values of LSWC mortars.



a) 15% zeolite content



b) 35% zeolite content



c) 55% zeolite content

Figure 4.42 Compressive strength development of GZ and BZ blended cement mortars prepared with MS

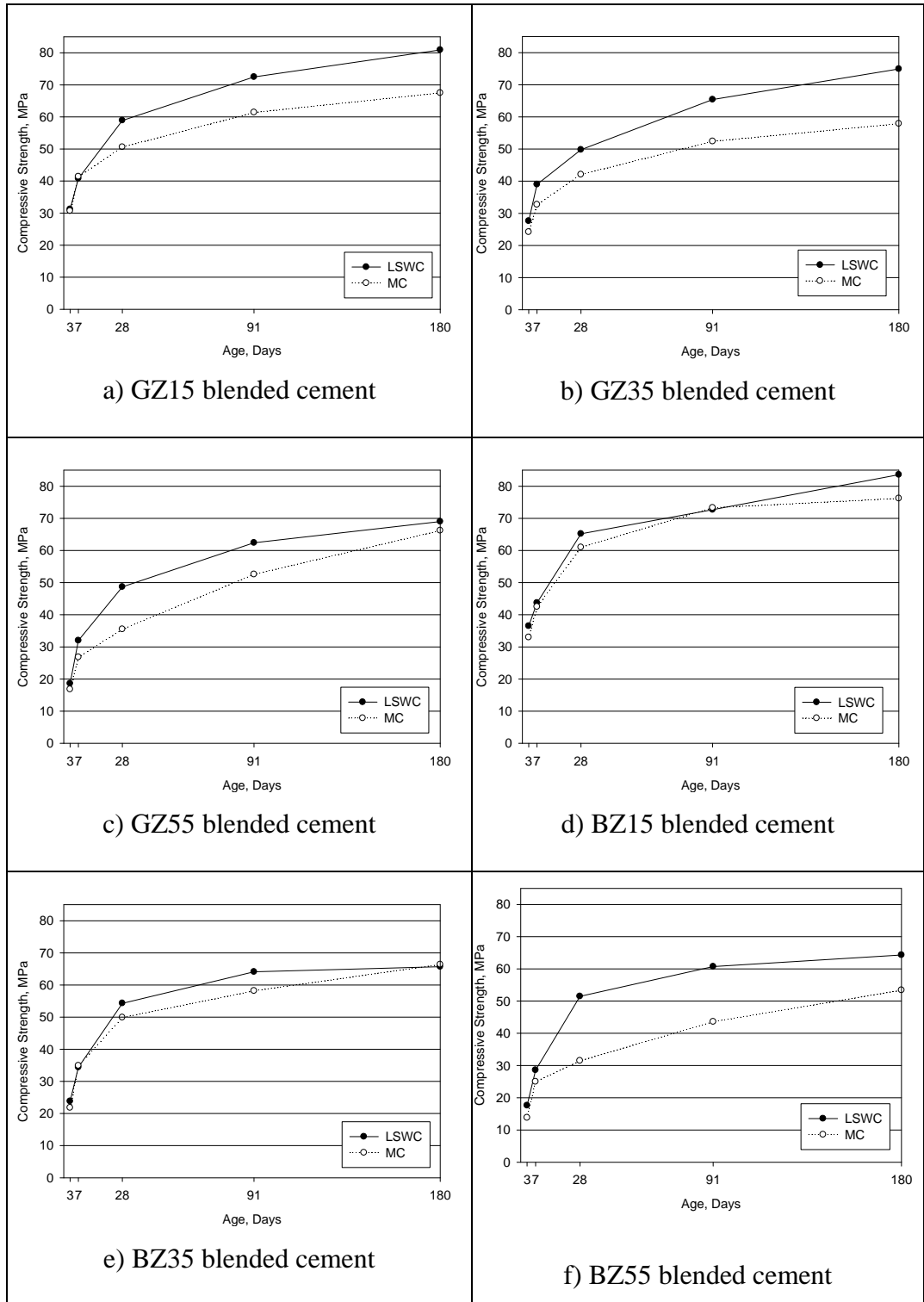


Figure 4.43 Comparison of compressive strength development of zeolite blended cement mortars for LSWC and MC conditions

For BZ blended cements, it was observed that MC did not result in considerably lower strength values of BZ15 and BZ35 blended cements, however, the strength reductions in the case of MC were significant for BZ55 mortar especially at 28 days and 91 days of age. The gap between strength development graphs of BZ55 mortar corresponding to LSWC and MC conditions narrowed at the end of 180 days, similarly to GZ55 mortar. It should be noted that the general discussions made on effect of MC on strength development of GZ blended cements are valid for BZ blended cements.

Only general discussions could be made on the effect of curing conditions on strength development of zeolite blended cements, therefore it is clear that more detailed experimental studies should be conducted individually for further explanations.

4.3 Properties of zeolite concrete mixtures

4.3.1 Properties of fresh concrete

The proportions of the concrete mixtures given in Table 3.12 in Section 3.3.3.1 are given again in Table 4.5.

Table 4.5 Proportions of the concrete mixtures

Mix Label	Portland cement kg/m ³	Natural zeolite kg/m ³	Water kg/m ³	w/cm	Aggregates			SP kg/m ³
					0-4mm kg/m ³	4-12 mm kg/m ³	12-20 mm kg/m ³	
C1	400	-	212	0.53	847	425	425	-
C2	400	-	180	0.45	890	447	447	2.8
ZC-GZ15	340	60 (GZ)	180	0.45	882	442	442	4.4
ZC-GZ35	260	140 (GZ)	180	0.45	875	439	439	6.0
ZC-GZ55	180	220 (GZ)	180	0.45	861	432	432	10.0
ZC-BZ15	340	60 (BZ)	180	0.45	882	442	442	3.6
ZC-BZ35	260	140 (BZ)	180	0.45	875	439	439	4.8
ZC-BZ55	180	220 (BZ)	180	0.45	861	432	432	4.9

As seen from Table 4.5, superplasticizer requirement of zeolite concrete mixtures increases with increasing zeolite replacement level and the concrete mixtures with BZ required less amount of superplasticizer when compared to the mixtures with GZ for a given replacement level. This is in line with the outcomes determined for zeolite blended cement mortars. ZC-GZ55 and ZC-BZ55 concrete mixtures required 10 kg/m³ and 4.9 kg/m³ superplasticizer, respectively, whereas 2.8 kg/m³ superplasticizer was adequate for plain portland cement concrete to provide the desired slump value of approximately 150 mm for 0.45 w/cm.

The slump, air content, unit weight and setting time of the fresh mixtures are given in Table 4.6.

Table 4.6 Properties of fresh concrete

Mix Label	Slump mm	Air Content %	Unit weight kg/m ³	Initial setting time hours: minute	Final setting time hours: minute
C1	140	1.9	2403	4:13	6:12
C2	150	2.2	2424	5:20	7:50
ZC-GZ15	140	1.6	2401	3:55	7:05
ZC-GZ35	150	1.3	2406	2:45	7:30
ZC-GZ55	150	1.6	2371	4:25	10:40
ZC-BZ15	160	1.8	2421	4:45	6:50
ZC-BZ35	155	1.7	2391	4:40	6:20
ZC-BZ55	160	1.2	2381	3:25	7:55

Air content of zeolite concrete mixtures was lower than that of the reference concrete mixtures C1 and C2, and generally air content decreased with increasing zeolite content, which is an expected result from concrete mixtures containing mineral admixtures.

The initial and final setting times of zeolite concrete mixtures varied depending on the type and amount of zeolite used in the mixture. Since it is well known that superplasticizer additions causes some delays in setting times especially at

relatively high dosages, the amounts of superplasticizer used in the mixtures should be considered for evaluation of setting times of the mixtures. Delaying effect of superplasticizer addition was observed clearly for initial and final setting times of control mixture C2 despite its lower w/c when compared to C1. Setting times of ZC-GZ15 and ZC-GZ55 mixtures were shorter than that of C2 control mixture having an equal w/cm despite delaying effect of increased amount of superplasticizer. This clearly indicates that zeolite addition results in shorter setting times as determined and discussed for blended cement pastes before. Due to considerably high amount of superplasticizer, ZC-GZ55 mix showed longer setting times not only than ZC-GZ15 and ZC-GZ55 mixtures but also than C2 mixture. Generally speaking, discussions on setting times of GZ concrete mixtures were valid for BZ mixtures, however, setting times of ZC-BZ55 were significantly shorter than ZC-GZ55 clearly due to lower degree of delaying effect attribute to lower amount of superplasticizer used in ZC-BZ55 mixture.

4.3.2 Compressive strength and splitting-tensile strength

Compressive and splitting-tensile strength of the concrete mixtures are given in Table 4.7 for 3, 7, 28, and 91 days of age.

Table 4.7 Compressive and splitting-tensile strengths of the hardened concrete mixtures

Mix Label	Compressive strength, MPa				Splitting-tensile strength, MPa			
	3 days	7 days	28 days	91 days	3 days	7 days	28 days	91 days
C1	32.2	35.3	42.4	48.5	2.9	3.5	3.5	3.5
C2	38.6	43.2	50.3	54.5	3.1	3.9	4.0	4.1
ZC-GZ15	32.5	41.3	65.6	73.3	2.5	3.2	5.1	5.3
ZC-GZ35	20.4	33.5	54.3	62.1	2.6	3.6	4.4	4.7
ZC-GZ55	11.8	27.6	53.0	62.4	1.1	3.1	3.4	3.6
ZC-BZ15	34.2	44.5	67.5	73.8	1.7	3.6	4.3	4.7
ZC-BZ35	22.6	38.7	60.0	64.5	2.1	3.5	3.7	3.8
ZC-BZ55	10.5	26.3	46.3	54.9	1.3	3.3	3.4	3.5

For an easy comparative evaluation, compressive strength data in Table 4.7 are graphically illustrated in Figure 4.44.

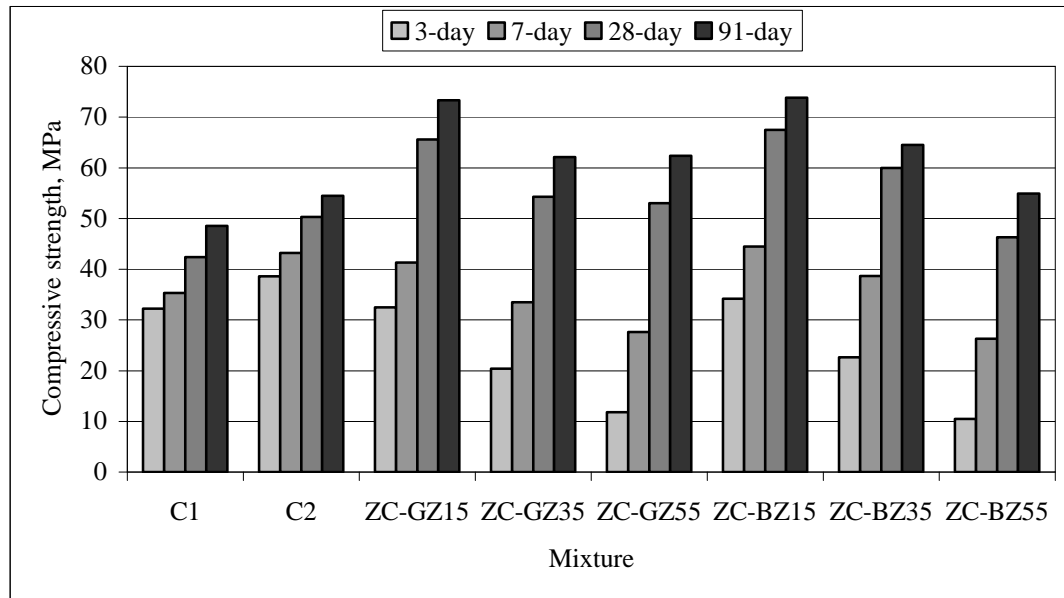


Figure 4.44 Compressive strength of the concrete mixtures

As shown from Figure 4.44, 3-day compressive strengths of ZC-GZ15 and ZC-BZ15 mixtures were similar to that of the traditional portland cement concrete without superplasticizer (C1) whereas they were slightly lower than that of the control mixture prepared by using 0.45 w/c with the help of superplasticizer (C2). 7-day compressive strengths of the zeolite concrete mixtures made with 15% replacement were similar to that of C2 control mixture. At 28 days, ZC-GZ15 and ZC-BZ15 mixtures exhibited 30% and 34% higher compressive strength, respectively, when compared to the control mixture prepared with the same w/cm and similar slump value (C2 mixture). This superior strength performance of concrete mixtures containing low (15% replacement) amount of the natural zeolites could be attributed to combined influence of pozzolanic activity and filler effect provided by finely ground natural zeolite particles as discussed for strength performance of mortar mixtures in Section 4.2.6.

The concrete mixtures containing moderate amount (35% replacement) of the natural zeolites performed approximately 15-20% lower 7-day compressive strength than C2 control mixture. However, at 28 day, ZC-GZ35 and ZC-BZ35 mixtures exhibited 8% and 19% higher compressive strength than C2 mixture. In other words, it was achieved to obtain high-strength concrete mixtures having 55-60 MPa 28-day compressive strength with only 260 kg/m³ portland cement dosage.

The concrete mixtures containing large amount (55% replacement) of the natural zeolites exhibited 28-day compressive strengths which are similar to that of C2 control mixture and higher than that of C1 control mixture. This means that 55% zeolite replacement allowed to produce concrete mixtures having approximately 25 MPa 7-day compressive strength and 45-50 MPa 28-day compressive strength with only 180 kg/m³ portland cement dosage.

Generally speaking, GZ and BZ concrete mixtures did not show a significantly different compressive strength performance for a given replacement level. However, it seems that BZ concrete mixture performed better than GZ mixtures for 15% and 35% replacement levels whereas the reverse is true for 55% replacement level.

Compared to control mixtures C1 and C2, zeolite concrete mixtures containing low (15% replacement) and moderate (35% replacement) amounts of the natural zeolites exhibited higher splitting-tensile strength at the ages of 28 days and 91 days, which is attributable to enhanced strength of the interfacial transition zone between aggregate and cement paste as a result of pozzolanic reaction. The pozzolanic reaction is slow but it has the effect of filling up the capillary voids with additional C-S-H. The relatively high late-age splitting-tensile strength of GZ concrete mixtures when compared to BZ mixtures is clearly attributed the same reason, namely pozzolanic activity, since it is known from data in previous sections that GZ has a slightly higher pozzolanic activity than BZ.

4.3.3 Modulus of elasticity

Modulus of elasticity (MOE) values of the concrete mixtures determined at the age of 91 days are presented in Figure 4.45. Compared to control mixture C2, zeolite concrete mixtures exhibited comparable or somewhat lower modulus of elasticity values varied between 29.8 and 41 GPa despite their relatively high compressive strengths. MOE values of GZ concrete mixtures decreased with increasing zeolite content, however this is not the case for BZ mixtures, that ZC-BZ55 mixture showed a similar MOE value to ZC-BZ15 mixture. Since air content is one of the factors affecting MOE of concrete [5], it is possible to express the relatively high MOE of ZC-BZ55 mixture with its relatively low air content (Table 4.6). Since porosity of paste matrix and porosity of interfacial transition zone are the other factors affecting MOE of concrete, it is difficult to express distinct mechanisms which are responsible for MOE values of zeolite concrete mixtures.

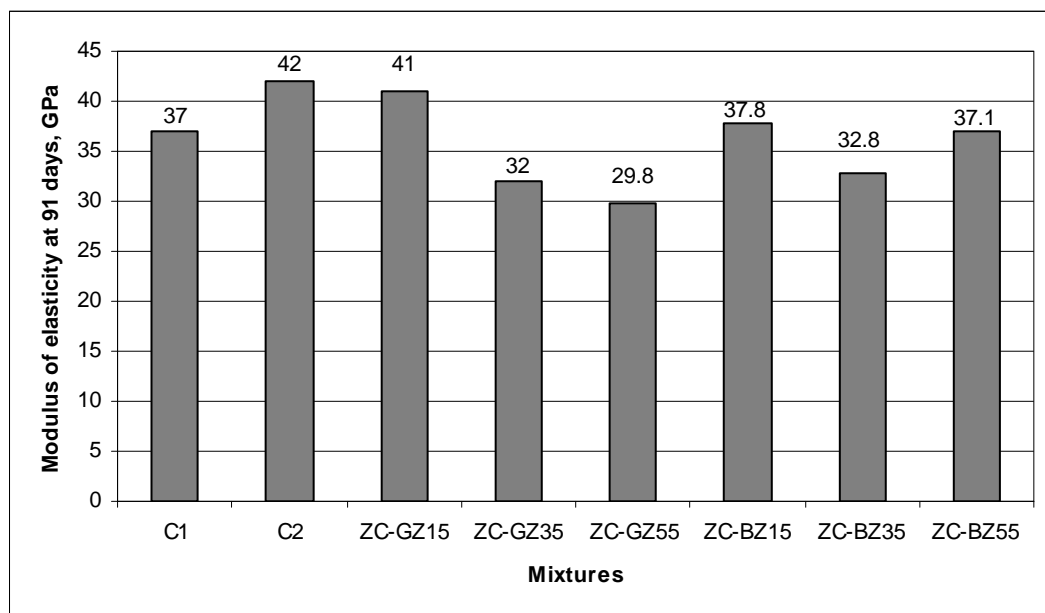


Figure 4.45 Modulus of elasticity of the concrete mixtures at 91 days

4.3.4 Chloride-ion penetration resistance (ASTM C 1202)

The data on the resistance of the concrete mixtures to chloride-ion penetration determined in accordance with ASTM C 1202 for the ages of 28 days and 91 days are shown in Figure 4.46. The concretes containing natural zeolites exhibited much higher resistance to the chloride-ion penetration (lower charge passed) when compared to the control mixtures C1 and C2. Chloride permeability of GZ and BZ concrete mixtures were found to be similar for a given zeolite replacement level. High-volume natural zeolite concrete mixtures (ZC-GZ55 and ZC-BZ55) exhibited “very low” chloride-ion penetrability, even at 28 days, in accordance with classification scheme proposed by ASTM C 1202 whereas the penetrability of the concrete mixtures containing moderate and low amount of zeolites classified as “low penetrability” at 28 days.

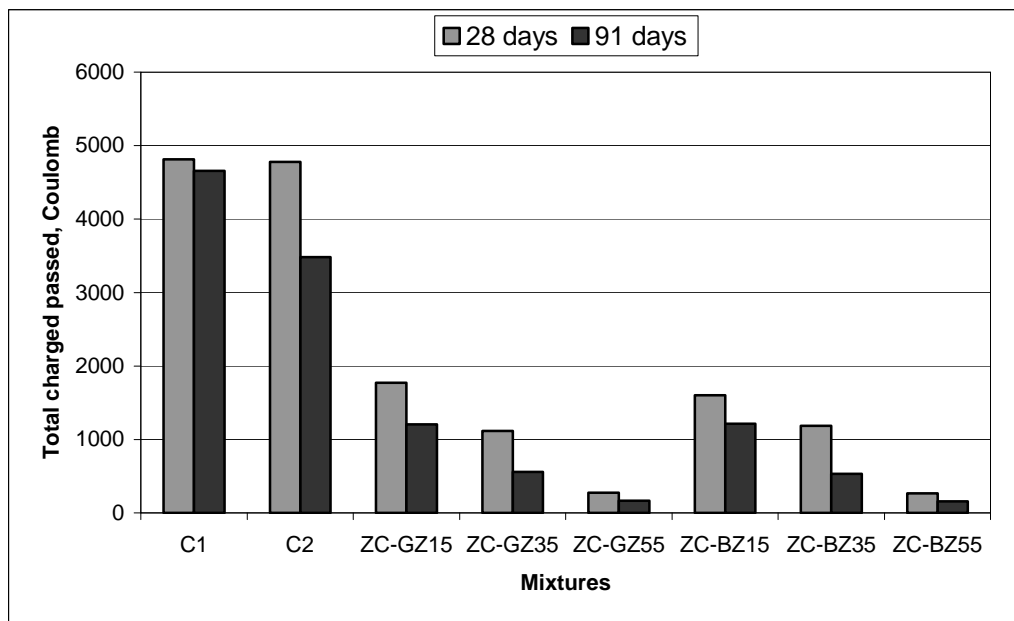


Figure 4.46 Total charged passed values as determined in accordance with ASTM C 1202

Chloride-ion penetrability of the zeolite concrete mixtures drastically decreased with increasing zeolite content. These drastic reductions could not only be related to improved microstructure of paste matrix as a result of pozzolanic reaction. Because the volume portion of permeable pores ($> 50\text{nm}$) in pastes of blended cements containing 55% zeolite was found to be comparable to the reference portland cement paste at 28 days by MIP analyses (Figure 4.21a). Accordingly some other factors should be considered to explain such low chloride-ion penetrability of the zeolite concrete mixtures. For instance, permeability of aggregate-paste interfacial transition zone and potential changes in pore solution chemistry in zeolite concrete mixtures could be responsible for low values of charged passed through concrete specimens. Especially, effects of mineral admixtures on pore solution chemistry and their potential side effects on charge values through the specimens are controversial points on the rapid chloride permeability test [79]. Natural zeolites may reduce the ionic concentration of pore solution in paste matrix and this might decrease the electrical conductivity and corresponding charge passed through water-saturated pores.

CHAPTER 5

CONCLUSIONS AND RECOMMENDATIONS

In this dissertation study, the natural zeolites obtained from two main deposits in Turkey (Gördes and Bigadiç) were experimentally evaluated in terms of pozzolanic activity, properties and hydration characteristics of zeolite blended portland cements, and performance of zeolite concrete mixtures. Blended cements and concrete mixtures were studied for three different zeolite replacement levels, namely low (15%), moderate (35%), and high (55%). The following conclusions can be drawn based on the experimental results of this study;

1. It was experimentally demonstrated that the natural zeolites (GZ and BZ) are more active than the fly ash and the non-zeolitic natural pozzolan used in the study, but less reactive than the silica fume, in terms of reactivity with $\text{Ca}(\text{OH})_2$. The reactivity of the zeolites at early ages was associated with their reactive SiO_2 content whereas their reactivity at late ages was attributed to their BET surface area as well as their reactive SiO_2 contents.
2. The natural zeolites, which have a crystalline structure, distinguished from the glassy pozzolanic materials by relatively low ratio of strength-to-amount of reacted lime. In terms of strength activity index which is a useful and widely-used parameter for practical evaluation of finely ground mineral admixtures, the natural zeolites showed a considerable performance when compared to the other materials. Specifically BZ exhibited higher 28-day

SAI value than all the other materials, even than SF, due to its more efficient filler effect in addition to its high pozzolanic reactivity.

3. Zeolite blended cements demonstrated faster initial and final setting time than the ordinary portland cement, which is probably due to relatively high BET surface area of the finely ground natural zeolites. In addition, median particle size of the ground natural zeolites was found to be another factor affecting setting times of the zeolite blended cements.
4. Lime production-consumption process in hydrating blended cement pastes was monitored via thermal analyses conducted on hardened cement pastes. In addition to Ca(OH)_2 consumption ability of natural zeolites, their contribution to Ca(OH)_2 production in blended cements by nucleation effect which enhances hydration of portland cement phase was also determined experimentally.
5. It was experimentally demonstrated that incorporation of finely ground Gördes and Bigadiç zeolites into blended cements provides refinement of pore size distribution of hardened pastes, i.e. transformation of larger pores into smaller ones. At 28 days and especially at 91 days of age, the volume fraction of pores larger than 50 nm in pastes of blended cements containing 15% and 55% natural zeolites was lower than that in reference PC paste, which is very beneficial when it is considered that capillary pores larger than 50 nm are more influential in determining the strength and impermeability of the pastes.
6. From XRD analysis of hardened cement pastes, tetra calcium aluminate hydrate ($4\text{CaO}\cdot\text{Al}_2\text{O}_3\cdot 13\text{H}_2\text{O}$) was found to be a common crystalline product of pozzolanic reaction in zeolite blended cements. It was observed no considerable difference between Gördes and Bigadiç zeolite blended cements in terms of crystalline phases in their hardened pastes.

Clinoptilolite peaks which got smaller on X-ray diffraction patterns of the hardened blended cement pastes between 7 days and 28 days of age indicated decomposition of clinoptilolite at a high alkaline medium caused from presence of calcium hydroxide at early days of hydration.

7. Backscatter-mode scanning electron microscopy studies on hardened cement pastes indicated that hardened pastes of blended cements containing 15% natural zeolites appear to have a denser microstructure when compared to PC paste, which is attributed to additional gel formation originated from pozzolanic reaction. In hardened pastes of blended cements containing 55% natural zeolites, it was concluded that some part of zeolite, especially relatively big grains, remains unreacted at 28 days of age. EDX analyses of outer rim of unreacted zeolite particles indicated a possible zeolite-decomposition on the surfaces.
8. Zeolite blended cements were found to be more compatible with the melamine-based superplasticizer, when compared to the naphthalene-based one, in terms of superplasticizer requirement and possible effects on compressive strength of mortars.
9. Zeolite blended cement mortars prepared by using superplasticizers exhibited very good strength performance when compared to ordinary portland cement mortar. Blended cements containing low amount (15%) of Gördes and Bigadiç zeolite demonstrated approximately 15% and 25% higher compressive strength of mortars, respectively, than the reference PC mortar, when prepared with melamine-based superplasticizer. Blended cement consisting of 55% Bigadiç zeolite and 45% portland cement exhibited a similar compressive strength of mortar to that of 100% portland cement. This is an extraordinary strength performance which could not be achieved with non-zeolitic natural pozzolans in previous studies [2, 3, 4, 5].

10. It was achieved to obtain high-strength (40MPa or more compressive strength at 28 days) zeolite concrete mixtures even for high amount of replacement of portland cement. 28-day compressive strengths of zeolite concrete mixtures made with 35% replacement of portland cement (260 kg/m³ portland cement and 140 kg/m³ zeolite dosages) were approximately 55-60 MPa. High-volume natural zeolite concrete mixtures made with 55% replacement (180 kg/m³ portland cement and 220 kg/m³ zeolite dosages) exhibited approximately 25 MPa 7-day strength and 45-50 MPa 28-day strength. This is a superior early and late age strength performance which can not be expected from an identical concrete mixture prepared with a non-zeolitic natural pozzolan.
11. Modulus of elasticity of the zeolite concrete mixtures at 91-days was found to be comparable or somewhat lower than that of plain portland cement concrete.
12. Natural zeolite concrete mixtures exhibited significantly higher resistance to chloride-ion penetration (lower charge passed determined in accordance with ASTM C 1202) compared to plain portland cement concrete and their resistance increased with increasing zeolite content, probably due to improved microstructure of cement paste matrix and interfacial transition zone.
13. Gördes and Bigadiç zeolites used in this study exhibited considerably different behaviors for some properties such as compressive strength of lime-pozzolan pastes, water requirement, strength activity index, and setting time of zeolite blended cements, in spite of the fact that their chemical and mineralogical compositions are not significantly different. It can be concluded that properties of cementitious systems containing natural zeolites are highly dependent to natural zeolite to be used. Therefore the experimental results in this study are only valid for the natural zeolites whose chemical, mineralogical and physical characterizations are given in a

detailed manner. On the other hand, the results on this study provide data in a wide-range of properties of cementitious systems containing the natural zeolites obtained from two major zeolite deposits in Turkey.

Further investigations are needed on cementitious systems containing natural zeolites. Similar kind of studies should be made for some zeolitic tuffs containing zeolite minerals other than clinoptilolite and for various purity levels. Use of finely ground natural zeolites together with some other mineral admixtures in concrete is another attractive topic which should be investigated. In addition, mechanical performance of natural zeolite concrete mixtures should also be determined for the mixtures without superplasticizer because superplasticizer cost may be a discouraging factor for widely use of concrete mixtures containing large amount of finely ground natural zeolites.

REFERENCES

1. CO₂ Emission from Cement Manufacture Have Been Underestimated, *Applied Catalysis B: Environmental*, Vol.13, No. 2, pp.N12-N13, 1997.
2. Uzal, B., Effects of High Volume Natural Pozzolan Addition on the Properties of Pozzolanic Cements, *Master of Science Thesis*, Middle East Technical University, 2002.
3. Uzal, B., Turanli, L., Studies on Blended Cements Containing a High Volume of Natural Pozzolans, *Cement and Concrete Research*, Vol.33, No.11, pp.1771-1781, 2003.
4. Turanli, L., Uzal, B., Bektas, F., Effect of Material Characteristics on the Properties of Blended Cements Containing High Volumes of Natural Pozzolans, *Cement and Concrete Research*, Vol.34, No.12, pp.2272-2282, 2004.
5. Turanli, L., Uzal, B., Bektas, F., Effect of Large Amounts of Natural Pozzolan Addition on Properties of Blended Cements, *Cement and Concrete Research*, Vol.35, No.6, pp.1106-1111, 2005.
6. Mehta, P.K., and Monteiro, P. J. M., *Concrete; Microstructure, Properties, and Materials*, 3rd Edition, McGraw-Hill, New York, 2006.
7. Tsitsishvili, G. V., *Natural Zeolites*, E. Horwood, New York, 1992.
8. Yücel, H., Zeolitler ve Kullanım Alanları, III. Ulusal Kil Sempozyumu Bildiriler, pp. 391-402, 1987.
9. Drzaj, B., Hocesvar, S., Slokan, M., Kinetics and Mechanism of Reaction in the Zeolitic Tuff-CaO-H₂O Systems at Increased Temperature, *Cement and Concrete Research.*, Vol.8, No.6, pp.711-720, 1978.

10. Sersale, R., Frigione, G., Natural Zeolites as Constituents of Blended Cements, Proceedings: International Symposium Zeolites, Synthesis, Structure, Technology and Application, International Zeolite Association, Portorose, 1985.
11. Blanco Varela, M.T., Ramirez, S.M., Erena, I., Gener, M., Carmona, P., Characterization and Pozzolanicity of Zeolitic Rocks from Two Cuban Deposits, *Applied Clay Science*, Vol.33, No.2, pp.149-159, 2006.
12. Ortega, E.A., Cheeseman, C., Knight, J., Loizidou, M., Properties of Alkali-Activated Clinoptilolite, *Cement and Concrete Research*, Vol.30, No.10, pp.1641-1646, 2000.
13. Poon, C.S., Lam, L., Kou, S.C., Lin, Z.S., A Study on the Hydration Rate of Natural Zeolite Blended Cement Pastes, *Construction and Building Materials*, Vol.13, No.8, pp.427-432, 1999.
14. Perraki, Th., Kakali, G., Kontoleon, F., The Effect of Natural Zeolites on the Hydration of Portland Cement, *Microporous and Mesoporous Materials*, Vol.61, No.1-3, pp.205-212, 2003.
15. Gottardi, G., Galli, E., *Natural Zeolites*, Springer-Verlag, Berlin, 1985.
16. Armbruster, T., Gunter, M.E., Crystal Structure of Natural Zeolites, *Reviews in Mineralogy and Geochemistry; Natural Zeolites (Editors D.L. Bish, D.W. Ming)*, Mineralogical Society of America, Vol. 45, Chapter 1, 2001.
17. Colella, C., Gennaro, M. de', Aiello, R., Use of Zeolitic Tuff in Building Industry , *Reviews in Mineralogy and Geochemistry; Natural Zeolites (Editors D.L. Bish, D.W. Ming)*, Mineralogical Society of America, Vol. 45, Chapter 16, 2001.
18. Virta, R.L., Annual Report on Zeolites, U.S. Geological Survey, Zeolites, 2002.
19. Kocakuşak, S., Savaşçı, Ö.T., Ayok, T., Doğal Zeolitler ve Uygulama Alanları, *Tubitak-Mam Malzeme ve Kimya Teknolojileri Araştırma Enstitüsü*, Rapor No: KM 362, 2001.
20. Massaza, F., Pozzolana and Pozzolanic Cements, *Lea's Chemistry of Cement and Concrete (Editor:P. C. Hewlett)*, Elsevier, 1998.

21. Shi, C., Day, R.L., Pozzolanic Reaction in Presence of Chemical Activators Part II. Reaction Products and Mechanism, *Cement and Concrete Research*, Vol.30, No.4, pp.607-613, 2000.
22. Shannag, M.J., Yeginobali, A., Properties of Pastes, Mortars and Concretes Containing Natural Pozzolan, *Cement and Concrete Research*, Vol.25, No.3, pp. 647-657, 1995.
23. Mehta, P.K., Studies on Blended Cements Containing Santorin Earth, *Cement and Concrete Research*, Vol.11, No.4, pp.507-518, 1981.
24. Galle, C., Effect of Drying on Cement-Based Materials Pore Structure as Identified by Mercury Intrusion Porosimetry A Comparative Study between Oven-, Vacuum-, Freeze-Drying, *Cement and Concrete Research*, Vol.31. No.10, pp. 1467-1477, 2001.
25. Diamond, S., A discussion of the Paper “Effect of drying on cement-based materials pore structure as identified by mercury porosimetry—a comparative study between oven-, vacuum-, and freeze-drying” by C. Galle, *Cement and Concrete Research*, Vol.33, No.1, pp.169-170, 2003.
26. Galle, C., Reply to the Discussion by S. Diamond of the paper “Effect of drying on cement-based materials pore structure as identified by mercury intrusion porosimetry: a comparative study between oven-, vacuum- and freeze-drying”, *Cement and Concrete Research*, Vol.33, No.1, pp.171-172, 2003.
27. Diamond, S., Mercury Porosimetry: An Inappropriate Method for the Measurement of Pore Size Distributions in Cement-Based Materials, *Cement and Concrete Research*, Vol.30, No.10, pp.1517-1525, 2000.
28. Chatterji, S., A Discussion of the Paper “Mercury Porosimetry-An Inappropriate Method for the Measurement of Pore Size Distributions in Cement-Based Materials” by S. Diamond, *Cement and Concrete Research*, Vol.31, No.11, pp.1657-1658, 2001.
29. Diamond, S., Reply to the Discussion by S. Chatterji of the Paper “Mercury Porosimetry-An Inappropriate Method for the Measurement of Pore Size Distributions in Cement-Based Materials”, *Cement and Concrete Research*, Vol.31, No.11, p.1659, 2001.

30. Wild, S., A Discussion of the Paper “Mercury Porosimetry-An Inappropriate Method for the Measurement of Pore Size Distributions in Cement-Based Materials” by S. Diamond, *Cement and Concrete Research*, Vol.31, No.11, pp.1653-1654, 2001.
31. Diamond, S., Reply to the Discussion by S. Wild of the Paper “Mercury Porosimetry-An Inappropriate Method for the Measurement of Pore Size Distributions in Cement-Based Materials”, *Cement and Concrete Research*, Vol.31, No.11, pp.1655-1656, 2001.
32. Olson, R.A., Neubauer, C. M., Jennings, H.M., Damage to the Pore Structure of Hardened Portland Cement Paste by Mercury Intrusion, *Journal of the American Ceramic Society*, Vol.80, No.9, pp.2454-2458, 1997.
33. Escalante-Garcia, J.I., Sharp, J.H., The Chemical Composition and Microstructure of Hydration Products in Blended Cements, *Cement and Concrete Composites*, Vol.26, No.8, pp.967-976, 2004.
34. Feng, N.Q., Peng, G.F., Applications of Natural Zeolites to Construction and Building Materials in China, *Construction and Building Materials*, Vol.19, No.8, pp.579-584, 2005.
35. Malhotra, V.M., Mehta, P.K., *Pozzolanic and Cementitious Materials*, Overseas Publishers Association, Amsterdam, 1996.
36. Martinez-Ramirez S., Blanco Varela, M.T., Erena, I., Gener, M., Pozzolanic Reactivity of Zeolitic Rocks from Two Different Cuban Deposits: Characterization of Reaction Products, *Applied Clay Science*, Vol.32, No.1-2, pp. 40-52, 2006.
37. Fragoulis, D., Chaniotakis, E., Stamatakis, M.G., Zeolitic Tuffs of Kimolos Island, Aegean Sea, Greece and Their Industrial Potential, *Cement and Concrete Research*, Vol.27, No.6, pp.889-905, 1997.
38. Gervais, C., Ouki, S.K., Performance Study of Cementitious Systems Containing Zeolite and Silica fume: Effects of Four Metal Nitrates on the Setting Time, Strength and Leaching Characteristics, *Journal of Hazardous Materials*, Vol.93, No.2, pp.187-200, 2002.

39. Canpolat, F., Yılmaz, K., Köse, M.M., Sümer, M., Yurdusev, M.A., Use of Zeolite, Coal Bottom Ash and Fly Ash as Replacement Materials in Cement Production, *Cement and Concrete Research*, Vol.34, No.5, pp.731-735, 2004.
40. Yılmaz, B., Uçar, A., Öteyaka, B., Uz, V., Properties of Zeolitic Tuff (clinoptilolite) Blended Portland Cement, *Building and Environment*, Article in Press.
41. Feng N.Q., Mukai, T., Ehara K., A Study on The Effect of Zeolite When Used as Strength Increasing Admixture for Concrete (in Japanese), *Journal of Structural and Construction Engineering (Transactions of AIJ)*, No. 388, pp.9-17, 1988.
42. Chan, S.Y.N, Ji., X., Comparative Study of the Initial Surface Absorption and Chloride Difusion of High Performance Zeolite, Silica Fume and PFA Concretes, *Cement and Concrete Composites*, Vol.21, No.4, pp.293-300, 1999.
43. Feng, N., Feng, X., Hao, T., Xing, F., Effect of Ultrafine Mineral Powder on the Charged Passed of the Concrete, *Cement and Concrete Research*, Vol.32, No.4, pp.623-627, 2002.
44. Sesale, R., Prigione, G., Porland-Zeolite Cement for Minimizing Alkali-Aggregate Expansion, *Cement and Concrete Research*, Vol.17, No.3, pp.404-410, 1987.
45. Feng, N.Q., Feng, X.X., Mechanism of Using Mineral Admixtures to Suppress Alkali-Silica Reaction, *Key Engineering Materials*, Vol.302-303, pp.111-119, 2006.
46. Feng, N.Q., Jai, H.W., Chen E.Y., Study on the Suppression Effect of Natural Zeolite on Expansion of Concrete Due to Alkali-Aggregate Reaction, *Magazine of Concrete Research*, Vol.50, No.1, pp.17-24, 1998.
47. Niu, Q.L., Feng N.Q., Effect of Modified Zeolite on the Expansion of Alkaline Silica Reaction, *Cement and Concrete Research*, Vol.35, No.9, pp.1784-1788, 2005.
48. Feng, X.X., Feng, N.Q., Han, D., Effect of the Composite of Natural Zeolite and Fly Ash on Alkali-Silica Reaction, *Journal of Wuhan University of Technology-Materials Science Edition*, Vol.18, No.4, pp.93-96, 2003.

49. Feng, N.Q., Hao, T.Y., Mechanism of Natural Zeolite Powder in Preventing Alkali-Silica Reaction in Concrete, *Advances in Cement Research*, Vol.10, No.3, pp.101-108, 1998.
50. TS EN 197-1, Cement-Composition, Specifications and Conformity Criteria, Part-1:Common Cements, Turkish Standards Institution, 2002 (in Turkish).
51. TS EN 196-2, Methods of Testing Cement-Part 2: Chemical Analysis of Cement, *Turkish Standards Institution*, 2002 (in Turkish).
52. ASTM C 311, “Test Methods for Sampling and Testing Fly Ash or Natural Pozzolans for Use as a Mineral Admixture in Portland Cement Concrete”, *American Society for Testing and Materials*, 2005.
53. Luxan, M.P., Madruga, F., Saavedra, J., Rapid Evaluation of Pozzolanic Activity of Natural Products by Conductivity Measurement, *Cement and Concrete Research*, Vol.19, No.1, pp. 63-68, 1989.
54. Paya, J., Borrachero, M.V., Monzo, J., Peris-Mora, E., Amahjour, F., Enhanced Conductivity Measurement Techniques for Evaluation of Fly Ash Pozzolanic Activity, *Cement and Concrete Research*, Vol.31. No.1, pp. 41-49, 2001.
55. ASTM C 109, Test Method for Compressive Strength of Hydraulic Cement Mortars (Using 2-in. or 50-mm Cube Specimens), *American Society for Testing and Materials*, 2005.
56. Erdogdu, K., Tokyay, M., Türker, P., Comparison of Intergrinding and Separate Grinding for the Production of Natural Pozzolan and GBFS-incorporated Blended Cements, *Cement and Concrete Research*, Vol. 29, pp. 743-746, 1999.
57. ASTM C 187, Test Method for Normal Consistency of Hydraulic Cement, *American Society for Testing and Materials*, 2004.
58. ASTM C 191, Test Method for Time of Setting of Hydraulic Cement by Vicat Needle, *American Society for Testing and Materials*, 2004.
59. Diamond, S., The Micro Structure of Cement and Concrete-A Visual Primer, *Cement and Concrete Composites*, Vol.26, No.8, pp.919-933, 2004.
60. TS EN 196-1, Methods of Testing Cement-Part 1: Determination of Strength, *Turkish Standards Institution*, 2002 (in Turkish).

61. ASTM C 143, Standard Test Method for Slump of Hydraulic-Cement Concrete, *American Society for Testing and Materials*, 2005.
62. ASTM C 138, Standard Test Method for Unit Weight, Yield, and Air Content (Gravimetric) of Concrete, 2000.
63. ASTM C 231, Standard Test Method for Air Content of Freshly Mixed Concrete by the Pressure Method, *American Society for Testing and Materials*, 2004.
64. ASTM C 403, Standard Test Method Time of Setting of Concrete Mixtures by Penetration Resistance, *American Society for Testing and Materials*, 2005.
65. ASTM C 39, Standard Test Method for Compressive Strength of Cylindrical Concrete Specimens, *American Society for Testing and Materials*, 2005.
66. ASTM C 496, Standard Test Method for Splitting Tensile Strength of Cylindrical Concrete Specimens, *American Society for Testing and Materials*, 2004.
67. ASTM C 469, Standard Test Method for Static Modulus of Elasticity and Poisson's Ratio of Concrete in Compression, *American Society for Testing and Materials*, 2002.
68. ASTM C 1202, Standard Test Method for Electrical Indication of Concrete's Ability to Resist Chloride Ion Penetration, *American Society for Testing and Materials*, 2005.
69. Rivera, A., Rodriguez-Fuentes, G., Altshuler, E., Time Evolution of a Natural Clinoptilolite in Aqueous Medium: Conductivity and pH Experiments, *Microporous and Mesoporous Materials*. Vol.40, No.1-3, pp.173-179, 2000.
70. Cebeci, Ö., Z., Pore Structure of Air-Entrained Hardened Cement Paste, *Cement and Concrete Research*, Vol.11, No.2, pp. 257-265, 1981.
71. ASTM C 1240, Standard Specification for Silica Fume Used in Cementitious Mixtures, *American Society for Testing and Materials*, 2005.
72. ASTM C 618, Standard Specification for Fly Ash and Raw or Calcined Natural Pozzolan for Use as a Mineral Admixture in Portland Cement Concrete, *American Society for Testing and Materials*, 2005.

73. Lawrence, P., Cyr, M., Ringor, E., Mineral Admixtures in Mortars Effect of Inert Materials on Short Term Hydration, *Cement and Concrete Research*, Vol.33, No.12, pp.1939-1947, 2003.
74. Rahhal, V., Talero, R., Early Hydration of Portland Cement with Crystalline Mineral Additions, *Cement and Concrete Research*, Vol.35, No.7, pp.1285-1291.
75. Chindaprasirt, P., Jaturapitakkul, C., Sinsiri, T., Effect of Fly Ash Fineness on Micro Structure of Blended Cement Paste, *Construction and Building Materials*, Vol.21, No.7, pp.1534-1541, 2007.
76. Gopalan, M.K., Nucleation and Pozzolanic Factors in Strength Development of Class F Fly Ash Concrete, *ACI Materials Journal*, Vol.90, No.2, pp.117-121, 1993.
77. Bentz, D.P., Stutzman, P.E., Evaluation of Porosity and Calcium Hydroxide in Laboratory Concretes Containing Silica Fume, *Cement and Concrete Research*, Vol.24, No.6, pp.1044-1050, 1994.
78. Taylor, H.F.W., The Chemistry of Cements, *Academic Press*, London, New York, 1964.
79. Shi, C., Effect of Mixing Proportions of Concrete on Its Electrical Conductivity and the Rapid Chloride Permeability Test (ASTM C1202 or AASHTO T277), *Cement and Concrete Research*, Vol.34, No.3, pp.537-545, 2004.

APPENDIX A

TGA PLOTS FOR LIME-POZZOLAN PASTES

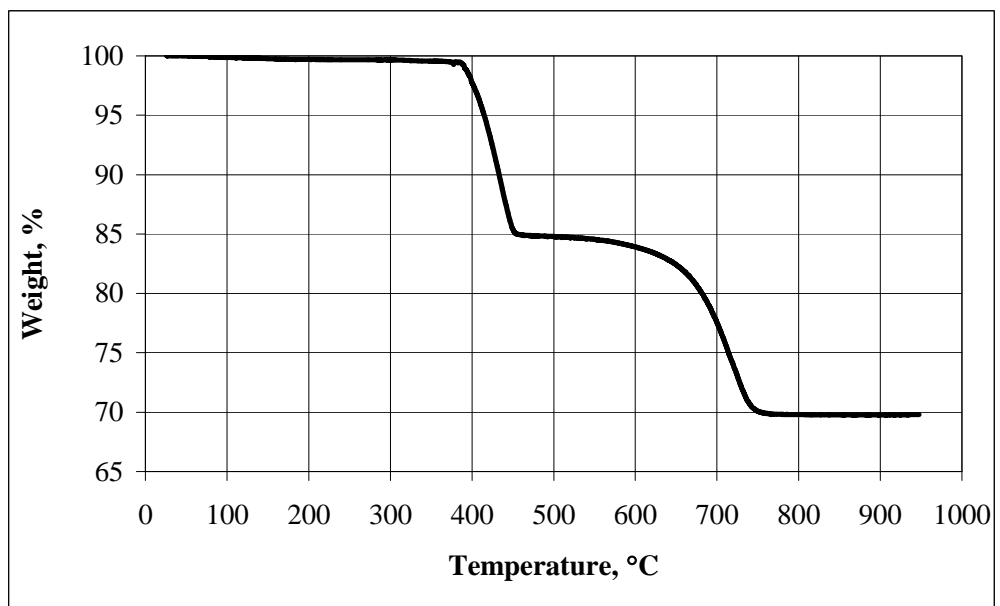


Figure A.1 TGA plot of the technical grade Ca(OH)₂ used in pozzolanic activity studies

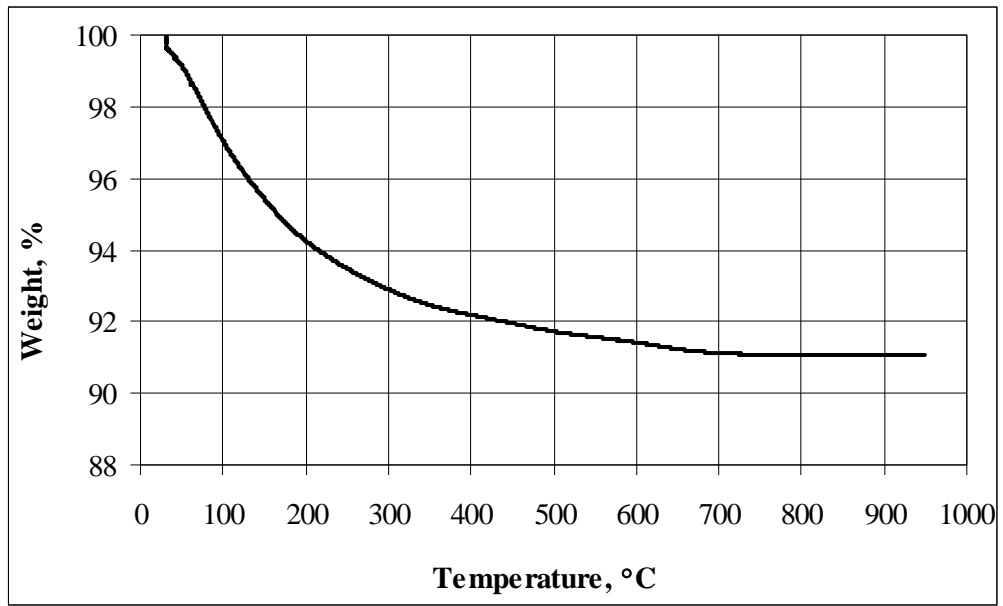


Figure A.2 TGA plot of Gördes zeolite (GZ)

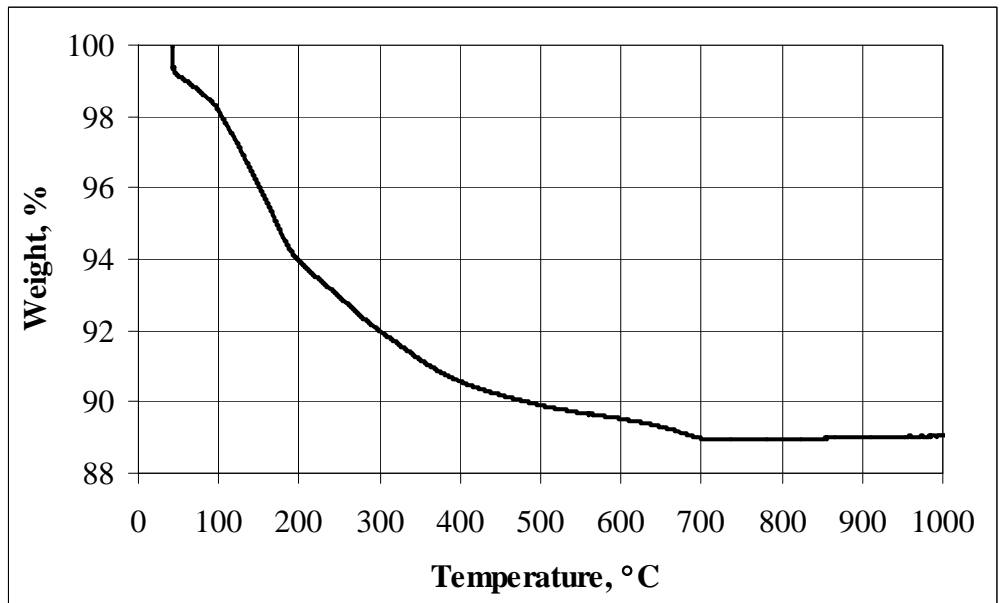


Figure A.3 TGA plot of Bigadiç zeolite (BZ)

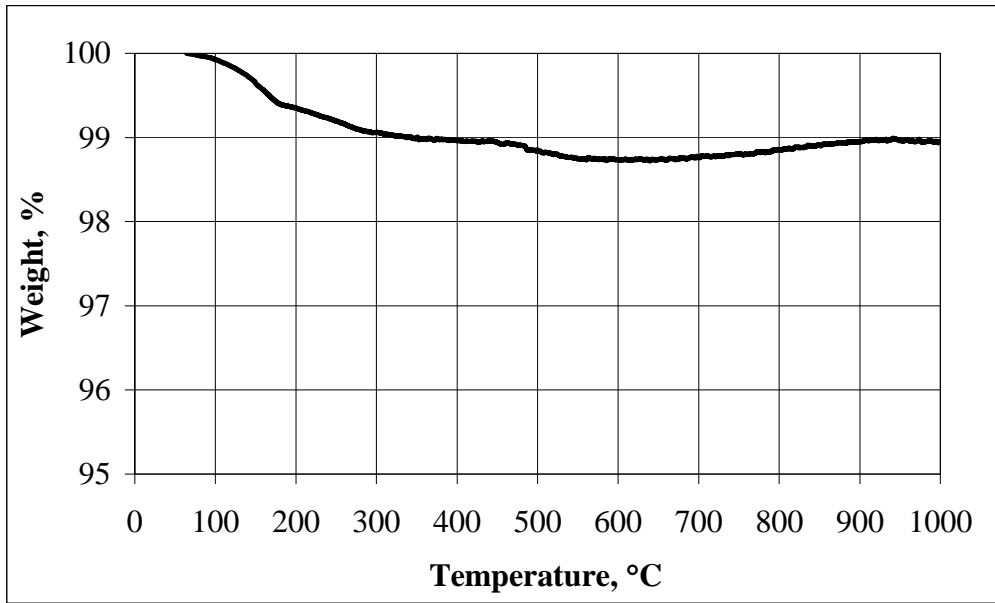


Figure A.4 TGA plot of the silica fume (SF)

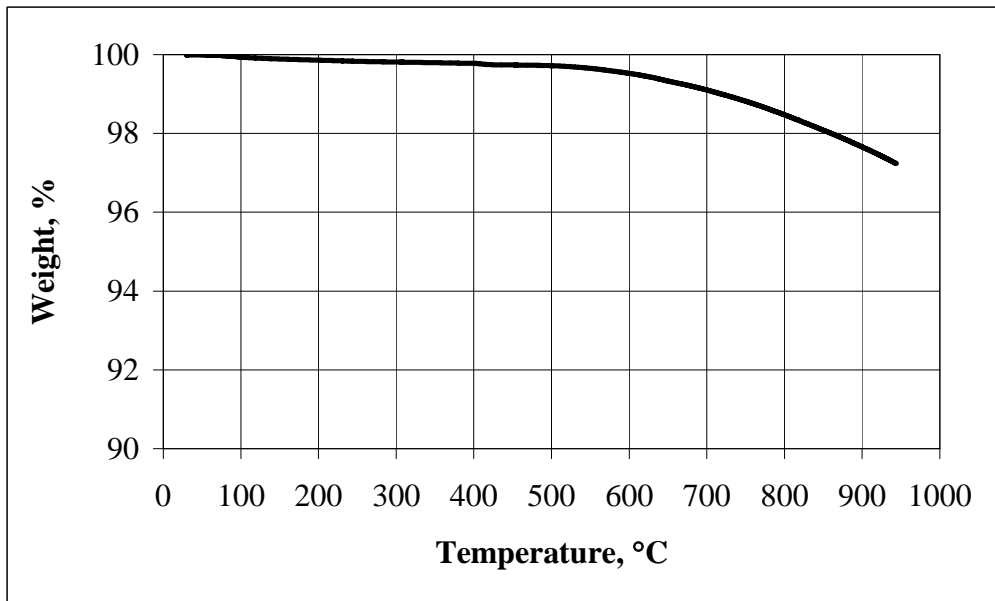


Figure A.5 TGA plot of the fly ash (FA)

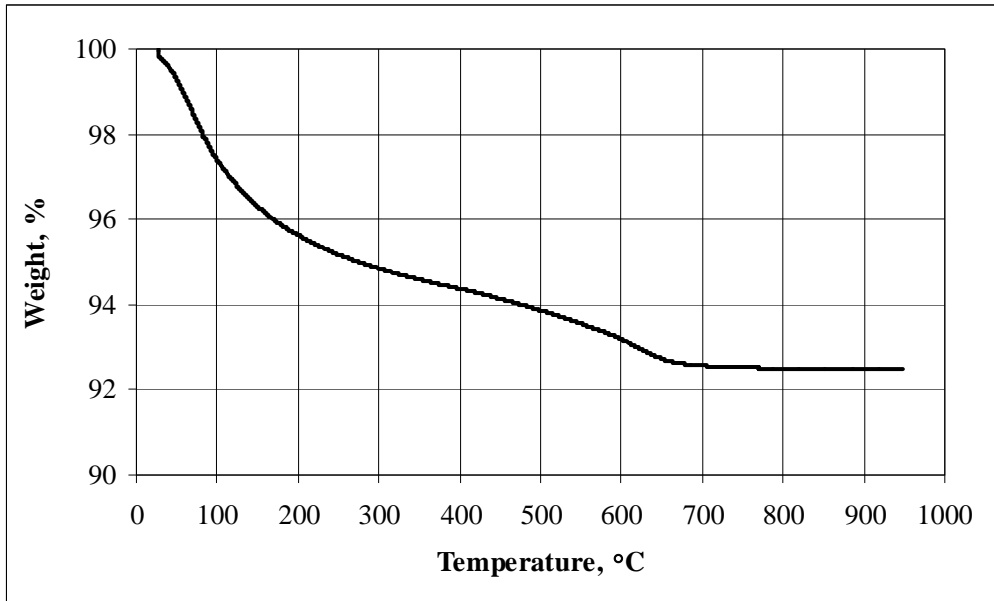


Figure A.6 TGA plot of the non-zeolitic natural pozzolan (NZP)

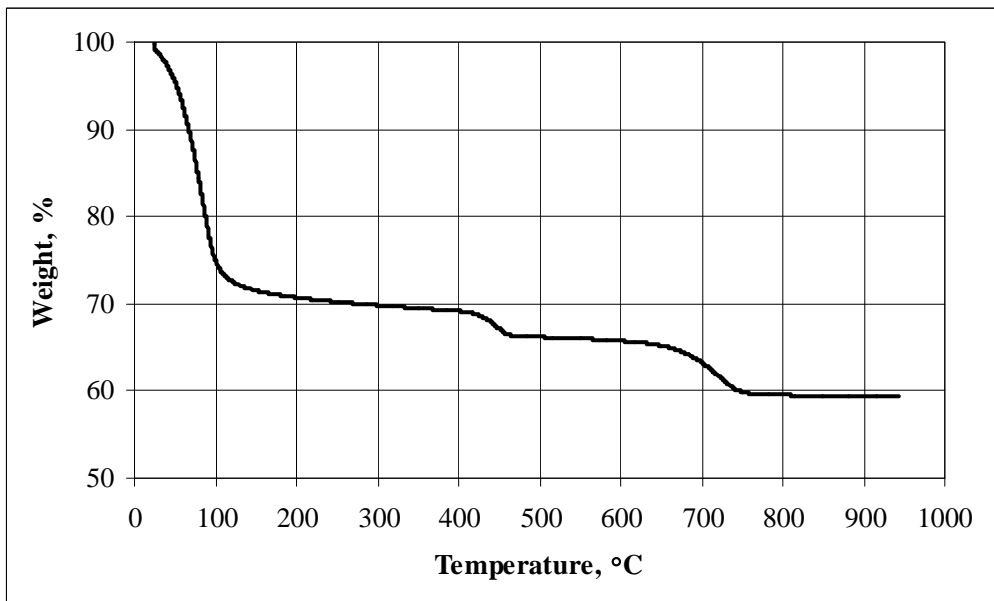


Figure A.7 TGA plot of the GZ-lime paste at 3 days

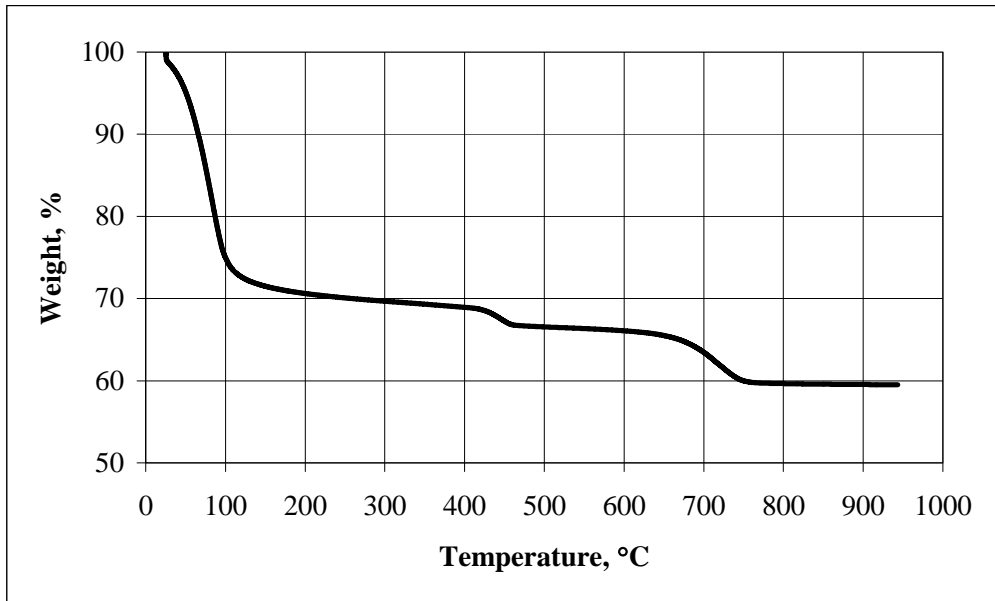


Figure A.8 TGA plot of the GZ-lime paste at 7 days

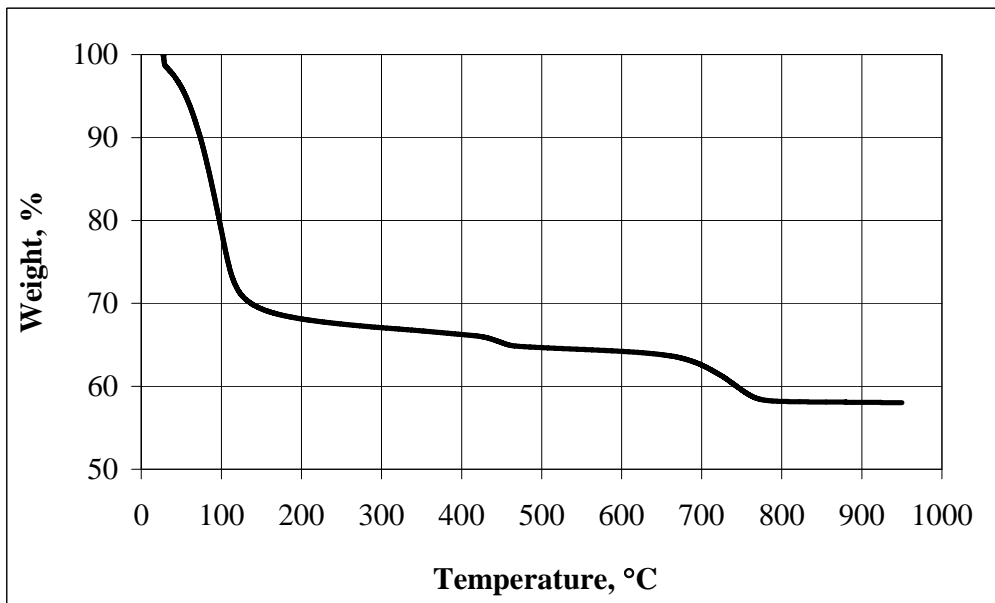


Figure A.9 TGA plot of the GZ-lime paste at 28 days

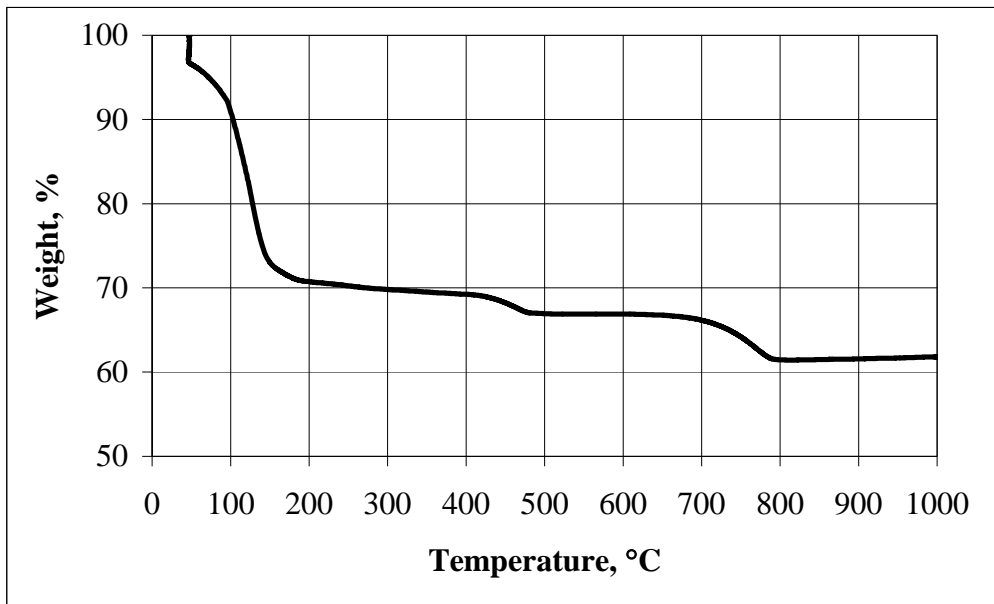


Figure A.10 TGA plot of the BZ-lime paste at 3 days

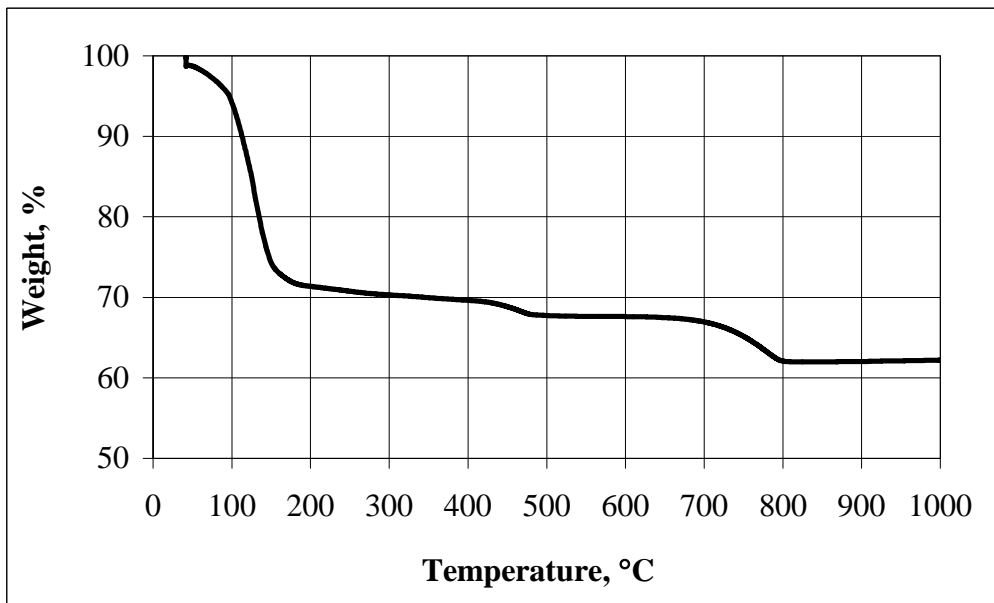


Figure A.11 TGA plot of the BZ-lime paste at 7 days

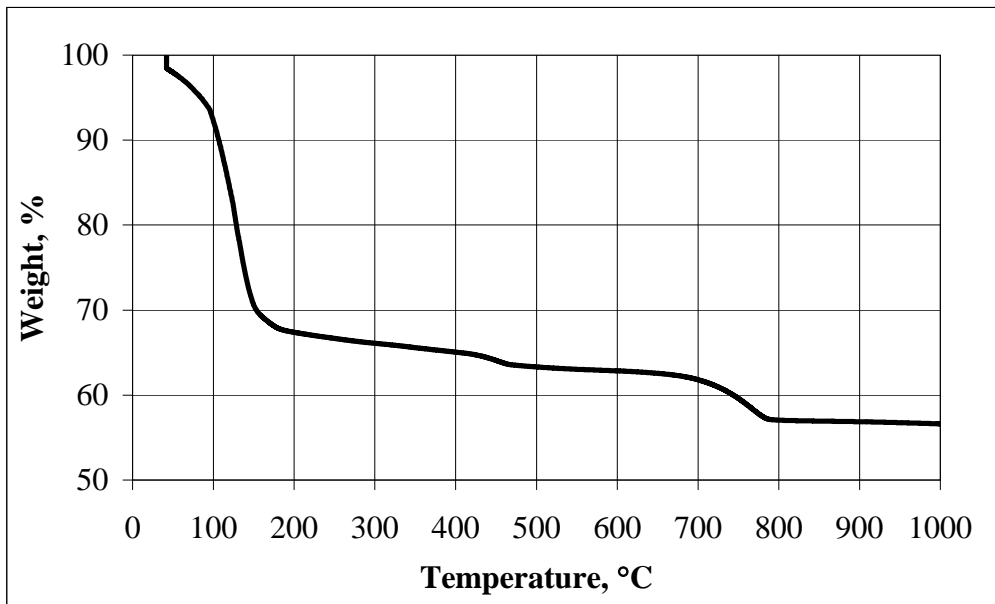


Figure A.12 TGA plot of the BZ-lime paste at 28 days

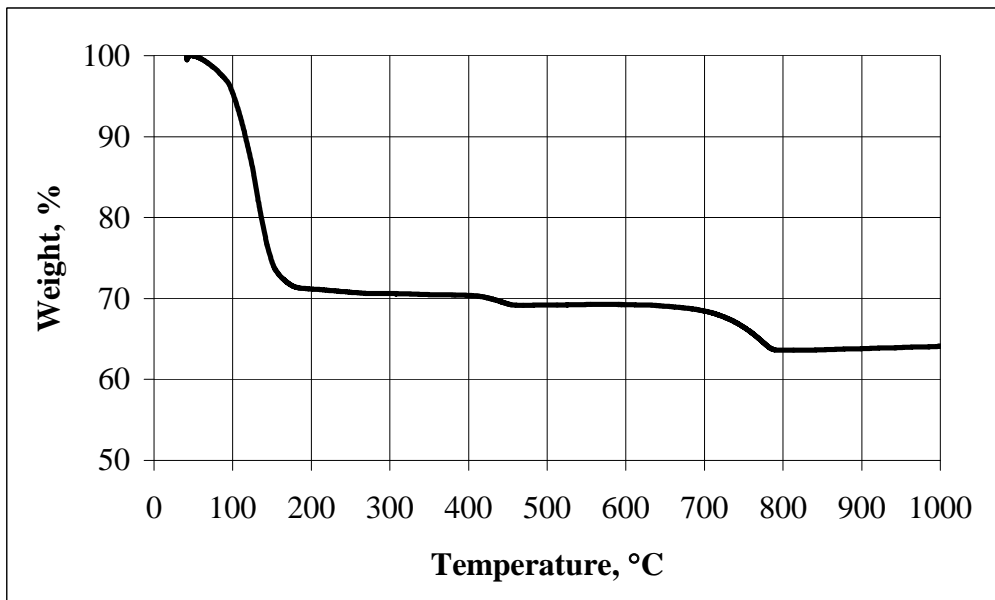


Figure A.13 TGA plot of the SF-lime paste at 3 days

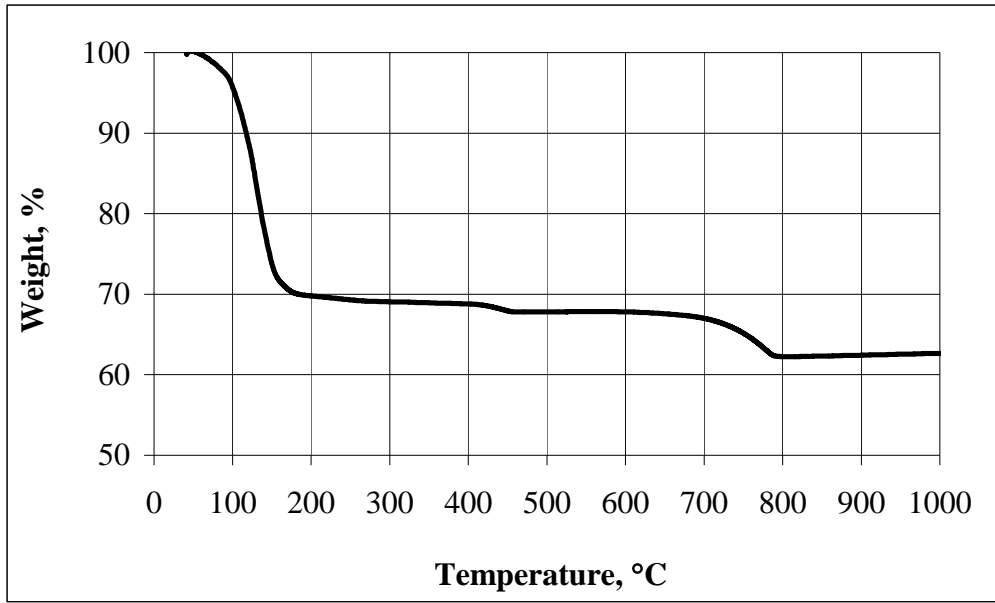


Figure A.14 TGA plot of the SF-lime paste at 7 days

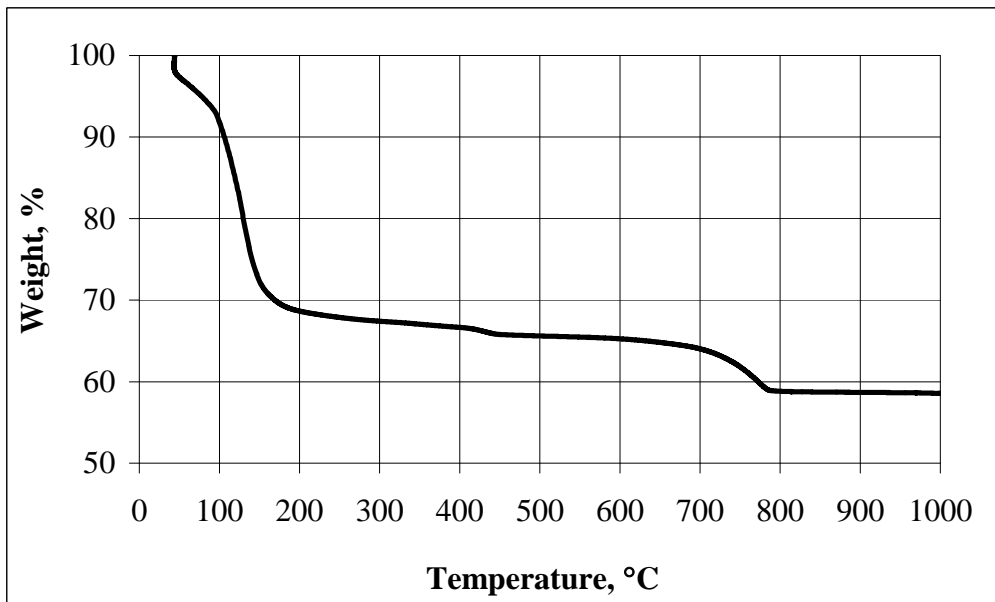


Figure A.15 TGA plot of the SF-lime paste at 28 days

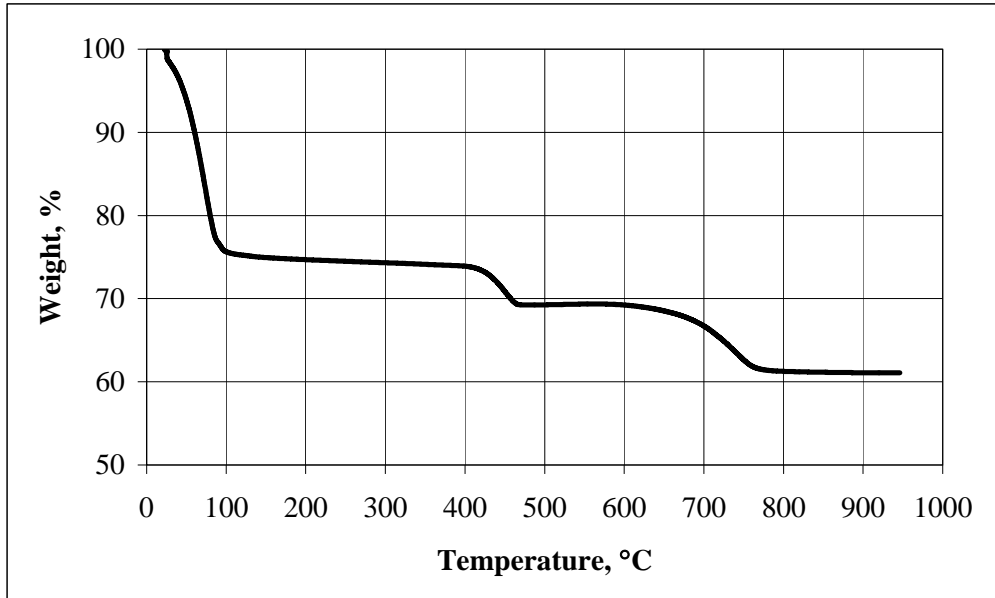


Figure A.16 TGA plot of the FA-lime paste at 3 days

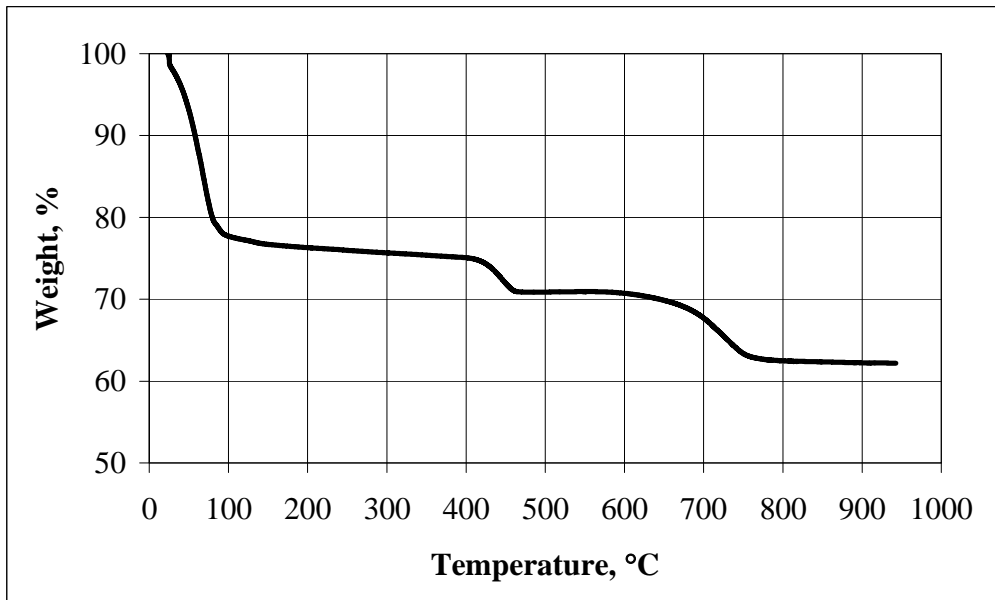


Figure A.17 TGA plot of the FA-lime paste at 7 days

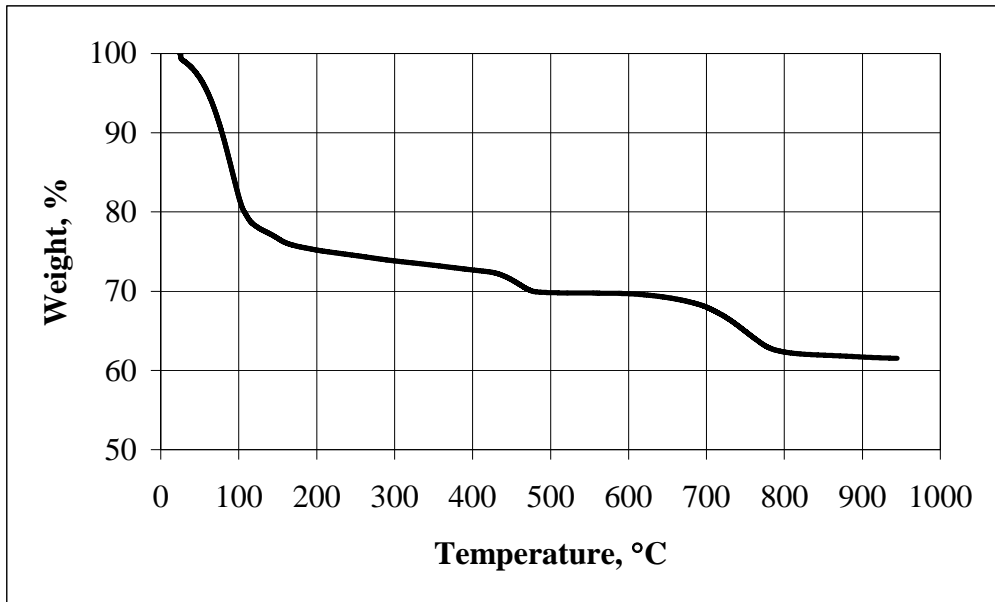


Figure A.18 TGA plot of the FA-lime paste at 28 days

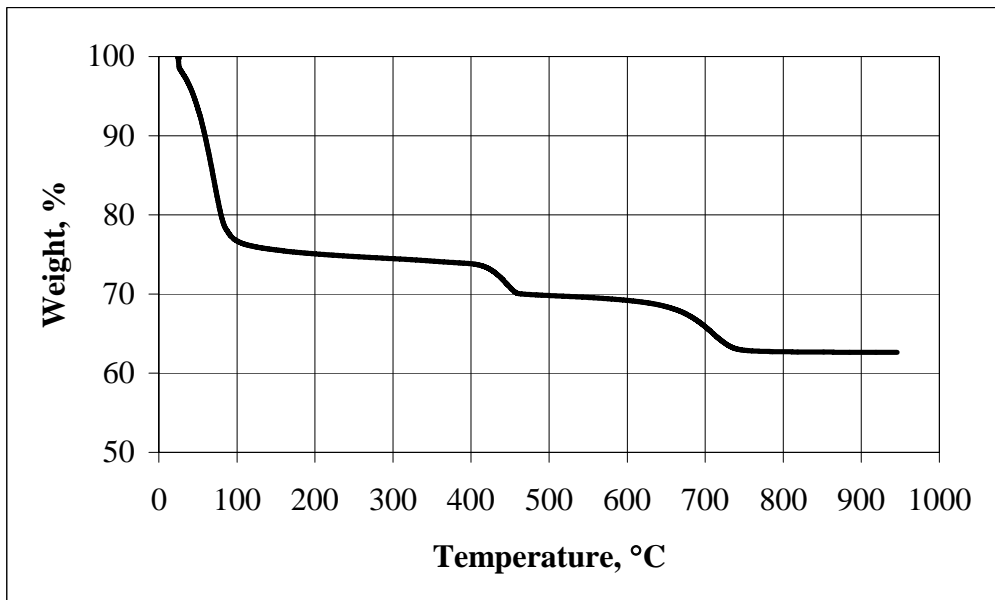


Figure A.19 TGA plot of the NZP-lime paste at 3 days

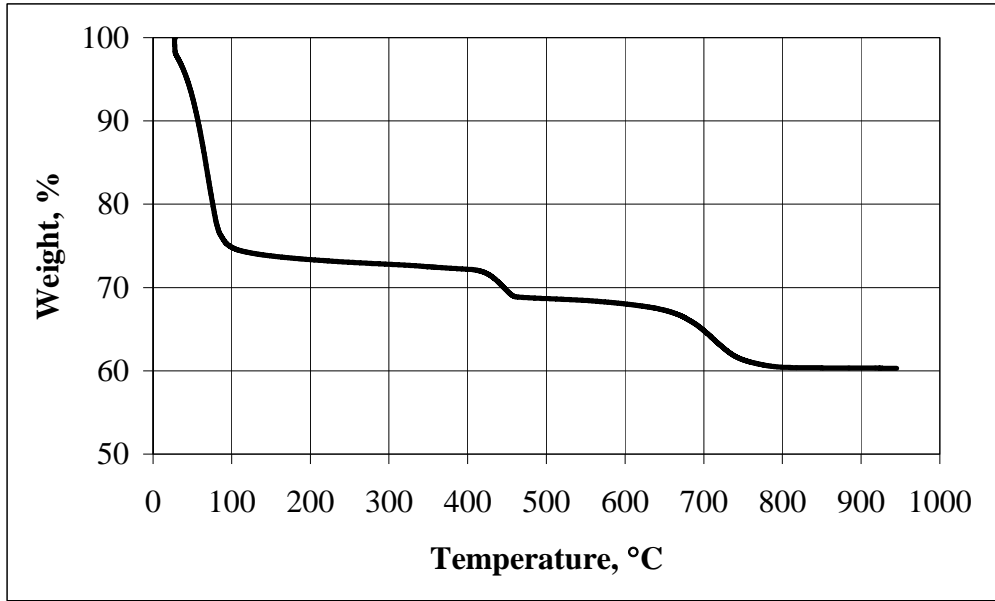


Figure A.20 TGA plot of the NZP-lime paste at 7 days

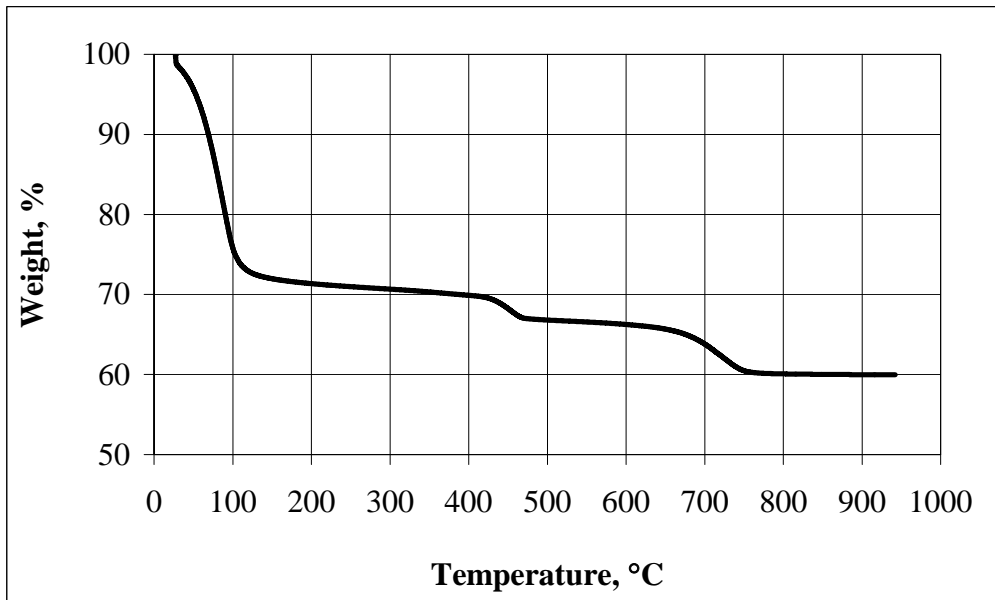


Figure A.21 TGA plot of the NZP-lime paste at 28 days

APPENDIX B

TGA PLOTS FOR HARDENED CEMENT PASTES

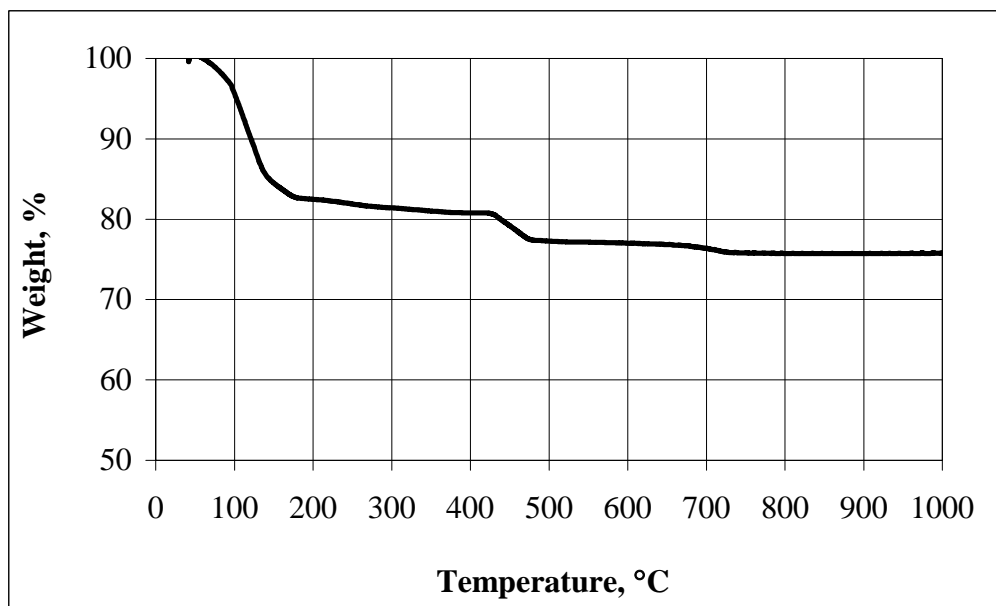


Figure B.1 TGA plot of PC paste at 3 days

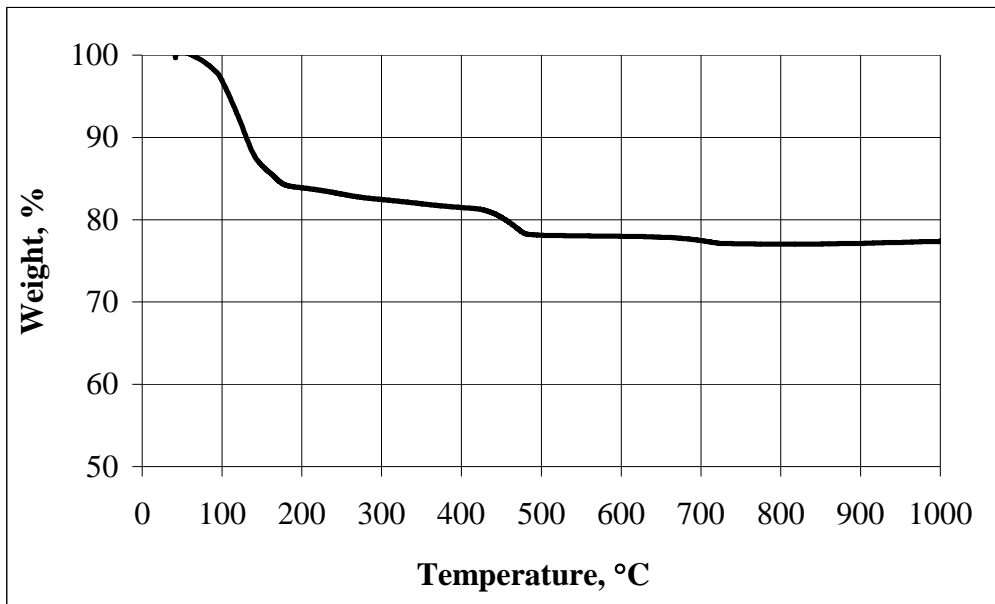


Figure B.2 TGA plot of PC paste at 7 days

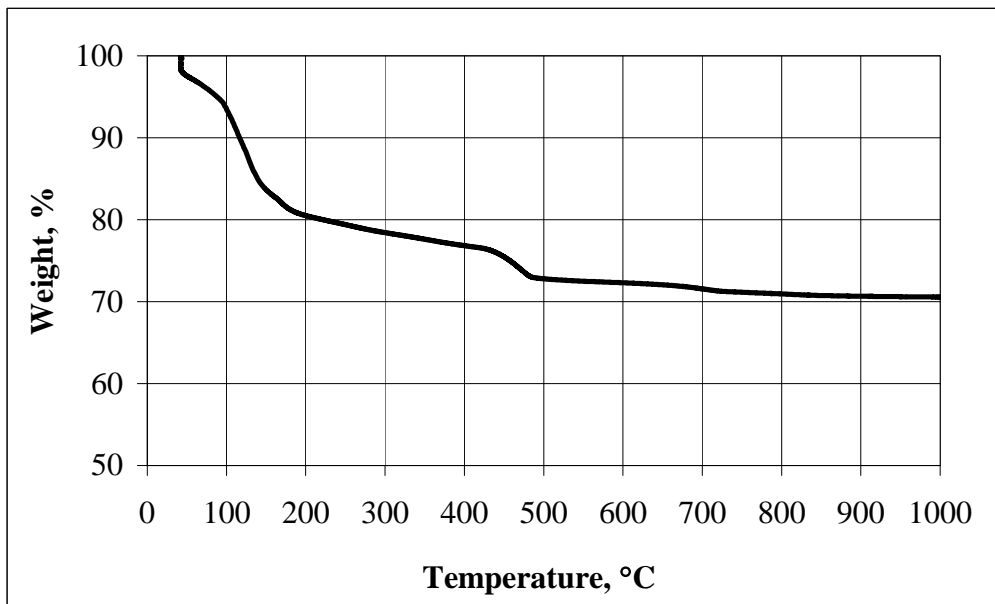


Figure B.3 TGA plot of PC paste at 28 days

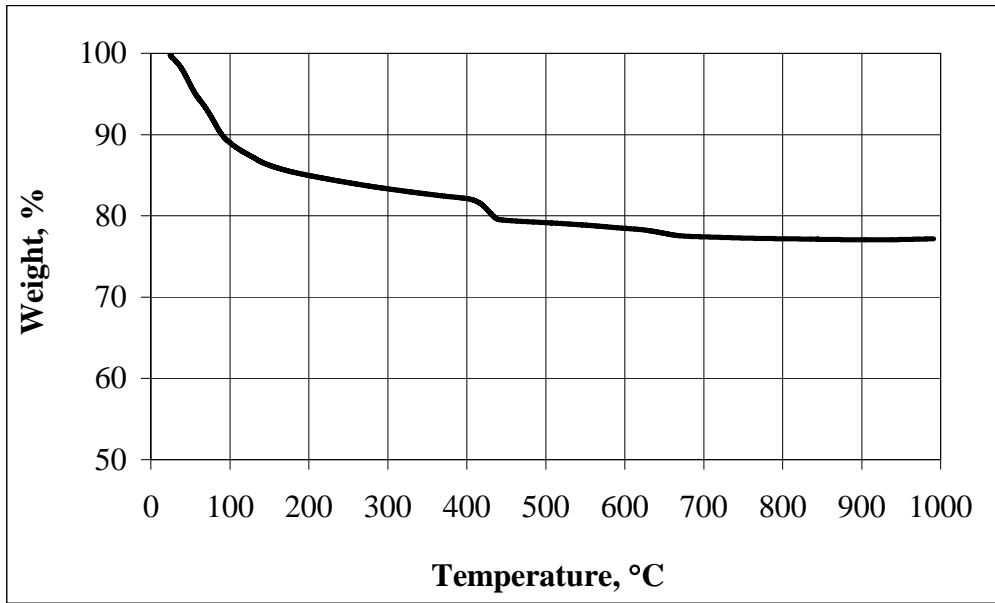


Figure B.4 TGA plot of GZ15 paste at 3 days

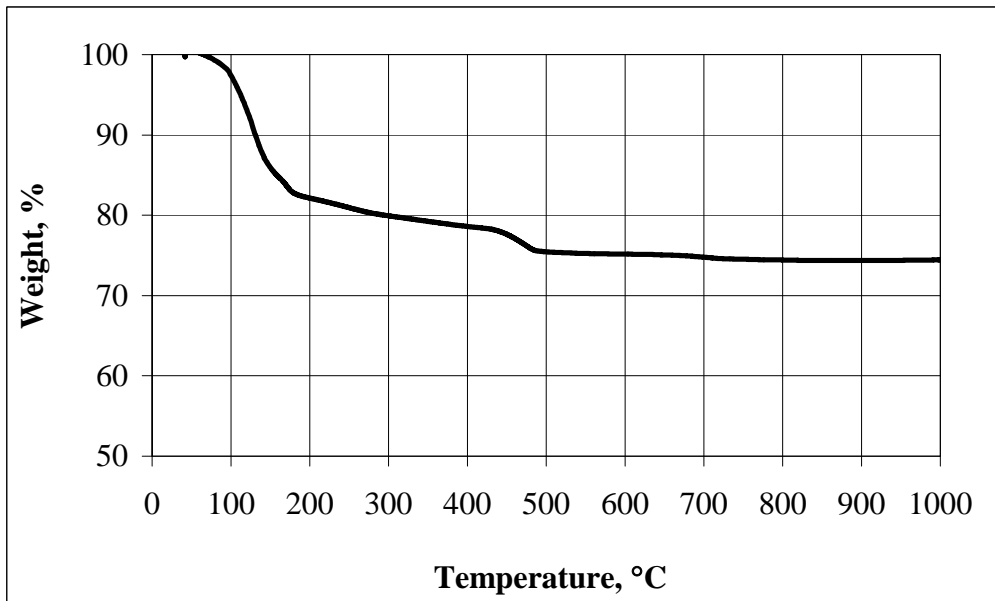


Figure B.5 TGA plot of GZ15 paste at 7 days

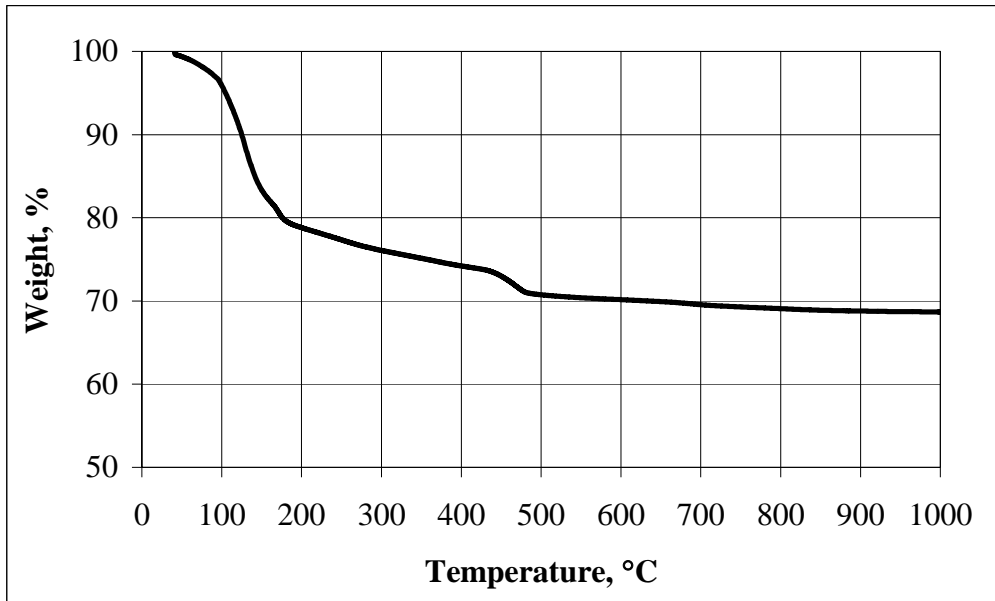


Figure B.6 TGA plot of GZ15 paste at 28 days

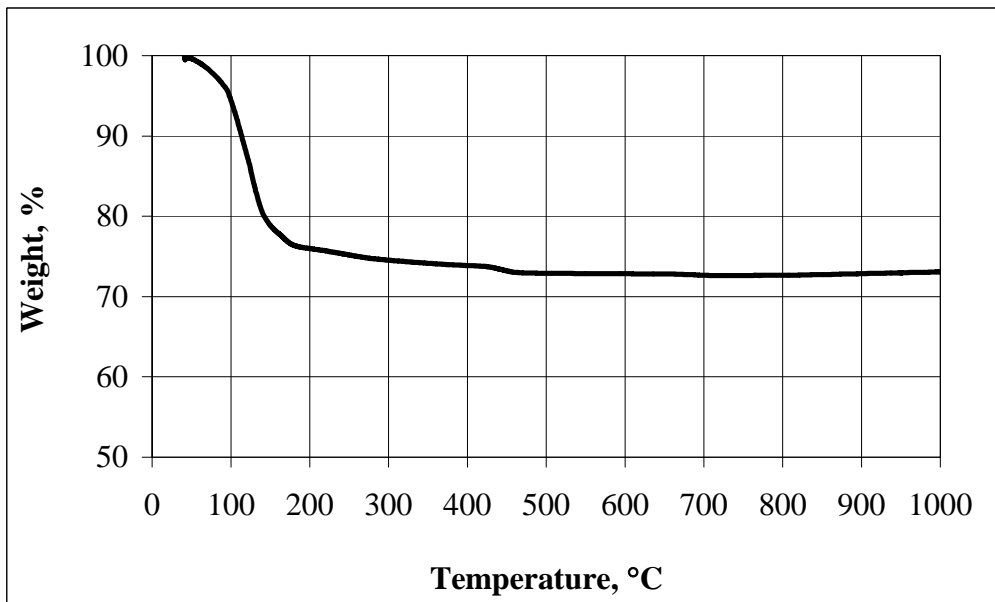


Figure B.7 TGA plot of GZ35 paste at 3 days

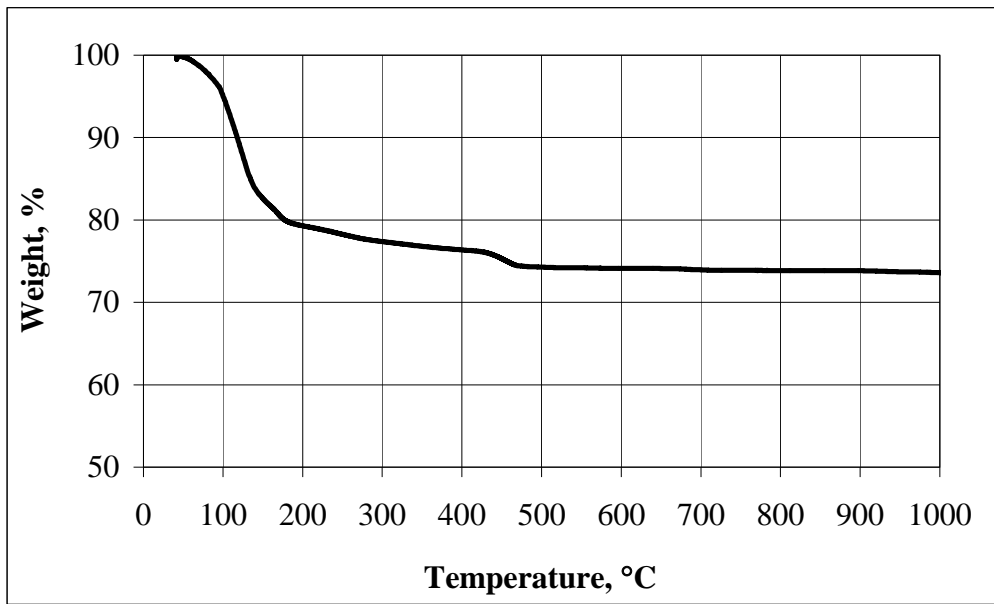


Figure B.8 TGA plot of GZ35 paste at 7 days

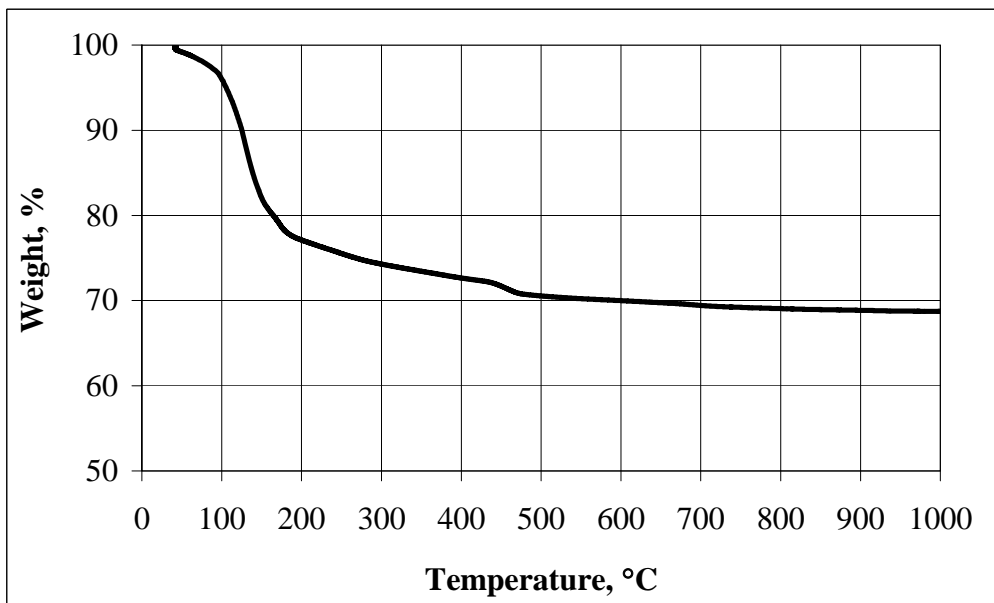


Figure B.9 TGA plot of GZ35 paste at 28 days

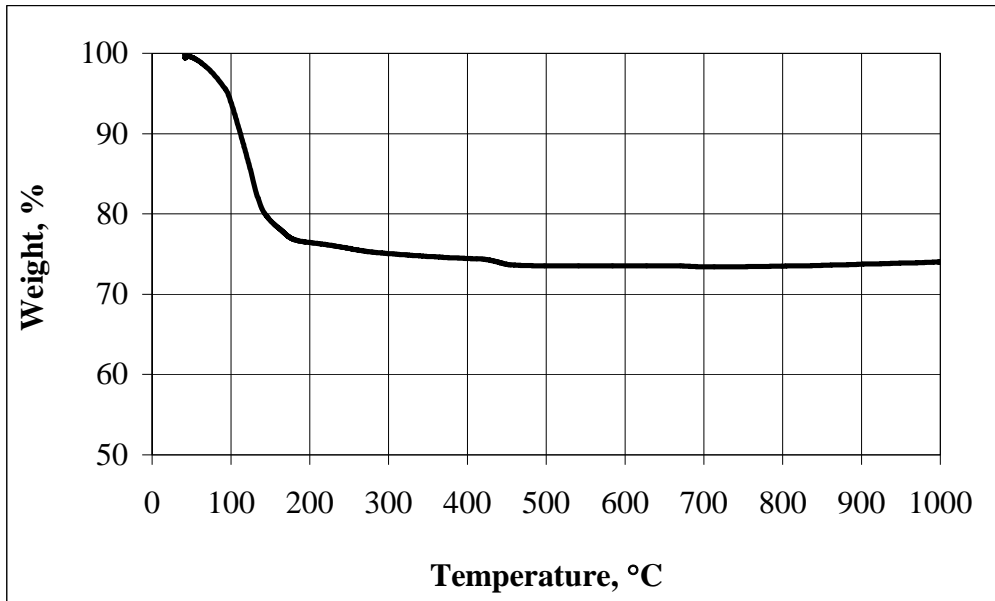


Figure B.10 TGA plot of GZ55 paste at 3 days

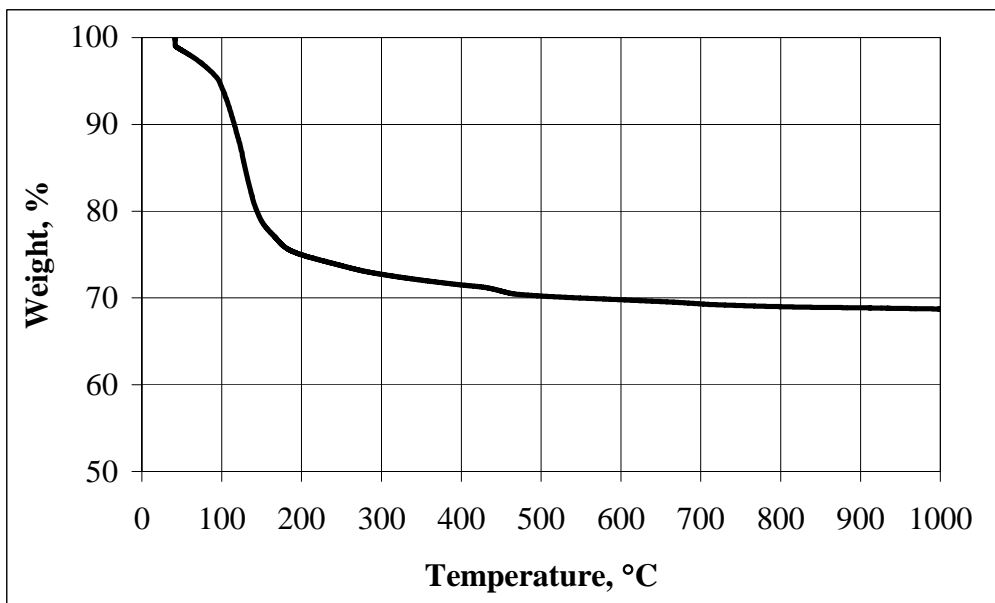


Figure B.11 TGA plot of GZ55 paste at 7 days

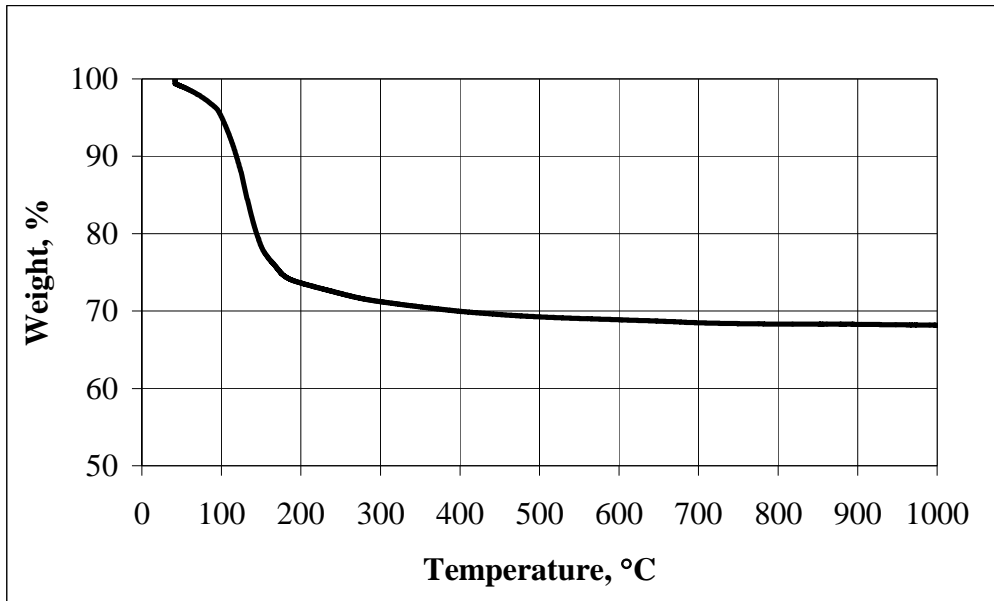


Figure B.12 TGA plot of GZ55 paste at 28 days

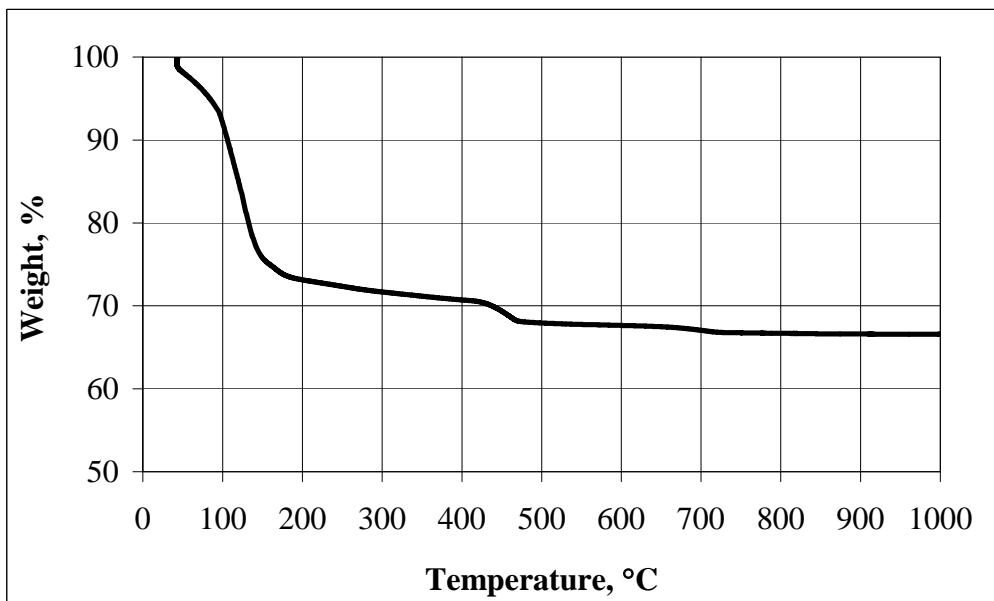


Figure B.13 TGA plot of BZ15 paste at 3 days

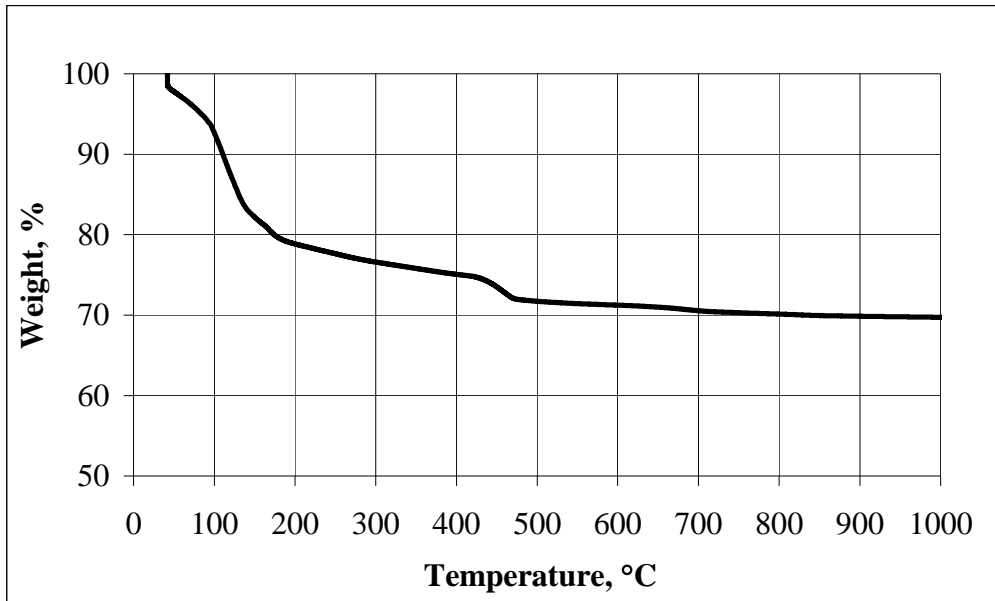


Figure B.14 TGA plot of BZ15 paste at 7 days

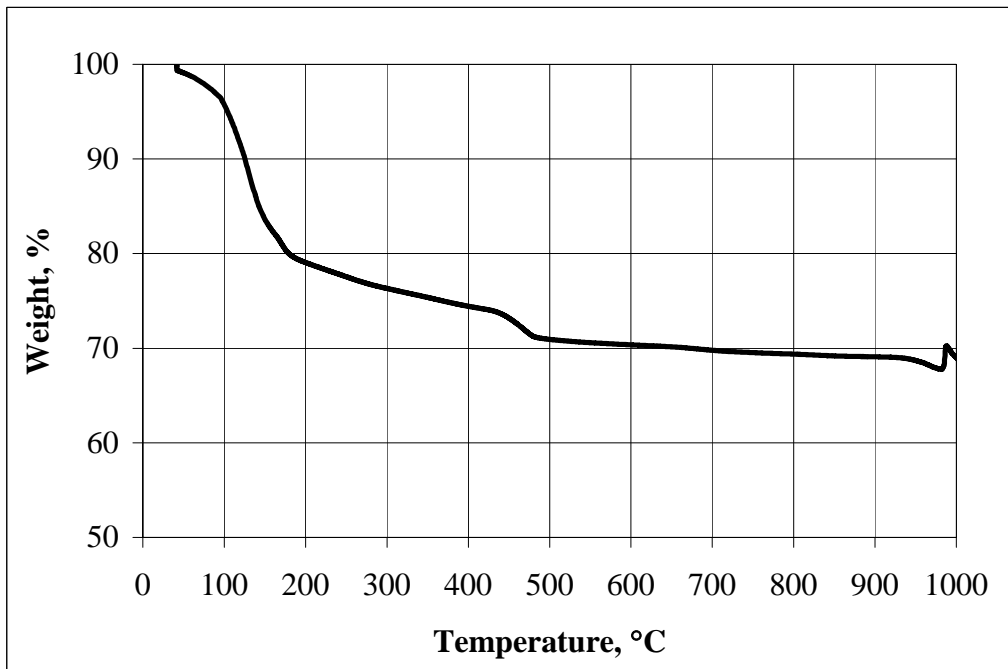


Figure B.15 TGA plot of BZ15 paste at 28 days

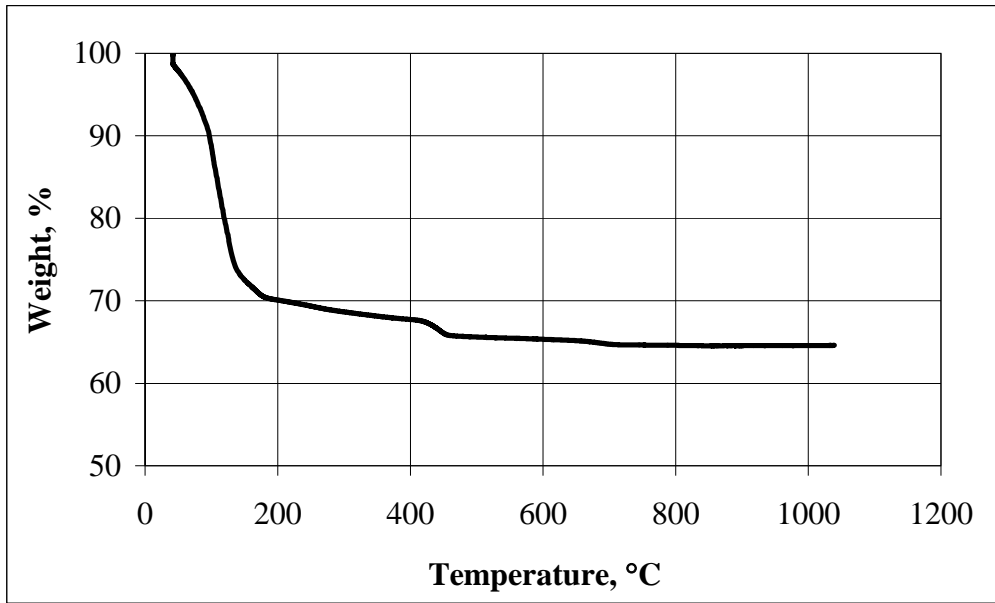


Figure B.16 TGA plot of BZ35 paste at 3 days

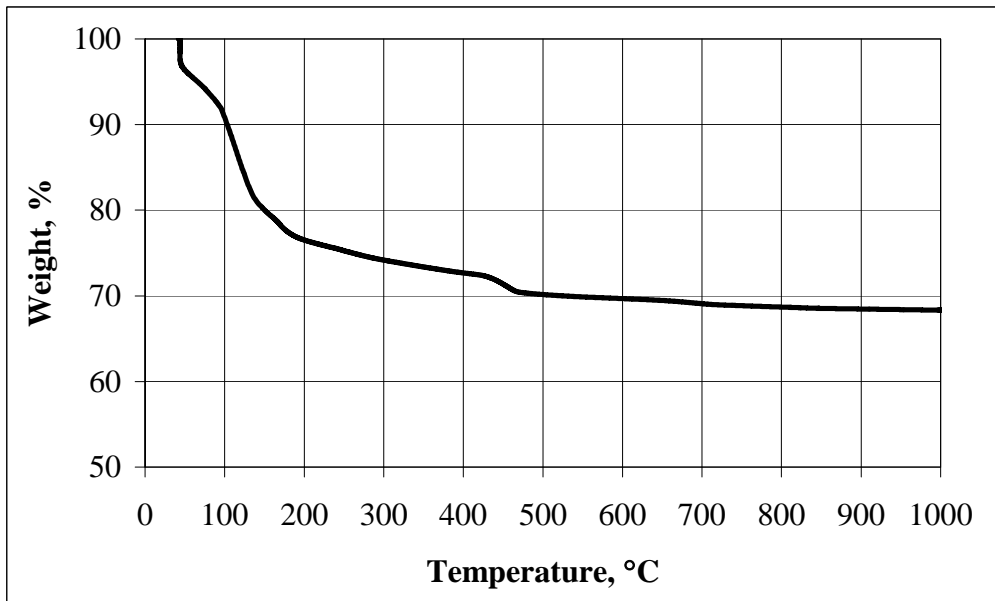


Figure B.17 TGA plot of BZ35 paste at 7 days

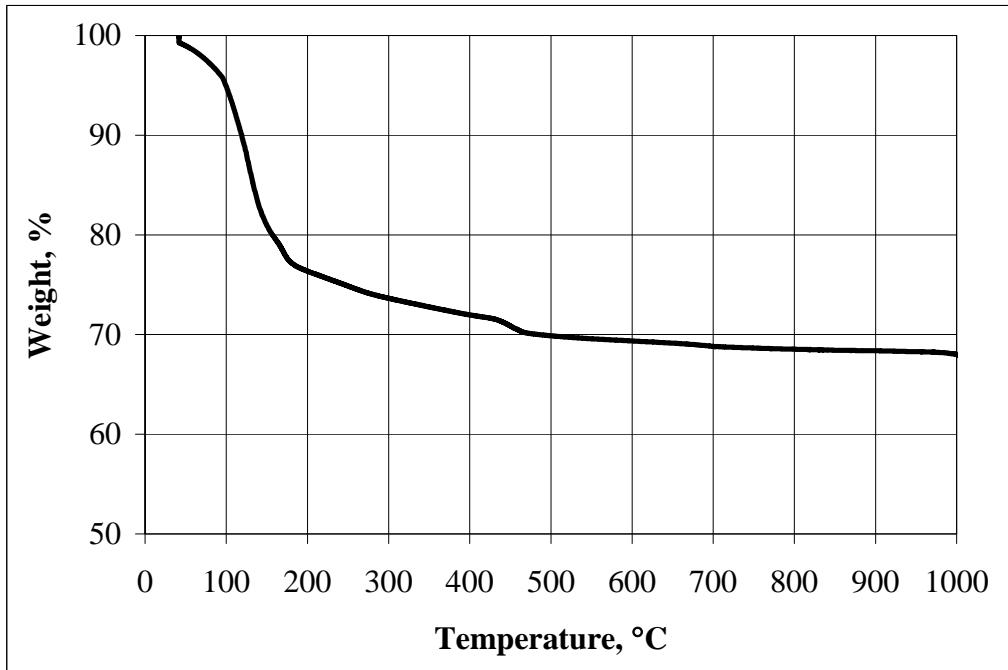


Figure B.18 TGA plot of BZ35 paste at 28 days

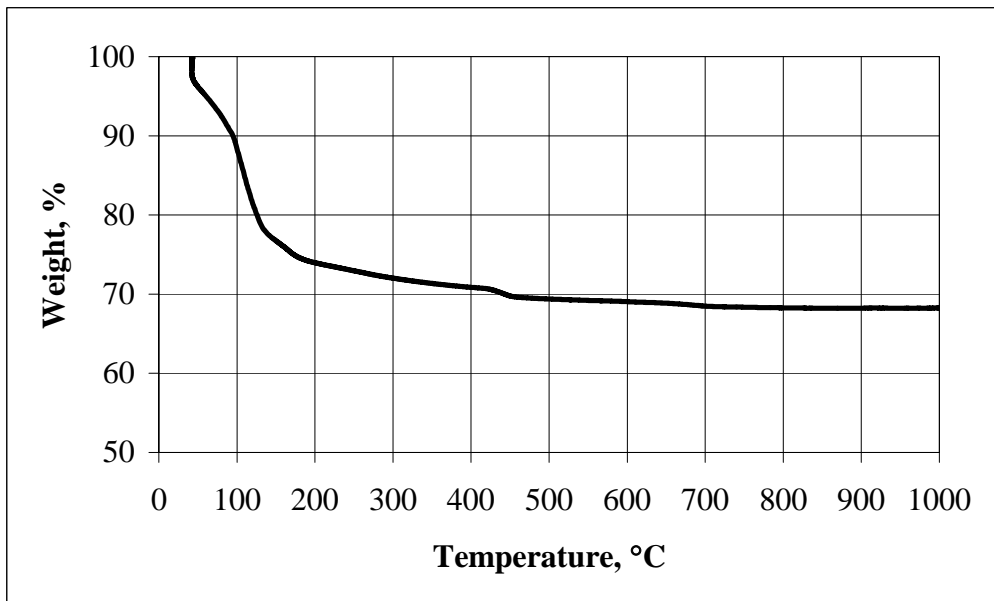


Figure B.19 TGA plot of BZ55 paste at 3 days

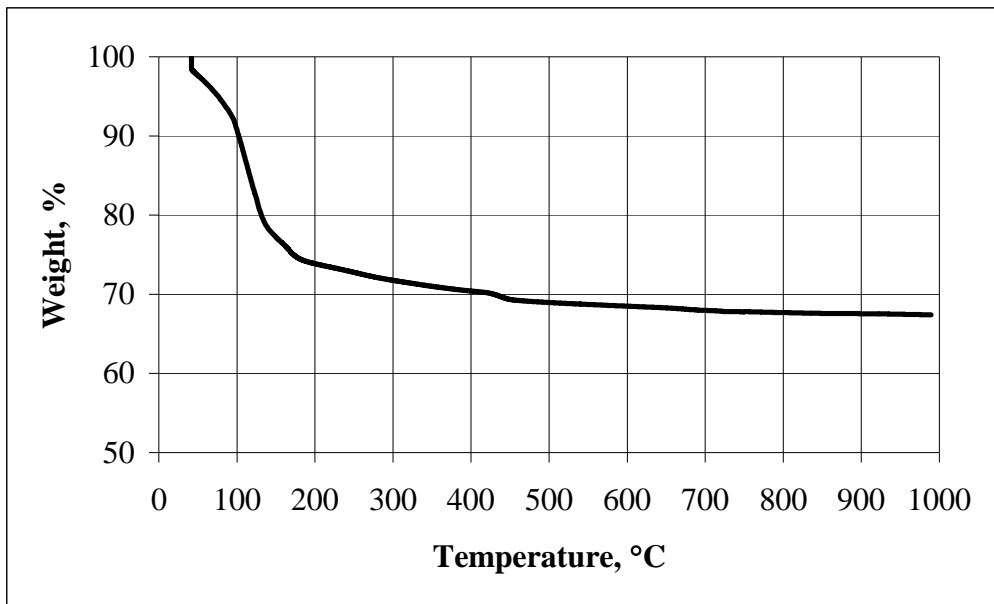


Figure B.20 TGA plot of BZ55 paste at 7 days

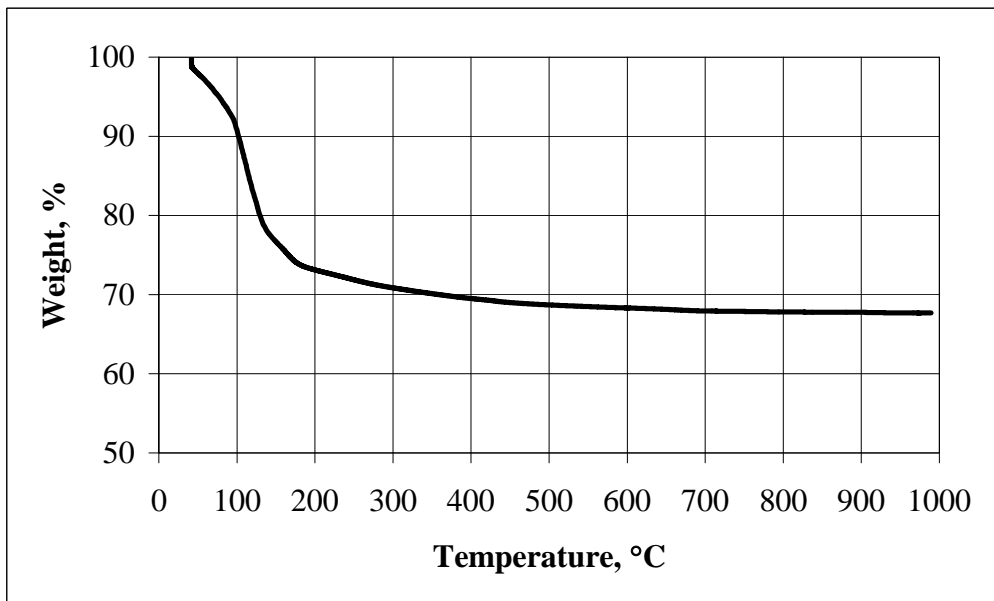


Figure B.21 TGA plot of BZ55 paste at 28 days

CURRICULUM VITAE

Burak UZAL

Date of Birth : 28-02-1978
Marital Status : Married
Phone : +90-312-2105497
Fax : +90-312-2101262
e-mail : uzal@metu.edu.tr , burakuzal@gmail.com

EDUCATION

Sept.1999 - Jan. 2002

- Middle East Technical University, Dept. of Civil Engineering, Materials of Construction Division (M.S.)

Sept. 1994 - Jul. 1998

- Selcuk University, Dept. of Civil Engineering (B.S.)

LANGUAGE SKILLS

English (Fluent)

COMPUTER SKILLS

- C/C++ Programming Languages
- MATLAB
- Office Tools

PROFESSIONAL EXPERIENCE

Sept.1999 - ...

- Research Assistant, Civil Engineering Department, Middle East Technical University at Ankara, Turkey

COURSES AND CERTIFICATES

- Short Course on Durable Concrete Structures-Modern Materials and Construction Practice, given by Professor P. Kumar Mehta from University of California at Berkeley, September 23-27, 2002, Ankara, Turkey.

- METU SEM (Continuous Education Center), Object-Oriented Programming with C++
- METU IDE A, Internet-Based Education A-synchronous, Information Technologies Certificate Program (On Going)

PROJECTS

- Researcher, Use of Natural Zeolites in Building Industry, TÜBİTAK 104M393, (Supervisor: Asoc.Prof.Dr. Lutfullah Turanlı, Other Researchers : Prof.Dr. Hayrettin Yücel (Chem. Eng. Dept.), Prof.Dr. Cemal Göncüoğlu (Geo. Eng. Dept.), Prof.Dr. Ali Çulfaz (Chem. Eng. Dept.)). Total Budget: 93.000 YTL
- Researcher, Study of Mass Concrete Ingredients of Deriner Dam and Hepp Project, AGUDOS-2002-03-03-2-002, Middle East Technical University at Ankara, Turkey, 2002.

PUBLICATIONS

Thesis

- Effects of High Volume Natural Pozzolan Addition on the Properties of Pozzolanic Cements (M.S. Thesis), Middle East Technical University at Ankara, Turkey (2002).

International Journals

- Studies on blended cements containing a high volume of natural pozzolans, (with L.Turanli), Cement and Concrete Research Vol.33 (2003) 1777-1781
- Effects of material characteristics on properties of blended cements containing high volumes of natural pozzolans, (with L. Turanli, F. Bektas), Cement and Concrete Research Vol.34 (2004) 2277-2282 .
- Effect of Large Amounts of Natural Pozzolan Addition on properties of blended cements, (with L. Turanli, F Bektas), Cement and Concrete Research Vol.35 (2005) 1106-1111.
- High-volume natural pozzolan concrete for structural applications, (with L. Turanli and P.K. Mehta), ACI Materials Journal Vol. 104 (2007) 535-538.

Proceedings

- High Volume Natural Pozzolan Blended Cements: Physical Properties and Compressive Strength of Mortars, Three-Day CANMET/ACI International Symposium on Sustainable Development and Concrete Technology, San Francisco, USA, 2001.
- Use of high volume natural pozzolan blended cements in suppressing alkali-silica reaction (with F. Bektas, L. Turanli), CANMET/ACI International Conference on Durability of Concrete, Thessaloniki, Greece (2003).

- Studies on Blended Cements Containing High Volume of Natural Pozzolans, (with L. Turanli) Sixth Canmet/ACI International Conference on Recent Advances in Concrete Technology, Bucharest, Romania, 2003.
- High-volume fly ash concrete for concrete pavements (with F. Bektas, L. Turanli), 9th International Symposium on Concrete Roads, Istanbul, Turkey (2004).
- Effect of chemical activation on consistency and compressive strength of superplasticized mortars made with blended cements containing large amounts of natural pozzolan (with F. Bektas, L. Turanli), 2nd International Symposium Non-Traditional Cement and Concrete, Brno, Czech Republic (2005)